

**University of Alberta**

**Frame stability considering member interaction and compatibility of  
warping deformations**

by

**Ian James MacPhedran**

A thesis submitted to the Faculty of Graduate Studies and Research  
in partial fulfillment of the requirements for the degree of

**Doctor of Philosophy**

in

**Structural Engineering**

Department of Civil and Environmental Engineering

©Ian James MacPhedran

Fall, 2009

Edmonton, Alberta

Permission is hereby granted to the University of Alberta Libraries to reproduce single copies of this thesis and to lend or sell such copies for private, scholarly or scientific research purposes only. Where the thesis is converted to, or otherwise made available in digital form, the University of Alberta will advise potential users of the thesis of these terms.

The author reserves all other publication and other rights in association with the copyright in the thesis and, except as herein before provided, neither the thesis nor any substantial portion thereof may be printed or otherwise reproduced in any material form whatsoever without the author's prior written permission.

## **Examining Committee**

Supervisor:	Gilbert Y. Grondin
External Examiner:	Robert Tremblay
Committee Chair:	Mohamed Al-Hussein
Committee Member:	Robert Driver
Committee Member:	Walied Moussa
Committee Member:	Josef Szymanski

## **Abstract**

Steel moment frames are often used in structures to provide lateral strength and stiffness to the structure. These frames are subject to failure modes including buckling in the out of plane direction in a lateral-torsional buckling mode. This failure mode is influenced by interactions of the members through their connections. While the flexural behaviour has been studied in depth and for some time, the effect of torsional warping interaction between members has not been studied extensively.

This work presents an analysis of the effect of including the effects of warping interaction or neglecting them, as is done in the current design practice. The issues of inelastic behaviour are considered, as well as the case of torsionally sensitive members. A joint element model is created to treat the warping displacements and their continuity through the joint.

The study finds that the current practice of neglecting the warping displacement continuity appears to be a conservative assumption. It is recommended that the present practice of neglecting the effects of warping in analysis of frames continues.

## **Acknowledgements**

The author wishes to thank the following:

The Alberta Ingenuity Fund (AIF) for funding this work through a Studentship, and University of Alberta for teaching and research assistantship bursaries and experience.

My graduate student colleagues including Yongjun Wang, Ming Jin and Georg Josi for their insight and discussion on my project and the problems I have encountered.

Faculty members Samer Adeeb, Alaa Elwi, and Robert Driver for their assistance in some of the tougher parts.

Gilbert Y. Grondin for his guidance, help and encouragement throughout this project.

And of course, Denise, always, and for everything.

# Table of Contents

1.	Introduction .....	1
1.1.	Specific aspects of this work.....	2
2.	Literature Review and Background.....	4
2.1	General structural mechanics .....	4
2.1.1	Bending and torsion .....	4
2.1.2	Local buckling behaviour.....	6
2.1.3	Buckling and out-of-plane behaviour.....	7
2.1.4	Plasticity and imperfections .....	11
2.1.5	Member interaction .....	12
2.2	Frame analysis.....	14
2.3	Current member design .....	15
2.4	Literature review .....	19
2.4.1	Torsion and beam columns .....	19
2.4.2	Frame analysis.....	23
3.	Finite Element Analysis of Torsional Warping Effects on Frame Buckling .....	36
3.1	Introduction .....	36
3.2	Brick and Shell Elements .....	38
3.3	Beam-Columns.....	39
3.3.1	Use of beam elements in current programs.....	40
3.4	Buckling analyses.....	41
3.4.1	Elastic buckling behaviour.....	42
3.4.2	Discrepancies in beam element elastic buckling.....	44
3.4.3	Inelastic buckling behaviour .....	49
3.4.4	Buckling analyses used within this work .....	50
3.5	Deformation of joint configurations.....	51
3.6	Inelastic modelling in a frame context .....	53
3.7	Member interaction using beam elements.....	55
3.8	Chapter summary .....	55
4.	Frame Analysis.....	70
4.1	Background: Frame behaviour, analysis and design.....	70
4.1.1	Advanced analysis.....	72
4.1.2	“Double $\omega$ ” .....	75
4.2	Interaction and Interactive Buckling.....	77
4.3	Interaction in Frames.....	79
4.3.1	Base plate fixity.....	83
4.4	Analysis Results .....	84
4.4.1	Effect of base plate.....	85
4.4.2	Effect of torsional susceptibility .....	86
4.4.3	Deep beams .....	88
4.4.4	Braced frames.....	89
4.4.5	Effect of warping direction .....	91
4.4.6	Effect of column length.....	92
4.5	Summary .....	94

5.	Joint Element with Warping Capability .....	143
5.1	Other joint elements .....	144
5.2	The shell element .....	144
5.3	The assemblage, or joint element.....	146
5.3.1	Sensitivity test .....	148
5.4	Substructuring .....	149
5.4.1	Deficiencies of the joint element as a substructure .....	152
5.4.2	Using the substructure in Abaqus .....	153
5.5	Frame analysis with the joint element.....	155
5.6	Summary .....	158
6.	Inelastic frame behaviour .....	177
6.1	Inelastic buckling considerations .....	177
6.2	Modelling .....	179
6.2.1	Analysis results .....	182
6.3	Summary .....	187
7.	Design Implications.....	209
7.1	Increase in Strength.....	209
7.2	Post Failure Considerations.....	210
7.3	Design Interaction Equations .....	211
7.4	Comparison With Standards.....	214
7.5	Costs.....	215
7.6	Summary .....	216
8	Summary and Conclusions.....	219
8.1	Conclusions .....	221
8.2	Further Work .....	222
	References .....	224
	Appendix A: Substructure generation .....	237

## List of Figures

Figure 2-1 Torsional warping displacement of section.....	27
Figure 2-2 Distortional buckling.....	28
Figure 2-3 Flexural and torsional buckling of column.....	29
Figure 2-4 Torsional buckling detail.....	30
Figure 2-5 Lateral-torsional buckling of beam – twist and weak axis moment.....	31
Figure 2-6 Lateral-torsional buckling of beam – torque produced by lateral flexure.....	32
Figure 2-7 Nomograph for effective length of columns in sway prevented frames .....	33
Figure 2-8 Mitre joint with diagonal stiffener.....	34
Figure 2-9 Decomposition of a bi-axially loaded beam-column into axial, flexural and torsional components.....	35
Figure 3-1 Analysis of buckling moment using various elements.....	59
Figure 3-2 Ratio of finite element analysis results to buckling equation prediction. Includes points of transition to inelastic behaviour for standard W-shapes.....	60
Figure 3-3 Difference between the Abaqus results and equation [3-3] for constant moment, beam ends are pinned-pinned with respect to flexure, and fixed-fixed with respect to warping. ....	61
Figure 3-4 ANSYS results for lateral torsional buckling analysis of simply supported beam, compared with the fitted surfaces for ANSYS and Abaqus.....	62
Figure 3-5 Ratio of FEA results to beam-column equation (Eq. [2-7]) prediction.....	63
Figure 3-6 Ratio of theoretical critical moment accounting for major axis curvature to simplified formulation versus the ratio of out-of-plane to in-plane moment of inertia. ...	64
Figure 3-7 Detail of stiffened box joint from finite element model.....	65
Figure 3-8 Joint Configurations .....	66
Figure 3-9 Finite element model of single storey building.....	67
Figure 3-10 Finite element model of a two storey frame.....	68
Figure 3-11 Load versus lateral displacement for the midpoint of beam in single storey frame, 8 m W200x27 beam with box joints, bottom flange restraint and elastic material. ....	69
Figure 4-1 Models for interactive lateral torsional buckling. (a) co-linear beams after Schmitke and Kennedy (1985) (b) braced frame formed with same beams .....	97
Figure 4-2 Portal Frame .....	98
Figure 4-3 Strength increase due to warping, 4 m columns, W200x27 beams and columns, fixed base.....	99
Figure 4-4 Alternate view of Figure 4-3, strength increase due to warping, fixed base ...	99
Figure 4-5 Strength increase due to considering warping, 4 m columns, W200x27 beams and columns, pinned column base (flexible base plate).....	100
Figure 4-6 Strength increase, 4 m columns, W200x27 beams and columns, rigid base plate (pinned end, warping rigid). ....	101
Figure 4-7 Transition length from torsional to flexural (weak axis) buckling for all standard rolled sections. ....	102
Figure 4-8 Torsional to flexural buckling transition and column slenderness reduction. ....	102

Figure 4-9 Strength increase due to considering warping, 4 m columns, W360x134 beams and columns, fixed column base. ....	103
Figure 4-10 Strength increase due to considering warping, 3 m columns, W360x134 beams and columns, fixed column base. ....	104
Figure 4-11 Strength increase due to considering reversed warping deformations, 3 m columns, W360x134 beams and columns, fixed column base.....	105
Figure 4-12 Strength increase due to considering reversed warping deformations, 4 m columns, W360x134 beams and columns, simply supported, flexible column base.....	106
Figure 4-13 Strength increase due to considering reversed warping deformations, 4m columns, W360x134 beams and columns, simply supported, rigid column base.....	107
Figure 4-14 Strength increase due to considering reversed warping deformations, 4 m columns, W690x125 beams and W200x27 columns, pinned, flexible column bases. ...	108
Figure 4-15 Strength increase due to considering reversed warping deformations, 4 m columns, W690x125 beams and W200x27 columns, pinned, warping fixed column bases. ....	109
Figure 4-16 Strength increase due to considering warping deformations, 3 m columns, W690x125 beams and W200x27 columns, fixed column bases.....	110
Figure 4-17 Braced frame, all members W200x27, 3 m columns, fixed column base. ...	111
Figure 4-18 Braced frame, all members W200x27, 4 m columns, fixed column base. ...	112
Figure 4-19 Braced frame, all members W200x27, 4 m columns, simply support column base.....	113
Figure 4-20 Braced frame, all members W360x134, 3 m columns, fixed column base. ....	114
Figure 4-21 Braced frame, all members W360x134, 4 m columns, fixed base, reversed warping.....	115
Figure 4-22 Braced frame, all members W360x134, 4 m columns, simply supported base. ....	116
Figure 4-23 Braced frame, all members W360x134, 4 m columns, warping rigid base. ....	117
Figure 4-24 Ratio of strengths for direct warping to reversed warping, a) 3 m and b) 4 m columns, W200x27 frame, fixed column bases, unbraced.....	118
Figure 4-25 Ratio of strengths for direct warping to reversed warping, a) 3 m and b) 4 m columns, W200x27 frame, simply supported column bases, unbraced. ....	119
Figure 4-26 Ratio of strengths for direct warping to reversed warping, a) 3 m and b) 4 m columns, W200x27 frame, fixed column bases, braced.....	120
Figure 4-27 Ratio of strengths for direct warping to reversed warping, a) 3 m and b) 4 m columns, W200x27 frame, simply supported column bases, braced. ....	121
Figure 4-28 Ratio of strengths for direct warping to reversed warping, a) 3 m and b) 4 m columns, W360x134 frame, fixed column bases, unbraced.....	122
Figure 4-29 Ratio of strengths for direct warping to reversed warping, a) 3 m and b) 4 m columns, W360x134 frame, simply supported column bases, unbraced. ....	123
Figure 4-30 Ratio of strengths for direct warping to reversed warping, a) 3 m and b) 4 m columns, W360x134 frame, fixed column bases, braced.....	124
Figure 4-31 Ratio of strengths for direct warping to reversed warping, a) 3 m and b) 4 m columns, W360x134 frame, pinned column bases, braced. ....	125
Figure 4-32 Length effects, W200x27 members, fixed base, unbraced frame. Column lengths are shown in the figure legends. ....	126



Figure 4-33 Length effects, W200x27 members, fixed base, unbraced frame, normalised .....	127
Figure 4-34 Length effects, W200x27 members, pinned base, unbraced frame.....	128
Figure 4-35 Length effects, W200x27 members, pinned base, unbraced frame, normalised .....	129
Figure 4-36 Length effects, W200x27+W690x125 members, fixed base, unbraced frame .....	130
Figure 4-37 Length effects, W200x27+W690x125 members, fixed base, unbraced frame, normalised .....	131
Figure 4-38 Length effects, W200x27+W690x125 members, pinned base, unbraced frame.....	132
Figure 4-39 Length effects, W200x27+W690x125 members, pinned base, unbraced frame, normalised.....	133
Figure 4-40 Length effects, W360x134 members, fixed base, unbraced frame .....	134
Figure 4-41 Length effects, W360x134 members, fixed base, unbraced frame, normalised .....	135
Figure 4-42 Length effects, W360x134 members, pinned base, unbraced frame.....	136
Figure 4-43 Length effects, W200x27 members, fixed base, braced frame .....	137
Figure 4-44 Length effects, W200x27 members, fixed base, braced frame, normalised	138
Figure 4-45 Length effects, W200x27 members, pinned base, braced frame.....	139
Figure 4-46 Length effects, W360x134 members, fixed base, braced frame .....	140
Figure 4-47 Length effects, W360x134 members, fixed base, braced frame, normalised .....	141
Figure 4-48 Length effects, W360x134 members, pinned base, braced frame.....	142
Figure 5-1 Shell element with degrees of freedom separated into a) flexural (out of plane) and b) membrane (in-plane) degrees of freedom .....	162
Figure 5-2 Joint element mesh, 4 elements across the face .....	163
Figure 5-3 Irregular mesh for cantilever (Jin, 1994).....	164
Figure 5-4 Displacement degrees of freedom in the joint element that form a single warping degree of freedom. ....	165
Figure 5-5 Joint element with warping displacement applied to one face, through the unified degree of freedom. ....	166
Figure 5-6 Side view of element with displacement on the warping degree of freedom. ....	167
Figure 5-7 Schematic of joint element showing the linear degrees of freedom expressed for the warping displacement. ....	168
Figure 5-8 Error in the S4R shell element model, relative to results from 32 element wide model.....	169
Figure 5-9 Relative error in the S4R shell element model, based on 32 divisions on the edge .....	169
Figure 5-10 Error in corner displacement relative to 64 elements across the face of the joint element.....	170
Figure 5-11 Schematic of spring model. ....	171
Figure 5-12 W200x27 frame – fixed base 2000 mm columns, joint element.....	172
Figure 5-13 W200x27 frame – fixed base 3000 mm columns, joint element.....	172
Figure 5-14 W200x27 frame – fixed base 4000 mm columns, joint element.....	173

Figure 5-15 W200x27 frame – fixed base 5000 mm columns, joint element.....	173
Figure 5-16 W200x27 frame – fixed base 6000 mm columns, joint element.....	174
Figure 5-17 W200x27 frame – fixed base 2000 mm columns, stiffer joint element. ....	174
Figure 5-18 W200x27 frame – fixed base 3000 mm columns, stiffer joint element. ....	175
Figure 5-19 W200x27 frame – fixed base 4000 mm columns, stiffer joint element. ....	175
Figure 5-20 W200x27 frame – fixed base 5000 mm columns, stiffer joint element. ....	176
Figure 5-21 W200x27 frame – fixed base 6000 mm columns, stiffer joint element. ....	176
Figure 6-1 Typical frame model, fully stiffened joints (box and diagonal stiffeners). ...	191
Figure 6-2 Results for 2000 mm beam second order analyses, full restraint. a) $F_y =$ 300 MPa, b) $F_y = 400$ MPa.....	192
Figure 6-3 Results for 4000 mm beam second order analyses, full restraint. a) $F_y =$ 300 MPa, b) $F_y = 400$ MPa.....	193
Figure 6-4 Results for 6000 mm beam second order analyses, full restraint. a) $F_y =$ 300 MPa, b) $F_y = 400$ MPa.....	194
Figure 6-5 Results for 8000 mm beam second order analyses, full restraint. a) $F_y =$ 300 MPa, b) $F_y = 400$ MPa.....	195
Figure 6-6 Results for 10000 mm beam second order analyses, full restraint. a) $F_y =$ 300 MPa, b) $F_y = 400$ MPa.....	196
Figure 6-7 Results for 2000 mm beam second order analyses, bottom flange restraint. a) $F_y = 300$ MPa, b) $F_y = 400$ MPa.....	197
Figure 6-8 Results for 4000 mm beam second order analyses, bottom flange restraint. a) $F_y = 300$ MPa, b) $F_y = 400$ MPa.....	198
Figure 6-9 Results for 6000 mm beam second order analyses, bottom flange restraint. a) $F_y = 300$ MPa, b) $F_y = 400$ MPa.....	199
Figure 6-10 Results for 8000 mm beam second order analyses, bottom flange restraint. a) $F_y = 300$ MPa, b) $F_y = 400$ MPa.....	200
Figure 6-11 Results for 10000 mm beam second order analyses, bottom flange restraint. a) $F_y = 300$ MPa, b) $F_y = 400$ MPa.....	201
Figure 6-12 Initial lateral displacement, in frame with 6 m beam and 2 m columns, out of plane restraint on all nodes at beam to column interface. All members W200x27, Grade 300W. ....	202
Figure 6-13 Further lateral displacement, same frame as in Figure 6-12. ....	202
Figure 6-14 Beam returning towards plane of frame, same frame as in Figure 6-12. ....	203
Figure 6-15 Beam acting as catenary / weak axis bending, same frame as in Figure 6-12. .....	203
Figure 6-16 Moment capacity based on $wl^2/12$ for a frame with full beam restraint, $F_y=300$ MPa. ( $l$ is the beam length, in mm).....	204
Figure 6-17 Moment capacity based on $wl^2/12$ for a frame with full beam restraint, $F_y=400$ MPa. ( $l$ is the beam length, in mm).....	204
Figure 6-18 Second order inelastic analysis compared to elastic buckling capacity for a frame with full beam restraint, $F_y=300$ MPa.....	205
Figure 6-19 Second order inelastic analysis compared to elastic buckling capacity for a frame with full beam restraint, $F_y=400$ MPa.....	205
Figure 6-20 Moment capacity based on $wl^2/12$ for a frame with bottom flange restraint, $F_y=300$ MPa. ( $l$ is the beam length, in mm).....	206

Figure 6-21 Moment capacity based on $wl^2/12$ for a frame with bottom flange restraint, $F_y=300$ MPa. ( $l$ is the beam length, in mm) .....	206
Figure 6-22 Second order inelastic analysis compared to elastic buckling capacity for a frame incorporating bottom flange restraint, $F_y=300$ MPa, .....	207
Figure 6-23 Second order inelastic analysis compared to elastic buckling capacity for a frame incorporating bottom flange restraint, $F_y=400$ MPa, .....	207
Figure 6-24 Equivalent moment coefficient from elastic analysis, full beam restraint. .	208
Figure 6-25 Equivalent moment coefficient from elastic analysis, compression flange restrained .....	208
Figure 7-1 Buckling load magnifier for 4 m W200x27 columns with W200x27 beam.	218

## List of Tables

Table 3-1 Summary of joint displacements for frame, all members W200x27, 3000 mm columns .....	57
Table 3-2 Strength ratios, based on portal frame .....	58
Table 4-1 Lateral buckling strength for various configurations of members.....	96
Table 4-2 Frames presented herein. ....	96
Table 5-1 Comparison between Aladdin and Abaqus elements, tip deflection of a fixed cantilever with rectangular cross section (inches).....	160
Table 5-2 Lateral displacement of flange tip for I-shaped cantilever experiencing torque, (inches).....	160
Table 5-3 Results from tests from Ojalvo and Chambers (1977) compared to theoretical warping fixed beam.....	161
Table 6-1 Frame joint configurations.....	189
Table 6-2 Summary of inelastic critical moments (kN m) and ratios for modelled yield strengths .....	190
Table 7-1 Analysis results for selected frame configurations for eigenvalue and second-order elastic-plastic analysis.....	217
Table 7-2 Design results from North American design guidelines .....	217

## Nomenclature

Symbol	Description
$a$	Torsional bending constant, mm
$A$	Area, mm <sup>2</sup>
$b$	Plate width (usually flange of I shaped section), mm
$C_b$	Equivalent moment factor (AISC) See also $\omega_2$ below.
$C_f$	Factored compressive load effect, N
$C_r$	Factored compressive resistance, N
$C_w$	Warping constant, mm <sup>6</sup>
$E$	Young's modulus, MPa (taken as 200 GPa for steel)
$F_y$	Yield strength, MPa
$\{F_i\}$	Vector of nodal forces, finite element analysis
$G$	Shear modulus, MPa
$h$	Distance between flange centroids, mm
$I_p$	Polar moment of inertia, mm <sup>4</sup>
$I_x$	Moment of inertia, major axis, mm <sup>4</sup>
$I_y$	Moment of inertia, minor axis, mm <sup>4</sup>
$J$	St Venant torsional constant, mm <sup>4</sup>
$k_x$	Effective length factor, strong axis
$k_y$	Effective length factor, weak axis
$k_w$	Effective length factor, warping
$K$	Effective length factor
$[k_e]$	Stiffness matrix, elastic
$[k_g]$	Stiffness matrix, geometric
$L$	Length, mm
$L_b$	Beam length, mm
$L_c$	Column length, mm
$M_{crw}$	Elastic buckling moment considering effective lengths, N mm
$M_u$	Elastic buckling moment, N mm
$M_{u+}$	Elastic buckling moment considering pre-buckling deflections, N mm
$M_{u0}$	Elastic buckling moment without modifications, N mm
$M_f$	Factored applied moment, N mm
$M_r$	Factored moment resistance, N mm
$M_\omega$	Bimoment in joint element development, N mm <sup>2</sup>
$N_x$	Number of elements across a joint element
$N_y$	Number of elements down a joint element
$N_z$	Number of elements between front and back faces of a joint element
$R_w$	Ratio of $M_u$ to the elastic buckling moment considering effective length factors or other slenderness effects.
$P$	Applied load, N
$P_t$	Load applied to flange tip for joint element, N
$P_x$	Buckling load, strong axis, N
$P_y$	Buckling load, weak axis, N

$P_z$	Buckling load, torsional, N
$r_p$	Polar radius of gyration, mm
$R_w$	Ratio of buckling strength of a restrained beam to that of a simply supported beam, considering the effective length factors of the beam.
$t$	Plate thickness, mm
$T_a$	Torque applied to member due to axial load, N mm.
$T_r$	Resisting torque in member, N mm.
$U_1$	Moment magnifier factor (P- $\delta$ effect and moment gradient)
$w$	Uniformly distributed load value, N/mm
$\alpha$	Multiplier for axial load, frame analysis.
$\beta$	Factor in S16 beam-column equation
$\Gamma$	Eigenvalues
$\delta$	Maximum displacement over length of member, measured from a line joining the member ends.
$\Delta$	Displacement of member ends relative to each other.
$\{\delta_i\}$	Vector of nodal displacements
$\theta$	Angle of twist at a location along a member, radians
$\theta'$	Rate of twist of a member along its length, radians / mm
$\lambda$	Column slenderness ratio
$\kappa$	Moment gradient, dimensionless.
$\nu$	Poisson's ratio. (Taken as 0.30 for steel)
$\omega$	Equivalent moment factor for beam-columns. (S16 previous to 1989.)
$\omega_2$	Equivalent moment factor for beam buckling. Also a general modifier for the elastic buckling moment.

# 1. Introduction

Many steel structures are based on the concept of a “moment frame”, a set of steel structural elements, known as beam-columns, that resist vertical (usually gravity based) loads and horizontal (usually wind or earthquake) loads. Within these frames, the interconnected members can act as a single structural element providing strength and rigidity to the structure. However, the members have long been considered to act as independent elements in design (Massonnet, 1976). From a design perspective, steel frames are designed to prevent the attainment of their maximum loads based on individual member stability or strength.

The Canadian design method for steel structures is based on the CSA standard CAN/CSA S16-01, “Limit States Design of Steel Structures” (CSA 2005). This will be used as the primary design document in this thesis, and will be referred to as “S16”. Design standards in general are based in the current building codes. The National Building Code of Canada (NRC 2005), referred to as “NBCC”, is the building code for most jurisdictions in Canada, although it may be amended for local conditions.

The design of beam-columns in S16 is based on satisfying four checks, based on various considerations and analysis procedures. In this work, only “Class 2” or better sections are considered. These are steel shapes that will not fail by local buckling of their elements (flanges or webs) before the attainment of a fully plastic section. Also, only doubly symmetric “I” shaped sections are considered. These are commonly used in steel frames and experience the warping deformations that are of interest. Hollow structural sections (HSS) are also commonly used in frames, but are selected due to their high torsional stiffness, of which the warping contribution is only a small part.

This work will present an evaluation of the torsional warping restraint provided by the connections of frame members on the stability of the frame. Interactive restraint between members requires that one member provides the extra restraint

when the other demands it. In other words, the stronger member is “supporting” the weaker one. It may be possible that, in the traditional design of beam-columns, the designer may be assigning a larger resistance to the member which is providing this “support” ignoring the extra demands on that member. This would lead to a potential for the member to fail before the frame’s ultimate design loads, potentially leading to collapse. The focus of this investigation is on how the deformations at member connections affect the behaviour of the frame and the members. The particular effect studied is the torsional warping displacements; how they are transmitted between members and what consequence the shared displacements have on the stability of the members and structure.

### **1.1. Specific aspects of this work**

This work is motivated by the desire to determine if the mutual warping interaction at frame connections provides a benefit or liability in the context of unbraced moment frames. Since the torsional restraint of beam-columns has received limited attention, there may be conditions where the demands of the torsion from the warping of one member may cause supporting members to fail before they might otherwise be expected to fail.

Full moment connections are required for this study. These connections permit the moments in one member to act on the connected members. As the warping displacements can be thought of as lateral bending actions, the moments and rotations for these degrees of freedom must be continuous. As described earlier, the warping behaviour can be thought of as the independent bending of each flange in opposite directions. This is similar to the out-of-plane bending of the member, save that the flanges would both move in the same direction. As a consequence of this similarity, it is difficult to separate the warping “effects” from the other moment and rotation effects on the connection and thus it is difficult to idealise this in a physical model. In an experimental program it would be difficult to isolate the lateral bending and the warping effects to see how these affect the buckling capacity.



While the limitation of consideration to class 1 or 2 “I” sections mirrors the special beam-column equations in S16, there are other reasons for this limitation. Closed sections, such as hollow structural sections (HSS), are very stiff torsionally, by the sole virtue that the St. Venant torsional constant is large, equal to the polar moment of inertia of the cross section. There is no warping for circular sections, and even for rectangular sections the St Venant torsion is large, so that the influence of warping is low. Other warping-sensitive sections with mono-symmetric sections (reduced flange “I” sections with unequal flange widths, or channel sections) or asymmetric sections (such as angles) are not commonly used in moment frames due in part to the complications arising from the eccentricity between the shear centre and centroid, and in part to difficulties in providing connections between members for full moment support.

The objective is to see whether the interaction of members, loads and deformations related to warping at steel frame joints will cause earlier instability or greater stability of the frame. It is hoped that this analysis will be of benefit to designers in determining the member sizes and connection detailing for such frames.

## **2. Literature Review and Background**

A principal concept of research is to build on the work of the past. This chapter will track some of the larger steps that have been made in the same direction as this work.

### **2.1 General structural mechanics**

A brief description of the major topics used in this work will be presented here.

#### **2.1.1 Bending and torsion**

The flexural considerations used in this thesis will be based on the Bernoulli-Euler beam theory, where the strain distribution is linear over the cross-section.

The applied torque is assumed to be resisted by two primary mechanisms, St. Venant torsion and warping torsion. Other mechanisms are not included in the analysis or other considerations. As torsional warping is of particular interest in this work, a short description is included herein. Where the term “warping” is used herein, it is meant to imply torsional warping.

St Venant torsion is the general response to torsion wherein the material experiences a shear stress relative to its distance from the rotational centre for closed sections that permit the stress to follow the closed path formed by the cross-section. For open sections, where the shear stress must travel both directions in each cross section element, the “skin” of each element carries the same shear flow in opposite directions, and this reduces linearly to zero at the centre of the element. The geometric property used for modelling this part of the torsion restraint is the St Venant torsional constant  $J$ , which for thin walled open sections can be approximated by one-third of the sum of the element length times the thickness cubed for all elements. Closed sections are very effective in resisting torsion, as the closed loop permits all material to participate to its full extent, and open sections are much less effective.

$$J = \frac{1}{3} \sum b t^3 \quad [2-1]$$

The doubly symmetric “I”-shaped cross section will be used throughout this work. This cross section shape experiences a relatively large amount of warping. As the “I”-shaped member’s ends rotate relative to each other, the member’s flanges will act as beams, bending in opposite directions (Figure 2-1). The moments in the two flanges will be equal, but acting in opposite directions. This two-moment combination is termed a bi-moment. The applied torque that twists the member is resisted by the flexural shear in the flange, multiplied by the distance between the flanges. As shear is the moment gradient along the beam length, the magnitude of the bi-moment must vary along the length of the member in order to restrain this torque. The effect of warping decreases with the length of the beam, whereas the effect of St Venant torsion remains relatively constant. Therefore, the importance of warping will be lessened for longer members.

The warping displacements may be fairly small, but their restraint can cause significant increases in the torsional stiffness of the member.

A study on combined torsion and flexure (Bremault *et al.* 2008) indicates that for many beams, flexural and torsional displacements cause serviceability problems before they exceed their strength. This is attributed to, in part, the softening effects of approaching lateral-torsional buckling capacities. However, for members stiff enough to provide sufficiently small deformations, the strength interaction can be delimited by a simple multi-linear curve. At its most severe, this is a straight line linking the point of maximum torsional strength and zero applied moment to the point of zero applied torque and maximum moment capacity.

### 2.1.2 Local buckling behaviour

While not the main topic of this investigation, there are cases where buckling phenomena affecting the cross section of the member play a role in the analysis and design of beam columns. There are two specific categories of importance. One is the buckling of the plates that form the cross sectional elements of the member in question. This is a buckling action of plates loaded in compression in the plane of the plate. The other is distortional buckling, where the web of the beam deflects out of plane. In both cases, the cross section of the member becomes deformed, and thus becomes unsymmetrical, leading to weakening of the member.

Local buckling is controlled in design through the use of limits on the plate slenderness, and the classification of the cross section based on those limits. The limits are based in part on classical plate buckling theory. The classification used by S16 is: if any part of the cross-section buckles before the material reaches its yield stress, the section is deemed Class 4; if no part will buckle before first yielding occurs, but will before full yielding of the section, the section is called Class 3; if all parts can sustain full plastification before buckling, it is Class 2; and if all parts can withstand full plastification of the section and develop sufficient additional rotation for “subsequent redistribution of the bending moment<sup>1</sup>”, it is Class 1. Dawe and Kulak (1986) provide an analysis of the local buckling requirements for beam-columns.

Distortional buckling is a more general buckling behaviour, but also one that affects the shape of the cross section. In this mode, the web bends out of the plane formed by its original position (Figure 2-2). This mode is not formally recognised in S16, but is in CSA S136<sup>2</sup> (CSA, 2007). While generally regarded as a mode that particularly affects members with very slender webs, there can be cases where distortional buckling is of interest in hot rolled members (Albert *et al.* 1992).

---

<sup>1</sup> § 11.1.1 (a), S16

<sup>2</sup> § C3.1.4 beams, § C4.2 columns, S136-07

### 2.1.3 Buckling and out-of-plane behaviour

Structural instability is caused by the combined effects of a load and the displacements caused by the load. As a load increases, the displacements caused by that load also increase. The destabilising effect increases as the combination of the load and its own displacement, and will increase in a non-linear manner. The displacement is resisted by the stiffness of the structure, up to the point where the displacements can grow without restraint.

This is called a “second order” effect. First-order effects are described as displacements and member forces that would result solely from the loads applied to the structure without other considerations. Second-order effects take into consideration the forces and moments resulting from the structural displacements and the applied forces acting on the deformed structure. In particular, the engineer is concerned about loads which cause displacements that continuously increase as these second order effects are calculated. This has been styled as “P- $\Delta$ ” (or “P- $\delta$ ”) analyses – “P” representing the load itself and “ $\Delta$ ” the displacement caused by the loading. The “ $\Delta$ ” effects are from relative displacements of member ends, whereas the “ $\delta$ ” effect results from deformation of the member between its ends.

While the term “buckling” is used often, the behaviour of real structures does not typically follow the “bifurcation” model of classical buckling described below. In general as the critical load is approached, there is a rapid loss of stiffness<sup>3</sup>, and potentially a loss of strength, that can precede a collapse. This complete “mechanism” is referred to as instability. The instability comes as the load’s effects increase more than linearly with the application of the load and there is a point where the effects overcome the structural resistance. In some cases, other structural mechanisms can start to pick up the load and its higher order effects to provide an increase in post-buckling strength.

---

<sup>3</sup> This was noted by Southwell (1932) and exploited as a plot of increasing flexibility versus lateral deflection to graphically determine the critical load.

The particular condition under consideration in this study is that of out-of-plane behaviour. In out-of-plane responses, the structure moves perpendicular to the plane in which the major moments and forces act. The mechanisms underlying the out-of-plane instability failure are lateral-torsional buckling, an instability due to applied moments about the major axis and the decrease in axial capacity due to the applied axial load and the buckling capacity, either lateral flexural or torsional. In the case of those sections where the centroid is not coincident with the shear centre, the axial load capacity may be governed by a combined flexural-torsional buckling failure mechanism. The governing equations for these mechanisms follow.

The most common buckling mode is flexural buckling, in which bending causes member instability. This bending is caused by the moment produced by the axial load and the member's deflection due to bending or initial imperfections (Figure 2-3). This moment is resisted by the flexural stiffness of the member. While this bending can occur about either principal axis, weak axis bending is of the greater importance to this work. This mode of buckling is represented by the following form:

$$P_y = \frac{\pi^2 E I_y}{(k_y L)^2} \quad [2-2]$$

Also caused by axial loading is a phenomenon known as torsional buckling. As the member twists, the elements of the cross-section become inclined to the axis of the member. The compressive axial force produces a lateral, or shearing, component that forces the member to twist further (Figure 2-4). The ratio of compressive load to torsional shear is equal to the product of the distance from the centre of rotation to the point under consideration, and the twist expressed in terms of the twist gradient ( $\theta'$ , radians per length). The centre of rotation is the shear centre. The twist gradient ( $\theta'$ ) is equal to the derivative of the twist angle ( $\theta$  radians) with respect to the distance along the length of the member. The moment arm for each particular shear component is also its distance from the shear centre.

Considering the compressive force to be uniformly distributed across the section, the forcing torque is:

$$T_a = \int r \sigma r \theta' dA = \frac{P \theta'}{A} \int r^2 dA = \frac{P I_p \theta'}{A} = P r_p^2 \theta' \quad [2-3]$$

The torque is resisted by the torsional stiffness of the member, which in turn has two components; a St. Venant torsional component and a warping component, as shown in Equation [2-4]. Equation [2-5] represents this failure mode for doubly symmetric cross-sections, where the shear centre and centroid are coincident. In those cases where the shear centre and centroid are not coincident, there is an interaction between the flexural and torsional buckling due to the displacement of the axial load as the centroid rotates about the shear centre.

$$T_r = GJ \theta' - E C_w \theta''' \quad [2-4]$$

$$P_z = \frac{A}{I_p} \left( \frac{\pi^2 E C_w}{(k_w L)^2} + GJ \right) \quad [2-5]$$

The warping portion of the torsional resistance becomes larger for shorter lengths. Many sources, for example Vacharajittiphan and Trahair (1974), use the formulation of another torsional constant,  $a = \sqrt{(E C_w)/(GJ)}$ , which has the dimensions of length, in describing the length of a member under torsion. A member that has a high  $L/a$  ratio is considered “long” and is governed by St Venant torsion. One with a low  $L/a$  ratio is governed by warping torsion.

For lateral-torsional buckling, the governing equation is presented as [2-6]. This phenomenon results from the assumed beam deflections resulting from a major axis bending moment causing twisting of the beam, producing a component of the applied moment that exerts bending about the weak axis (Figure 2-5); and an out-

of-plane bending that produces a component of the major axis moment that causes a torque about the beam axis (Figure 2-6). As these two components are linked (the torque is caused by displacements from the lateral bending and the lateral bending is caused by the rotation caused the torque), both the lateral bending stiffness and torsional stiffness must be considered. This is separated into three parts: a factor to account for the effects of the shape of the moment distribution along the member ( $\omega_2$ ), the weak axis flexural stiffness, and the torsional stiffness.

$$M_u = \omega_2 \sqrt{\frac{\pi^2 E I_y}{(k_y L)^2}} \sqrt{\frac{\pi^2 E C_w}{(k_w L)^2} + GJ} = \omega_2 \sqrt{(P_y) (r_p^2 P_z)} \quad [2-6]$$

The latter part of equation [2-6] shows the critical moment in terms of the axial buckling loads. The second component is the torsional buckling load multiplied by the polar radius of gyration about the shear centre,  $r_p$ . These expressions rely on the beam being restrained from twisting at its ends. Without rotational support, the member would “fall over” rather than buckle.

All of these modes will interact in reducing the member’s capacity from its ideal ultimate strength if the moment and axial compression act simultaneously. This inter-modal interaction is a fundamental concept underlying beam-column theory. Many approximate relationships are proposed to measure this reduction, such as equation [2-7], which provides a reduction in lateral-torsional buckling capacity due to the “softening” effect of an axial load applied to equation [2-6], along with the increased moment due to the moment magnifier factor  $(1 - P/P_x)$ . However, for design purposes, these are presented in the form of interaction inequalities. These interaction relationships will be discussed in more detail in a following section.

$$M_u = M_{u0} \sqrt{\left(1 - \frac{P}{P_y}\right) \left(1 - \frac{P}{P_z}\right)} \cdot \left(1 - \frac{P}{P_x}\right) \quad [2-7]$$



### 2.1.4 Plasticity and imperfections

The stability considerations above are based on members remaining elastic throughout their deformation. In actual steel structures, the initiation of inelastic behaviour often occurs at load levels lower than those required to produce elastic buckling. As the stiffness of the member is drastically lowered when yielding starts, and as stability is a function of stiffness, the instability effects increase as parts of the section begin to yield.

The manufacturing process for sections under consideration involves the deformation of hot steel bars through rollers, which shape the bar into the form of an “I”. The resulting shape cools unevenly. The parts that cool first (the flange tips, then the middle of the web) also gains stiffness and strength first and can sustain stresses while the rest of the cross-section still possesses a very low yield strength. As the bar continues to cool, the hotter steel continues to shrink, “pulling” on the cooler, more rigid steel. At the end of the cooling process, there is an internal set of stresses in the bar, ranging from compression at the points of first cooling (flange tips) to tension at the points that cooled last (the flange-web junctions). These are called residual stresses and can govern where the member will start to yield when external stresses are applied (Kulak and Grondin<sup>4</sup>, 2006). As the flange tips are furthest from the centroid, they have the greatest influence on the flexural stiffness of the member, and as they have residual compressive stresses, they will yield first in compressive loading. Thus, the typical residual stress pattern is disadvantageous for stability.

The geometric imperfection of the member influences the strength and stiffness as well. The nominal case considered by the theoretical stability equations is for a member that is perfectly straight; perfectly prismatic (every cross section along the length has the same measurements); and perfectly shaped (there is no deviation from the perfect “I” shape – the individual pieces of the cross section all

---

<sup>4</sup> Section 4.3 “Behaviour of Cross-Section”

meet at right angles and are piecewise straight). The major concern for all overall buckling modes is that the member is straight. If it is not straight, there are second order moments created in the member as soon as it is loaded, which softens the member. For torsional buckling, there is also a concern that the member has no initial twist, which would immediately impart a torque into the member when loaded.

In general these imperfections, both material and geometric, will reduce the strength of the member. This phenomenon has been known for some time. Ayrton and Perry (1886) developed their column strength equation to incorporate the effects of inelasticity and geometric imperfections in columns, and they reference earlier works by Tredgold and Gordon who also made similar approximations for columns.

### **2.1.5 Member interaction**

The influence of the interaction between members in frames is well known and has been studied in the context of flexural buckling for a long time. The basic equations produced graphical design aids as long ago as 1936 by N.J. Hoff (per CRC Guide (1960)<sup>5</sup>) and have continued to be used in the effective length nomographs. The latter are also known as the Jackson-Moreland alignment charts, from the firm that originally produced them in 1957. The aids are used to determine the effective length for flexural buckling of columns in sway and non-sway frames. These charts are integral parts of the design process of columns and beam-columns in many jurisdictions, including Canada. (Appendix G of CSA S16-01 provides an example of these.) These charts consider only the mutual flexural restraint offered by the flexural stiffnesses of connected members. An example of the side-sway prevented (braced frame) nomograph is reproduced in Figure 2-7.

Trahair (1968a) coined the phrase “interactive buckling” to describe the behaviour of interconnected beams when they experience joint lateral-torsional buckling.

---

<sup>5</sup> pp 26-27

The influence of end restraints has been considered to increase the lateral-torsional buckling behaviour of members, in general. Flint (1951) notes that if the ends are permitted to rotate, or in his words there is “elastic torsional movement of the end supports” then there is decreased capacity compared to equation [2-6] (with  $k_y = k_w = 1$ ). However, the general expression depends on total torsional fixity at the ends, so this is to be expected.

Schmitke and Kennedy (1984) provide an excellent summary<sup>6</sup> of the history of interactive buckling of continuous beams. The reader is directed there for a more thorough description of work until that time.

Trahair (1968b) presents a discussion of the extreme case of a beam completely fixed at one end and pinned at the other (a “propped cantilever”) and leads into a discussion of the interaction between multi-span continuous beams (Trahair, 1968c). While the first paper discusses I-sections briefly, both papers focus on narrow rectangular sections. Trahair (1968b) introduces an iterative method of finding the critical load for rectangular sections. This technique had some problems in reaching convergence for I-shaped sections if the St Venant and warping expressions  $(GJ\theta')$  and  $(EC_w\theta''''/L^2)$  are approximately equal. A numerical solution technique, specifically the finite difference method, was recommended. However, a first order finite difference method technique proved to be unsatisfactory and a finite integral method was used as the final solution. The second paper describes a linear interaction equation that illustrates the increase in the critical load when two or three adjacent, loaded spans of a continuous beam are considered. The loading described was for single point loads at midspan, and uniformly distributed loads.

The interaction between members and its influence on lateral torsional buckling has not been incorporated into the design process in Canada<sup>7</sup>.

---

<sup>6</sup> Chapter 5, “Continuous Beams”

<sup>7</sup> Masarira (2002) implies that DIN-18800 and DIN-4114 may incorporate some of this in their joint stiffness considerations.

Work by Nethercot and Trahair (1976a, 1976b) used the flexural buckling charts for mutual restraint considerations to determine the effective length of continuous beams. Continuing work, such as that of Schmitke and Kennedy (1985) did not directly consider the restraint based on the nomograph, but also concentrated only on the flexural resistances of the members and their mutual influence. The resistance from the torsional components, and especially that of the restraint of torsional warping deformations, is not included in the factors under consideration.

## **2.2 Frame analysis**

The particular condition under consideration in this study is that of out-of-plane behaviour. This is a situation where the displacement of the structure is out of the plane formed by its members. This plane is typically also the plane in which all loads are applied, if the frame is considered to be a planar structure. In real structures, the loads are not applied strictly within the plane of the frame. The out-of-plane failure mechanism is not critical in unbraced structures (Wongkaew 2000) unless the lateral (flexural) buckling stiffness is substantially less than the in-plane buckling stiffness.

A key part of frame analysis is to account for the  $P-\Delta$  effects in the analysis (Wood, *et al.* 1976a). Recommendations were given in appendices of previous editions of S16 (CSA, 1989) for including these effects in the analysis.

The concept of notional loads has been introduced in frame analysis to permit first order analyses to adequately model the second order effects of loads. In Canadian design, these were first introduced into S16 in 1989 (CSA 1989). “Notional” loads are so-named because they are not actual loads applied to the structure, but are rather a conceptual tool. They provide a simulation of the effects experienced by the frame from the second order effects. Usually, notional loads in a frame analysis are point loads introduced into the structure laterally (horizontally) at the floor level, and are some fraction of the gravity (vertical) loads added to the structure at that floor. However, in strictest practice, these are to be added to the

structure at the same point (or height) that the respective vertical load is introduced into the structure.

At a minimum, the notional load should represent the equivalent moment produced by a reasonable allowance for the initial vertical imperfections (out-of-plumb) in the columns of the frame. For example, if the code of practice for a given standard were to permit an out-of-plumb ratio of  $1/500$  times the length of member, the minimum notional load would be  $0.002$  times the gravity loads. This produces an overturning moment equal to the vertical load times the initial off-plumb value.

Other uses for notional loads and modifications from the base condition are explored in Clarke and Bridge (1995). Some design standards use modifications to account for the number of storeys, yielding of the members or their connections, or the slenderness of the columns. At least one standard, the AISC (2005) Specification, uses a reduced stiffness (reduced modulus) approach in conjunction with the notional load to determine the frame design requirements.

## **2.3 Current member design**

This work considers the provisions of the current Canadian steel building design standard (S16-01, CSA 2005) with respect to frame and beam-column design. These provisions and their development are detailed in Essa and Kennedy (2000). A summary of the historical development of Canadian steel beam-column design to this point is provided by MacPhedran and Grondin (2007b).

Beam-columns are analysed and designed individually, separated from their environment in the frame. The loads on the member are determined from a structural frame analysis, and considered, through an interaction inequality, with the individual member capacities for axial and flexural loads. While the mutual member restraint mentioned earlier can be used to account for restraint in braced frames, unbraced frames are analysed slightly differently and the restraint is incorporated into the loads applied to the member. This translates into the use of

effective length factors less than one for the columns in a braced frame, and the use of an effective length factor of one for columns in a sway-permitted frame.

The frame analysis specified by the design standard incorporates the inelastic behaviour of the structure and second order effects of loading. This is specified via notional loads in the current version of the standard. With the approach used in S16, the notional load is actually larger than the nominal value (1/500) required to match initial imperfections. A higher value of the notional load is used as that gives results consistent with more exact analyses that account for the effects of distributed plasticity (Kennedy *et al.* 1993). The notional load is applied at each storey and is 0.005 times the gravity loads applied at that storey. By representing the geometric imperfections and presumed deformation with a load, the notional load “*transforms a sway buckling problem into a bending strength problem*” (Essa and Kennedy, 2000) simplifying the analysis. In other words, the notional load replaces the initial imperfections and the sway effects are accounted for by the second order analysis. Thus, the entire P-Δ effect is compensated for, and the effective length factor of columns in sway frames analysed with notional loads can be set to 1, rather than the longer effective lengths previously used.

Trahair (1986) outlines the types of failure associated with beam-columns. These are: exceeding the cross sectional strength of the member; buckling of the member in the direction of applied moments, usually in the plane of the frame; buckling of the member perpendicular to the applied moment, usually out of the plane of the structure; and the potential that biaxial bending will exceed the member strength. Each of these points is addressed by S16 separately. For the members considered here, Class 1 and 2 I-shaped sections, the design objective is to provide members sized so that the inequality [2-8] is satisfied for these conditions.

$$\frac{C_f}{C_r} + \frac{0.85U_{1x}M_{fx}}{M_{rx}} + \frac{\beta U_{1y}M_{fy}}{M_{ry}} \leq 1.0 \quad [2-8]$$

The components on the left hand side of [2-8] are: the factored load effects,  $C_f$  and  $M_f$ , where the moment may be applied about either or both the strong ( $M_{fx}$ ) or weak ( $M_{fy}$ ) axes; the factored resistances,  $C_r$  and  $M_r$ ; and the factor,  $U_I$ , that accounts for the increased moment due to the axial load and the P- $\delta$  effect  $(1 - P/P_x)$  and the decrease in moment severity due to moment gradient,  $\kappa$ ; ( $\omega_1 = 0.6 - 0.4\kappa \geq 0.4$ ), as determined by Austin (1961). The value 0.85 is a shape parameter that is specific to I-shaped sections.

**Strength:** The conditions are based on using differing values for the factored resistances in the equation. The first condition is that the plastic strength of the section is not exceeded. Equation [2-9a] is invoked for this contingency. The maximum strength parameters are used for strong-axis bending and compressive resistance – the lengths for beams and columns are taken to be zero. This check need only be done for braced frames, as stability concerns will govern in sway permitted frames.

$$\frac{C_f}{C_r(\lambda = 0)} + \frac{0.85U_{1x}M_{fx}}{M_{rx}(L = 0)} + \frac{0.6U_{1y}M_{fy}}{M_{ry}} \leq 1.0 \quad [2-9a]$$

**Overall buckling:** The second condition is a stability criterion (Equation [2-9b]) considering the effects of column buckling. Here, the column resistance is calculated for the weaker plane that has an applied moment, usually the major or “strong” axis. This value is calculated with an effective length factor of 1. Lateral-torsional buckling of the section in bending is not considered in this check. The effects of bending about the weak axis are increased as the member’s compressive slenderness ratio about the weak axis increases, to account for plastic softening of the cross section (Essa and Kennedy, 2000).

$$\frac{C_f}{C_r(K = 1)} + \frac{0.85U_{1x}M_{fx}}{M_{rx}(L = 0)} + \frac{(0.6 + 0.4\lambda_y)U_{1y}M_{fy}}{M_{ry}} \leq 1.0 \quad [2-9b]$$

**Lateral torsional buckling:** The third criterion is the one of most interest in this work, where lateral torsional buckling is considered in determining the strong axis factored moment resistance, and the column factored axial resistance is based on the weakest buckling mode, usually this is the flexural weak axis buckling mode.

$$\frac{C_f}{C_r(\min)} + \frac{0.85U_{1x}M_{fx}}{M_{rx}} + \frac{(0.6 + 0.4\lambda_y)U_{1y}M_{fy}}{M_{ry}} \leq 1.0 \quad [2-9c]$$

**Biaxial bending:** As the moment contributions are reduced in the interaction equations above, it may be that a member controlled by bending may “pass” the other interaction equations, but still not have the capacity to support the bending moments. To prevent these situations, equation [2-9d] is included to check if the moment capacity is exceeded.

$$\frac{M_{fx}}{M_{rx}} + \frac{M_{fy}}{M_{ry}} \leq 1.0 \quad [2-9d]$$

As an example of the theoretical basis for these equations, the following is a modification of Trahair’s (1993) derivation<sup>8</sup> of a simple interaction relationship based on equation [2-7]. If the reduced moment capacity,  $M_u$ , was considered as the applied moment,  $M$ , at the same time as the axial load,  $P$ , equation [2-7] could be expressed as:

$$\frac{M}{\left(1 - \frac{P}{P_x}\right)M_{u0}} \leq \sqrt{\left(1 - \frac{P}{P_y}\right)\left(1 - \frac{P}{P_z}\right)} \quad [2-10]$$

The inequality is introduced to demonstrate that smaller values of  $M$  are “safe”. It is conservative to replace both terms  $P_y$  and  $P_z$  on the right hand side with the lesser of the two, simplifying the expression under the radical. Assuming the lesser to be  $P_y$ , this rearranges to:

---

<sup>8</sup> pages 207-208



$$\frac{P}{P_y} + \frac{M}{\left(1 - \frac{P}{P_x}\right) M_{u0}} \leq 1 \quad [2-11]$$

That is the same as equation [2-9c], considering elastic behaviour, strong axis bending, uniform moments and general cross sections. If the torsional buckling load,  $P_z$ , governs, this case would also be treated by equation [2-9c], as the designer must check the lowest axial capacity.

Typically, design aids are available to the designer from the steel industry associations. The Canadian association provides a general handbook (CISC, 2006) as well as publications specific to torsional design (CISC 2002). The American institute also provides a handbook, as well as design guides for torsional behaviour (Seaburg and Carter, 1996).

## 2.4 Literature review

This section presents a discussion of two main topics: the first is the development of the theory of torsion and beam-column action; and the other is the development of frame analysis and how it affects the design of beam columns.

### 2.4.1 Torsion and beam columns

Torsion represents an important component of the out-of-plane strength of members. With wide flange sections, the warping portion of the torsional stiffness can be a significant contribution, especially for shorter beam lengths.

The consideration of buckling of beams has been investigated for over a century. Trahair (1993) indicates<sup>9</sup> that A.G.M. Michell (1899) and L. Prandtl independently published on lateral torsional buckling in 1899, for narrow rectangular sections; and S.P. Timoshenko introduced warping torsion into the equation in 1905. The work by Wagner (1936) presented the general torsional analysis for open shapes, including warping.

---

<sup>9</sup> pages 3-4

Vlasov (1961) is also a significant contributor to the work on torsional behaviour. The details of Vlasov's work include the concept of effective length factors for the warping and flexural components of the lateral torsional buckling phenomenon. This concept, if not the exact values calculated by Vlasov, will be used later in the analysis of the finite element results found in this work.

There are two works of note with respect to practically restraining warping in experimental tests. Each of these shows the difficulties in trying to restrain the warping displacements.

Dinno and Gill (1964) tested small specimens machined from 5/8 inch square steel rods into I shapes with solid ends to determine the effects of plasticity on the torsional behaviour. In order to restrain warping, the solid ends were 2 inches long – over 3 times the dimension of the cross section – a very stiff member when warping is considered.

Ojalvo and Chambers (1977) tested specially stiffened I-shaped beams. The stiffeners were composed of two channel sections welded to both flanges and the web of the beam at both ends. These provided “warpingly stiff” beams, as the ends were almost encased in a tube section. These tests showed that even very stiff warping restraints do not provide full torsional warping rigidity and can only provide a certain amount of extra rigidity.

Vacharajittiphan and Trahair (1974) presented a set of finite element analyses of joints between equal sized steel I-sections considering the warping restraint at the joints. They came to the conclusion that ignoring the restraint is conservative, but produced equations similar to those for the flexural restraint nomographs. One comment was that for three pairs of stiffeners, the joint could be considered rigid with respect to warping. Ojalvo (1975) responded to some of the points raised, indicating that some of the end restraints were not sufficiently rigid, leading to the paper described previously.

While an important work that should be mentioned in this context, Ettouney and Kirby's (1981) work focuses on the influence of warping restraint on beam strength only, but provides a finite element beam element which considers warping. An application to short members in three dimensional frames is presented.

Yang and McGuire (1984) present a description of a finite element that models variable restraints of the warping of members. This restraint was provided by warping "springs" that provide a flexibility of 0 (warping fully restrained) to 1 (fully free to warp). Further development of this work led to a development of an element that would model non-linear geometric behaviour (Yang and McGuire, 1986), including the presentation of a geometric stiffness matrix to permit eigenvalue solution of the buckling problem.

Krenk and Damkilde (1991) consider stiffened connections for equal sized I-sections. Finite element models were constructed of two members whose webs are coplanar and that meet at an angle. They mention the importance of cross-section distortion of the members at the joint as being part of the member interaction, and propose a small "spring-like" stiffness matrix to account for this interaction.

Morrell *et al.* (1996) investigated similar two-member "frames" made of steel channel sections. These again had equal sized sections joined, only at right angles, with various stiffener configurations. One member was loaded in torsion and the other acted only to restrain that load. Distortion of the joint was also noted as being important. The warping of the loaded member determined to amount and direction of twisting of the frame.

There are two recent studies into the behaviour of frames considering the warping restraints at shared joints.

Masarira (2002) presented a study that looked at the interaction of members and joints considering warping. This considered finite element models of several joint types with an applied bi-moment to determine the warping stiffness. A set of

equations are presented to determine the joint stiffness and an approach is proposed using a coefficient for the stiffness of the joint when analysing the strength and stiffness of the frame. These coefficients are used in the German design standards DIN/18800 and DIN/4114 for consideration when determining the lateral torsional buckling capacity of members.

Zinoviev and Mohareb (2004) also investigated portal frames, in the form of pipe racks, in terms of out-of-plane behaviour. The frames investigated are laterally unsupported, with fixed column bases, and thus likely to fail in out-of-plane behaviour. Two joint configurations were investigated as to their warping stiffness through finite element analysis using shell elements. The design procedure proposed uses geometric stiffness matrices and determines the eigenvalue thereof to find the critical loadings.

Tong *et al.* (2005) also present transmission of warping through joints in two member frames. In this case, only one type of joint is presented, a mitre joint with a diagonal stiffener. This joint configuration, illustrated in figure 2-8, is one where the connecting members' flanges and webs are joined, and the flanges that would otherwise cross the web are removed. A diagonal stiffener joins the flange intersections. A stiffness modification is introduced into the analysis to account for the warping restraint of the diagonal stiffener. When compared to direct transmission of warping, this advanced treatment shows a small reduction in the rotation of the members, and little to no difference for the lateral displacements of the column or beam.

Masarira (2002), Zinoviev and Mohareb (2004), and Tong (2005) used numerical simulation exclusively. There have been limited experimental data available. While not directly related to stability and frames, two reports involving reduced beam section tests in seismic frames, Chi and Uang (2002) and Zhang and Ricles (2006), do mention certain aspects of warping at connections in steel moment frames. Chi and Uang mention that early lateral-torsional buckling in beams with a reduced cross section (a configuration used in seismic frame design to force

plastic hinges to form outside the connections) cause the beam's axial force to produce an eccentric thrust against the columns, producing a torque in the column. They also mention that deep beams will produce a high warping stress in columns. Zhang and Ricles determined that Chi and Uang may have overestimated the warping contribution but also indicate that the columns did undergo significant torsional rotation post failure.

Both of these experimental studies involve significant plastic deformation of the columns and beams after cyclic loading, involve post buckling behaviour, and are beyond the scope of this research. However, they do indicate possible future directions.

## **2.4.2 Frame analysis**

The history of the development of steel frame analysis and design is lengthy. Baker (1936) presents an interesting account of the progress at that time in Britain. Baker's presentation was to introduce a new British national code of practice formulated by the Steel Structures Research Committee. This included extensive recommendations including such topics as wind load variance with height, and live load reduction factors, but more relevantly, effective lengths for columns ( $K = 1$ , except for continuous columns,  $K = 0.7$  and intermediate values between), analysis methods and assumptions (such as simply supported beams on continuous columns), and design equations (the Perry-Robertson formula). This was also the point in time at which Massonnet (1976) begins his review of the history of beam-column design.

The evolution of the Canadian design process, outlined in MacPhedran and Grondin (2007b), started from more humble beginnings, as fairly simple stress addition formulae originally without consideration of slenderness for beam-columns, but changed rapidly during the periods of intensive research into beam-columns. Shortly after the British changes listed above, the Canadian standard S16-1940 moved to include slenderness effects as well. The "new" Canadian standard adopted the Perry-Robertson column strength formulation. Since that

time there has been continuous refinement in the methods used in frame analysis and beam-column design. A comparison between the current methods summarised previously and these earlier standards shows that the designer today has (or should have) a greater comprehension of frame behaviour and design methodology for steel beam-columns.

The corollary of this is that the methods of design for frames, or rather the process of sizing beam-columns has become complex, and intensive for the engineer. While some standards have tried to maintain simplicity, for example the AISC Specification (AISC 2005), which uses a two part two equation to cover all modes of failure, others (such as S16) have tried to match the growing complexity with more equations to handle the various modes, and still others, like EuroCode 3 (CEN 2005) use more exact coefficients to properly account for the  $P-\Delta$  and  $P-\delta$  second order effects in the beam column equations.

Currently, there is much discussion on the alliterative techniques of “Advanced Analysis” and “Direct Design”. A brief description of this can be found in Surovek *et al.* (2006), but the idea behind “advanced analysis” is that it is an analysis that considers all the relevant structural “limit states,” given sufficient information on the structure – the material, including inelastic properties, residual stresses; and the geometry, including initial geometric imperfections. The Europeans have coined the mnemonics “GMNIA” for Geometric and Material Nonlinearities and Imperfections Analysis and “SOPHIA” for **S**econd **O**rders **P**lastic **H**inge **A**nalysis of imperfect members (Ofner, 1997) for these analysis procedures. These analyses present member behaviour including the effects of “stability” – or second order effects of loadings and the resulting deformations – and plasticity to directly establish if the members have the strength to support the given loads. Thus all beam-columns could be reduced to only a “strength” check – a more direct design method, and a continuation of the notional load concept to all frame failure conditions.

One of the early researchers of beam-column analysis and design, Charles Massonnet, provided the summary below as to why current beam-column design practice does not present the full picture of frame design.

“However, the story is not ended, because the concept of the classical isolated beam-column is an oversimplification for two reasons:

first, an actual beam-column is an object behaving in a three-dimensional space, and ought to be studied as such. This justifies the growing trend towards research and experiments on columns subjected to buckling with bi-axial bending, of which we have still much to learn. Such research is also justified by the fact that there is a trend toward designing and analyzing structures as space frames, in which it becomes necessary to introduce the biaxial bending of columns.

second, and perhaps more important, is the fact that the isolated beam-column is an object that only exists in theoretical models and testing machines. All actual columns are linked, in one way or other, to the remainder of the structure, and the behavior of each column is influenced by the overall behavior of the structure.”

Massonnet, (1976)

While many advances have been made in the intervening time, much of what the above quote says is still true. One point that Massonnet did not explicitly mention is that in the analysis of beam-columns with bi-axial bending the torsional behaviour must also be considered. A contemporary work by Chen and Atsuta (1977) demonstrates this requirement, and their illustrative diagram has been reproduced in Figure 2-9. The combination of axial load and biaxial bending moments (Figure 2-9a) can be converted to a single eccentric point load (Figure 2-9b) that should express the sum of all the external loads. However, if the three components were expressed separately as point loads (Figure 2-9c, 2-9d, and 2-9e) there is an imbalance in the sum of these point loads that can be only resolved by the addition of a bimoment (Figure 2-9f).

To date, those studies of member interaction and compatibility of warping deformations do not test the assumptions made in the analyses for current design practice that these effects can be neglected in design. There has been no

examination to see if there is a harmful consequence of this practice. This study is being conducted to determine if there is an inherent problem or if there is an unexploited benefit that can be made from including these factors in our design process.



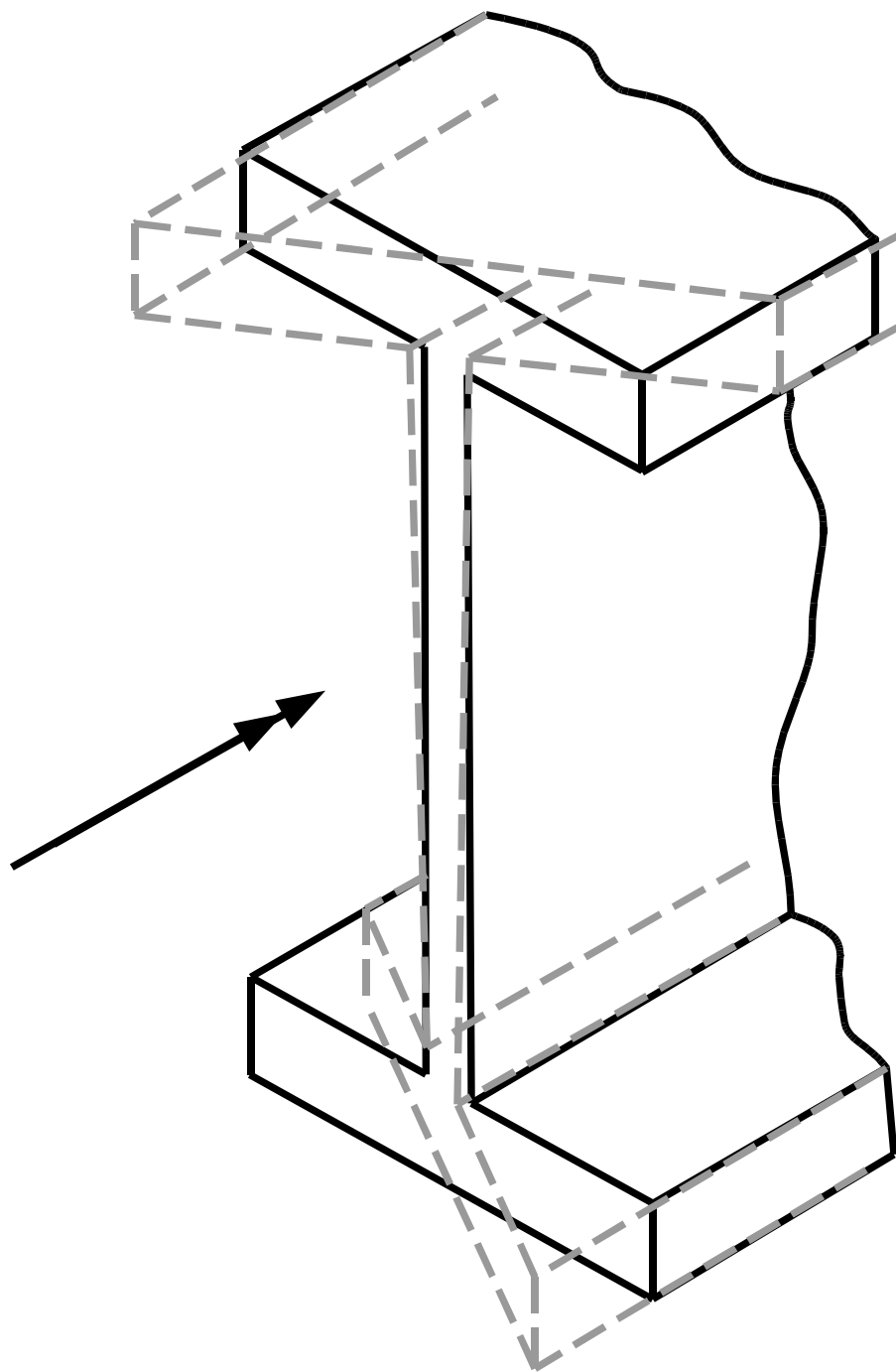


**Figure 2-1 Torsional warping displacement of section. (After Attard & Lawther, 1989)**

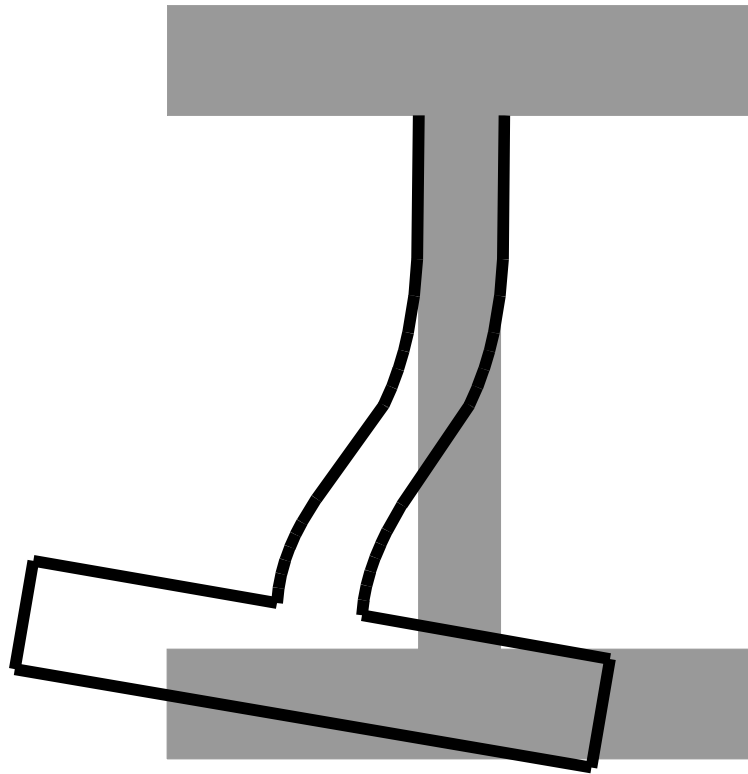


**Figure 2-2 Distortional buckling**

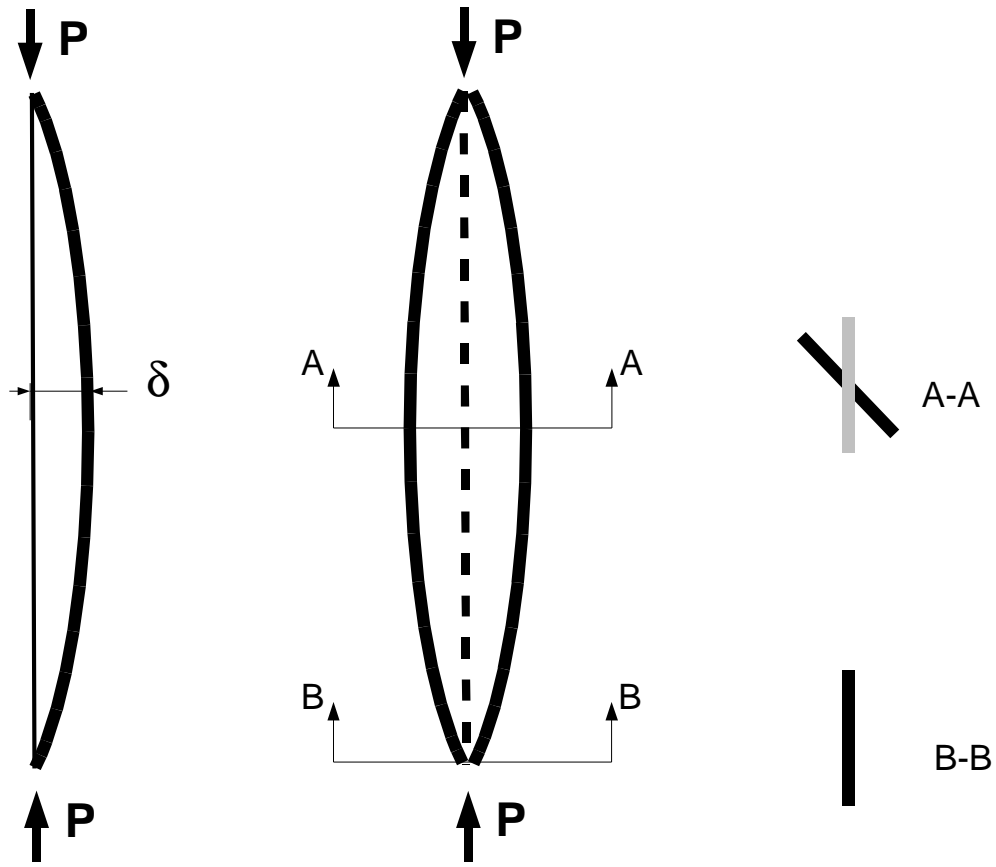


Figure 2-3 Flexural and torsional buckling of column

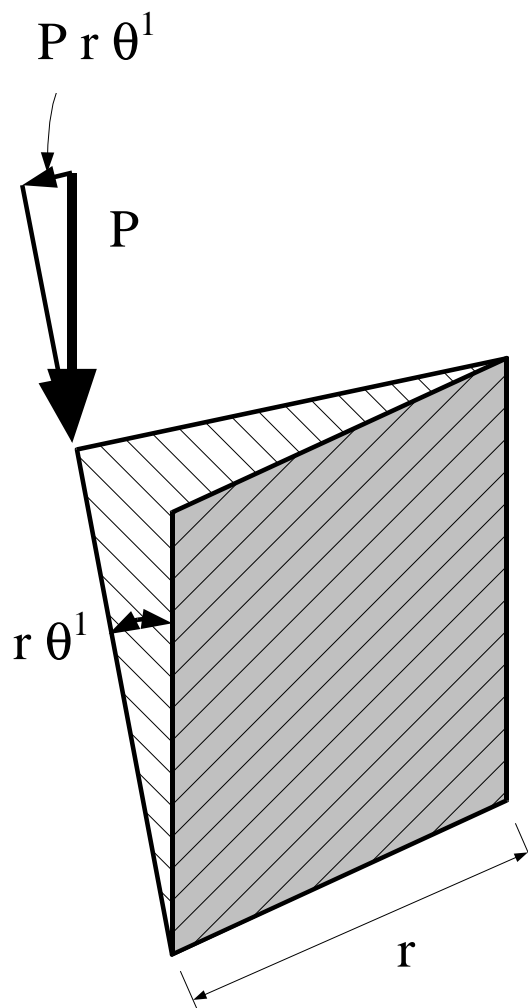
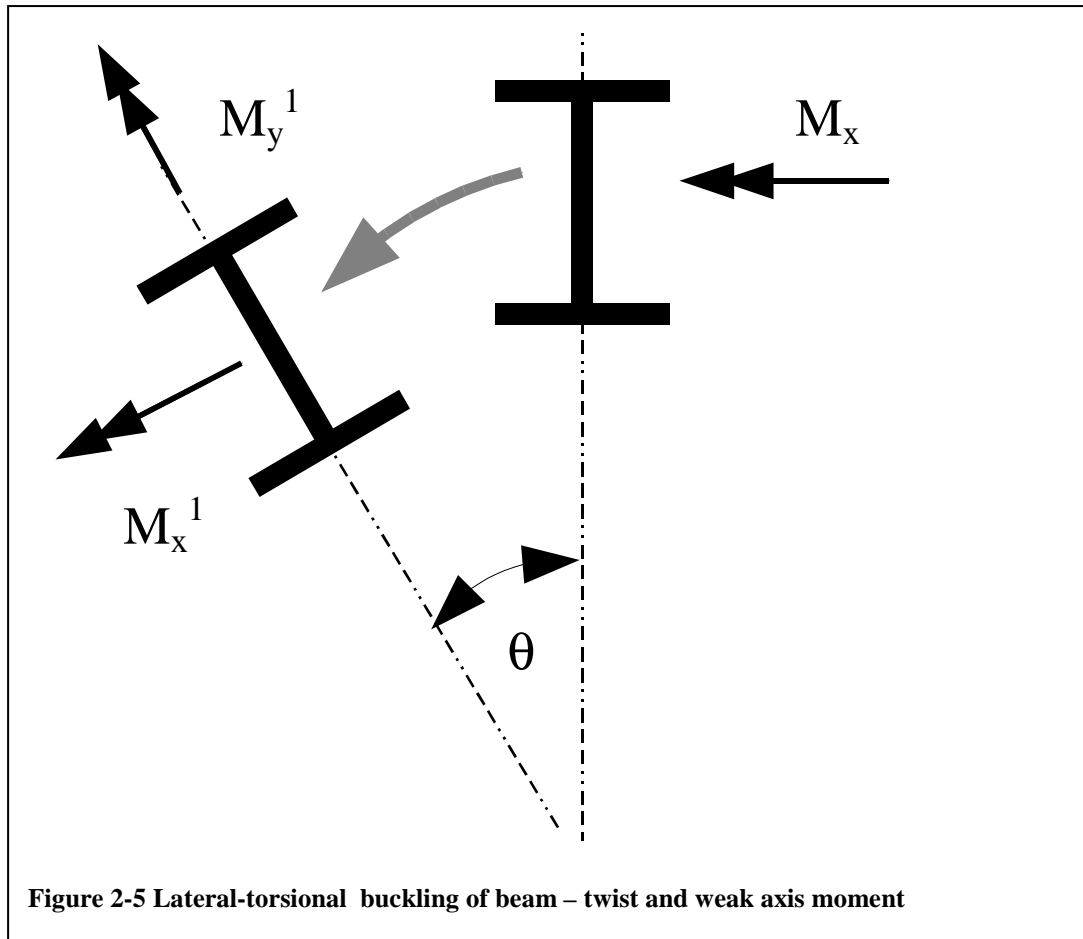
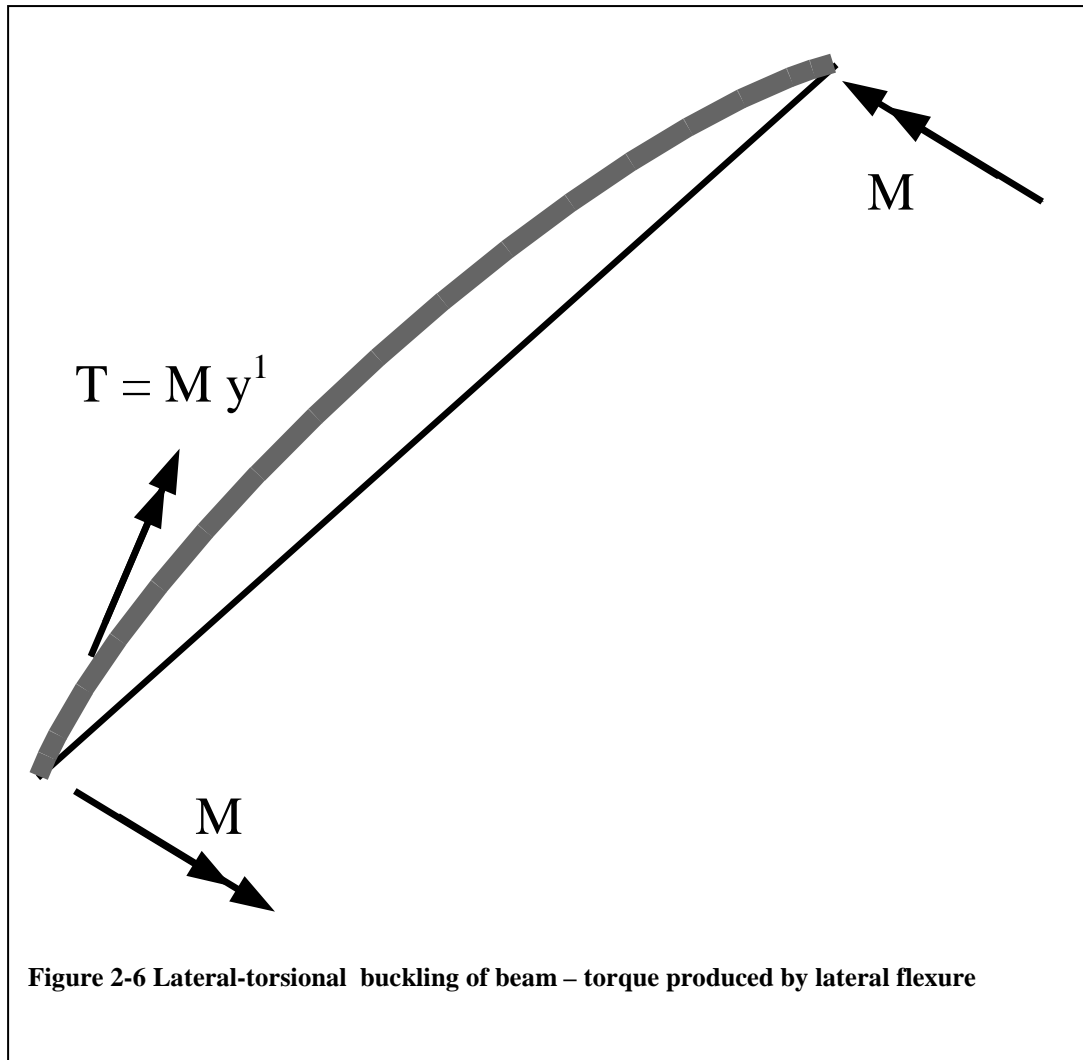
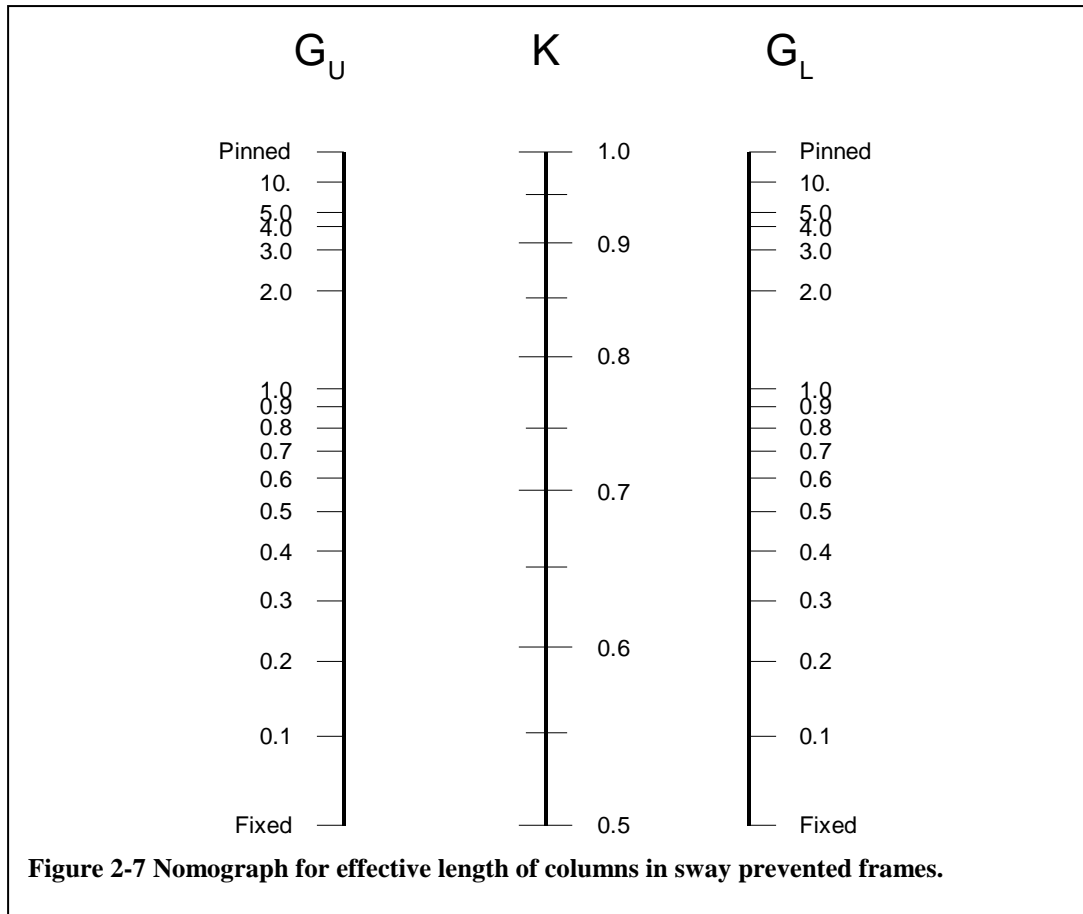


Figure 2-4 Torsional buckling detail







**Figure 2-7 Nomograph for effective length of columns in sway prevented frames.**

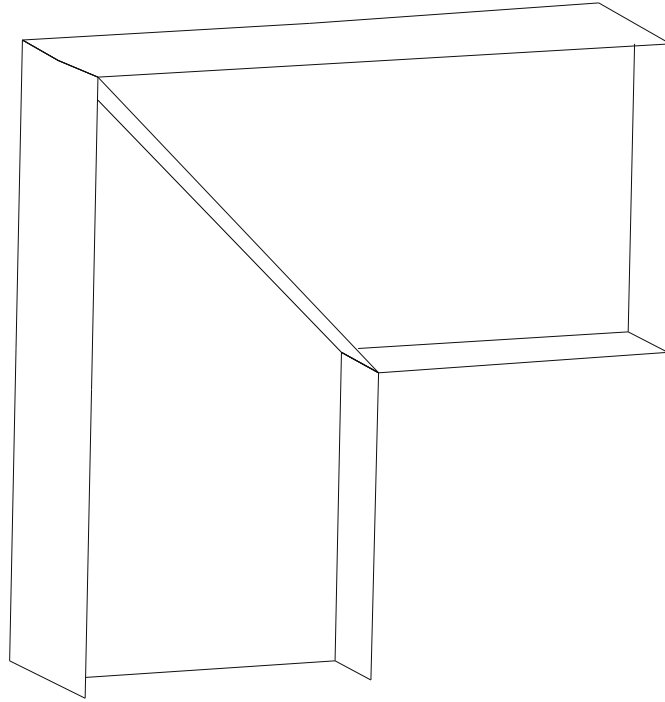
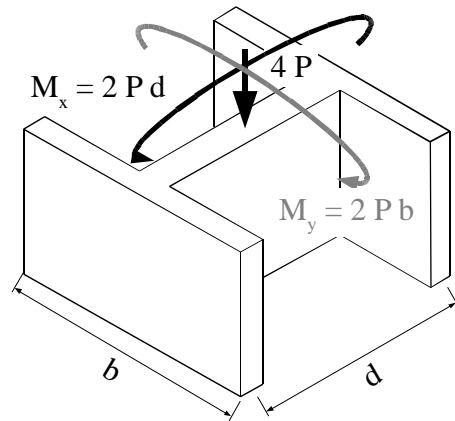
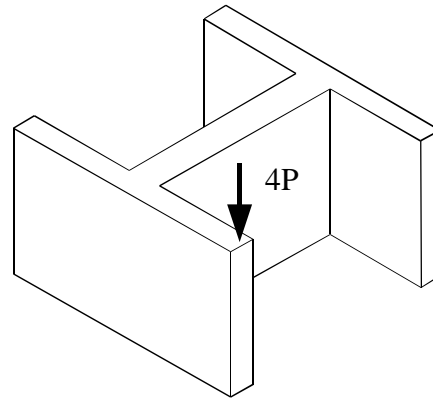


Figure 2-8 Mitre joint with diagonal stiffener

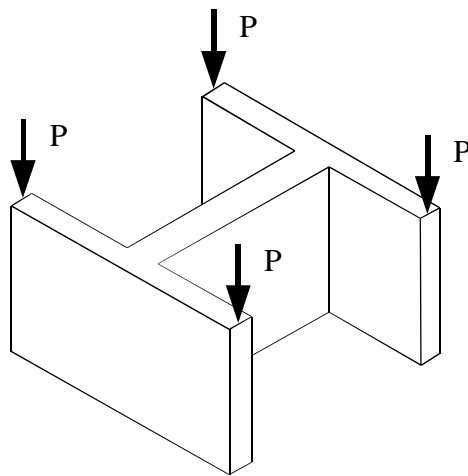




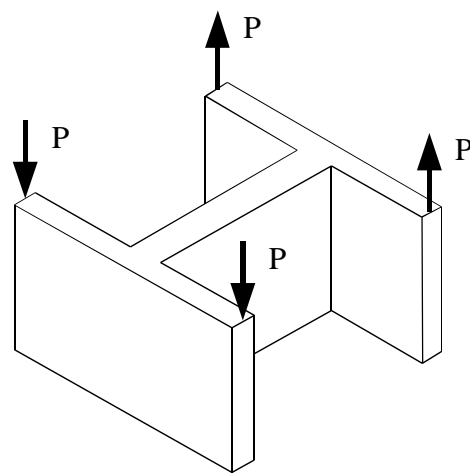
(a) Beam-column with axial load and bi-axial bending



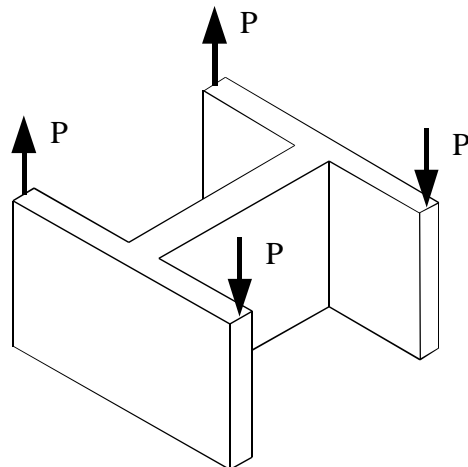
(b) Equivalent eccentric point load



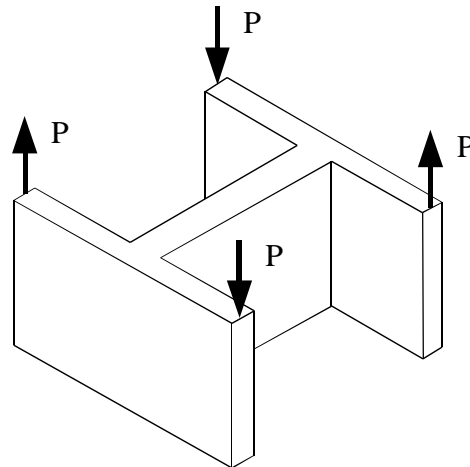
(c) Distributed axial force ( $F = 4 P$ )



(d) Strong axis bending, ( $M_x = 2 P d$ )



(e) Weak axis bending, ( $M_y = 2 P b$ )



(f) Warping bi-moment

**Figure 2-9 Decomposition of a bi-axially loaded beam-column into axial, flexural and torsional components. (After Chen and Atsuta (1977), Figure 1.6.).**

## **3. Finite Element Analysis of Torsional Warping**

### **Effects on Frame Buckling**

#### **3.1 Introduction**

The finite element method is a numerical analysis technique that uses approximate solutions over small subsets, or elements, of a partial differential equation problem to gain an approximate solution to the whole problem. The collection of elements and the boundary conditions for the problem are called a model. While approximate, the solutions for the model can approach the exact solution very closely.

There are several conditions that must be satisfied to obtain good results from finite element analyses. The foremost is that the model must match the physical problem. That is, the loading and restraints on the model must closely represent those in the physical problem. The geometry of the physical specimen must be accurately brought into the numerical model. The material properties assumed in the finite element analysis also need to be similar to those used in the physical test. Such properties as the stress versus strain relationship – for steel, this would include the modulus of elasticity, and yield strength at a minimum – should be taken from the actual materials being used. The analyses presented in this chapter are elastic only – the effects of yielding are not incorporated into the analyses presented here.

The modelling technique must also be appropriate to the type of analysis performed and the required results. The element types need to be able to model the effects of interest. In the particular case under consideration, the elements must be able to provide support for inclusion of torsional warping effects in its formulation. Solid and shell elements would support this effect as a consequence of their modeling of the full behaviour of the shape. However, beam elements

must support an extra degree of freedom to model the warping. For specialised analyses, it is also required that the analysis procedure can provide the desired results. For those models that require non-linear material or geometric analyses, the analysis procedure must support an iterative analysis process. The model and boundary conditions must also be amenable to convergence, as this also has a great influence on successful non-linear analysis, even with programs capable of non-linear analyses.

The model may also be sensitive to the geometry of the elements. The elements might work best when they have particular dimensions – as an example, the element may have been developed for a case where all of the element edges are approximately the same length and the effectiveness of the element decreases as its aspect ratio deviates from the ideal. In the case of equal length sides, the ideal is an aspect ratio of 1.0. The element may also work better when oriented in a particular direction with respect to the principal stresses or strains.

The mesh, or general arrangement of the elements, can also influence the accuracy of the model and how well the solution conforms to the real response of the physical problem. In general, the more elements that are used in the model, the better the solution is. However, the analyst can use different meshing techniques to use the elements in appropriate locations. Parts of the model that have higher strain gradients would require elements placed more closely together than would other parts with lower strain gradients. Elements that have a more complex approximation (higher order elements) can also be used to increase the accuracy in some of these regions of interest.

For structural and solid mechanics problems, the analysis uses a particular type of element based on generalised displacements (these include translations and rotations), or degrees of freedom, and forces (including moments) to model portions of the whole structure. The structure is discretised into elements and nodes supporting degrees of freedom. In general, the more degrees of freedom that are provided in a model, the more accurate the model is. (This is a highly

simplified statement as there are many factors to consider, such as the relative size of the elements, and where they are located in the model.)

The following is an assessment of how well finite element analysis performs in the study of the stability of frames, incorporating the effects of torsional warping. This includes a discussion of problems or shortcomings with available elements and analysis procedures, as well as their adequacies. A summary of the results of basic beam and column buckling analyses considering warping effects are also presented.

## **3.2 Brick and Shell Elements**

“Brick” elements are solid elements that only permit translational displacement degrees of freedom at their nodes. In the three dimensional models, they can appear as “wedge” (5 faces) or hexahedral (6 faces) bricks, and, in the most simple configuration, tetrahedral (4 faces) elements. The lack of rotational, and thus flexural, degrees of freedom is usually compensated for by using more elements. The larger number of degrees of freedom increases the accuracy of the solution, more closely approximating true flexural behaviour.

Shell elements are structural finite elements that support both translational and rotational degrees of freedom at each node. This permits both “in-plane” and “out-of-plane” forces to be studied. In-plane, these are the membrane forces and the “drilling” moment. The drilling degree of freedom accommodates the twist of the material within the plane of the element. This is expressed as a rotation about the plane perpendicular to the surface of the element. Out-of-plane degrees of freedom are shear, perpendicular to the plane of the element, and two orthogonal moments. While similar behaviour can be captured by the solid elements, the shell elements directly support moment and rotational degrees of freedom, which is more convenient for the analyst. Using shell elements reduces the total number of degrees of freedom in the model, and the detail required for the mesh.

The shell elements used in this study are the Abaqus elements called “S4” and “S4R”. Both are general purpose quadrilateral elements. The “S4R” element type has been used quite successfully in previous numerical stability studies (Grondin, *et al.*, 1998). It uses a reduced integration method, where the number of Gaussian integration points for an element is reduced. This technique is used to reduce the stiffness of the element, which is often overestimated by the formulation method (Bathe<sup>1</sup>, 1996). In the case of the quadrilateral element, this reduces to one Gauss point and this can cause other numerical problems. As there is only one reference point, there are displacement modes that can be mistakenly identified by the finite element analysis solver. These are referred to as “zero energy” or “hourglass” modes (Abaqus 2002)<sup>2</sup>. There are corrections that can be applied to the element stiffness matrix to compensate for this, but the earliest analyses in this program used the “S4” element to avoid the hour-glassing problem.

### 3.3 Beam-Columns

Beam-columns, as has been noted previously, are a general member in the construction of steel structures. They can be modeled by a one-dimensional element in structural finite element analysis. General beam-column elements provide displacement degrees of freedom in all three translational Cartesian directions, as well as rotations about all three axes. Using local coordinate systems, this translates into the requirement for the element to support an axial load, bending about two perpendicular (i.e. principal) flexural axes, and torsion about the element’s axis. These elements are typically considered as a straight-line segment, but those developed with higher order shape functions may be curved.

Barsoum and Gallagher (1970) introduced the first elements to include support for warping degrees of freedom. This work permitted analysis of both the warping and St Venant torsional behaviour for open cross-sections like wide-flange

---

<sup>1</sup> § 5.5.6 “Reduced and Selective Integration” p. 476

<sup>2</sup> § 3.6.5 “Finite-strain shell element formulation”

sections. By extension, torsional, torsional-flexural and lateral-torsional instabilities could be modelled. The element thus created has an extra degree of freedom at each node to support the warping behaviour.

While elements with warping capabilities continue to be developed, for example as recently as Alemdar and White (2008), where a version of this element was developed for the commercial finite element program RAM Advanse, the technology is currently mature enough to use existing elements in the analysis of steel frames and their stability. However, many of the common programs used in analysis of frames do not yet include this ability and thus the design procedure commonly used must evaluate the torsional aspects separately (Galambos, 1998).

There is also work ongoing to develop elements with enhanced capabilities. Extended capabilities include the nonlinear, non-uniform warping stiffness<sup>3</sup> (Trahair, 2003), exact formulations (Mohareb and Nowzartash, 2003), and plastic hinge for simple analyses (Ziemian *et al.*, 2008). While these have much promise for analysis in the future, the elements used in this work were the ones available in commercial packages.

### **3.3.1 Use of beam elements in current programs.**

Current programs that use beam-column elements with warping degrees of freedom include Abaqus (2002) and ANSYS (2002), among others. The Abaqus element is called B32OS, and the ANSYS element is named BEAM189. These are three dimensional beam elements that assume an open section, i.e. one with potentially significant torsional warping. Both elements are quadratic, having three nodes along their length. There are some differences between the implementations, but in general the force degree of freedom for warping is a bi-moment, produced when the flanges develop opposing shears and thus opposing moments, separated by the distance between the flanges. The displacement degree

---

<sup>3</sup> Also referred to as the Wagner, corkscrew, or helix effect. Extreme fibres travel further laterally than interior fibres under torsion, forming a helix. Compatibility of displacements across the section forces the exterior fibres to lengthen and interior fibres to shorten, producing a resisting torque, which acts to stiffen the member.

of freedom is the in-plane rotation angle of the flange in ANSYS and the flange tip displacement out of the plane of the cross section in Abaqus. The choice of this implementation in Abaqus means that joining beam members of differing cross section collinearly requires a constraint equation to be used in all cases to ensure compatibility of warping deformations. In ANSYS, the constraint equations are required for sections with differing heights. While unused in this work, the elements in both programs also support Timoshenko beam theory, allowing the provision of including shear deflections as well as flexural deflections.

For non-linear analysis involving displacements, the element formulation involves the concept of “co-rotational” elements, which are formulated expressly separating the rigid-body and “flexible” body displacements (Felippa and Haugen, 2005). This mirrors the separation of  $P-\Delta$  and  $P-\delta$  effects considered in frame and beam-column analysis. However, the underlying assumptions require that the “local” member deformations are much smaller than the rigid body displacements. This is usually the case for sway-permitted frames, though braced frames may experience the opposite effects (Essa and Kennedy, 2000). Accuracy can be increased by using smaller elements. In this case, the element deformations are reduced, and the member deformations are captured as rigid body displacements of the smaller elements.

Higher order beam elements, as mentioned above, may also be used to increase accuracy, in place of, or along with, smaller elements. These elements have nodes between their “ends” that will capture internal deflections, and thus can include  $P-\delta$  effects directly in the element moments.

### **3.4 Buckling analyses**

While the finite element analysis technique has historically been used for analysis of stresses and strains in structures, it can be, and has been, used for buckling analyses as well. The techniques for elastic buckling and inelastic behaviour are

slightly different, but both can be handled by advanced finite element analysis programs.

### 3.4.1 Elastic buckling behaviour

A strictly elastic buckling analysis can be done using a “geometric stiffness” matrix and an eigenvalue solver. The geometric stiffness matrix is a matrix that includes the second order effects of loads and the subsequent softening (compressive loads) or stiffening (tensile loads) of the structure.

The complete solution to the finite element problem is presented in Equation [3-1], with the elastic stiffness of the system  $[k_e]$  and geometric stiffness  $[k_g]$  simultaneously acting on the global displacements to produce the global load vector.

$$\left( [k_e] + [k_g] \right) \{ \delta_i \} = \{ F_i \} \quad [3-1]$$

There are many references through which one can find geometric stiffness derivations. Rajasekaran (1977) presents the geometric stiffness matrix for a beam-column element including warping effects. Chang (2004) provides the derivation of a beam-column element’s geometric stiffness matrix for a higher order element formulation, although the warping degree of freedom is not incorporated.

The general solution is to take the general stiffness matrix and combine it with the geometric stiffness matrix with a multiplier, usually scalar. When the sum is zero, the physical implication is that the overall stiffness of the structure has vanished. The general form of this is shown in Equation [3-2], with the scalar multiplier being the vector,  $\Gamma$ , known as the eigenvector. As this problem deals with matrix manipulation, the result of zero is the same as the determinant of the resulting reduced stiffness matrix being zero. This reflects the classical bifurcation concept



of buckling and gives a good approximation of the elastic buckling load for the structure. The method by which the critical load is determined is by eigenvalue extraction (Bathe<sup>4</sup>, 1996, Bathe and Wilson, 1976).

$$\left[ \left[ k_e \right] - \{ \Gamma \} \left[ k_g \right] \right] = 0 \quad [3-2]$$

This is an elastic solution. It is impractical to use the eigenvalue procedure for inelastic behaviour, as the geometric matrix must be updated to account for the softening due to yielding. If the matrix must be updated, the analysis can more easily incorporate the effects of displacement in the updated matrix and use a non-linear analysis considering the updating of geometry and material properties, than use multiple eigenvalue solutions.

The eigenvalue extraction procedure is used by many finite element programs, and specifically by Abaqus and ANSYS. The first analyses done by this method for several cross sections examining the lateral-torsional buckling mode showed remarkable differences from the capacities predicted by elastic theory. An example of the results of this form of analysis is presented in Figure 3-1. Here, a W200x27 beam is analysed for various lengths and two different end conditions, using both shell and beam elements. The two end conditions are included to illustrate different extremes of behaviour. Simply supported conditions, where the effective length factors with respect to warping and lateral flexure are equal to 1, give the simplest results. The second case, where the beams ends are still simply supported considering flexure, but fixed so that the flanges do not warp, represent a much more complex situation. In this case there is interaction between the warping and lateral flexure modes, and the effective length factors are related. In this case  $k_y$  is 0.940 and  $k_w$  is 0.492 (Galambos, 1968). For longer members, both types of elements give the same results, in very good agreement with the elastic buckling theory. For shorter members, however, there is a decrease in strength.

---

<sup>4</sup> Chapter 11, Solution Methods for Eigenproblems

This decrease is relative to a theoretical, increasing buckling moment. The shell elements are capturing the effects of local buckling, and can be readily explained using elastic buckling theory.

### **3.4.2 Discrepancies in beam element elastic buckling**

The beam elements used in Abaqus show a decrease in buckling capacity relative to theory. This is shown in Figure 3-2 as a contour plot of the ratio of the results of the eigenvalue buckling solution to the theoretical buckling moment. This is for simply supported beams, with a uniform moment applied. The diamond markers in the upper portion of the figure (well within the 99% boundary) represent the length for which the elastic buckling moment is equal to the full plastic capacity for all of the wide flange rolled shapes available in North America. This length is a reasonable measure of the limits on the effect of elastic behaviour in the members. It is shorter than the limit at which the design standard S16 acknowledges full elastic behaviour, i.e. the length at which the buckling moment is two-thirds of the plastic moment. The length used is also longer than the limit used by S16 to indicate that the behaviour is fully plastic, where the buckling moment is approximately 2.15 times the plastic moment.

Beams elements are not capable of modelling local buckling of the beam web or flanges. Therefore, the decrease in buckling capacity below the theoretical value requires additional explanation. Other potential explanations for the difference between the beam analysis results and the theoretical predictions also fail. If this were a reduction due to shear flexibility that is being captured by the Timoshenko beam theory, changing the cross sectional area or shear stiffness factor should change the buckling load. It does not. If this were a higher order torsional effect, such as the Wagner effect mentioned earlier, the buckling load should increase. (This element should not capture that effect in any case.) As the detailed analyses showed that the capacity did not vary with the cross sectional area, the torsional

axial buckling capacity is not a direct influence. It may be, given that the effect is most pronounced at higher torsional stiffness, that there may be a numerical truncation or underflow error occurring when flexibilities are being used. The latter possibility is impossible to check without access to the inner workings of the solver. So, while the differences between beam theory and element behaviour are as of yet unexplained, they can at least be measured, and a subsequent parametric analyses (MacPhedran and Grondin, 2007a) provided the relationships presented below.

Figure 3-3 presents the results of an Abaqus eigenvalue analysis for a beam simply supported with respect to flexure, but fixed with respect to warping at the ends. As was done in Figure 3-2, the eigenvalue results were divided by the theoretical buckling moment to illustrate the discrepancy. The discrete results from the Abaqus analysis are joined by a grid, to enhance the continuity of the results and plotted as the lighter solid line, and the prediction Equation [3-3] is plotted as the darker dashed line.

$$\omega_2 = \frac{R_w}{\sqrt{1 - \frac{1.3J}{I_P} \left( 1 - \frac{\pi^2 a^2}{(k_w L)^2} \right)}} \quad [3-3]$$

The value  $R_w$  in the above equation is the ratio of the lateral-torsional buckling moment for restrained beams,  $M_{crw}$ , to that for a simply supported beam,  $M_{cr}$ . For this particular case, a simply supported beam, the theoretical solution should be a flat plane at a value of 1.0.

$$R_w = \frac{M_{crw}}{M_{cr}} = \frac{\frac{1}{k_y} \cdot \sqrt{1 + \frac{\pi^2 a^2}{k_w^2 L^2}}}{\sqrt{1 + \frac{\pi^2 a^2}{L^2}}} = \frac{\sqrt{(k_w L)^2 + \pi^2 a^2}}{k_y k_w \sqrt{L^2 + \pi^2 a^2}} \quad [3-4]$$

Equation [3-4] illustrates that warping restraint affects longer members less than shorter members. Theoretically, the value  $R_w$  for a very long beam would be  $1/k_y$ , and that for a very short beam would be  $1/(k_y k_w)$ , though this would not be achievable in real structures, as other failure modes governed by material properties or local buckling would be more critical. This also implies that any negative effects of warping would also affect shorter beams and beam-columns more than shorter members.

Analysis results from ANSYS are plotted on Figure 3-4. The surface of the analysis results presented in Figure 3-4 are the equations: [3-3] for Abaqus, and [3-5] for ANSYS. These equations were developed by visually fitting a surface to the finite element analysis results. A numerical procedure, such as least squares, was not used as the equations contain a singularity at the point where the denominator is zero that causes numerical problems. The match between the equation's predictions and the finite element solution are very close at locations far from the points  $\left(\frac{\pi a}{k_w L}\right)^2 = 1 - \left(\frac{I_p}{n J}\right)$ , where  $n = 1.33$  for Abaqus and  $n = 1.0$  for ANSYS.

$$\omega_2 = \frac{0.99 R_w}{\sqrt{1 - \frac{J}{I_p} \left(1 - \frac{\pi^2 a^2}{(k_w L)^2}\right)}} \quad [3-5]$$

The beam-column elements perform satisfactorily when compared with a simple lateral-torsional buckling beam-column model (Equation [2-7]). Figure 3-5 shows the results of the finite element analysis compared to the predictions of the equation. The contours in this figure show the ratio of the results from Abaqus buckling analysis to the results predicted by elastic theory for lateral torsional buckling in the presence of an axial load. The extremes of equal moments of inertia about both axes and axial load equal to the buckling load were not included. In the case of the axial load being equal to the buckling load, the applied

moment that would cause lateral-torsional buckling would be negligible, and this would reduce to a pure flexural Euler buckling analysis. In the case of equal moments of inertia about the orthogonal axes, lateral torsional buckling should not happen. The effects of major axis curvature are neglected in the predictive formula used in the comparison made in Figure 3-5, as this exercise was intended to illustrate how the finite element program handles this phenomenon.

While the capacity predicted by finite element analysis did vary with the moments of inertia about the major and minor axes, there was no measurable influence from the ratio of these two values. This indicates that the effect of curvature is not being considered during the analysis. The effect of curvature about the axis of flexure, which is related to the ratio of the moments of inertia about the plane of bending and the orthogonal plane, has been long known to influence the buckling moment (Michell 1899, Flint 1951). This is due to a coupling of the curvature of the member about the strong axis to the curvature about the weak axis and to the twist about the long axis, as shown by Trahair and Woolcock (1973). This is neglected in the usual derivation of the lateral-torsional buckling expression, Equation 2-6. Equation 3-6 from Trahair and Woolcock (1973) illustrates the full effect, including torsion and flexure. In this equation,  $M_{u0}$  is the lateral torsional buckling moment ignoring the effect of major axis curvature,  $M_u^*$  is the lateral-torsional buckling moment corrected for the effect of bending curvature; and  $I_x$  and  $I_y$  are the moments of inertia about the axis of bending and the out of plane axis, respectively. These two axes are also the principal axes of the beam. If  $I_x$  is less than  $I_y$ , then the solution requires imaginary numbers. This is consistent with the observation that beams bent about their weak axis typically do not experience lateral torsional buckling (Yura and Widiyanto, 2005).

$$\frac{M_{u0}}{M_u^*} = \sqrt{\left(1 - \frac{EI_y}{EI_x}\right)} \sqrt{\left(1 - \frac{GJ}{EI_x}\right) \left(1 - \frac{\pi^2 E C_w}{(EI_x - GJ)(L)^2}\right)} \quad [3-6]$$

Considering only the effects of the first term, which relates the lateral bending stiffness to major axis bending stiffness, the increase in capacity for current rolled “W” sections from North American rolling mills can be up to 25% (MacPhedran and Grondin, 2008). This increase is presented for all ratios of  $I_y/I_x$  in Figure 3-6. This benefit is only apparent for elastic analyses, as inelastic effects will provide an upper limit for beam capacity.

While it may appear that the torsional component is as important as the flexural one in determining the increase in strength,  $EI_x$  will always be larger than  $GJ$ . The maximum  $J$  occurs in closed sections where it is the same as the polar moment of inertia,  $I_p$ . The ratio of  $I_p$  to  $I_x$  is at its maximum value of 2 when  $I_x = I_y$ . As equation 3-7 shows, this expression reduces to a function of Poisson’s ratio. As Poisson’s ratio is positive for normal materials<sup>5</sup>, this will ensure that the increase in strength due to the torsional component will always be finite. For steel with a nominal Poisson’s ratio of 0.3, the maximum increase in the buckling moment due to the St. Venant torsional component is a factor of 2.08.

$$\left(1 - \frac{GJ}{EI_x}\right) = \left(1 - \frac{GI_p}{EI_x}\right) = \left(1 - \frac{2G}{E}\right) = \left(1 - \frac{2E}{2(1+\nu)E}\right) = \left(1 - \frac{1}{(1+\nu)}\right) = \frac{\nu}{1+\nu} \quad [3-7]$$

The stiffening effect of major axis curvature is likely excluded from the analysis due to the effect being considered a pre-buckling phenomenon. That is to say, it is a higher order effect than simple buckling. However, this can be seen as advantageous as most design standards ignore the effect, so that the analysis results may be misinterpreted. Fortuitously, this exclusion avoids some numerical problems, as including the effect could give rise to division by zero or the determination of the square root of a negative number. The buckling analysis may be inaccurate for real-world conditions, where it is unlikely for beams to experience lateral-torsional buckling when bent about their minor axis.

---

<sup>5</sup> Materials that have a negative value for Poisson’s ratio are called “auxetic.” Auxetic materials are very rare and are not used in structural engineering.

Exceptions to this exist if the beam loads are applied above the shear centre (Kennedy *et al.*, 1993) or if there is a significant pre-existing curvature, i.e. camber, that must be countered by the applied moment (Yura and Widiyanto, 2005). However, since this effect always increases the capacity of the member, the results of analyses neglecting it are conservative when used for structural design.

### **3.4.3 Inelastic buckling behaviour**

The ultimate load states of many steel frames go well past the point of first yield (ASCE 1971). The high ductility of steel that permits this behaviour is exploited in the design of frames that must carry lateral seismic loadings to dissipate the energy put into the structure.

The steel that has yielded is not considered to provide any stiffness (Yura, 2006) in stability analysis and thus the buckling capacity is lowered once yielding occurs. In design this is often accounted for by using a tangent (reduced) modulus of elasticity to represent the weakening of the member (Galambos, 1998). In finite element analysis, this can be taken into account when updating the system stiffness matrix for the structure, as the analysis progresses. If the displacements of the structure are also reflected in the updated matrix, both the second order effects and the effects of plasticity are incorporated into the solution.

As there are possibilities for the analysis to stop prematurely when instabilities are reached in the numerical model, special techniques may need to be employed to generate a solution in the analysis of inelastic instability. Such a technique used by Abaqus is the Riks method (Riks 1979, 1984). This is a method for following the equilibrium path of an analysis, where that path may include unloading of the structure, such as for a “snap-through” buckling problem, where a structure will suddenly lose stiffness, then regain it at a larger displacement, thus permitting the analyst to progress past the point of instability and providing post buckling

behaviour. This requires that the stiffness matrix be updated to reflect the new position of the structure.

The Riks method approaches the solutions of instability problems as being an equilibrium “path” of the load vector (scaled by a varying scalar value) versus a generalised displacement vector. Starting at a known point on the equilibrium path, a solution is sought further down the path, at a distance called an “arc length.” The initial arc length is specified by the user of Abaqus (2002). The direction from the known solution point to the next trial solution is determined by the tangent to the equilibrium path at the known point. This produces an assumed applied force and a displacement vector. The trial solution is tested for convergence, or equilibrium between applied load and the restoring force from the displaced structure. If there is an imbalance in the two forces, the assumed applied force and displacements are adjusted. However, the new trial solution is restricted to load and displacement vectors in a set that is orthogonal to the initial tangent. If this problem were reduced to a 3 dimensional one, the solution set would be a plane, perpendicular to the initial tangent to the equilibrium path.

If convergence cannot be reached within a previously specified number of iterations, the procedure goes back to the last known equilibrium point and uses a shorter arc length to provide a trial solution.

### **3.4.4 Buckling analyses used within this work**

Both elastic and inelastic buckling analyses are used in this work. The elastic buckling analysis provides a tool to see how a frame will behave when loaded, while considering differing warping interactions between the frame members. The elastic buckling analyses give a good picture of the maximum benefits or penalties that are possible when the effects of warping interaction are included in analyses.

Members analysed in this study were not significantly susceptible to the deviation of the FEA lateral torsional buckling behaviour from the theoretical behaviour



noted above, in section 3.4.2. No corrections were made for the effect of major axis curvature. This was ignored as those effects are neglected in design of these members, and were also not provided in the generally available analysis.

The inelastic buckling analyses used in this work included non linear geometric analysis, wherein the stiffness matrix is updated to include the displacement of the structure at each load step. The solution technique also includes the Riks analysis technique

### 3.5 Deformation of joint configurations

The effect of joint configuration on frame behaviour was investigated (MacPhedran and Grondin, 2005). For this portion of the work, several joint configurations, summarised in Figure 3-8, were modelled using S4 shell elements. These joint configurations were selected as they have been modelled by other researchers (Vacharajittiphan and Trahair (1974), Ojalvo and Chambers (1977), Krenk and Damkilde (1991), Wongkaew and Chen (2002)) and include the common joint details, as well as some that are less common. Common joint details that do not transfer significant moment, for example shear tabs or web clips that only connect one member by its web, are not included as they do not impart significant moment or torsion, and thus no warping is transferred between the joined members.

Modelling was done with the W200x27 rolled wide flange section. This section was chosen due in large part to its relatively high torsional bending constant,  $\sqrt{EC_w/GJ}$ , of 1088 mm. This implies that the effects of warping are applicable for a relatively long beam length, and would illustrate better the effects of warping interaction between the members. The section is also a class 2 section in flexure for yield strengths below 460 MPa, so that a plastic hinge could be formed before local buckling of the section. The beam also has a short minimum bracing requirement. The characteristic length,  $L_u$ , value (i.e. the maximum unbraced length for which the fully braced capacity can still be developed) is 2.04 m for

300 MPa steel to 1.63 m for 450 MPa. These values are based on CAN/CSA-S16-01 (CSA, 2005).

There can be significant imbalances in the warping deformation of the flanges when the flanges are not equally restrained. This is exemplified in the case of one story versus two story frames modelled in the first phase of this project (MacPhedran and Grondin, 2005). Here, elastic buckling analyses were conducted for two types of frames modelled using shell elements. Nodal displacements, a measure of the warping stiffness of the joint, were measured for a unit torque of 1 kN·m. This warping stiffness relates fairly closely to the complexity of the connection and to the elastic buckling strength of the frame.

One frame type was a simple portal frame (Figure 3-9), the other a two storey frame (Figure 3-10). In the two storey frame, the joints under consideration were those at the structure's mid-height. All joint types were included for the single storey frame. However, for the two storey frame, the impractical joint types were not included. (These are those joint configurations where the column flanges are not continuous through the joint.) In these analyses, the single storey frames were loaded with a uniformly distributed load on the beam. The two storey frames were loaded only on the lower beam, again as a uniformly distributed load. The buckling load is calculated as a multiplier of the applied load. Thus, the total buckling load is the product of the original load and the buckling multiplier.

The results for the analyses of these frames are presented in Table 3-1. The single storey frame is listed on the left; the two storey frame is on the right. The buckling load, presented as the total uniformly distributed load is given, followed by the maximum warping displacements of the top and bottom flanges of the beam determined as described above. The actual buckling load is less interesting than the relative change in buckling capacity as determined by the joint connection details. To focus on the relative change in this factor, the buckling load is normalised with respect to the lowest buckling strength, in this case the beam through joint. This value is also presented in the table.

The joints in the single storey frame show a discrepancy between the warping displacements in the top flange, which is restrained only by the joint, and the bottom flange, which is restrained by the joint and column. The restraint provided to both flanges by the continuous column in the two storey frame permits the warping displacements of the two flanges to become more similar. Thus, the lack of restraint for the top beam flange in the single storey frame induces an unsymmetric warping displacement in the connection. This is somewhat problematic if the warping bi-moment and displacements are assumed to be equally distributed to both flanges, as they will be in models using beam elements.

### **3.6 Inelastic modelling in a frame context**

In the second phase of this project (MacPhedran and Grondin, 2006), models were developed to investigate how the inelastic behaviour of the members influenced the structural response. The W200x27 cross section was used in modelling a series of portal frames. The frames formed by these sections were loaded with a uniformly distributed load acting vertically down through the shear center of the beam.

The models were constructed of the S4R shell element type. The modelling process for the frames was to analyse the frame with the elastic buckling (i.e. eigenvalue) solver of Abaqus and then apply the eigenvectors (buckled shapes) to the shape to introduce initial imperfections to the model. The maximum imperfection was scaled to  $L/200$  ( $0.005L$ ), which is somewhat larger than the maximum likely imperfections, which are on the order of  $L/1000$ . The value of  $L$  is the length of the horizontal beam in the frame. The larger imperfections were used to promote the onset of buckling in the frame. Only the first buckling mode was applied at this level, two higher modes were applied at half this value. However, higher modes did not play a large part in the model's response. The models with initial imperfections were then re-analysed using the Riks approach.

Beam end restraints were modelled as two conditions. The first consists of a set of displacement constraints on the bottom flange of the beam at the beam-to-column connection. These prevented the displacement of the flange out of the plane of the frame. This was to prevent unrestrained twisting of the column. The other set was applied to all the nodes at the beam-to-column joint, allowing only displacements in the plane of the frame, and preventing twist of the beam while allowing warping of the cross-section. The two end conditions were applied to examine the differences in the restraint provided. The flange restraint models a more practical restraint, where a single point is restrained at the joint, and the joint stiffness is used to prevent twist at the joint. The full section restraint more closely models the joint conditions when beam elements are used. That case would assume that there is no deformation of the joint and the webs of the members. An example of one joint modelled is shown in Figure 3-7. The first restraint condition is shown as solid arrows on the lower flange, the second end restraint consists of the solid arrows and the hollow arrows.

As lateral-torsional buckling has a significant post-buckling strengthening effect, (Ioannidis *et al.*, 1993<sup>6</sup>, Woolcock and Trahair, 1974<sup>7</sup>) the major indicator of lateral-torsional buckling was the loss of lateral stiffness in the models. This loss of stiffness was evidenced by reversals in the deformations or rapidly increasing lateral deformations. This can be seen in Figure 3-11, which shows the results of a plastic analysis of a portal frame made of W200x27 members.

The strength increase in the frame when modelled with two yield strengths, 300 MPa and 400 MPa, are summarised in Table 3-2. The strength increase matches the predictions of Kirby and Nethercot (1979), wherein the strength ratio is about that of the square root of the yield ratios.

While not reflected in the analytical model, the non-uniform warping behaviour from the “helix” effect could also increase the stiffness of the member (Trahair,

---

<sup>6</sup> A numerical study of I-shaped, stocky beams, was conducted.

<sup>7</sup> Slender rectangular cantilever, I-shaped cantilever and I-shaped simply supported beam, experimental and numerical work.

2003). This effect is a torsional strengthening of the member due to extension of the extreme fibre, and resulting compression of the member's core. This effect would be captured somewhat by the shell models, though not at all by beam element models. This effect is considered to be negligible in the cases modelled here, as the rotation required to mobilise this mechanism is very high.

### **3.7 Member interaction using beam elements**

The ultimate phase includes elastic modelling of portal frames with beam elements to determine the interaction of members considering the warping displacements supported by those elements (MacPhedran and Grondin, 2007a). The frames considered are similar to that in Figure 3-9.

As the beam elements support the option of disabling or enabling warping connectivity at the ends of the members, the influence of this mechanism can be separated in one model or incorporated into another. A comparison of these two models illustrates the effect of warping displacements on buckling analyses. The beam elements also support plastic behaviour, and can give an idea of how the warping can affect the inelastic buckling strength.

### **3.8 Chapter summary**

This chapter presents a brief overview of the finite element analysis used in this work. There are some discrepancies between the results of the analysis and the theoretical solutions of the test cases used. For most practical situations, the results from the analysis are conservative, but not overly so, in that they will slightly under-predict the capacity of the structure when compared to theoretical strength predictions. The results can be extremely different from the theoretical predictions, but those cases are outside the practical range of conditions: the affected members are either very short or closed sections.

The results from beam elements are affected by numerical artefacts that, while inexplicable, do not greatly affect the strength predictions for practical lengths and sizes of beams.

The stiffness of a frame model increases with the amount of complexity of the connections at the joints of the frame. This may seem an obvious observation, yet it is a behaviour that is not well captured in the beam element models.

**Table 3-1** Summary of joint displacements for frame, all members W200x27, 3000 mm columns.

One Bay, One Storey Portal Frame						One Bay, Two Storey Frame			
Beam Length (mm)	Joint (See Figure 3-8)	Buckling Load, kN/m	Warp of Top Flange (mm)	Warp of Bottom Flange (mm)	Relative Buckling Load	Buckling Load, kN/m	Warp of Top Flange (mm)	Warp of Bottom Flange (mm)	Relative Buckling Load
4000	Beam Through	19.4	0.385	0.370	1				
	Mitre	20.7	0.406	0.402	1.07				
	Column Through	26.9	0.374	0.362	1.39	32.6	0.362	0.359	1
	Box	32.9	0.185	0.144	1.70	43.9	0.121	0.115	1.35
	Mitre + Diagonal	32.9	0.205	0.235	1.70				
6000	Box + Diagonal	40.7	0.067	0.057	2.10	51.2	0.056	0.057	1.57
	Warping Rigid	50	N/A	N/A	2.58	63.7	N/A	N/A	1.95
	Beam Through	11.1	0.512	0.485	1				
	Mitre	12.1	0.535	0.529	1.09				
	Column Through	12.8	0.496	0.474	1.15	15.5	0.476	0.471	1
8000	Box	15.3	0.245	0.168	1.38	19.8	0.153	0.142	1.28
	Mitre + Diagonal	15.6	0.248	0.305	1.40				
	Box + Diagonal	17.8	0.086	0.067	1.60	22.2	0.070	0.070	1.43
	Warping Rigid	20.8	N/A	N/A	1.86	26	N/A	N/A	1.68
	Beam Through	6.9	0.571	0.533	1				
10000	Mitre	7.7	0.592	0.584	1.11				
	Column Through	7.5	0.552	0.521	1.08	9.1	0.527	0.520	1
	Box	8.7	0.282	0.170	1.25	11.1	0.170	0.153	1.22
	Mitre + Diagonal	9	0.261	0.343	1.30				
	Box + Diagonal	9.8	0.097	0.070	1.41	12.1	0.077	0.077	1.33
	Warping Rigid	10.6	N/A	N/A	1.53	13.7	N/A	N/A	1.51
	Beam Through	4.7	0.598	0.550	1				
	Mitre	4.9	0.617	0.607	1.05				
	Column Through	4.9	0.578	0.538	1.05	6	0.549	0.541	1
	Box	5.5	0.307	0.162	1.18	7	0.178	0.156	1.18
	Mitre + Diagonal	5.4	0.260	0.367	1.15				
	Box + Diagonal	6.1	0.104	0.069	1.30	7.6	0.080	0.080	1.26
	Warping Rigid	6.7	N/A	N/A	1.44	8.4	N/A	N/A	1.40

**Table 3-2** Strength ratios, based on portal frame

Joint Type (Figure 3-8)	Yield Stress (MPa)	Beam Length (mm)				
		2000	3000	4000	6000	8000
Beam Through	300	30.0	32.5	32.5	30.6	28.7
	400	34.3	37.1	37.1	35.5	33.5
	Ratio	0.875	0.877	0.877	0.862	0.855
Mitre	300	46.5	41.0	37.1	33.0	30.0
	400	55.2	47.8	42.8	37.3	33.4
	Ratio	0.842	0.858	0.867	0.885	0.898
Column Through	300	63.8	56.2	49.2	41.3	37.2
	400	80.1	67.9	59.4	50.1	45.1
	Ratio	0.797	0.827	0.829	0.823	0.826
Box	300	74.4	69.3	62.1	52.3	47.2
	400	93.9	85.9	76.1	64.5	60.6
	Ratio	0.793	0.807	0.816	0.812	0.779
Stiffened Box	300	81.4	81.8	75.4	67.0	63.4
	400	104.6	101.9	92.0	84.6	80.2
	Ratio	0.779	0.803	0.819	0.792	0.791



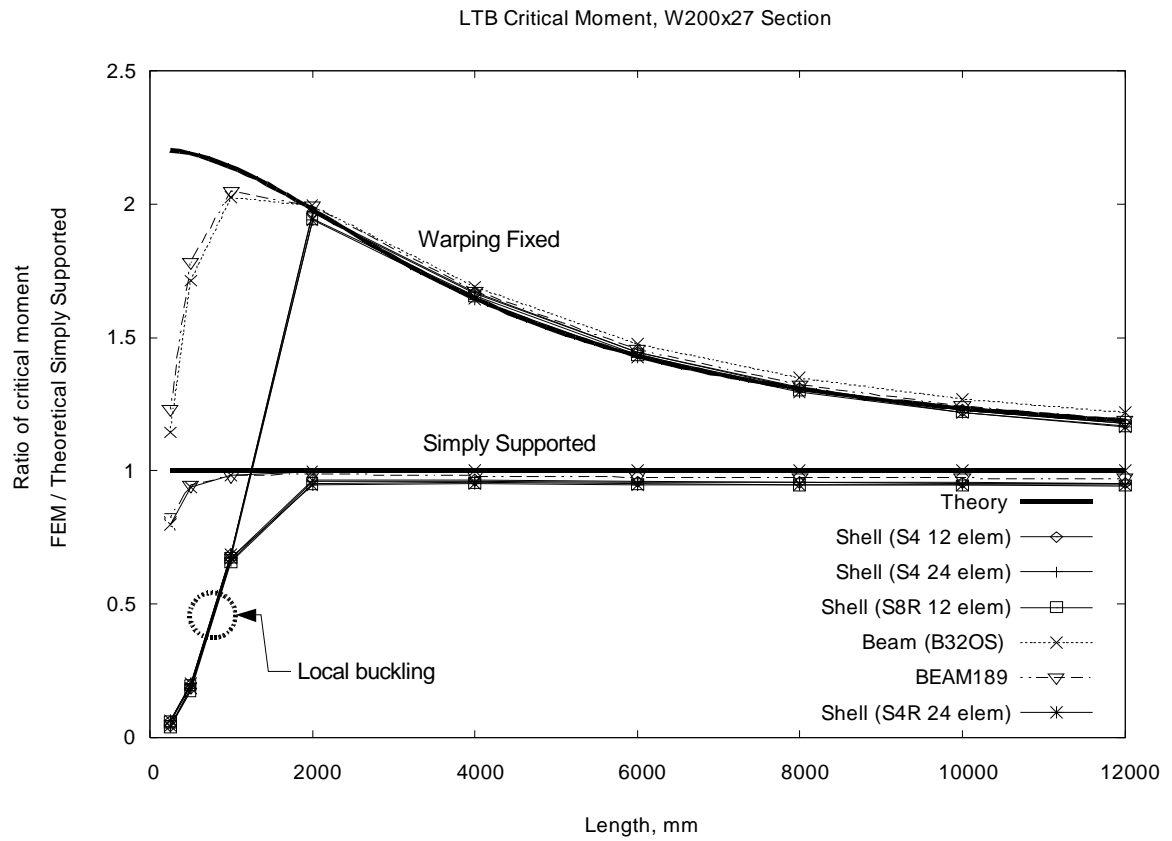


**Figure 3-1** Analysis of buckling moment using various elements.

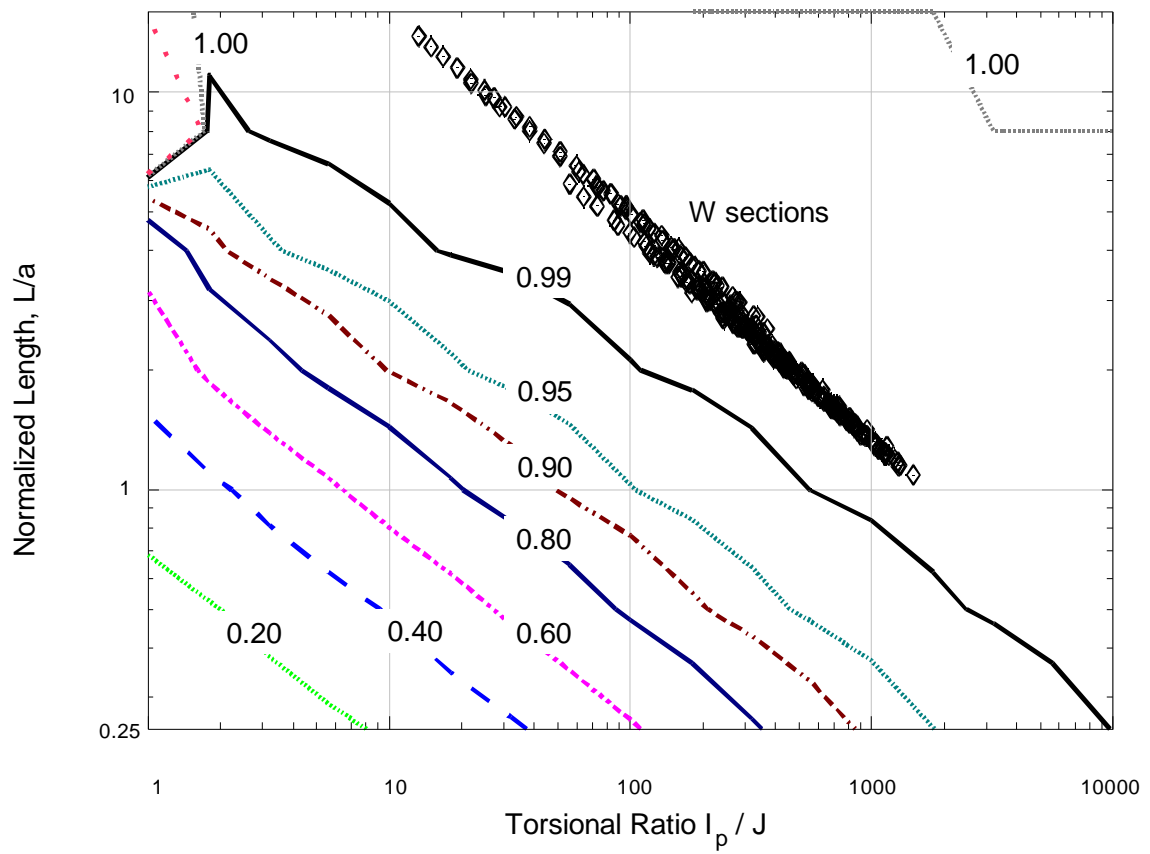


**Figure 3-2** Ratio of finite element analysis results to buckling equation prediction. Includes points of transition to inelastic behaviour for standard W-shapes.

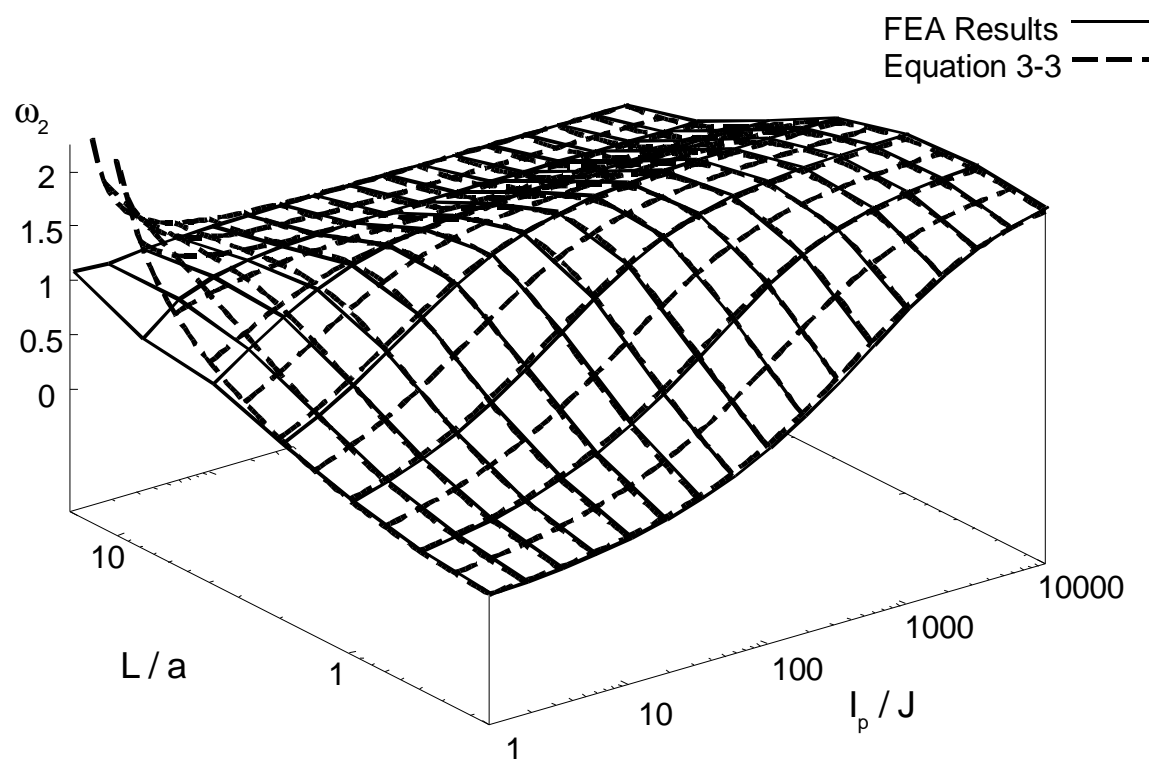


**Figure 3-3** Difference between the Abaqus results and equation [3-3] for constant moment, beam ends are pinned-pinned with respect to flexure, and fixed-fixed with respect to warping.

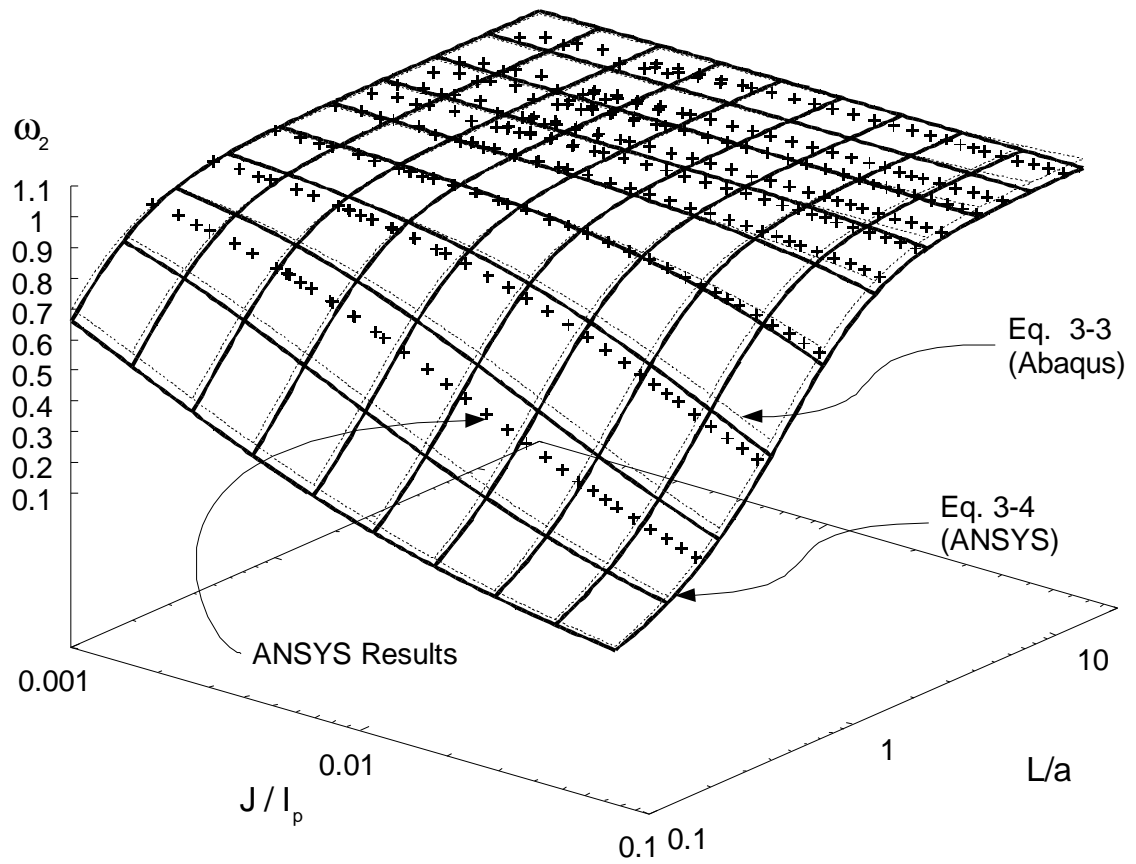


**Figure 3-4** ANSYS results for lateral torsional buckling analysis of simply supported beam, compared with the fitted surfaces for ANSYS and Abaqus.

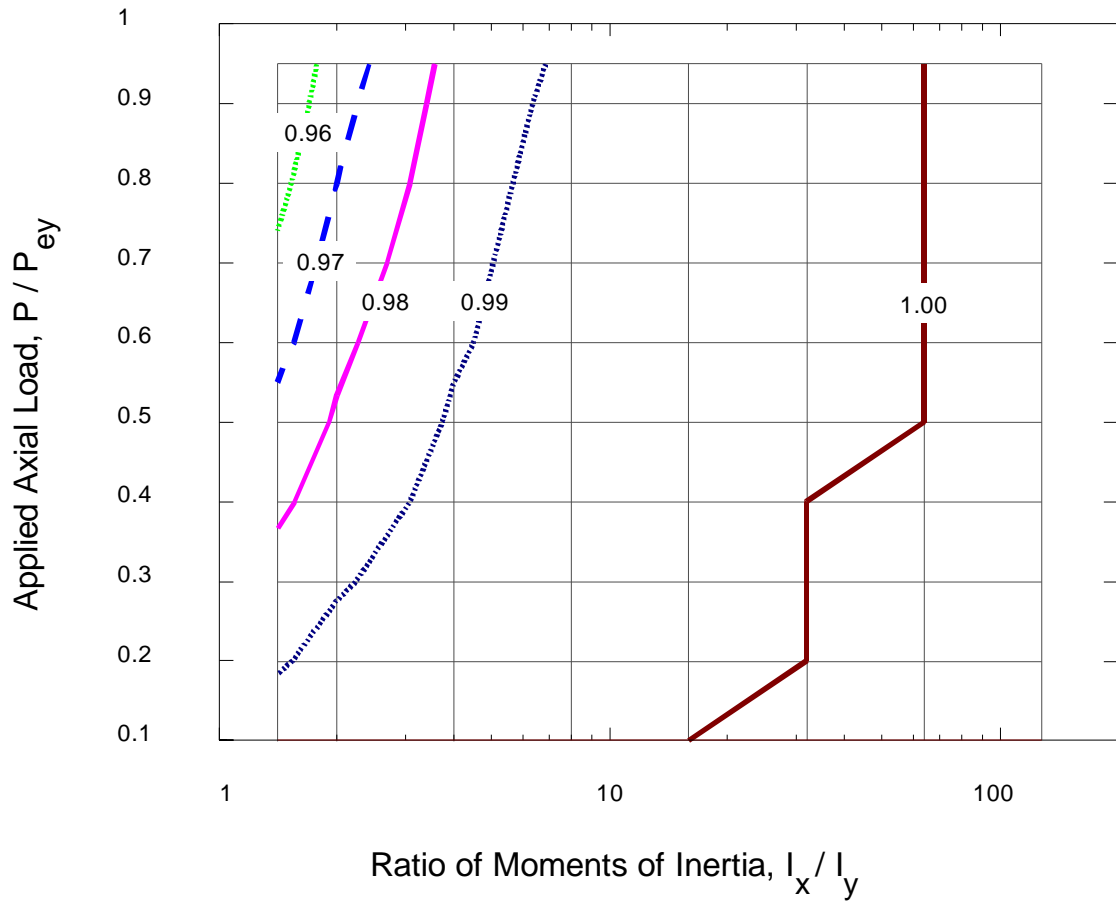


**Figure 3-5** Ratio of FEA results to beam-column equation (Eq. [2-7]) prediction.

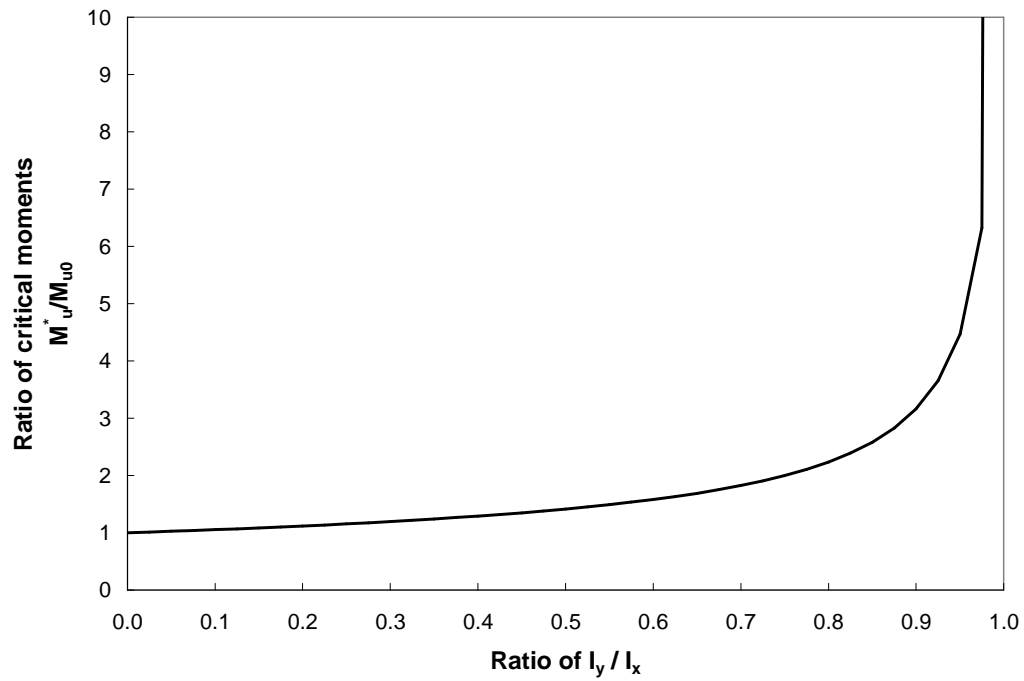


**Figure 3-6** Ratio of theoretical critical moment accounting for major axis curvature to simplified formulation versus the ratio of out-of-plane to in-plane moment of inertia.

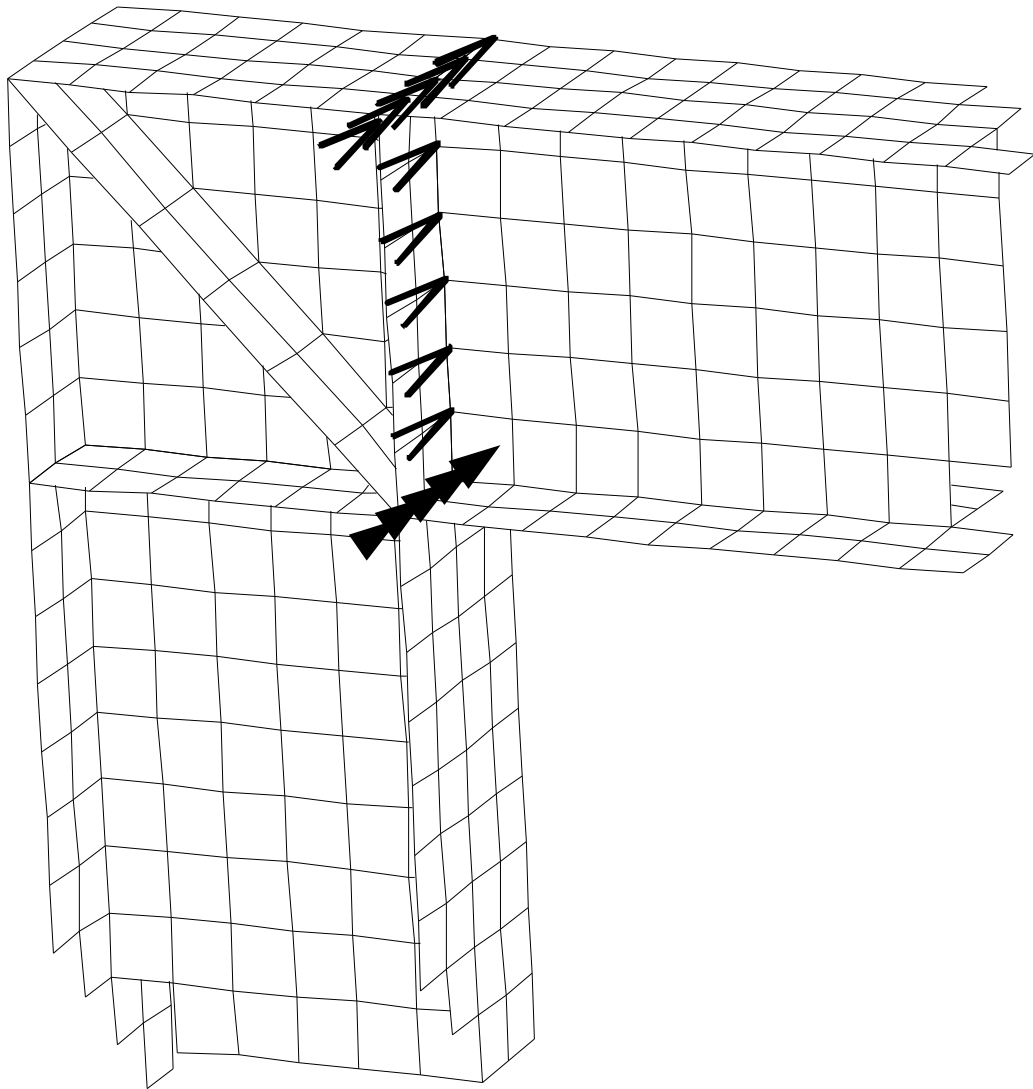
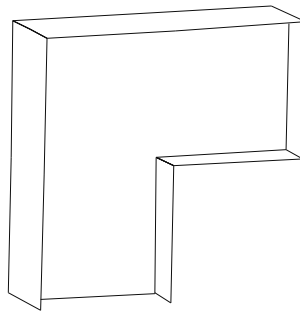
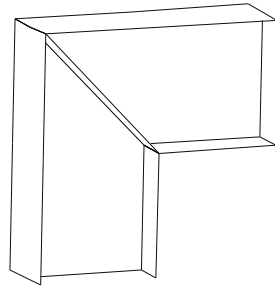


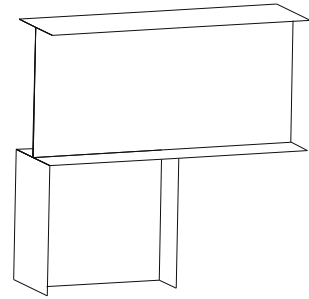
**Figure 3-7 Detail of stiffened box joint from finite element model.**



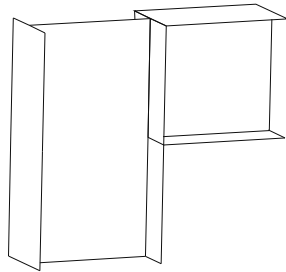
Mitre Joint



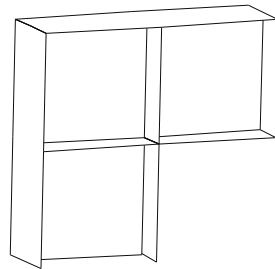
Mitre & Diagonal



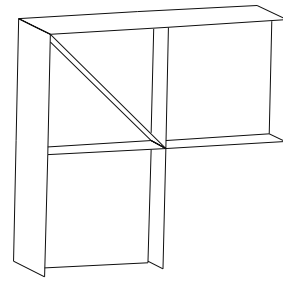
Beam Through



Column Through



Box



Box & Diagonal

**Figure 3-8** Joint Configurations



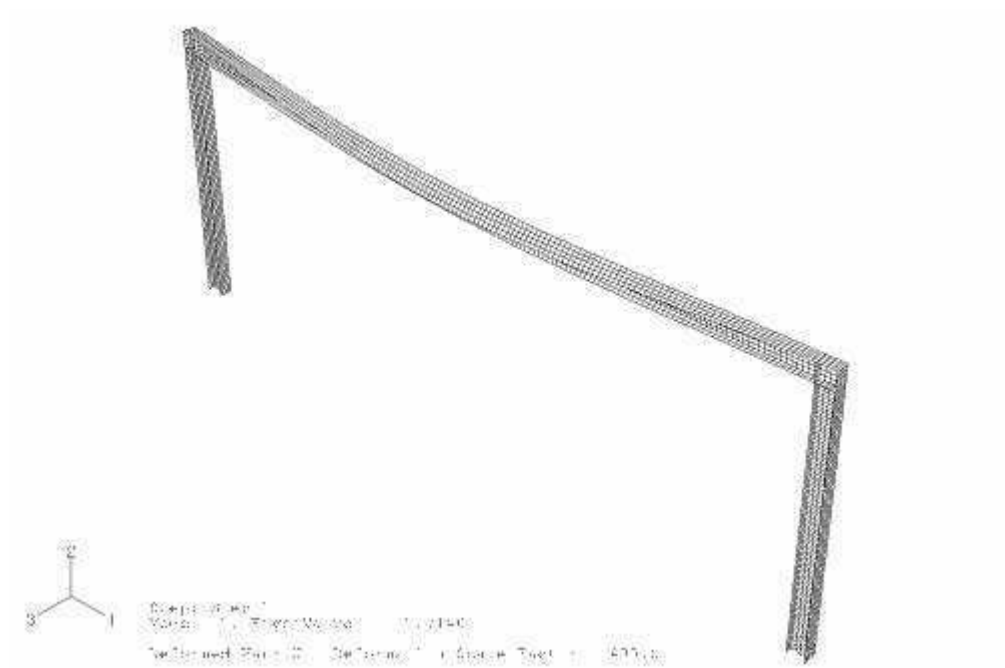


**Figure 3-9** Finite element model of single storey building.

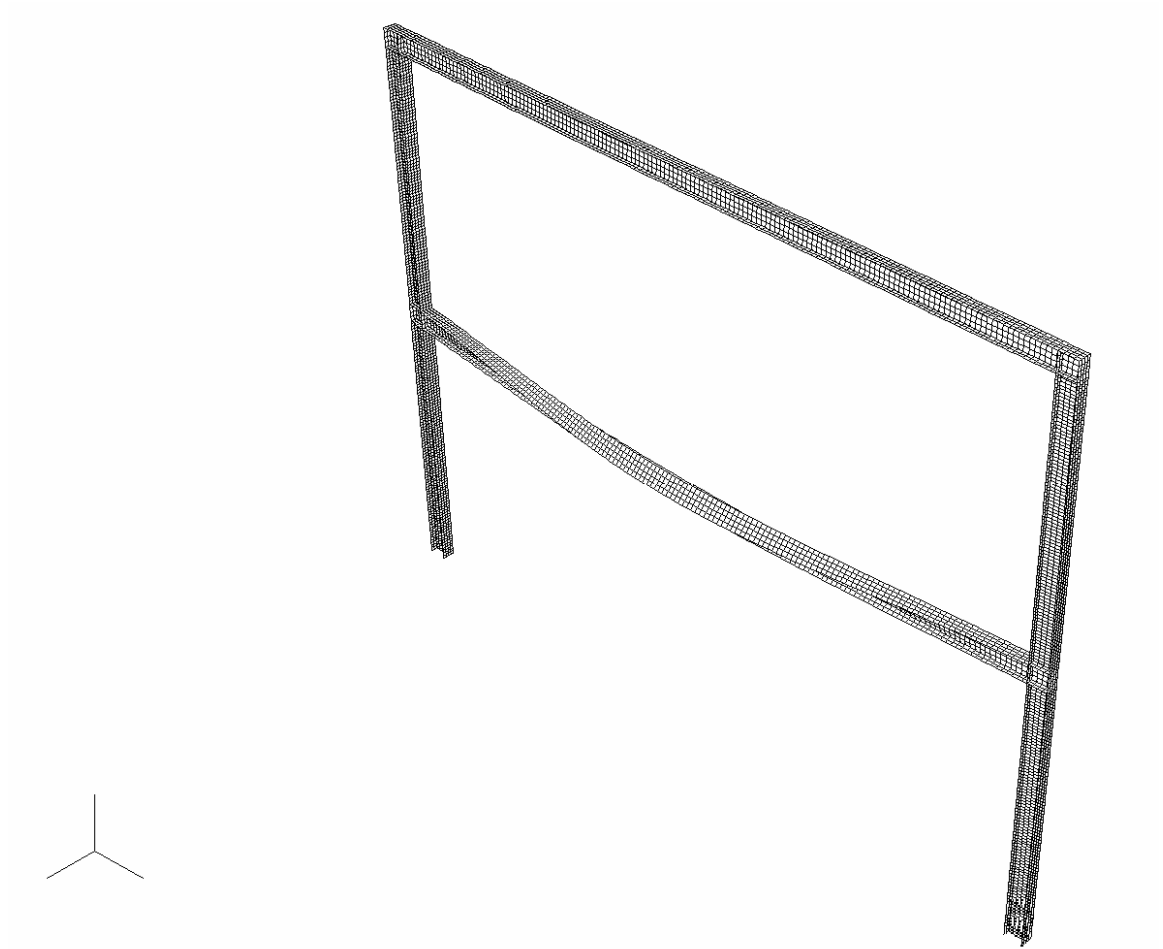


**Figure 3-10** Finite element model of a two storey frame.

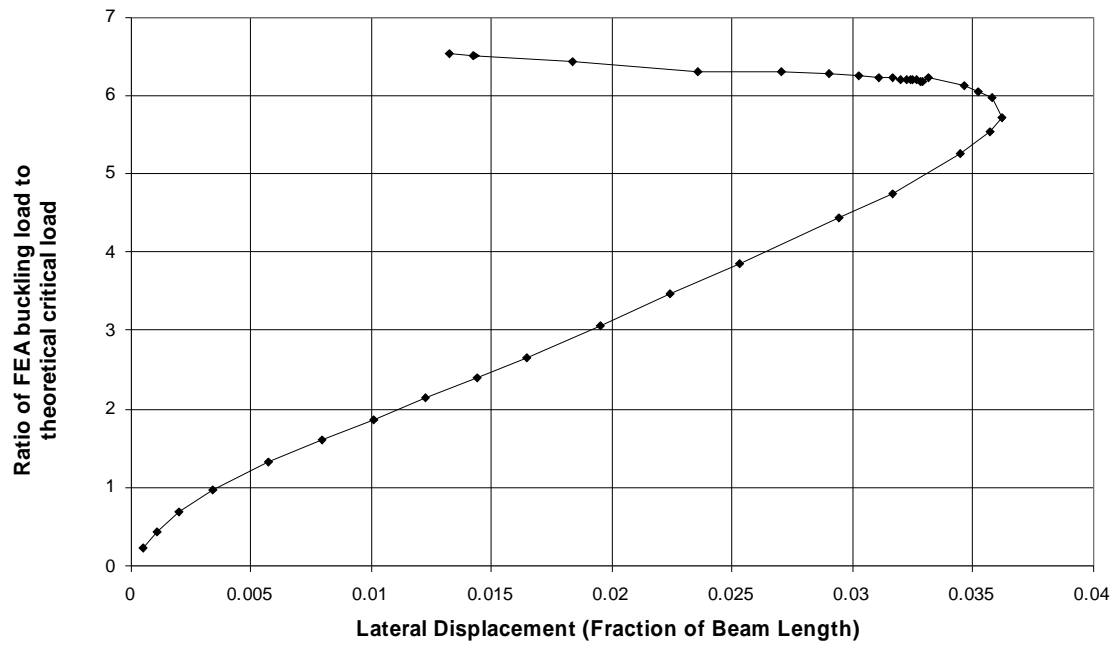


**Figure 3-11** Load versus lateral displacement for the midpoint of beam in single storey frame, 8 m W200x27 beam with box joints, bottom flange restraint and elastic material.

## 4 Frame Analysis

How does the consideration of warping affect the analysis of the stability of steel frames? To answer this question, the inter-member and inter-modal interaction considering torsional warping must be addressed. As the situation is only of interest in determining the predicted design capacity and the elastic behaviour of the members and structure of the frame, a comparison needs to be made of how the members interact, and how this interaction is changed when the torsional warping is considered in the analysis.

This chapter will consider this question using a single storey portal frame to investigate the effect of warping on the analysis of the forces / stability in the frame. This is done through elastic buckling analyses, as the intent is to determine if the elastic stability is affected by warping.

### 4.1 Background: Frame behaviour, analysis and design

A brief examination of the current design and analysis processes is presented in the following. There are many resources (Galambos, 1998, Kulak and Grondin, 2006) that describe frame behaviour, analysis and design. The main point of most reviews is that the analysis and subsequent design must consider the second order effects on the structure as lateral loads and gravity loads are applied to the frame.

The Canadian design procedure in CSA-S16 (CSA, 2005) is presented as a representative method. Most other design philosophies follow similar procedures (Galambos<sup>1</sup>, 1998), The S16 method requires either a second order analysis or a first order analysis modified by moment magnifiers to account for the P- $\Delta$  effects.

---

<sup>1</sup> Chapter Sixteen, Frame Stability, Section 16.5. This covers design procedures for four of the major English language steel design standards, including the AISC Specification, EuroCode 3, Australia's AS4100 and S16. This chapter is the process of being updated to cover the current versions of these standards,

These analyses would include the application of “notional loads,” lateral loads applied to the structure to account for the imperfections in the vertical alignment, or “out-of-plumb” of the vertical members (ASCE, 1997). The Canadian approach for notional loads is to use a load of 0.005 times the gravity load, more than would be required to match the out-of-plumb imperfections of the vertical members (Clarke and Bridge, 1995). The larger value is meant to account for the softening effect of member yielding in the structure (Essa and Kennedy, 2000). In general, the application of notional loads is a globally accepted practice, with variations in detail. For example, the American analysis (AISC, 2005) uses a reduced stiffness to account for material softening and lower notional load of 0.002 times the gravity load that only reflects the out-of-plumb of the structure (Surovek, *et al.* 2005).

The moment magnifier approach requires separate calculation of the gravity load effects, preventing sidesway with external restraints if required, and of lateral load effects, that include any restraining forces that were required in the gravity load analysis to prevent sway. The lateral load analysis will always include the notional loads. As this is a linear elastic (first order) analysis, the effects from each load can be combined in a linear fashion. The lateral load effects are multiplied by a moment magnifier, called  $U_2$  in S16, and added together with the unmodified gravity load effects.

Full second order analyses that consider the secondary moments from load displacement do not require moment magnifier factors. However, these are not linear analyses and so each load combination requires a separate analysis, whereas the magnified first order analyses permit the linear scaling and combination of the load effects. Notional loads would still be required for elastic analyses to account for initial out-of-plumb and material inelasticity. However, the magnitude of the notional load may be reduced for those analyses that incorporate any geometric imperfections in the original model.

Full second order analyses that include the effects of inelastic behaviour, initial geometric imperfections and residual stresses (“Advanced Analyses”) would not require notional loads. In these cases, the conditions captured by the notional load are taken into account by direct inclusion of the initial out-of-plumb and incorporation of inelastic behaviour in the analysis of the frame members.

#### **4.1.1 Advanced analysis**

If the analysis were to consider all of the relevant details in the frame, then many of the other approximations, such as effective length factors, moment magnifiers, and the current design column and beam column curves can be eliminated. The primary requirement is that the second order effects must be accounted for – the displacements of the structure must be considered in the analysis, and equilibrium must be found for the forces on the deformed structure. The initial displacements, or geometric imperfections, in the frame and members must also be included in the analysis. The out-of-plumb is described above, but the displacement of member between its ends also contributes to the second order effects. The initial out-of-straight imperfection of the member, and the shape of the imperfection must also be incorporated into the model. For flexural stability, initial rotation of the beam and displacements of the beam perpendicular to the direction of bending also have an effect on the lateral-torsional buckling behaviour. Also, the true position of loading needs to be considered throughout the analysis. This can be important for conditions such as the position of loads relative to the vertical position of a beam’s shear centre. All of the flexural and torsional responses would need to be considered for complete second order modelling. An argument can be made to include axial member deformations due to the compressive (or tensile) loads they experience, but these deformations would be small compared to the gross displacement of member ends relative to each other due to flexural shortening.

Material nonlinearities and imperfections are also required. This would include the initial imperfections that result from residual stresses in the cross section

created during its fabrication. These play a great part in how the cross section first yields and how plastification progresses in the member. The material's stress-strain behaviour is also needed to model this behaviour.

The behaviour of the connections in the frame also contributes to the behaviour of the structure. This thesis addresses a portion of this topic. While this work considers that fully stiffened moment connections are used and that these keep the connected members at the same angles throughout deformation, there are many connection details that permit some differential rotation between the connected members<sup>2</sup>. Current design provisions only require that the member's angle of twist be considered. Specifically, the member is considered to be prevented from twisting at brace points. The torsional warping behaviour is neglected for the most part.

The true cross section should also be modelled – the thickness of the member's web and flanges, their length, any imperfections in the shape of the cross section, such as out-of-square, out-of-parallel, or web off-centre can also have an effect, as can the amount of twisting imperfection along the length of the member. At this point, it must be noted that in all practical senses, there is a limit to the accuracy of the analysis. For the most part, the analysis is to provide guidance on the final design of the structure, when the real geometry of the frame is roughly known and the member sizes unknown. Details at the level of the cross section would be impossible to establish in the finished structure, and cannot be modelled. The analyst can only use idealised values for many of the parameters considered above. Idealised imperfections for the geometry, the stress-strain behaviour of the material and the residual stress magnitude and patterns can be used.

Analyses that fully model the second order effects and imperfections in the members and the structure also no longer require buckling checks, and the design check is strictly a strength check. This offers obvious advantages for the designer. However, the analysis is very intensive and can be time consuming. The

---

<sup>2</sup> These are known as partially restrained connections. See Surovek *et al.* (2005) for some design guidelines

analyst/designer is required to model all potentially critical load combinations individually. The other method permits the designer to model only the base load cases – dead, live, wind, etc. – and combine those analysis results. The latter is much simpler. Also, there are only few inexpensive programs that are capable of carrying out these analyses. Thus, this is not a truly viable option. As well, considering lateral torsional buckling, many of the analysis packages do not provide sufficient capabilities to adequately model the torsional warping effects and structural response so that the full advanced analysis advantage can be used (Galambos, 1998). While research has been done to incorporate torsional effects in advanced analysis (Trahair and Chan, 2003, Wongkaew and Chen, 2002), this has not yet found its way into the standard design methodology.

Member behaviour after yielding begins plays a critical part in the detailed plastic analysis of steel frames. The stiffness for both warping and lateral flexure drops fairly rapidly with the onset of inelastic behaviour, as the flange tips are affected first in compression. This reduction is due to higher compressive residual stresses being generated at the flange tips during the fabrication of I shaped sections, and those areas would reach their yield stress first. Once the material starts to yield, the stiffness of the yielded portion of the cross section is effectively reduced to zero. The effective warping constant and the lateral bending stiffness are more sensitive to the loss of stiffness in the flange tips, than in the tensile yielding of the web-flange junction. As noted by Wongkaew and Chen (2002)<sup>3</sup>, there is a further complication in that an initially symmetric I-shaped section no longer acts as a doubly symmetric section after yielding. Even assuming yielding patterns that are perfectly symmetrical about the weak axis, the shear centre will shift towards the stiffer, i.e. tension, flange.

Inelastic behaviour also provides a common limit to the strength developed in structural steel members. Members that can sustain large deformations without local buckling, have a maximum design capacity that is restricted to the full plastic capacity of the section. Elastic instability effects will reduce the member

---

<sup>3</sup> Page 950



strength below full plastic strength, but cannot increase the member capacity above that value.

Local yielding in the members can lead to large localised inelastic deflections as noted in the testing programs of Chi and Uang (2002) and Zhang and Ricles (2006). However, this is a condition that would be beyond the point of failure in most design philosophies and would be the subject for post-failure or structural integrity design considerations.

#### 4.1.2 “Double $\omega$ ”

A further argument for the advancement of “advanced analysis” for the design of frame members is a phenomenon that Trahair (1986) calls “double  $\omega$ ”. There is a problem in accounting for the “moment magnifier” effect of the axial load and the moment distribution in a beam column. The effect, simply stated, is that there is a secondary moment created as the product of the axial load and the lateral displacement of the member due to the applied moments. (This is the P- $\delta$  effect. This may include a pre-existing  $\delta_0$  deflection, which is the out-of-straightness of the member.)

The problem, as Trahair indicates, is that the then-existent moment magnifier value, the equivalent moment factor,  $\omega$ , did not properly converge to 1.0 as the applied axial load approached zero. As the same  $\omega$  factor was used in the calculation of the lateral-torsional buckling moment, he used the term “double  $\omega$ ” to describe this.

This had been previously mentioned by Massonnet (1959) when he wrote<sup>4</sup>, comparing an interaction formula similar to the S16 formula with another formula:

“For large values of this ratio  $[M/M_p]$ , [...] the interaction formula slightly over-estimates the strength of the

---

<sup>4</sup> Point 2, page 107.

column. This slight defect is a result of using the same expression  $M_{equiv} = \sqrt{0.3(M_1^2 + M_2^2) + 0.4M_1M_2}$  for both phenomena, i.e. collapse by bending in the plane of applied moments and buckling by torsion-bending normal to this plane. Actually two different expressions should be used to cover these cases, but at the expense of simplicity in the interaction formula. In the opinion of the author, there is no need to introduce such a complication.”

Trahair apparently had a differing opinion and did suggest more complex formulae for the appropriate consideration of both the axial and flexural components in  $\omega$  for moment magnification, based in large part on the work of Cuk and Trahair (1981). Among current design standards, Eurocode 3 (CEN, 2005) also presents a fairly complex computation of an expression equivalent to  $\omega$ . As Massonnet indicated, these do complicate the design.

However, this all presumes that only a first order, elastic analysis is required to determine the design load effects. If a complete second order analysis, including all flexural and torsional behaviours and all imperfections, is performed on the members, as well as on the frame in general, all of the higher order effects are accounted for in the member load effects. The member loads already reflect the moment magnification, and this eliminates the need for  $U_2$ ,  $U_1$ , and thus  $\omega_1$ , greatly simplifying member selection. The effects of moment uniformity, reflected in  $\omega_2$ , would also be included in the analysis results.

As mentioned earlier, most analysis packages do not include modelling of the torsional behaviour of the member, especially with respect to torsional warping. For these packages, and even those that support this mechanism, the modelling of the second order effects with respect to torsion-related imperfections is difficult. The imperfections that are of concern are lateral out-of-straightness imperfections, where the member deviates horizontally from the line joining the ends and rotational defects, where the principal axes of the member rotate with respect to the configuration at the ends. The former imperfection provides an initial curvature that produces a torsional component from the applied strong axis

moment, as well as a torque from the product of beam shear and the lateral distance from the line joining the endpoints. The latter imperfection produces an initial weak axis bending component of the bending moment, which is nominally applied to the strong axis, and a larger torque from vertical loads that do not occur at the shear centre of the cross-section.

Kim and White (2008) propose a modelling imperfection whereby the compression flange has a sinusoidal “sweep” of  $L/1000$ , and the tension flange has no lateral imperfection. This produces both a twist and a curvature imperfection in the member. However, the model used was for shell elements, and this imperfection is not possible for beam elements.

In turn, the warping displacements in the beam flanges due to the applied loads on the beam may drive the column to an earlier than otherwise predicted axial buckling failure. The interaction that is considered here is that the displacements will cause an equivalent initial twist in the column, or a forcing torque, that would accelerate the torsional buckling of the column. Any reduction in the torsional buckling capacity would also reduce the lateral torsional buckling capacity of the member.

The torsional buckling of an axially loaded member is initiated by the rate of change in the angle of twist of the member, as it relates to the length of the member, and the axial load. The beam’s warping displacements are caused by the component of the applied major axis moment that produces torque on the beam. The warping displacements are thus fairly small. The twist-per-unit-length considering the elastic warping of the members would be low, if the column is reasonably stiff in torsion. Torsional buckling of the column for doubly symmetric sections (i.e. I-shaped sections) would not likely occur.

## **4.2 Interaction and Interactive Buckling**

The interaction between the members and this interaction’s effect on the buckling strength of the structure can be determined through various methods. Schmitke

and Kennedy (1985) present a method that can be used to model the interactive buckling of a collinear set of beams. The example used in that paper was also modelled in the Abaqus finite element program to see how well the results of that method and of finite element analysis agreed. A continuous beam with the cross-sectional properties of a W310x28 rolled section was modelled as in Figure 4-1 (a).

The beam conditions in the Schmitke and Kennedy work were such that the beam was very close to the inelastic buckling point as defined in S16.1–M84, the then extant Canadian steel design standard. As the design curve for steel beams has not changed in this standard since the advent of limit states design in 1974, these provisions are still in effect. The behaviour was considered sufficiently close to that of elastic beams so that elastic buckling theory can be used. Thus, the beam was analysed for the elastic eigenvalue buckling magnifier load. The beam capacity predicted by Schmitke and Kennedy was 1.050 times the given loading condition. The finite element analysis predicts a buckling capacity 1.078 times the given load. This difference is due to the capacity predicted by Schmitke and Kennedy being based on the design standard's capacity prediction as that calculation includes inelastic effects, ignored in this finite element analysis.

However, there is another aspect to the work presented here that is beyond the simple case of a collinear beam presented in Schmitke and Kennedy. The members are no longer to be considered as collinear, but are perpendicular to each other, as in Figure 4-1 (b), forming a single storey, single bay, braced frame. To ensure that the analyses used for frames are as effective as those used for collinear beams, the frame configuration should also be analysed for the inter-member interaction phenomenon. To model such a frame in a manner similar to the collinear beam, there must be no interaction between bending moments and axial loads. To prevent this force-moment interaction, all four joints of the structure were constrained so as to prevent the introduction of axial loads into all members. This also prevents relative displacements of the joints, making the structure a braced frame.

One difference between the collinear beam and braced frame that must be considered when comparing the analysis results is the torsional fixity of the members. In the collinear beam, the segments are all restrained against twist at their ends. In the frame, if this condition is strictly applied, the joints between vertical and horizontal members would be restrained against both twist and lateral rotation, a much stiffer restraint than in the collinear beam. To offset this, the possible restraint conditions were all modelled to see which of these best related to the original problem. These results are presented in Table 4-1. As expected, if all members are restrained at the joint, the strength is higher than for a continuous beam. If no additional restraint is provided – the twist of each member is restrained by the lateral flexural stiffness of the perpendicular member – then the structure is somewhat weaker. However, if the vertical members were the ones restrained from twisting, implying that the horizontal member was restrained from bending laterally at the joints, the strength (1.079) is in close agreement with that of the collinear beams (1.078).

### **4.3 Interaction in Frames**

The frame analyses results presented below are based on elastic eigenvalue buckling analysis. This incorporates a form of second order analysis, though it does not incorporate the imperfections of the frame nor of its members. As this is an elastic analysis, any effects of inelastic behaviour are also ignored. It is recognised that the warping effects may be significantly influenced by inelastic behaviour, elastic analyses are the first step, as the focus of this work is to examine the warping behaviour of the members, which will be more pronounced in the elastic domain.

The primary frame model used in this part of the study is a single storey, single bay, unbraced moment frame. The schematic of this frame is illustrated in Figure 4-2.

As the target is to determine the stability contribution of the continuity in torsional warping through the frame, the frame was first analysed with warping displacements discontinuous at the joints. This required that the members connected at each joint all be independent with respect to warping. In the finite element model, the warping degree of freedom on the members at the nodes representing the joints was released. This frame model is then analysed to determine its buckling loads.

In the physical realm, this is an impossible situation. A moment connection at the beam to column connection will transmit moments about both the strong and weak axes. Thus, the bi-moment resulting from the warping deformation must also be transmitted into the connection, as it can be considered as weak axis bending of the member, but with the flanges bending in opposite directions. The physical test that separates the flexural fixity from the warping fixity is impossible. However, in structural analysis the standard frame modelling philosophy ignores the warping effects.

The second analysis incorporates the warping displacements being transmitted into the members connected at each joint. This is done by directly connecting the warping degrees of freedom of joined members together at the connection. In cases where the joint connects members of differing sizes, a correction is made to adjust the warping from one member to that in the other member. This is accomplished in Abaqus by the use of constraint equations, which can force the transfer of partial displacements between elements. This is required in Abaqus as the degree of freedom for the torsional warping displacement is the maximum displacement of the flange. The correction is calculated as the ratio of the column width to the beam width, so that the warping deflection of the beam is multiplied by the ratio and used as the warping deflection in the column. This relationship is applied using constraint equations, which are created using the \*EQUATION command in Abaqus.

The two elastic buckling analyses produce critical loads that are multiples of the applied loads. To assess the effect of considering warping in analysis, the buckling load from the analysis considering warping was divided by that determined from the analysis that neglected warping, for the same moment/axial load ratio. The ratio of buckling loads provides an indication of how the warping affects the capacity – either increasing or decreasing the capacity if the ratio is greater than 1.0 or less than 1.0, respectively. It also directly gives a measure of the amount of increase or decrease.

The applied loading should ensure that the column and beam both be close to their respective buckling capacities. If the frame were loaded with a uniformly distributed load on the beam, the relationship in Equation [4-1] would need to be satisfied to produce lateral-torsional buckling in the beam simultaneously with weak axis buckling in the column. This would give the nonlinear relationship for beam to column length in Equation [4-2].

$$\frac{\pi^2 EI_{yc}}{(k_y L_c)^2} = \frac{6 \omega_2}{L_b} \sqrt{\left( \frac{\pi^2 EI_{yb}}{L_b^2} \right) \left( GJ + \frac{\pi^2 EC_w}{L_b^2} \right)} \quad [4-1]$$

$$\frac{L_b^2}{(k_y L_c)^2} = \frac{6 \omega_2}{\pi^2 EI_{yc}} \sqrt{\left( \pi^2 EI_{yb} \right) \left( GJ + \frac{\pi^2 EC_w}{L_b^2} \right)} \quad [4-2]$$

However, this would require very stiff beams to produce the loading required for simultaneous buckling of both members. As an example, W200x27 columns would require short span beams of W690x125 sections for shorter columns. To enable the beams to be stiff enough to support the required loadings, the beam was braced at mid-span against lateral displacement and twist. Short span beams would likely exhibit considerable inelastic behaviour, rather than elastic buckling. This was considered undesirable behaviour for this project, as the effects of warping on the frame strength would not be as large when the frame's resistance is governed by fully plastic capacity. Also, while deep beams and relatively slender columns are used in practice for frames, the majority of previous research

(Krenk and Damkilde 1991, Morrell *et al.* 1996, Tong *et al.*, 2005) used beam and column members of the same size. To include these types of frames here, the method of loading should permit equal sized members. Also, the loading method used should not exclude members of different sizes.

The loadings chosen for the models were moments and vertical loads applied at the connections, as shown in Figure 4-2. The gravity load was set to be a ratio of the buckling capacity,  $\alpha$ , ranging from 0 to 1. The moment capacity of the beam was then calculated using the reduced buckling moment capacity in the column,  $M_{cc}$ , and the buckling moment capacity of the beam,  $M_{cb}$ . While these did not always produce the exact critical load due to variability in the support conditions assumed in determining the buckling loads, the loads are scaled appropriately during the buckling analysis.

Lateral torsional buckling often governs the design of beam-columns in braced frames. Out-of-plane buckling is rare in frames that are not braced against in-plane sway displacements, but are braced against out-of-plane sway. For out-of-plane buckling to occur, the expression  $k_x / k_y \leq \sqrt{I_x / I_y}$  must be satisfied (Wongkaew, 2000). This is difficult, as  $k_x$  in this context is greater than one. Of the relatively few standard rolled wide flange sections that satisfy this criterion, the W200x27 section was chosen for modelling the majority of the frames. This had been selected as a representative section earlier in the project as it met several other criteria, including a relatively long “ $a$ ” (torsional bending constant,  $\sqrt{(EC_w)/(GJ)}$ ) value and not being susceptible to local buckling before full section yielding, i.e. it is at least Class 2 in bending for commonly available steel grades.

The columns in the frame model have initial maximum imperfections of 0.002L out-of-plumb. This is a linearly scaled defect, so that at one end of the column the value of the imperfection is zero, and at the other end the imperfection is 0.002L. The column also has an out-of-straightness imperfection of 0.001L. This imperfection is a half sine wave, with a maximum value half the distance between



supports. As the beams are braced at their midspan, they have a maximum out-of-straightness of  $0.0005L$ , and the imperfection is a full sine wave over the length of the beam. A rotational imperfection was not included, as the beam element doesn't support this. Each element must be rotated a certain amount – the nodes cannot be assigned a rotation.

### 4.3.1 Base plate fixity

Varying base plate fixity conditions were modelled to test the effect of the far end conditions on the change in frame performance due to warping consideration at the member connections. The three support conditions modelled were: a fully fixed conditions, where all displacements, rotations and warping are restrained at the base plate; a simple or “pinned” connection where the base plates only provide restraint from translation and no resistance to rotation or warping; and a pinned support with full warping and translational fixity (“warping rigid”), but no rotational restraint. The last condition would be equivalent to a very thick plate welded to the end of the column, preventing torsional warping of the column's cross section, but the plate is still free to rotate at the base.

These conditions are modelled by manipulating the beam element's restraint conditions on the appropriate degrees of freedom. For the fixed base, all seven degrees of freedom are prevented from displacing. For the pinned base, only the three translational degrees of freedom are fixed. And for the pinned, but rigid with respect to warping, base the degrees of freedom restrained are the three translational and the warping degree of freedom.

The conditions for the two pinned base conditions were selected as providing extremes bounds for the actual restraint provided at the base of columns. The simple support condition is somewhat less than the actual restraint typically provided, as recognised in S16, where column bases that are treated as “simply supported” may be given a higher restraint than a pinned support<sup>5</sup>. The warping

---

<sup>5</sup> Appendix G, CAN/CSA-S16-01, clause G4.

displacements at the base plate would not be fully restrained, as no base plate could provide that much rigidity. However, this will give an “upper bound” solution to the problem. The true warping behaviour of the base plates would lie between the two conditions used for the pinned bases.

## 4.4 Analysis Results

The model described above was analysed using Abaqus. Other variables were introduced to compare various effects to the reference configuration of an unbraced frame composed entirely of W200x27 members, with column base plates that provide full rigidity with respect to bending about both major axes, and thus, full warping fixity.

The element type used is a three dimensional beam element, Abaqus beam element B32OS. The “2” in the designation means that the underlying shape function is quadratic, which requires a midspan node. The “OS” indicates that this is an open-section element, meaning that it supports the warping degree of freedom. While not pertinent to the analyses herein, the element also supports Timoshenko beam theory, where shear deformations are incorporated into the stiffness matrix. For the purposes of this analysis, shear deformation does not affect the buckling behaviour of the element, and the difference between the Timoshenko beam element behaviour and that of a Bernoulli-Euler beam is negligible. However, the standard Bernoulli-Euler beams in Abaqus incorporate cubic shape functions, though they lack the warping degree of freedom. To ensure that sufficient degrees of freedom were used to adequately capture the buckling responses, several of the quadratic elements were used to model each frame member. Each member was modelled with segments that were 250 mm long.

The analysis results are presented starting with Figure 4-3. Each frame is typically represented by a pair of graphs, one showing the “surface” for the analysis results for varying lengths of beam, given a constant column height, and for varying load ratios ( $\alpha$ ) as presented in Figure 4-2. This graph is presented in an orientation that

provides the best view of the surface's features. The second graph is a contour plot of the surface, presented in the standard two-dimensional plot format. The values measured are the increase in capacity considering warping transmission, **relative to the buckling capacity that does not assume warping displacement transmission**. They do not represent absolute buckling capacities. This capacity ratio, designated  $R_w$  on the graphs, was chosen so that differing frame configurations could be compared directly.

#### 4.4.1 Effect of base plate

The first effects that are apparent are those that represent the effects of the base plate fixity. Three base plate conditions were selected to represent the available idealised end constraints: a base plate that prevents all translations, rotations and warping, hereafter called the “fixed base”; a base plate that prevents all translations, but does allow free rotations and warping displacement, the “pinned base”; and a pinned base that prevents warping displacements, the “warping rigid base.” The results for a representative frame using 4 m columns is presented through Figures 4-4, showing the fixed base condition, 4-5, showing a pinned base connection and 4-6, showing a warping rigid base.

There are marked differences between the fixed base condition and the others. However, the difference between the pinned base and warping rigid base is negligible. In general, this holds true for most of the frames analysed. The torsionally susceptible column discussed below is the only one for which the warping rigidity of the base plate makes a difference.

The fixed condition presents an interesting profile, with a “valley” separating two increased capacity regions. These represent different buckling modes for the frame, dominated by column buckling behaviour for higher axial loads and shorter beams and beam buckling behaviour for longer beams and lower axial loads. The “valley” marks the decline of the contribution of each mode.

## 4.4.2 Effect of torsional susceptibility

The length at which torsional buckling of a column will govern over flexural buckling about the weak axis is found by setting the torsional and flexural buckling loads equal (Equation 4-3) and solving the resulting relationship. This results in the series of steps outlined below (Equations 4-4 and 4-5), using doubly-symmetric I-shaped sections where the warping constant,  $C_w$ , can be represented by  $I_y(d-t)^2/4$ .

$$\frac{A}{I_p} \left( JG + \frac{\pi^2 C_w E}{L^2} \right) = \frac{I_y \pi^2 E}{L^2} \quad [4-3]$$

$$J \frac{E}{2(1+\nu)} = \frac{I_y \pi^2 E}{L^2} \left( \frac{I_p}{A} - \frac{(d-t)^2}{4} \right) \quad [4-4]$$

$$L^2 = \frac{I_y \pi^2 2(1+\nu)}{J} \left( \frac{I_p}{A} - \frac{(d-t)^2}{4} \right) \quad [4-5]$$

For the standard rolled steel I-shape sections available in North America, most of the values of  $L^2$  in equation [4-5] are negative, indicating that the torsional buckling load is always higher than the weak axis flexural buckling load, for effective length factors of 1.0 for both weak axis bending and warping. Of the 67 shapes found to be susceptible to torsional buckling, the longest length for which torsional buckling will govern is 3235 mm, for a W360x134 section. The mode transitions for these 67 cross sections are shown in Figure 4-7 plotted as the weak axis slenderness ratio for a yield strength of 350 MPa versus member length at which the failure mode changes from torsional buckling to flexural buckling on the horizontal axis. Bjørhovde (1972) indicates that for a slenderness less than 0.15, the full yield strength can be reached, so many of these transitions would occur after the full yield capacity was reached. Converting the transition points from slenderness to column strength using the S16-01 column formula for

flexural buckling gives Figure 4-8 where the column strength relative to the full section capacity is shown as a function of the transition length.

The columns that are most slender flexurally at the transition to torsional buckling are sections that do not meet the local buckling requirements in compression for a yield strength of 350 MPa. Most of those sections do not meet the web local buckling requirement. The most slender section (W360x237) has a slenderness ratio of 0.31 at the transition length (2390 mm), which gives a design strength of 96.9% of the yield strength according to the provisions of S16-01 (CSA, 2001). Data points circled on these graphs indicate that the member indicated will experience local buckling before the predicted load can be reached.

Those members that do not meet the web slenderness requirement for columns and should be designed according to CSA S136-07 (CSA, 2007). Some of these sections do not satisfy Class 2 slenderness requirements for flexure. Most lengths at which the buckling mode changes from weak axis flexural buckling (just longer than the transition length) to torsional buckling (just shorter than the transition length) are such that the column behaviour is almost completely dominated by inelastic behaviour, at least for the common yield strength of 350 MPa. This is shown in Figure 4-8, as the minimum strength of any column is 0.91 times its full yield capacity.

Local buckling and inelastic considerations were set aside to permit an elastic buckling comparison with the considerations used previously for sections susceptible to flexural buckling. An elastic buckling analysis using the procedure described above for a portal frame was conducted with a W360x134 section. This section has a transition length of 3235 mm. The elastic buckling analysis does not consider the local buckling of the cross section. (The plates composing the section are not included in the section properties used to determine the stiffness of the finite elements used.) It also is not restricted by inelastic effects, so any buckling effects will not be masked by yielding.

The results from these analyses are similar to those for the other cross sections in that the strength is never reduced by considering the effects of warping. However, there is an interesting development in that there is a large range of beam lengths and axial load ratios for which there is almost no change in capacity ratio,  $R_w$ , when considering warping deformations. This occurs for the case of fixed-based columns (Figures 4-9, 4-10, and 4-11) and pin-based columns with plates capable of restraining warping (Figure 4-13). This is not evident in those frames with simply supported column bases (Figure 4-12). These all occur in those cases with longer beam lengths and higher axial load ratios. This indicates that the critical buckling modes for this frame do not include a torsional component, and are unaffected by the beam's warping.

The frames with pinned column supports do not show marked differences in the capacity increase over the range of analysed conditions. There is an increase in capacity throughout, but the surface plot of the analysis (Figure 4-12) shows gradual changes to the increases, and a flatter profile throughout. This indicates that the frame strength is influenced primarily by the columns being stiffened torsionally by the rest of the frame. The exception to the trend mentioned earlier in pinned ends occurs here. A comparison of the pinned base plate (Figure 4-14) and the pinned, but warping rigid plate (Figure 4-15) shows that there is little to no change in buckling capacity. This likely illustrates a change of buckling modes from torsional buckling to flexural (major axis) buckling for these conditions.

### **4.4.3 Deep beams**

The majority of the work done by other researchers up until the start of the 21<sup>st</sup> century was done considering the horizontal and vertical members in the frame were of the same cross section. This was primarily the focus of the work described herein as well, but the work of Chi and Uang (2002) and Zhang and Ricles (2006) indicate that the use of a larger beam can produce post-failure behaviour that shows significant warping displacements.

Tests conducted by Zhang and Ricles (2006) include composite action between the steel members and concrete floor slab. While this is the construction method that would be expected in real structures, the floor slab would stiffen the beam's top flange, reducing the amount of warping experienced by the frame. It would also provide significantly higher warping resistance to all members of the frame at service, and perhaps ultimate, load levels.

Extending the observation made earlier that if one were to look at achieving the simultaneous buckling of both column and beam, a larger beam would not require central bracing that was required for the more slender beam modelled above. This type of frame needs to be examined.

A representative frame was modelled, using W200x27 vertical members with a W690x125 horizontal member. The model was constructed similarly to those mentioned previously, and included the warping displacement correction described earlier. The results from these analyses are plotted similarly in Figure 4-16, for a representative fixed based frame, Figure 4-14 for a pinned base frame, and Figure 4-15 for a warping rigid base.

The frames with simply supported columns have no significant differences for the two different warping restraint base conditions. There is a marked difference in the fixed base column condition (Figure 4-16), where noticeable increases in capacity for short beam lengths and high axial loads contrast with relatively (and absolutely) low increases for long beams and high moments. This may reflect that the influence of warping effects is less significant for long beams.

#### **4.4.4 Braced frames**

Braced frames are more susceptible to out-of-plane buckling, as the  $P-\Delta$  effects are not as severe for strong axis buckling. The columns of these structures are more susceptible to weak axis buckling, and also lateral-torsional effects. A set of frames, similar to the unbraced set described above but braced against sway by a single restraint at the right column, were analysed using the same conditions and

measurements as above. Both of the single cross section frames are presented – the W200x27 frame and the W360x134 frame. The results of these analyses are presented as Figures 4-17 through 4-23.

One important difference from the unbraced frame analysis previously conducted with the torsionally sensitive W360x134 members is the disappearance of the “plateau” where the buckling capacity is unchanged by the inclusion of warping. A comparison of Figures 4-10 and 4-20 illustrate this difference. This change supports the presumption that the buckling modes for those conditions are not affected by warping, and indicates that these cases are dominated by the strong axis buckling of the columns, as suggested by Wongkaew (2000).

Contrasting the braced and unbraced frame behaviour for the frame composed of W200x27 sections for both columns and beam draws a different picture. The unbraced frame behaviour (exemplified by Figures 4-3 and 4-4 for 4 m columns with fixed bases) and that of the braced frame (the analogue braced frame is shown in Figure 4-18) shows negligible differences in the values of the warping effect. This forces the conclusion that for frames with columns that buckle about the weak axis, the braced condition does not significantly affect the effect of warping transmission. The effect of column length in braced frames can be seen by comparing Figure 4-17 with Figure 4-18. The frame with a longer column length has a primary buckling mode based on the column for a longer range of beam lengths than frame with shorter columns. This difference in behaviour can also be seen in the frames with W360x134 members, represented in Figures 4-20 and 4-21.

A comparison between Figure 4-18 and Figure 4-19 illustrates that the effect of base plate restraint can be fairly important. In Figure 4-19, the frame with a pinned column base shows a uniform strength increase, indicating that a single buckling mode is dominant for all beam lengths considered. This is also reflected in Figures 4-22 and 4-23, where the single mode is dominant over the lengths and loads investigated. There is a small exception to this, in Figure 4-23, for the



region of the graph representing high axial load and long beams, where another mode appears dominant. As this mode is not affected by warping restraint, this mode would be a flexural buckling mode in the columns.

#### **4.4.5 Effect of warping direction**

There are two conditions for continuity of the warping displacements (Basaglia, *et al.* 2007), one where the warping displacements may be transferred directly through the joint, and another where they reverse sign. Which of these are active depends on the joint configuration. The typical displacement is the one in which the warping displacements are directly transferred. The reversed direction occurs with some diagonal stiffener configurations. The cases presented below have been modelled with both direct warping displacements and reversed warping displacements. The reversed warping was also modelled to determine if this condition could be forcing instability in the rare conditions where it is produced.

The warping displacements have been noted as being either directly applied or reversed in direction when they are transmitted through the connection. For the most part, the differences between the results from these two analyses are small. The effect is plotted for the fixed and pinned column support conditions for the two column lengths of 3000 and 4000 mm. The frames composed of W200x27 members in Figures 4-24 (fixed base, unbraced); 4-25 (pinned base, unbraced); 4-26 (fixed base, braced); and 4-27 (pinned base, braced). The W360x134 frames are shown in Figures 4-28 (fixed base, unbraced); 4-29 (pinned base, unbraced); 4-30 (fixed base, braced); and 4-31 (pinned base, braced).

The fixed base columns show more complex surfaces for these plots. In part, this seems to change in concert with the dominant buckling mode. There does not appear to be one warping direction that is more advantageous for strength. In some cases, such as Figure 4-27, the direct warping transfer provided more strength (ratios larger than one) and in others, exemplified by Figure 4-28, the reversed warping provided more strength (ratios smaller than one). In most cases

the range was about 4% strength increase for either condition. However, the torsionally sensitive cross section (W360x134) did display more variance. The range is from 1.04 in Figure 4-25 to 0.926 in Figure 4-30.

#### **4.4.6 Effect of column length**

Several column lengths (2 m, 3 m, 4 m, 5 m and 6 m) were also modelled to examine the effect that the relative lengths of beam and columns have on the effects of mutual warping restraint on the system buckling loads. The results from selected frames are presented in Figures 4-32 to 4-48. Each curve on the charts represents the change in frame capacity for varying beam lengths for a single column length. The relevant column length, in millimetres, is noted in the legend of the graph. A single series of curves present the strength increases for a particular  $\alpha$  (ratio of applied axial load to buckling capacity) value. These charts show the increase in buckling capacity for the direct warping transmission case. For each frame, three load cases are selected (those being axial loads of 30, 50, and 70 percent of the buckling load, i.e.  $\alpha = 0.3, 0.5$  and  $0.7$ ). These are representative of the general trends for most of the frames analysed. Only two column base conditions, fixed and pinned, are represented in the graphs. The condition of pinned base, with a rigid warping condition, follows the same general trend as the pinned base case.

The most obvious effect is that shorter columns experience a larger change in buckling strength compared to that of longer columns for pinned base columns. Examples of this can be found in Figures 4-34, 4-38, 4-40, 4-42, 4-45, 4-46, and 4-48. This effect agrees with the general thought that warping is more important for shorter members and any effects, beneficial or adverse, would be larger for shorter members. However, there are exceptions to this trend, particularly in the case of fixed column bases and shorter beam lengths, such as can be found in Figure 4-32.

Some of the gains do seem unrealistic. There appears to be an increase to more than twice the capacity for short columns and short beam combinations. Figure 4-48 is likely the best example of this. It must be noted that for simply supported member, Equation [3.5] predicts buckling capacities to rise to over 2 if the warping were completely suppressed at both ends. The apparent greater stabilisation effect for shorter columns must be countered by noting that in practical columns, yielding and plastic behaviour will dominate the capacity. Thus, these “gains” are not achievable in real frames.

A comparison of normalised beam lengths, that is where the data is graphed with the beam length divided by the column length, shows some common patterns for the capacity changes. One striking example is for the frame with W200x27 columns and a W690x125 beam, shown in Figures 4-36 and 4-37. The pattern shown there is quite similar to the increase in buckling capacity for a beam with simple supports and warping restraint shown in Figure 3-1. The same comparison made with other pairs of graphs shows other interesting trends.

Frames with pinned column bases show no definite trends whether the beam lengths are normalised or not. The comparable pairs of figures: Figures 4-34 and 4-35 using W200x27 for all members; and Figures 4-38 and 4-39 for W200x27 columns with W690x125 beams, show the same lack of sensitivity to a change in beam length. While the corresponding normalised graph is not shown for Figures 4-42 and 4-45, the graphs also show no apparent correlation between beam length and frame resistance.

The frames constructed with the W360x134 members, presented in Figures 4-40 and 4-41 for the unbraced, fixed base configuration, show that for high axial loads, the transition to the strong axis buckling mode occurred at the same beam length. As this buckling mode dominates the high axial load region of the graph, the normalised graph does not show a good correlation between the behaviours of the frames based on the normalised beam length. The corresponding braced frame shown in Figures 4-46 and 4-47 shows no similar transition to strong axis

buckling, and presents a better correlation for the normalised beam length graph. The unrealistic strength increase for short columns is also shown in Figures 4-46 and 4-47.

The behaviour of the braced frame with fixed column bases composed of W200x27 members, is presented in Figures 4-43 and 4-44. Figure 4-43 shows that behaviour of the frames with longer beams and lower axial loads matches when the absolute beam lengths are compared. However, the transition point between buckling modes matches the normalised beam length much better, as shown in Figure 4-44.

In all, there are features in the behaviour of the frames that are better represented by the normalised beam lengths, particularly for the transition between column buckling and beam buckling modes. The beam buckling mode correlates more to the absolute beam length. The frames with no rotational support at the base do not show a trend with either the absolute or normalised beam lengths.

## **4.5 Summary**

Finite element analysis can capture the interaction of members in buckling when considering moment (rotation) transfer at the member connections, as illustrated in section 4.2 above. This has been extended later in this chapter to look at the transfer of bi-moments (or flange warping displacements) across member connections.

This chapter also presented the results of a series of frame models that measured the contribution of mutual warping restraint on the elastic stability of steel moment frames. The five basic frames models presented are summarised in Table 4-2.

For each frame, there are three base conditions modelled for the columns: fixed, simply supported and simply supported but rigid with respect to warping. There are 5 column heights (lengths) represented 2, 3, 4, 5 and 6 m, and 13 beam

lengths: 3 m to 15 m, with a 1 m increment. There were 11 load cases that spanned the buckling capacity of the frame, considering the axial load in the columns to be from zero load to full buckling capacity. For each of these load cases, the columns were loaded in a combination of axial and flexural loads that would bring them close to the buckling point. This was done to measure the influence of the warping deformations at or near the critical loads. Three types of warping transmission at the beam-to-column connection are also considered for the comparison: no warping transmission (the base case), full direct warping transmission, and fully reversed warping transmission. There are small differences between the latter two cases, but these are not significant when compared to the differences between the case of no warping consideration and full treatment of the warping displacements.

In almost all cases, the buckling capacity of the frame is increased when the warping of the beam and that of the column are jointly considered, when compared to the typical case where warping is neglected in the analysis of the frame. Transitions between various buckling modes are apparent in many analysis results, where the buckling capacity shows differing profiles. A striking example is Figure 4-11, where three modes are evident. However, some frames simply show a monotonic buckling increase over the capacity determined without consideration of the transmission of warping displacements.

There are no cases where the buckling strength is decreased. However, there are cases where there is no apparent increase in capacity when warping transmission is considered. Some columns in unbraced frames will be controlled by strong axis column buckling and are unaffected by the strengthening effect provided to other frames by warping. However, bracing the frame will tend to change the dominant buckling mode of columns to a lateral (weak axis) or, in some extremely rare cases, torsional buckling mode.

**Table 4-1** Lateral buckling strength for various configurations of members.

<b>Restraint conditions</b>	<b>Ultimate Strength</b>
co-linear beams	1.078
joints restrained for torsion for horizontal member	1.011
joints restrained for torsion for vertical members	1.079
joints restrained for torsion for all members	1.162
joints restrained only by member interaction	0.917

**Table 4-2** Frames presented herein.

<b>Column Section</b>	<b>Beam Section</b>	<b>Unbraced</b>	<b>Braced</b>
W200x27	W200x27	X	X
W200x27	W690x125	X	–
W360x134	W360x134	X	X

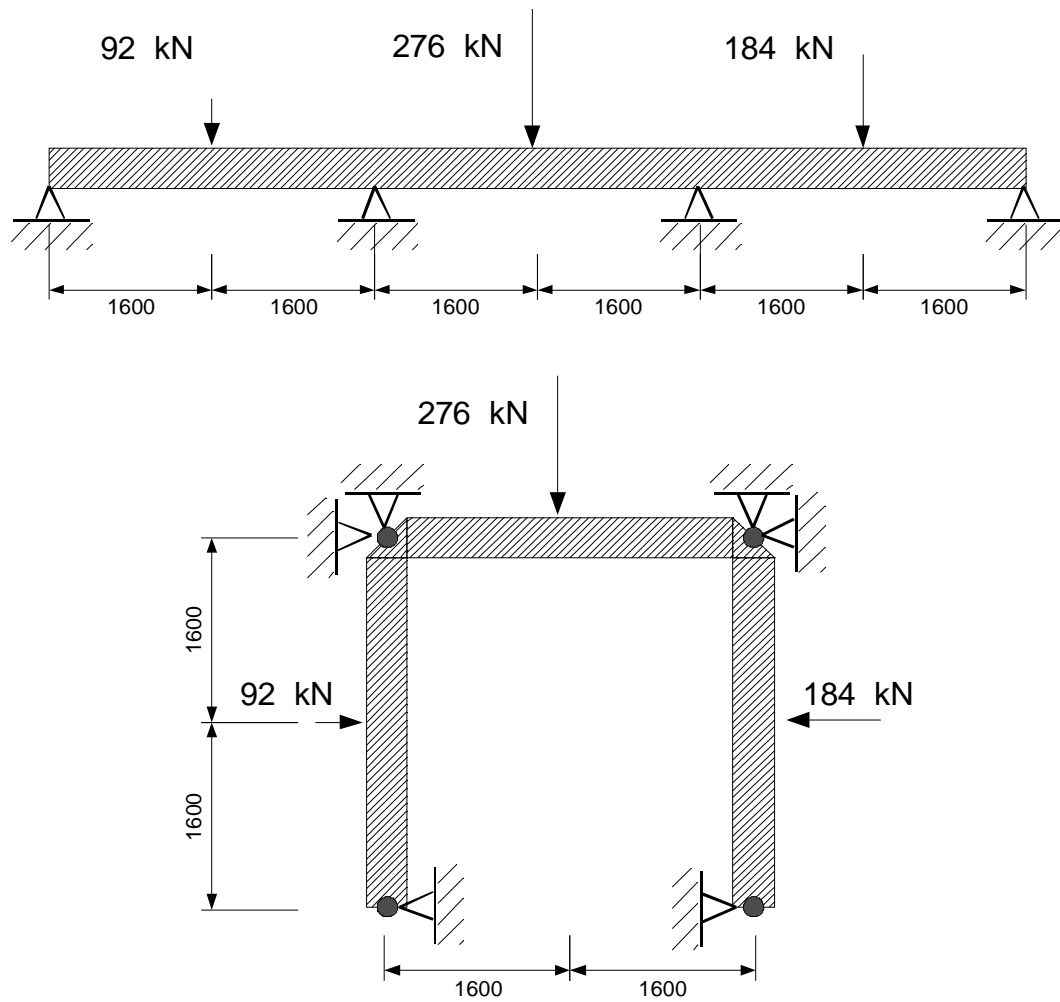


**Figure 4-1** Models for interactive lateral torsional buckling. (a) co-linear beams after Schmitke and Kennedy (1985) (b) braced frame formed with same beams

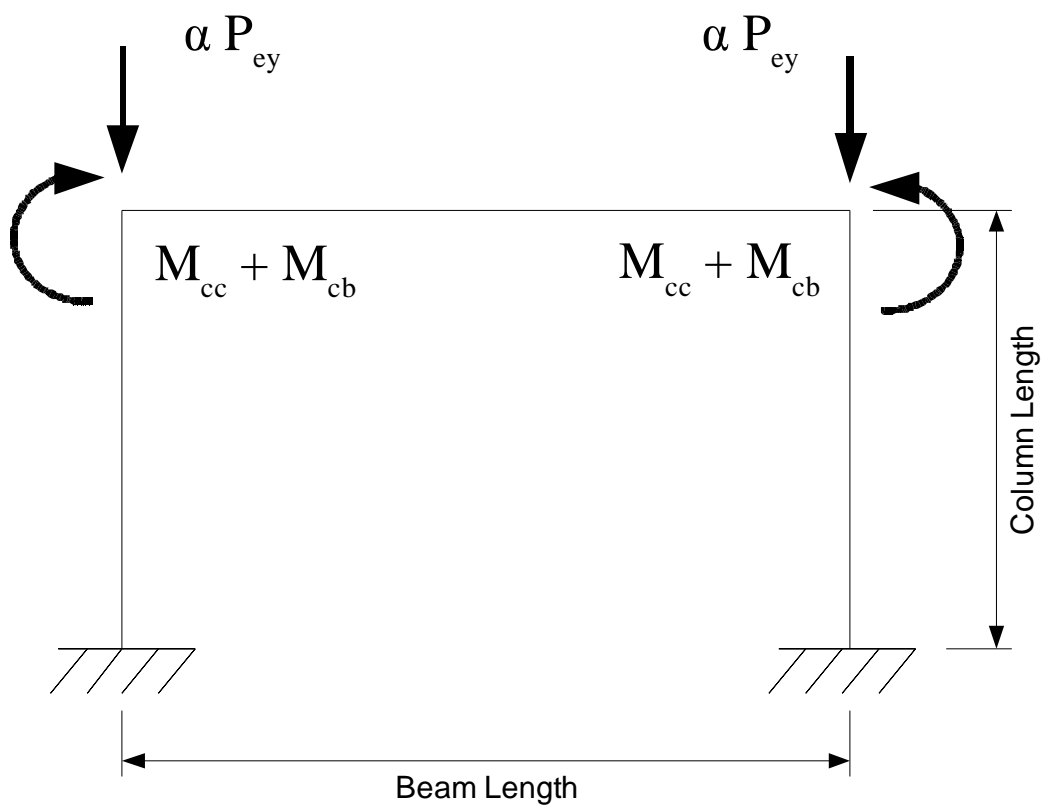


**Figure 4-2** Portal Frame



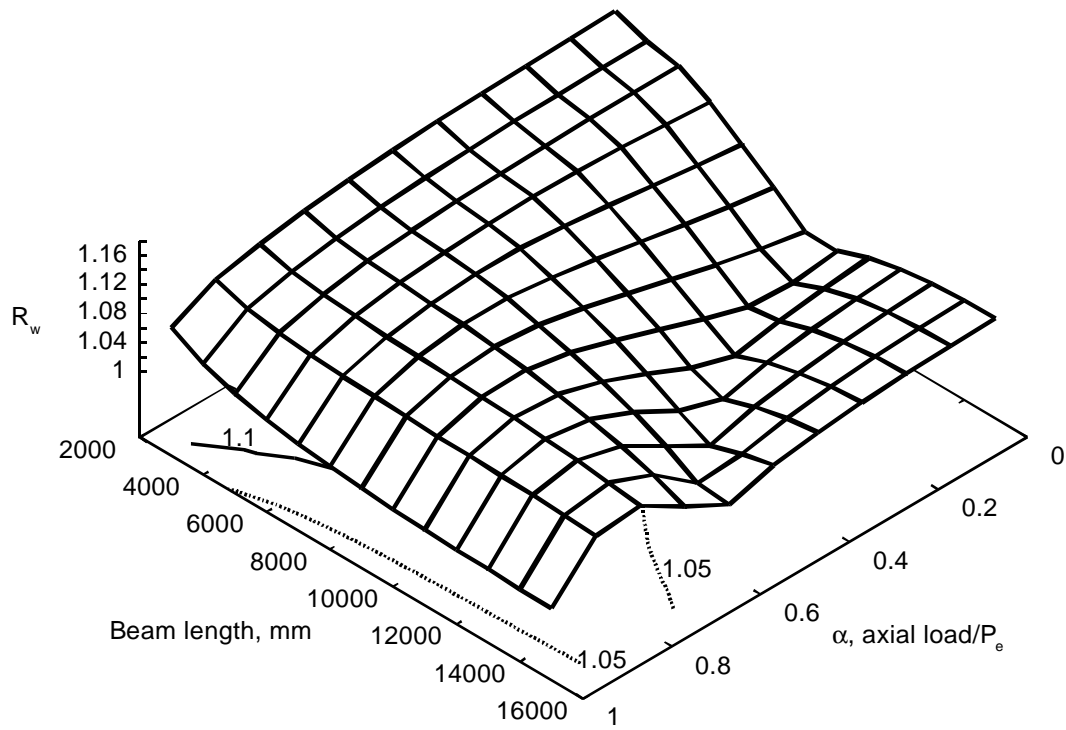


**Figure 4-3** Strength increase due to warping, 4 m columns, W200x27 beams and columns, fixed base.

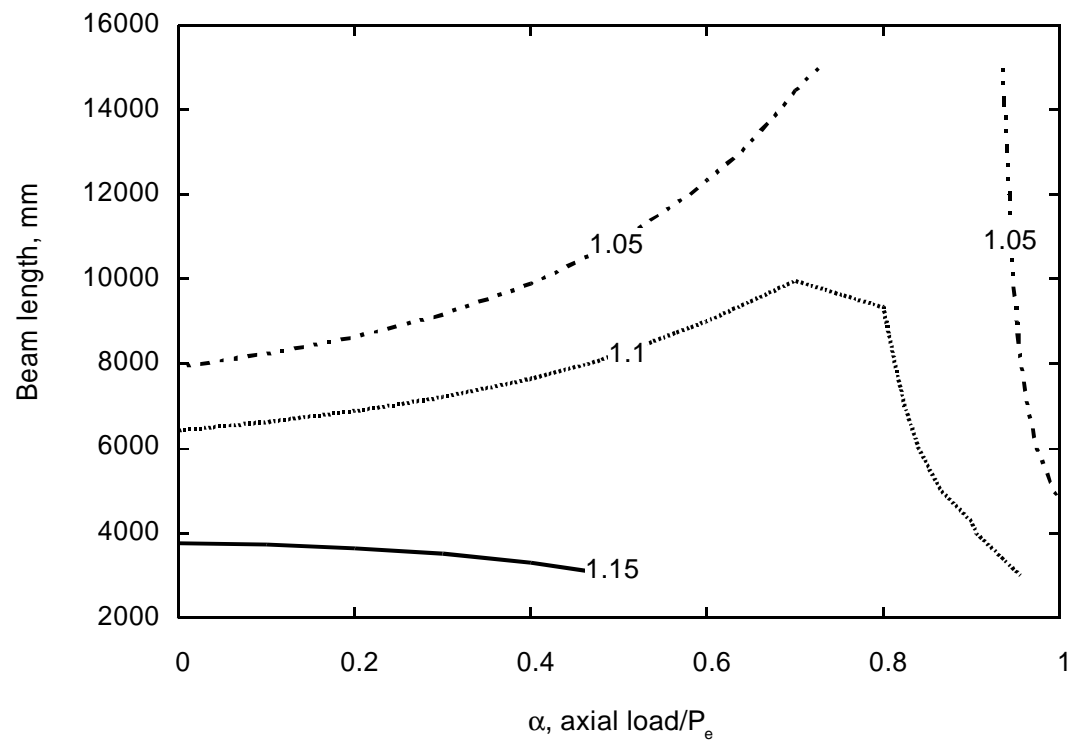


**Figure 4-4** Alternate view of Figure 4-3, strength increase due to warping, fixed base

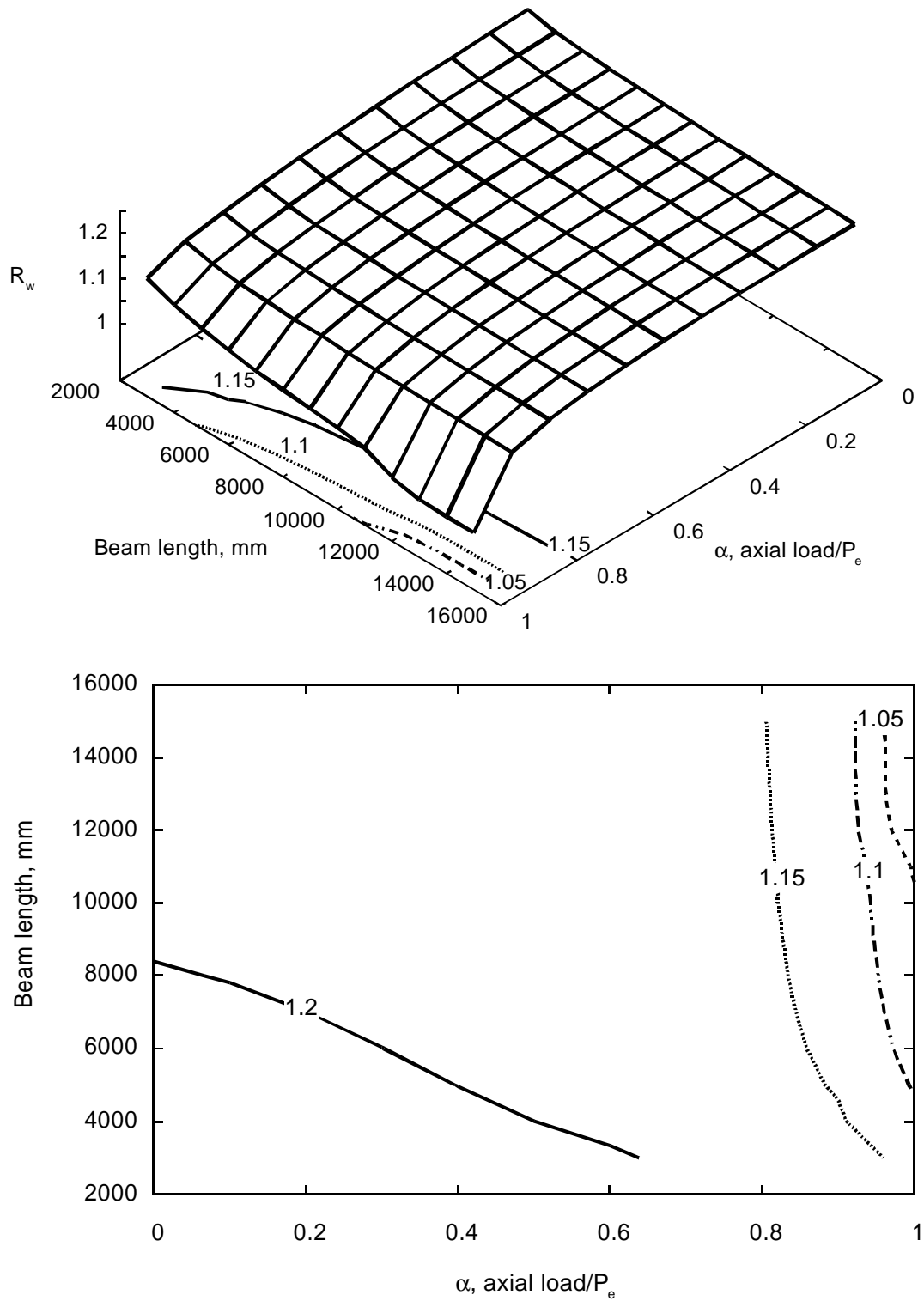


**Figure 4-5** Strength increase due to considering warping, 4 m columns, W200x27 beams and columns, pinned column base (flexible base plate)

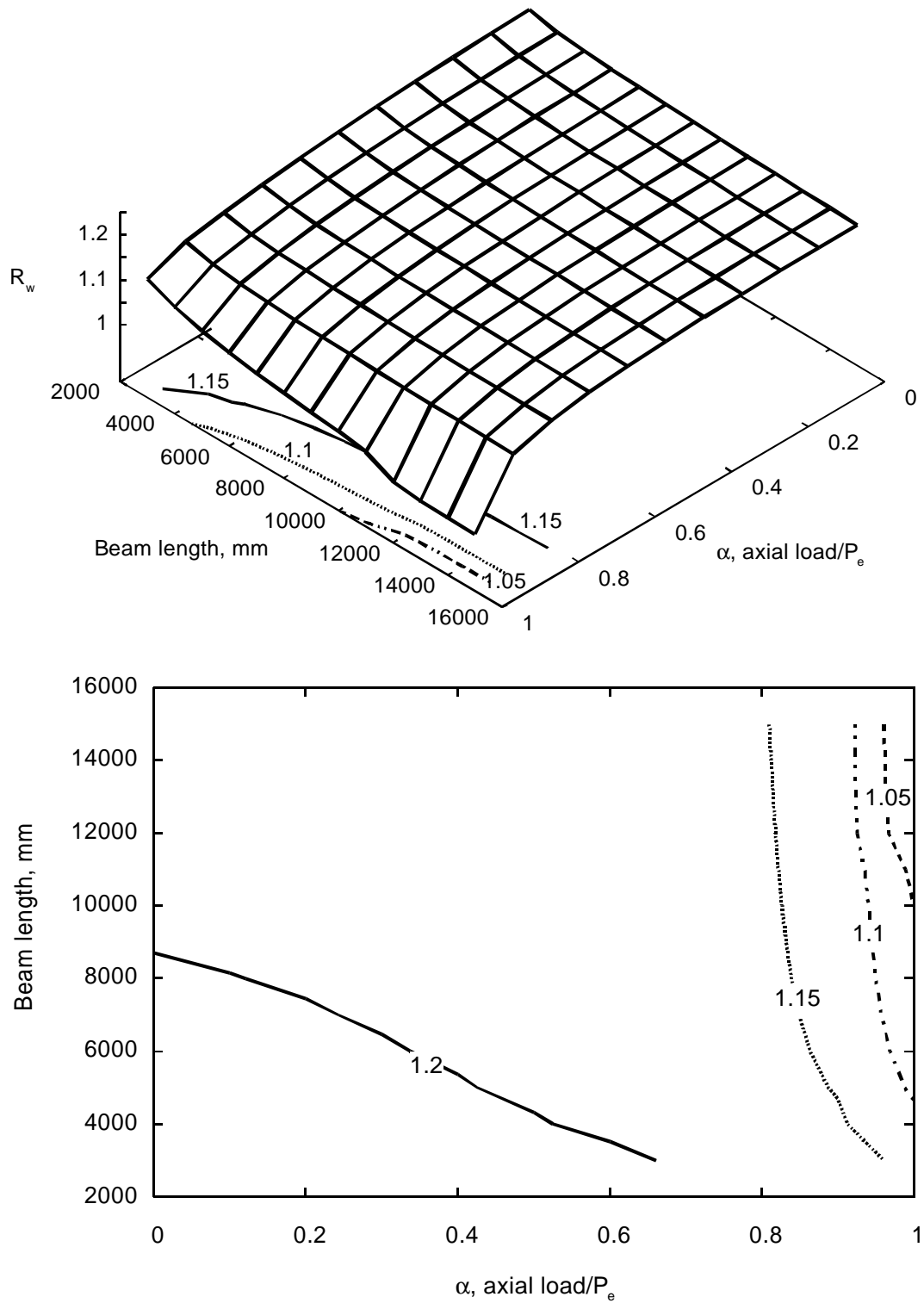


**Figure 4-6** Strength increase, 4 m columns, W200x27 beams and columns, rigid base plate (pinned end, warping rigid).

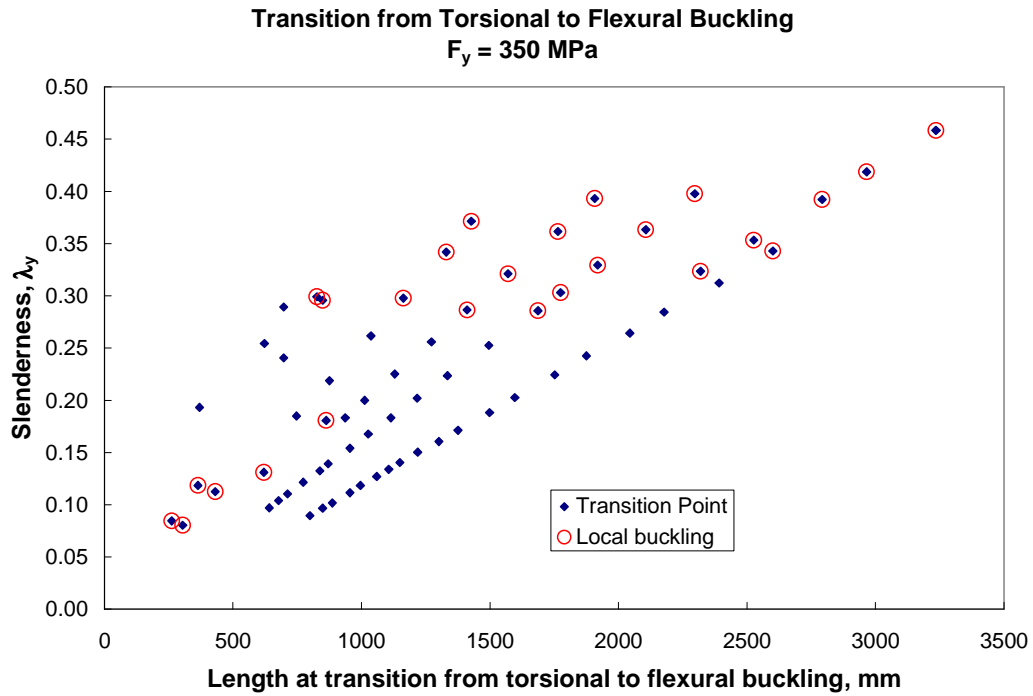


**Figure 4-7** Transition length from torsional to flexural (weak axis) buckling for all standard rolled sections.

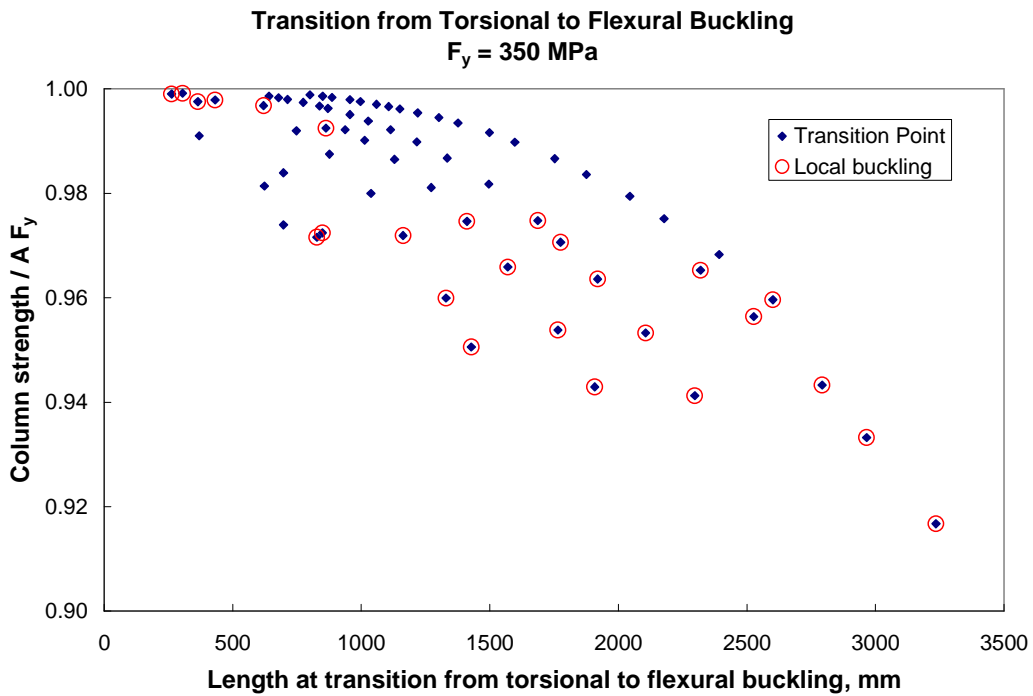


**Figure 4-8** Torsional to flexural buckling transition and column slenderness reduction.

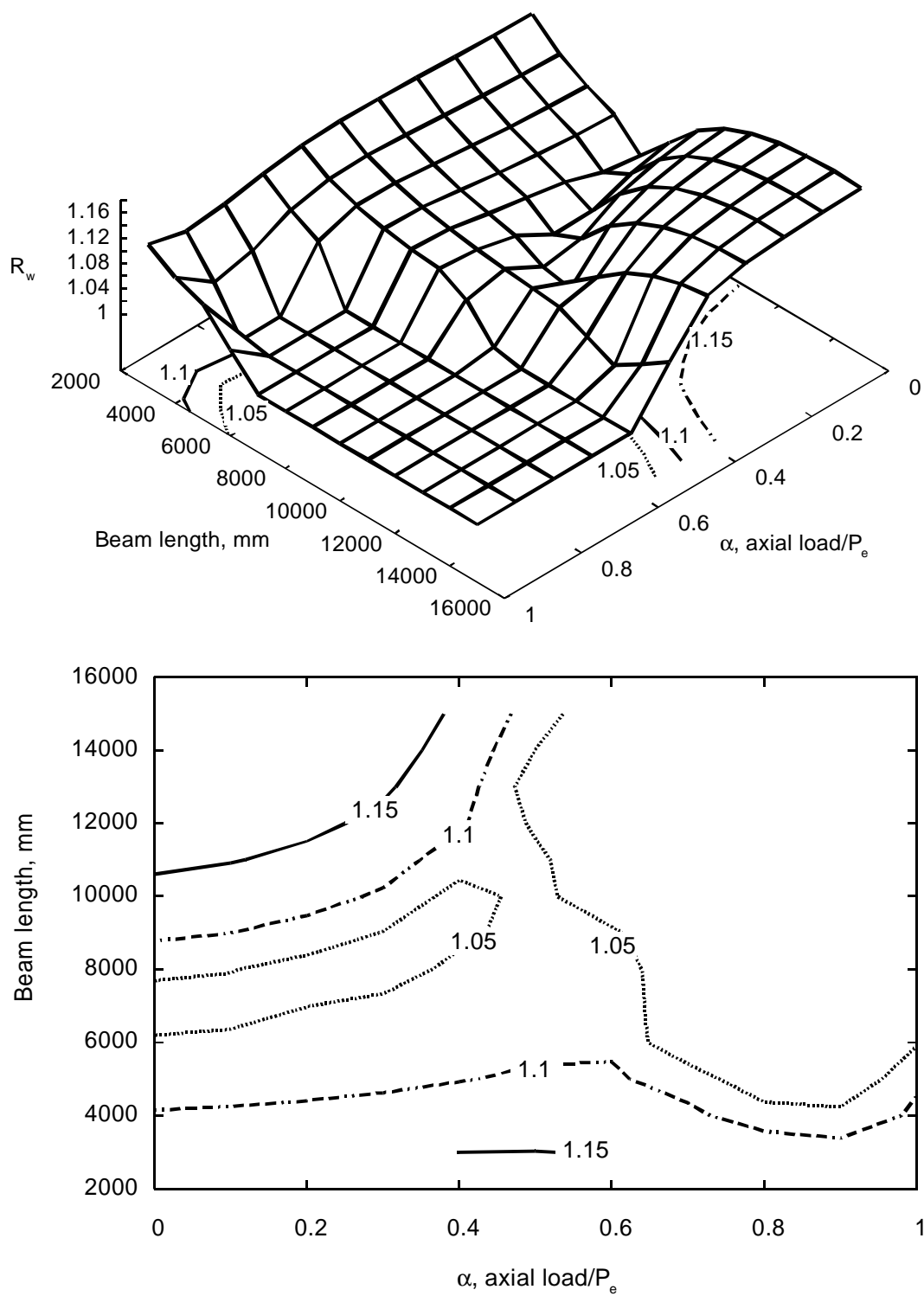


**Figure 4-9** Strength increase due to considering warping, 4 m columns, W360x134 beams and columns, fixed column base.

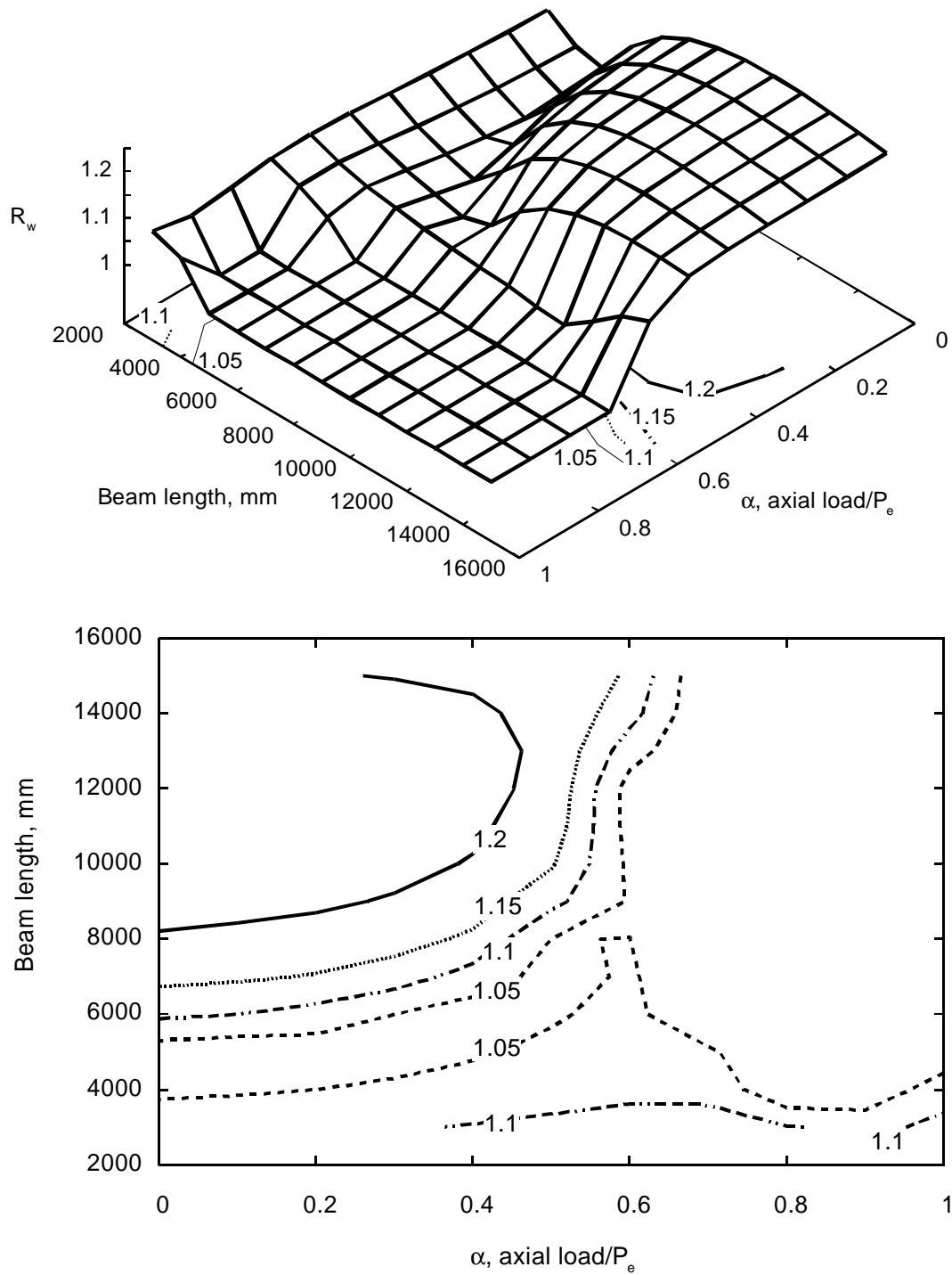


**Figure 4-10** Strength increase due to considering warping, 3 m columns, W360x134 beams and columns, fixed column base.

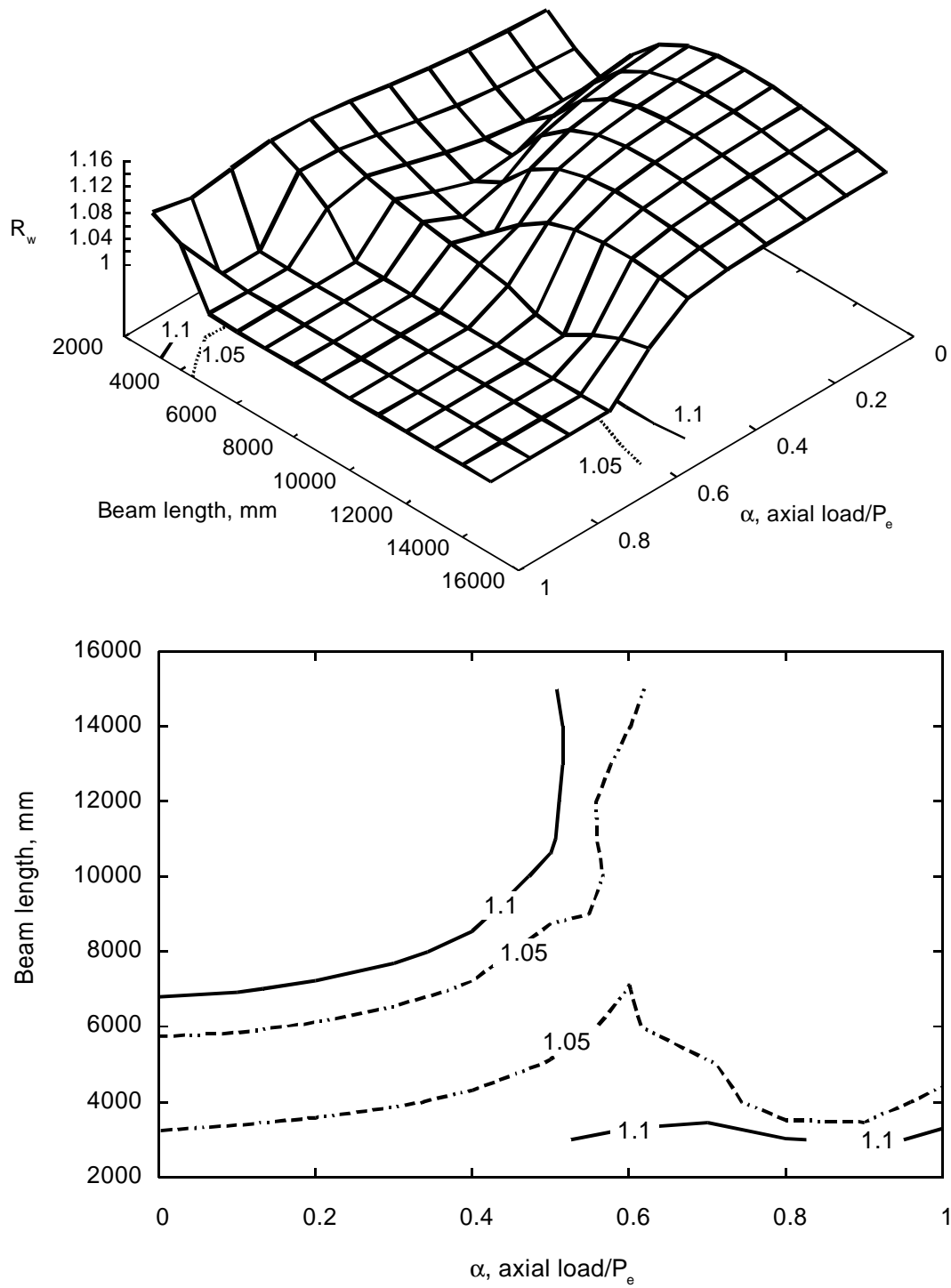


**Figure 4-11** Strength increase due to considering reversed warping deformations, 3 m columns, W360x134 beams and columns, fixed column base.

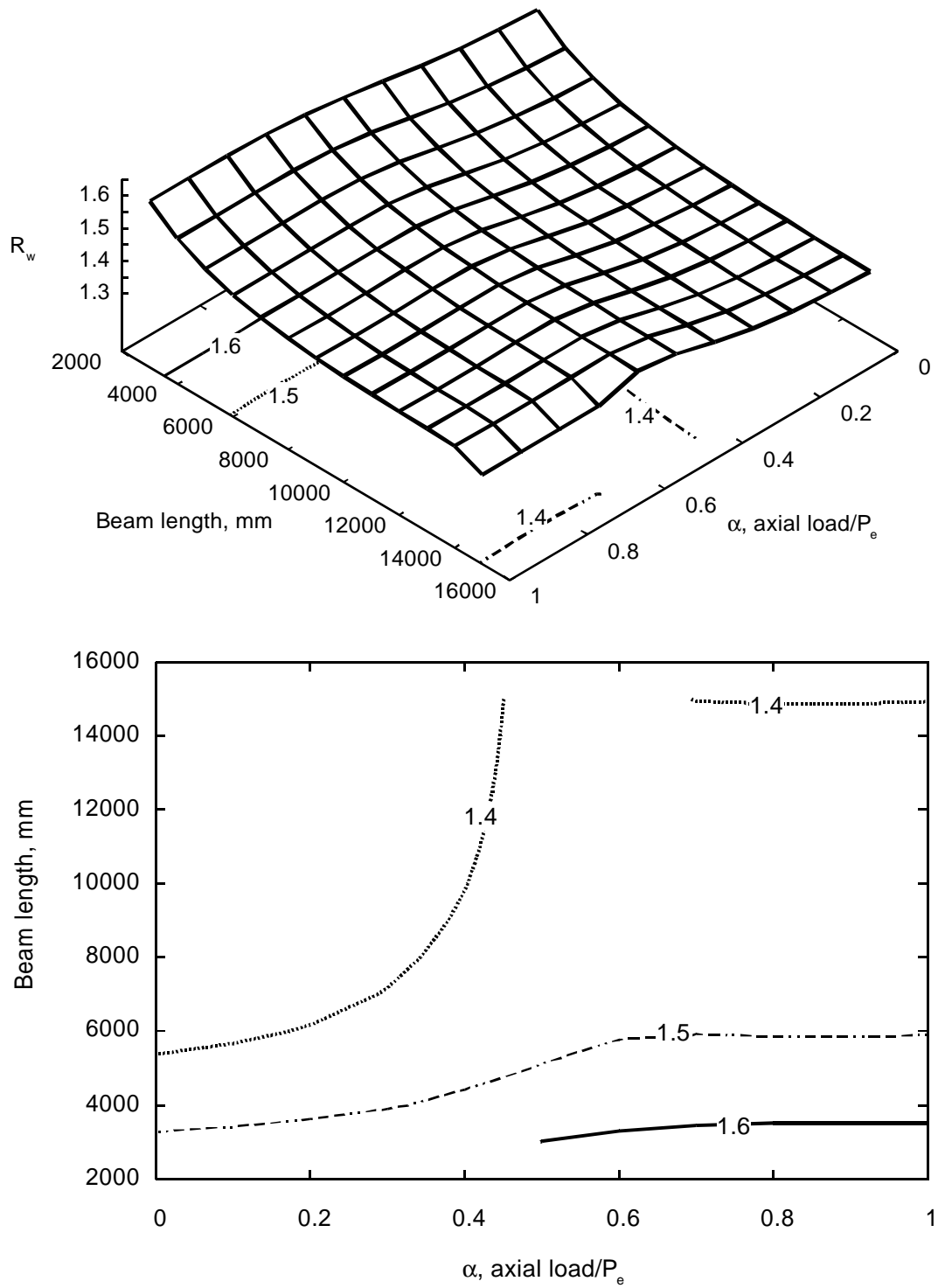


**Figure 4-12** Strength increase due to considering reversed warping deformations, 4 m columns, W360x134 beams and columns, simply supported, flexible column base.



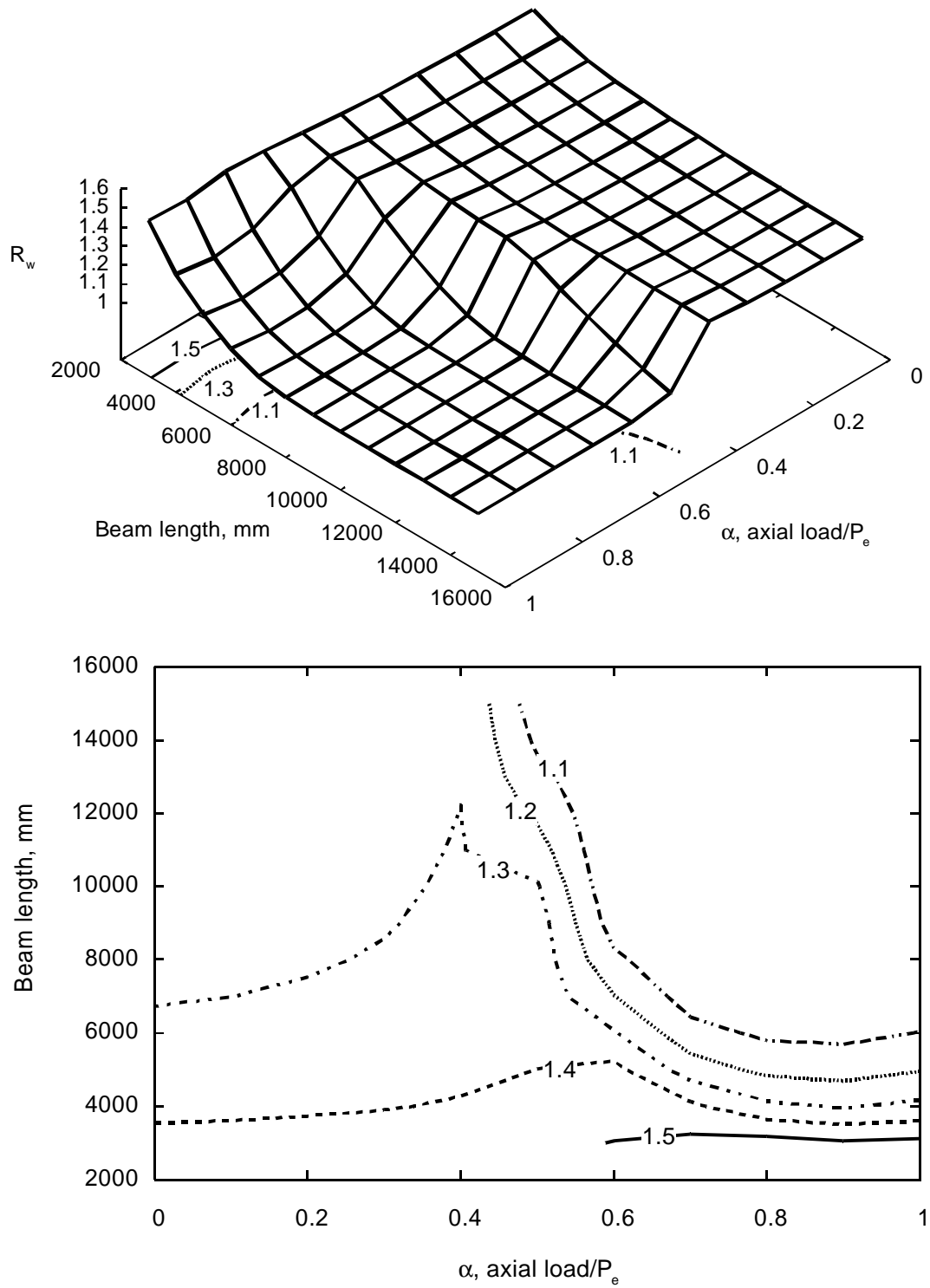


**Figure 4-13** Strength increase due to considering reversed warping deformations, 4m columns, W360x134 beams and columns, simply supported, rigid column base.

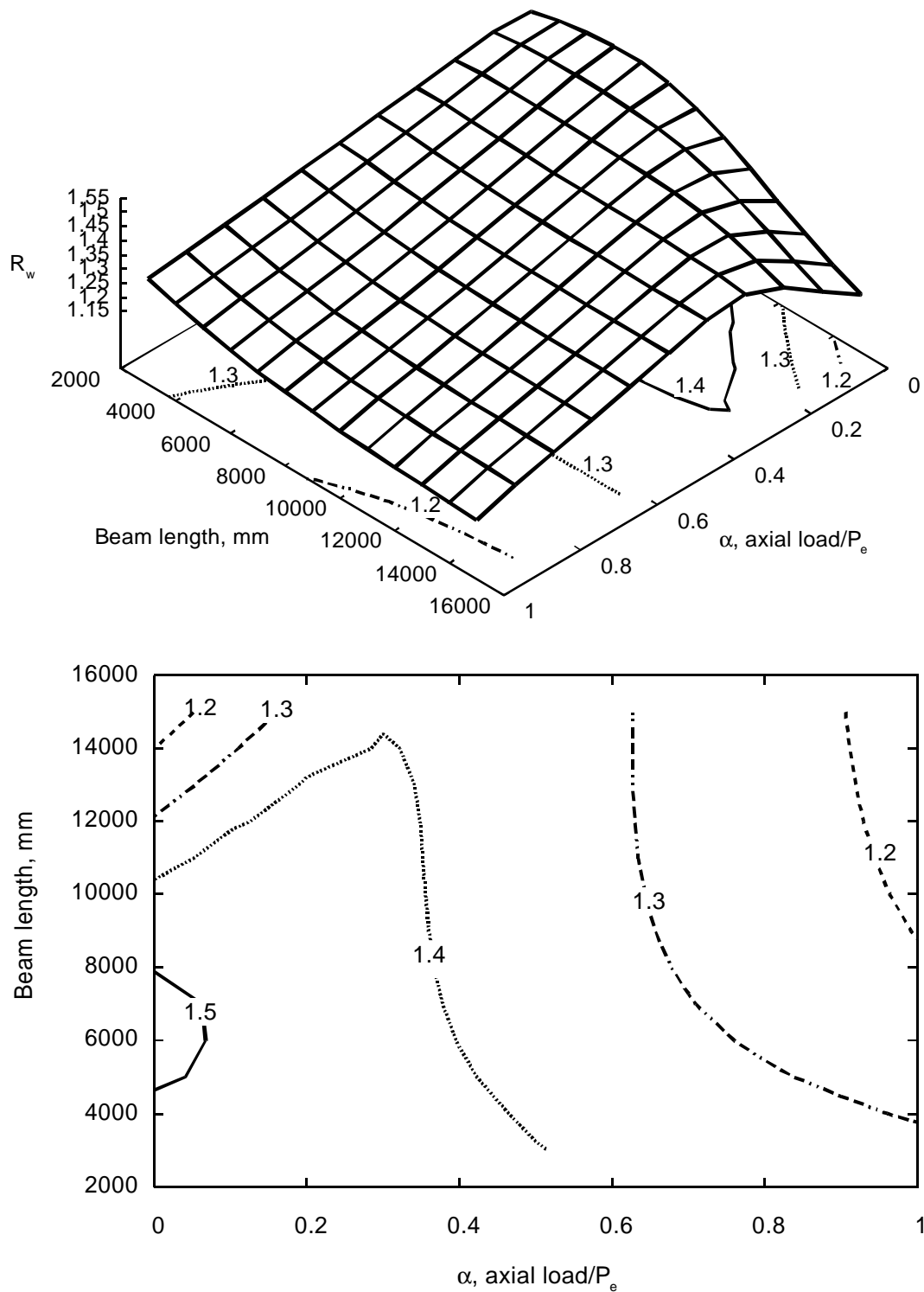


**Figure 4-14** Strength increase due to considering reversed warping deformations, 4 m columns, W690x125 beams and W200x27 columns, pinned, flexible column bases.

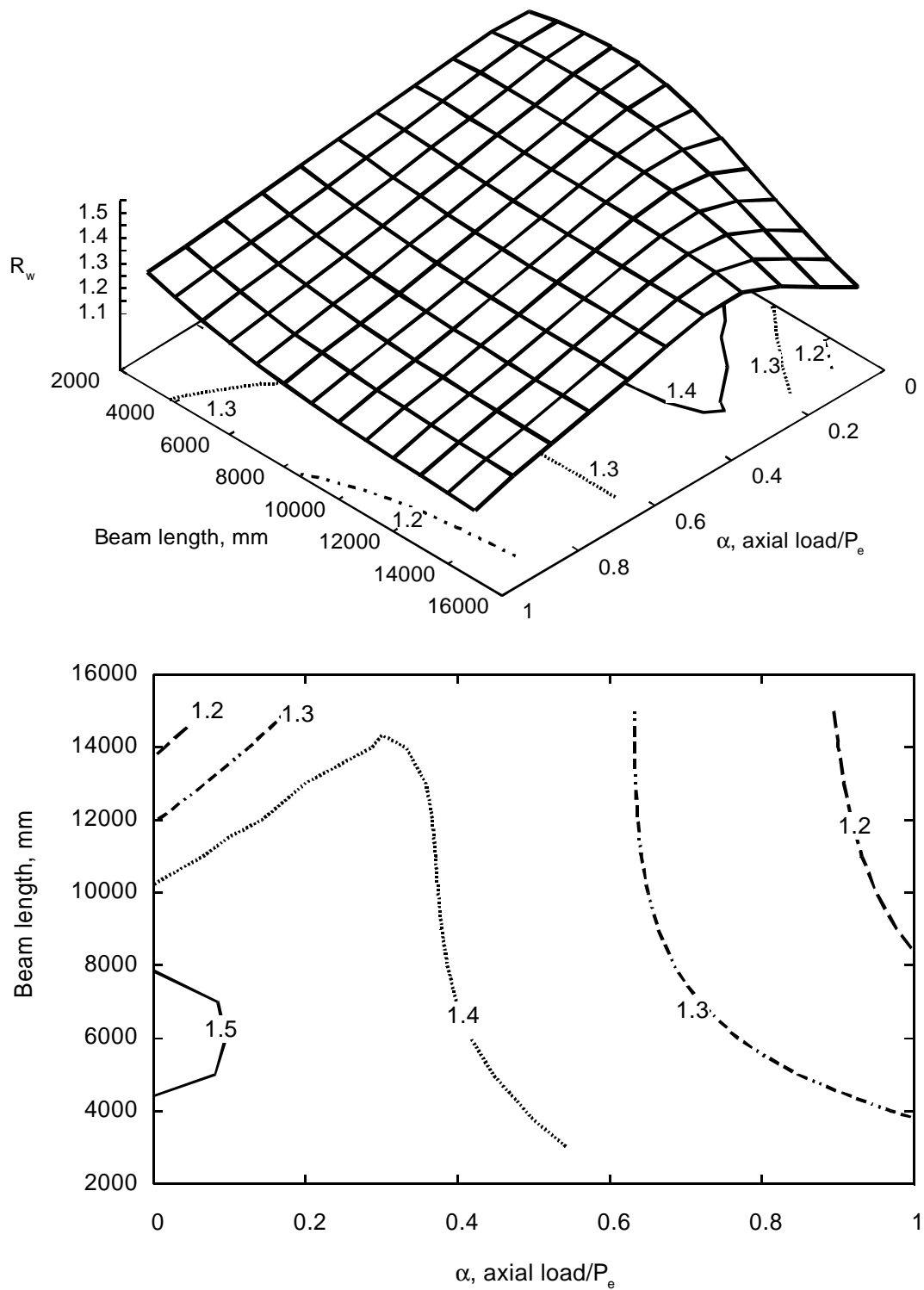


**Figure 4-15** Strength increase due to considering reversed warping deformations, 4 m columns, W690x125 beams and W200x27 columns, pinned, warping fixed column bases.

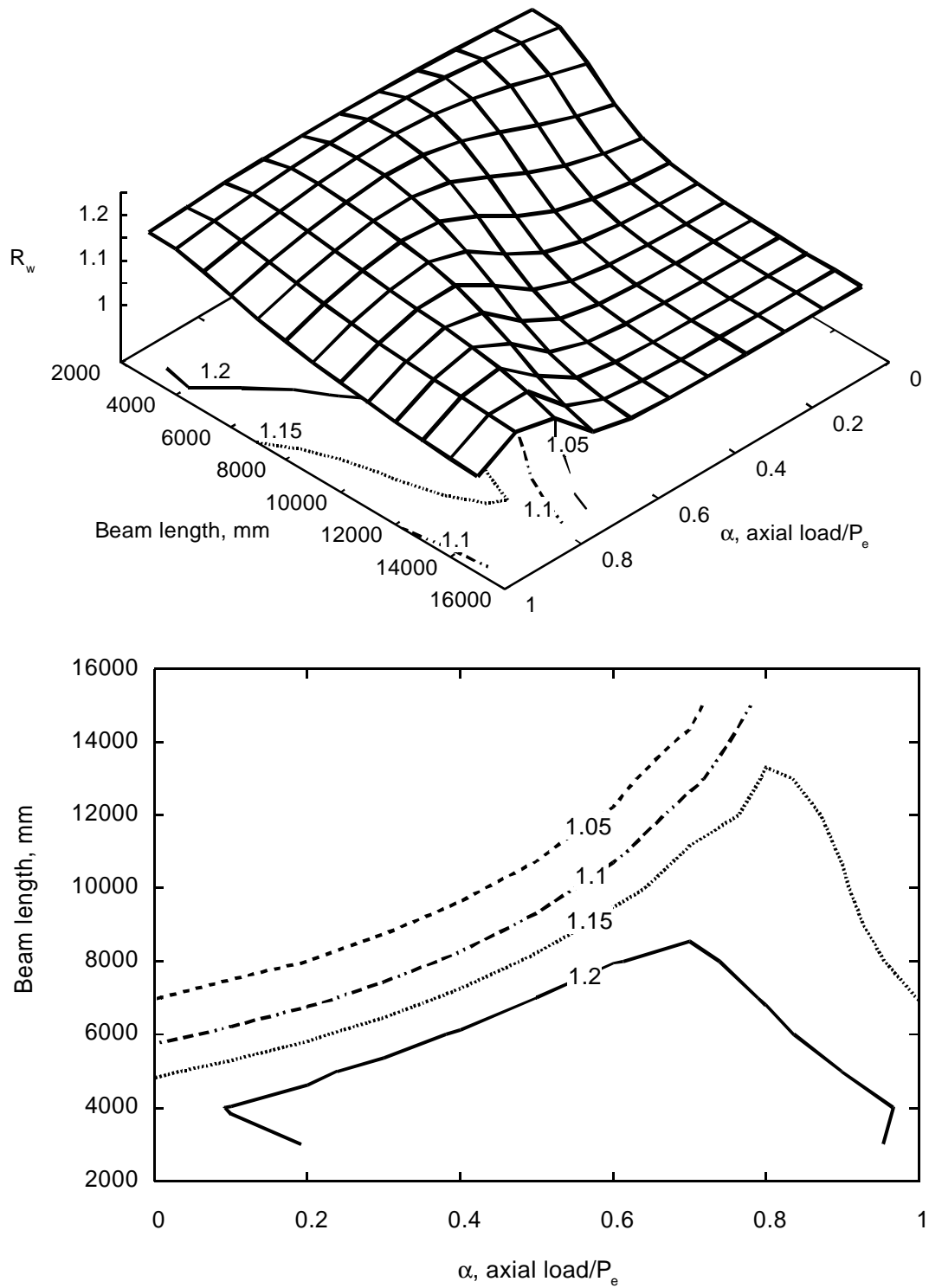


**Figure 4-16** Strength increase due to considering warping deformations, 3 m columns, W690x125 beams and W200x27 columns, fixed column bases.

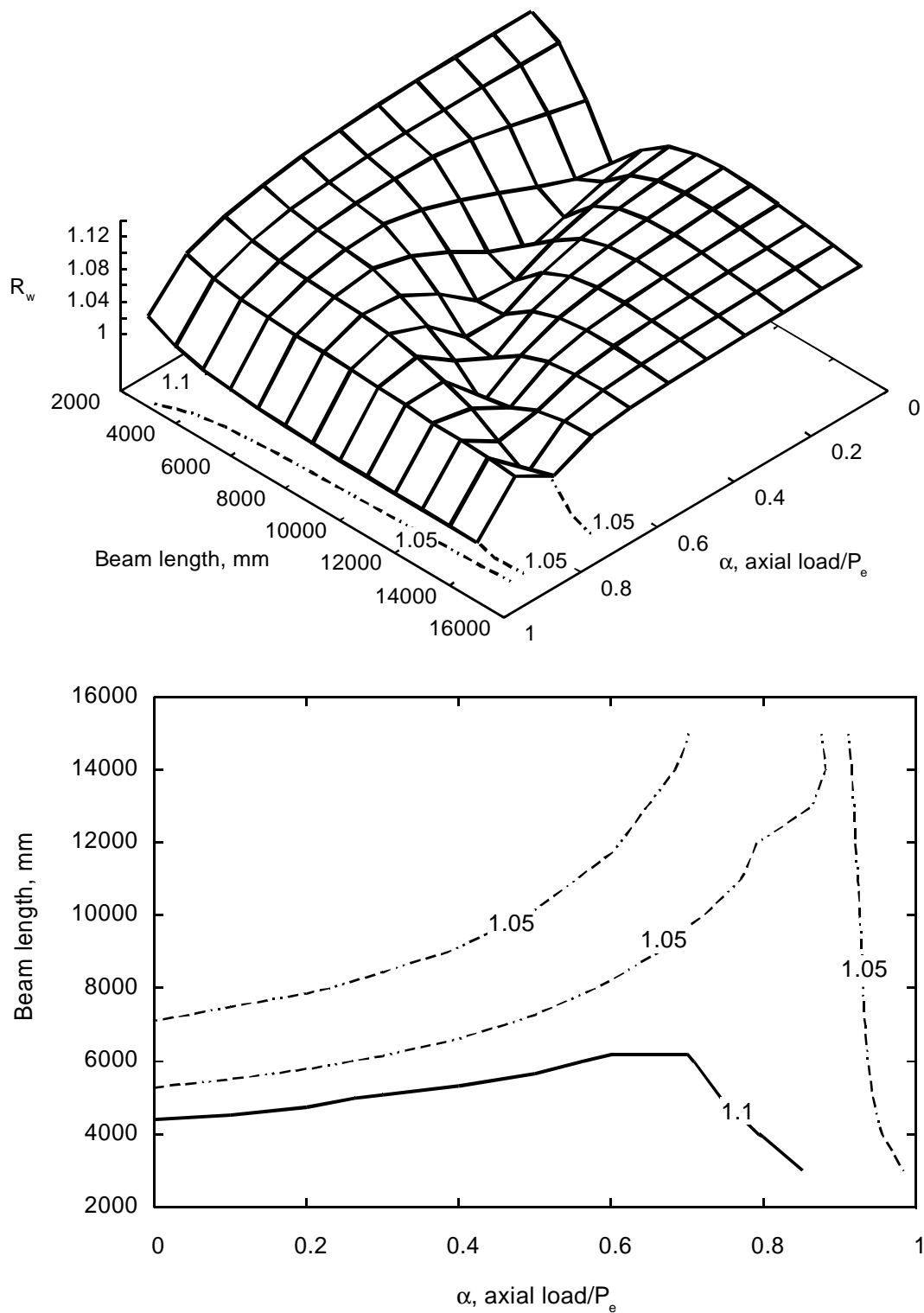


**Figure 4-17** Braced frame, all members W200x27, 3 m columns, fixed column base.

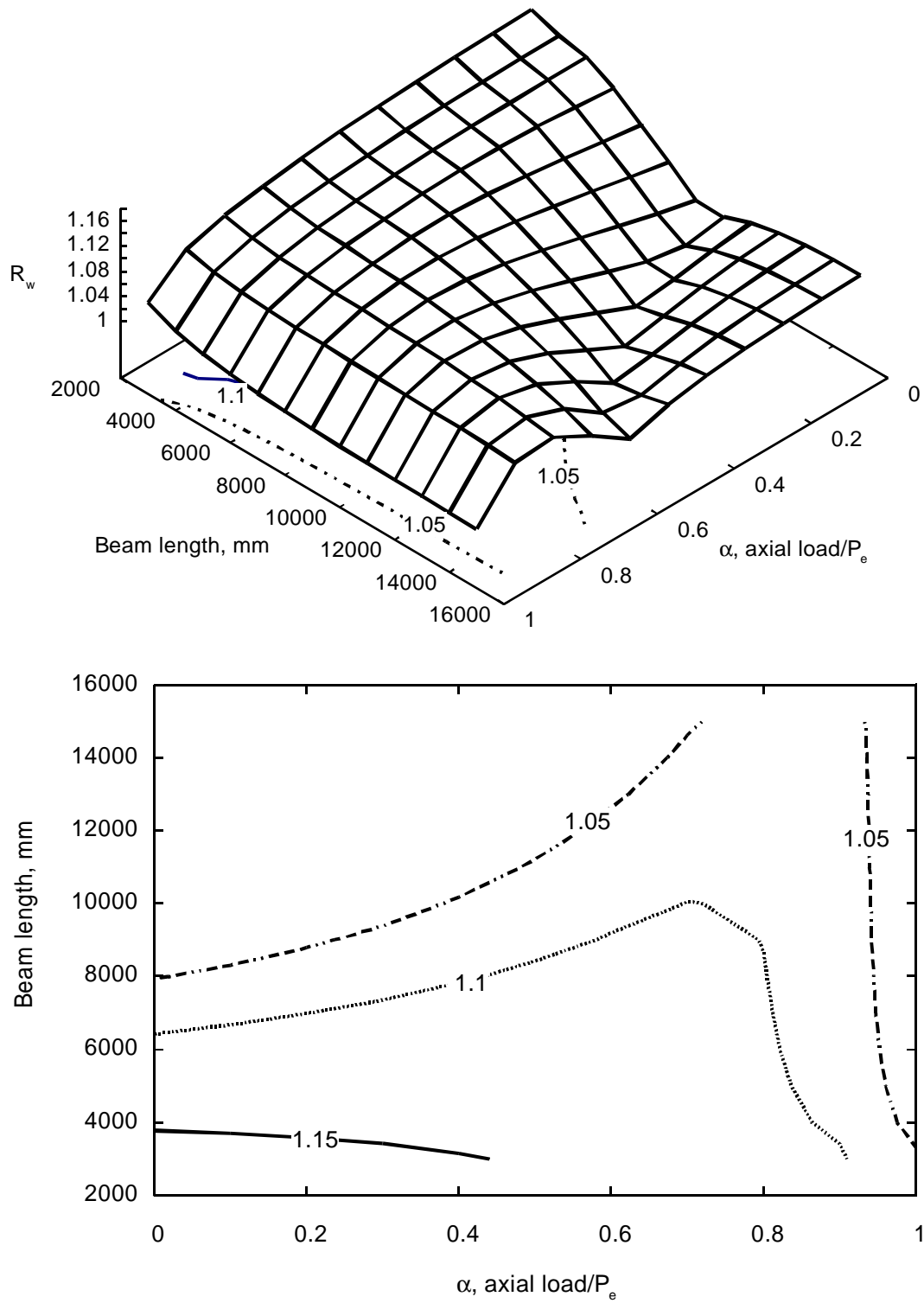


**Figure 4-18** Braced frame, all members W200x27, 4 m columns, fixed column base.

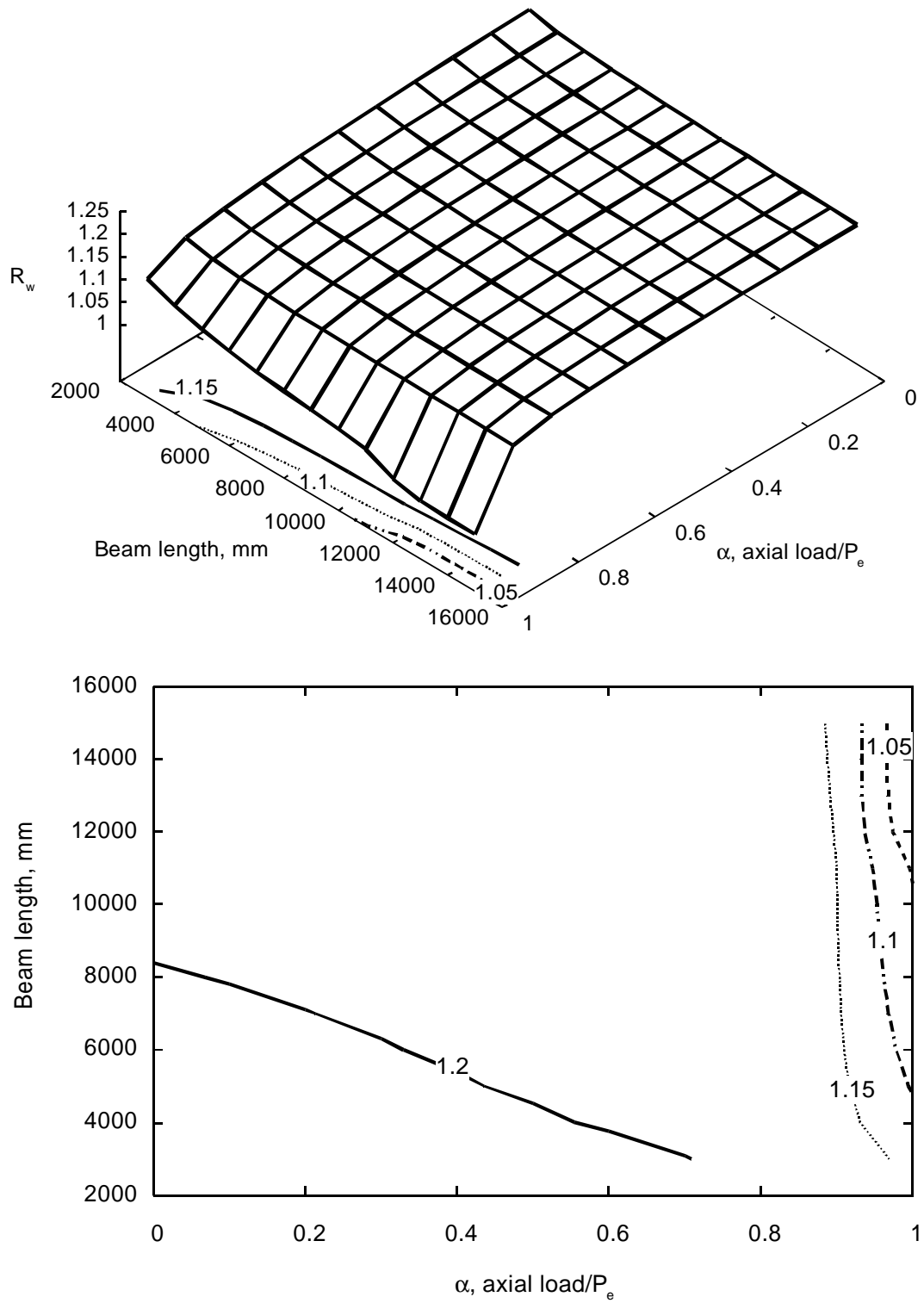


**Figure 4-19** Braced frame, all members W200x27, 4 m columns, simply support column base.

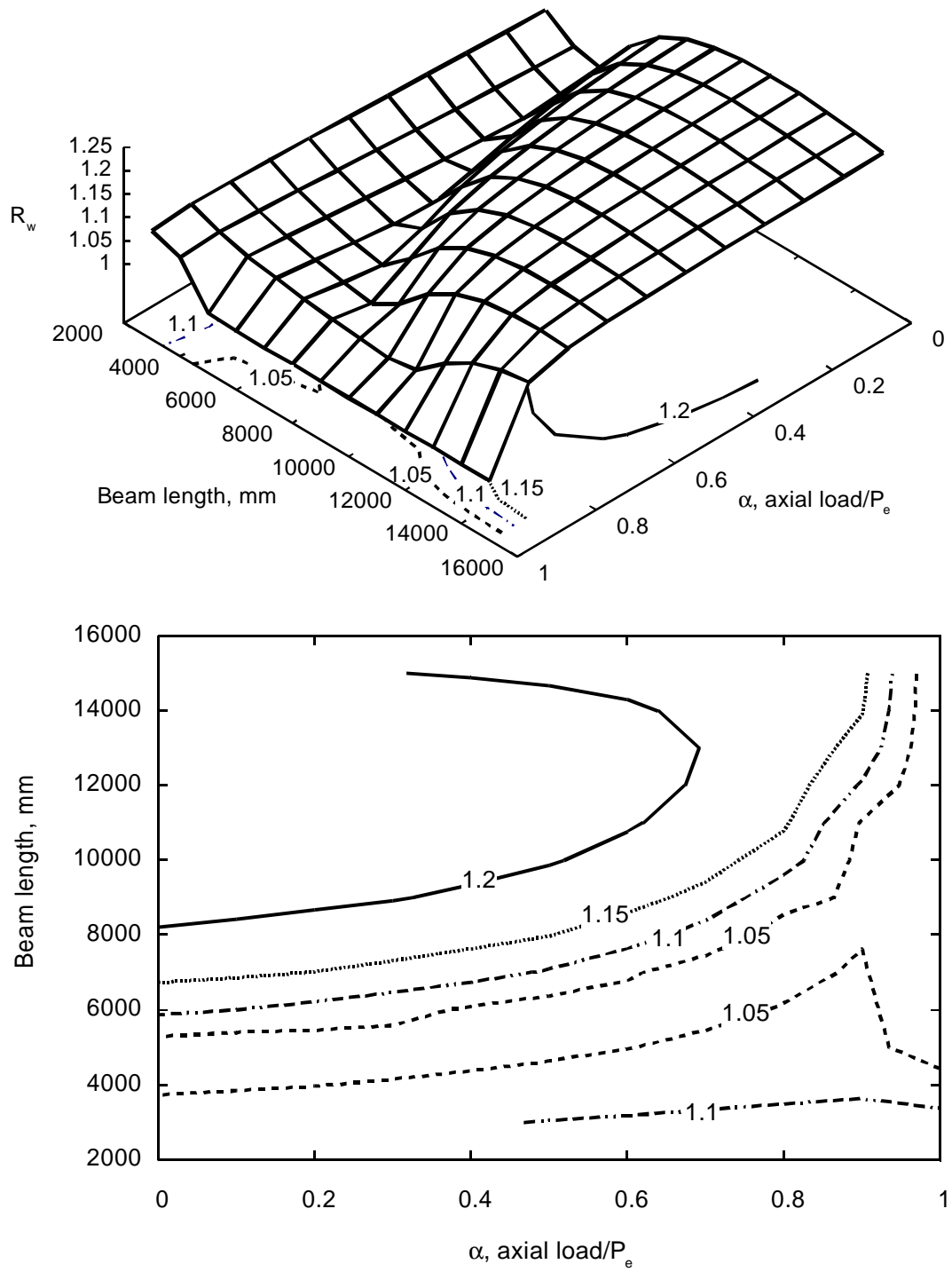


**Figure 4-20** Braced frame, all members W360x134, 3 m columns, fixed column base



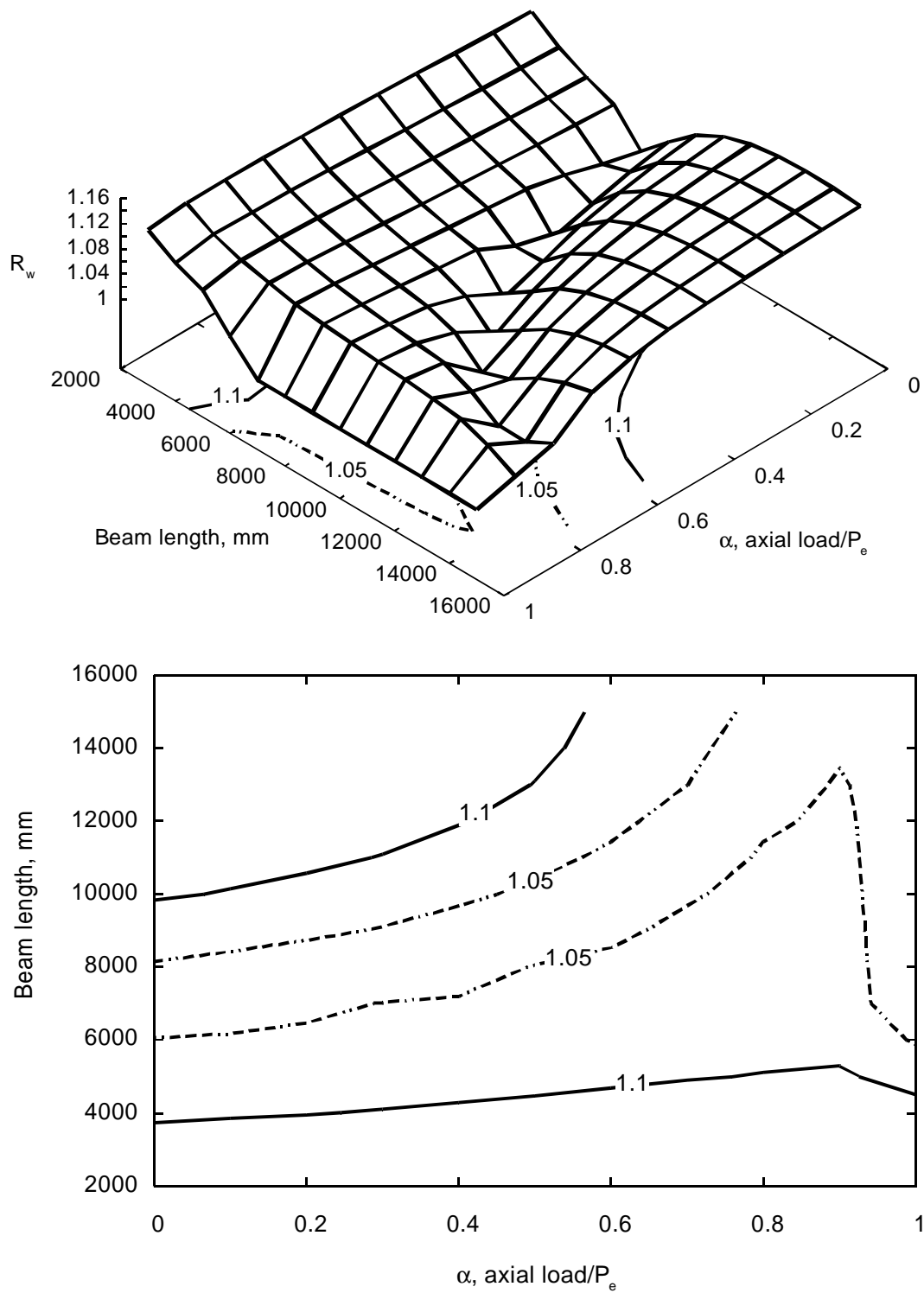


**Figure 4-21** Braced frame, all members W360x134, 4 m columns, fixed base, reversed warping.

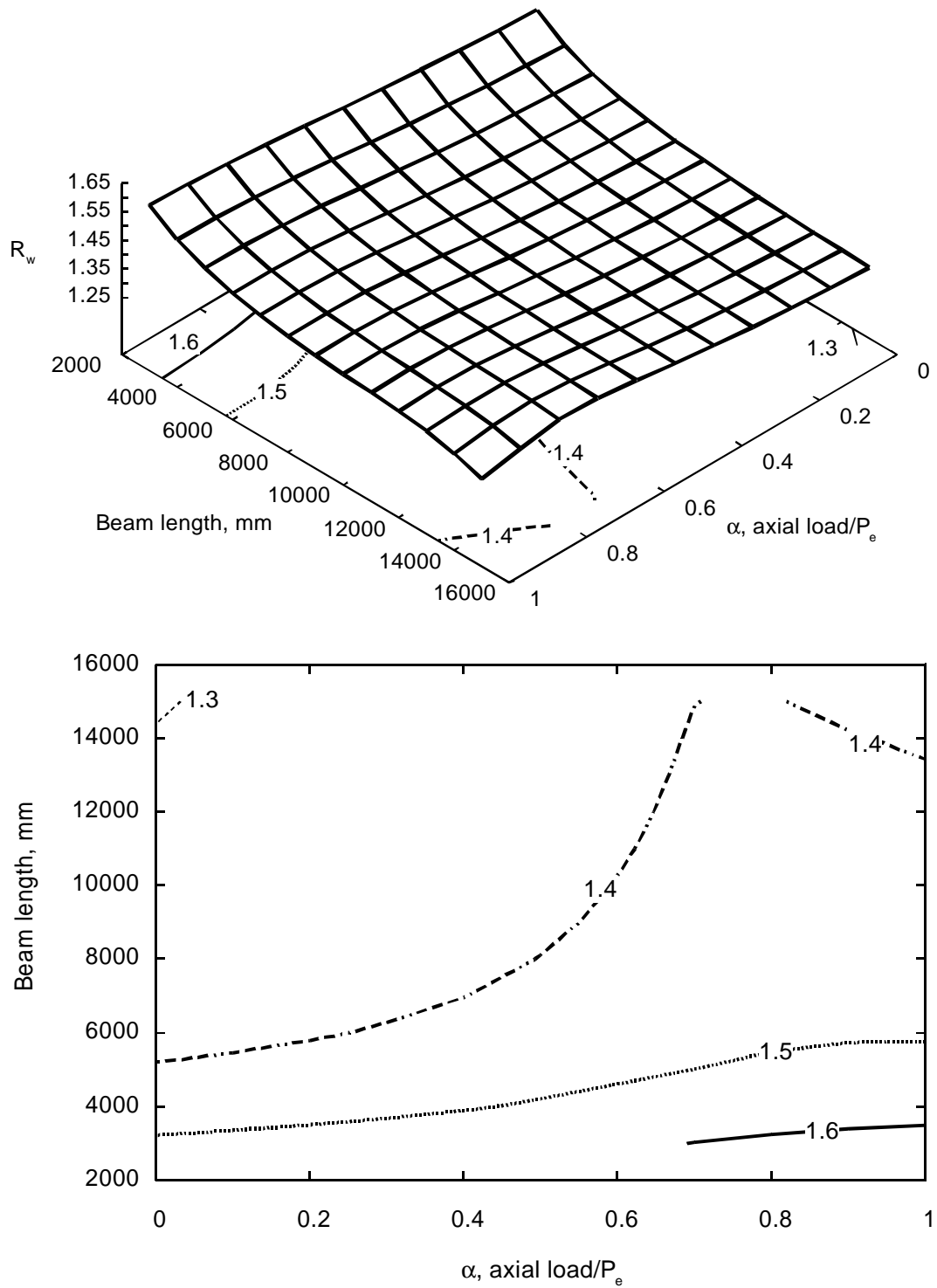


**Figure 4-22** Braced frame, all members W360x134, 4 m columns, simply supported base.

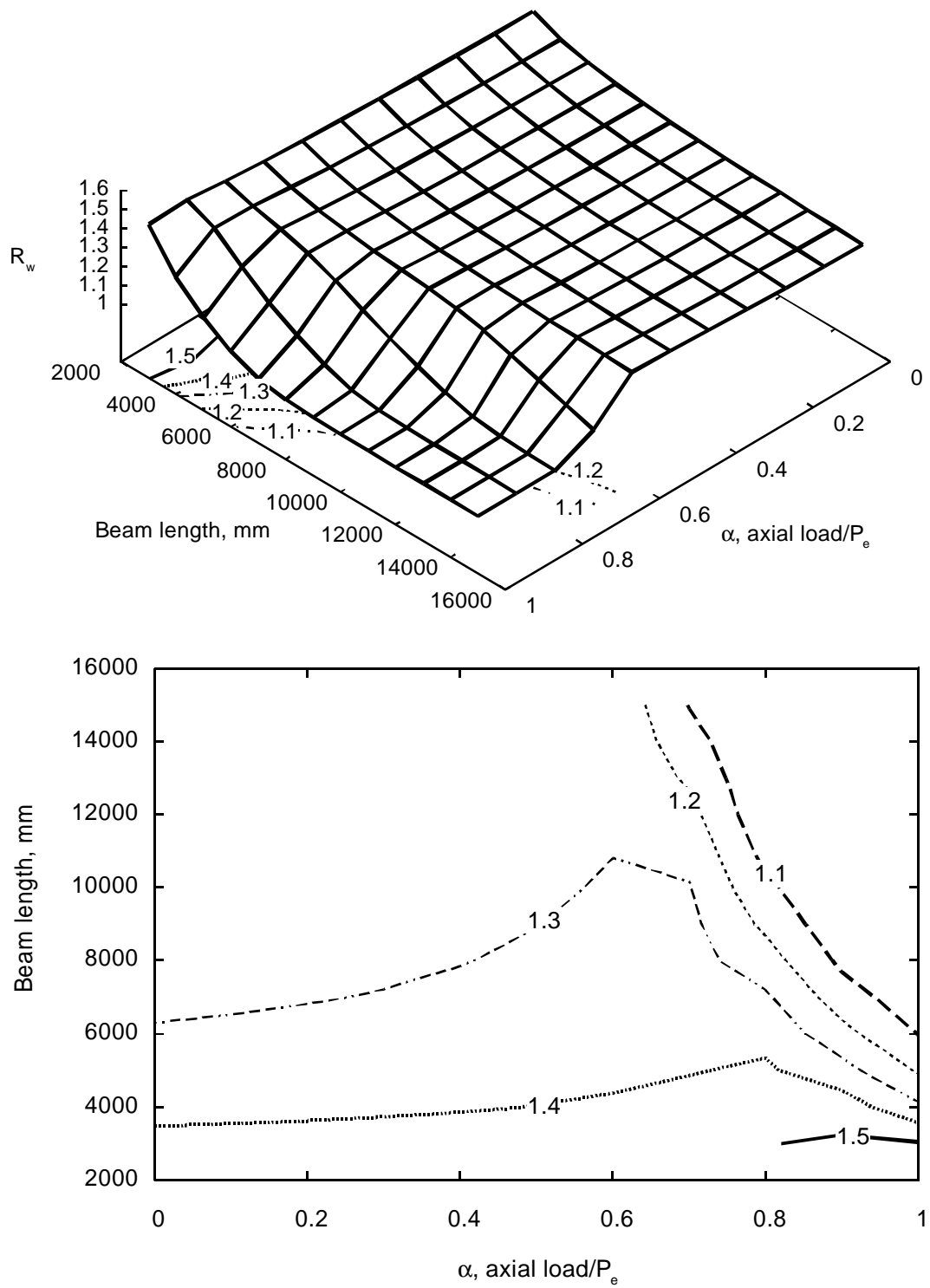
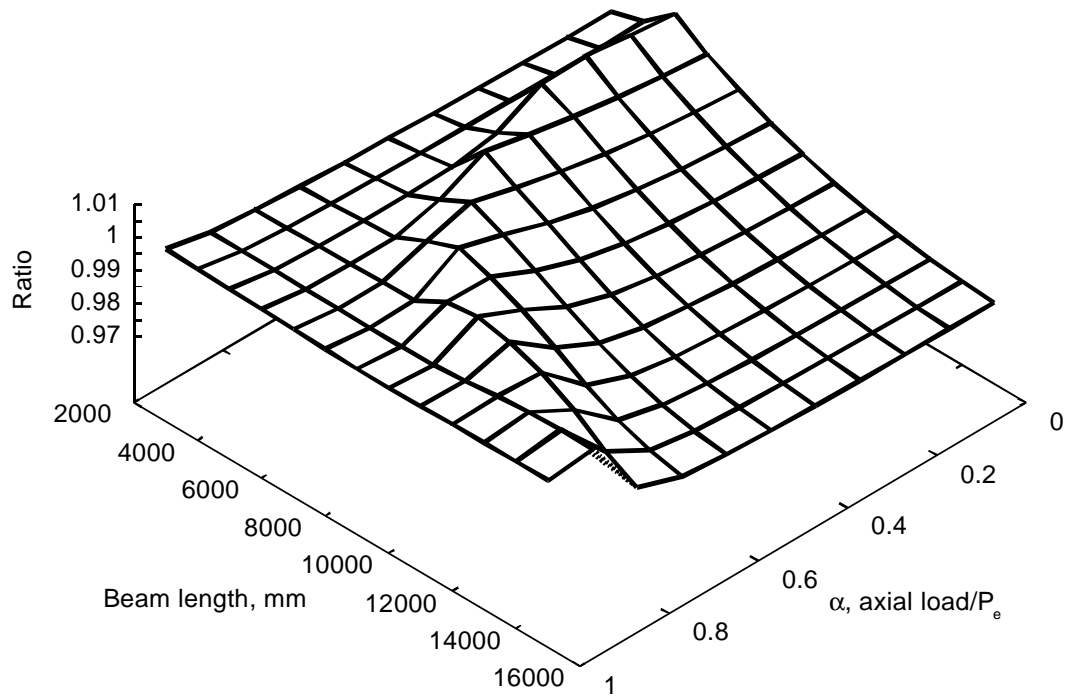
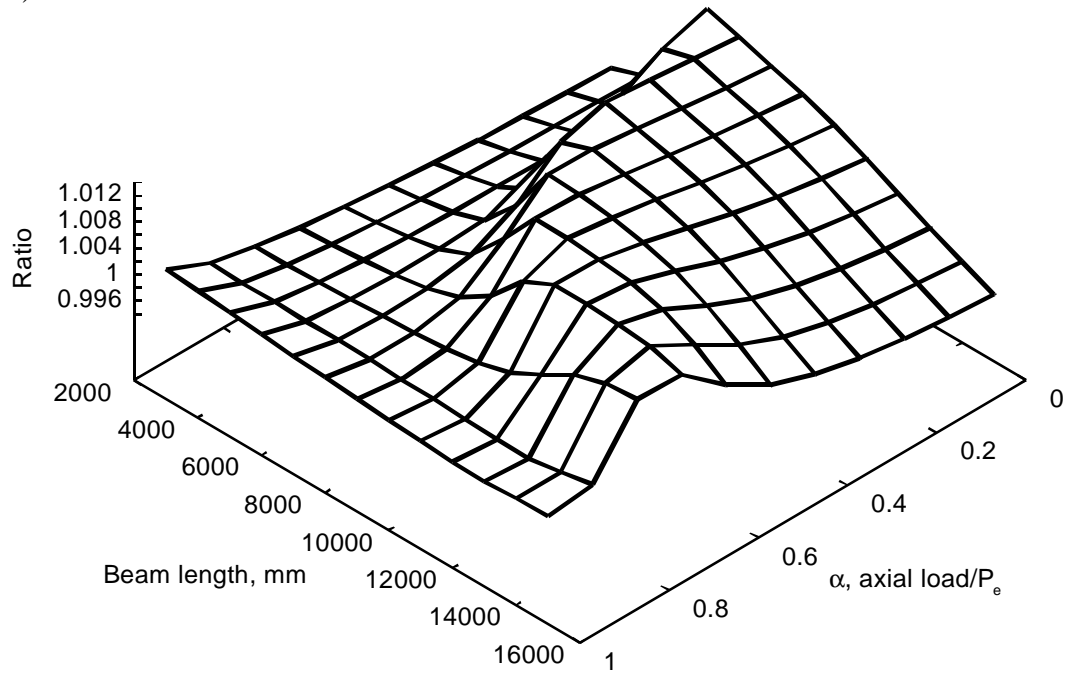


**Figure 4-23** Braced frame, all members W360x134, 4 m columns, warping rigid base.

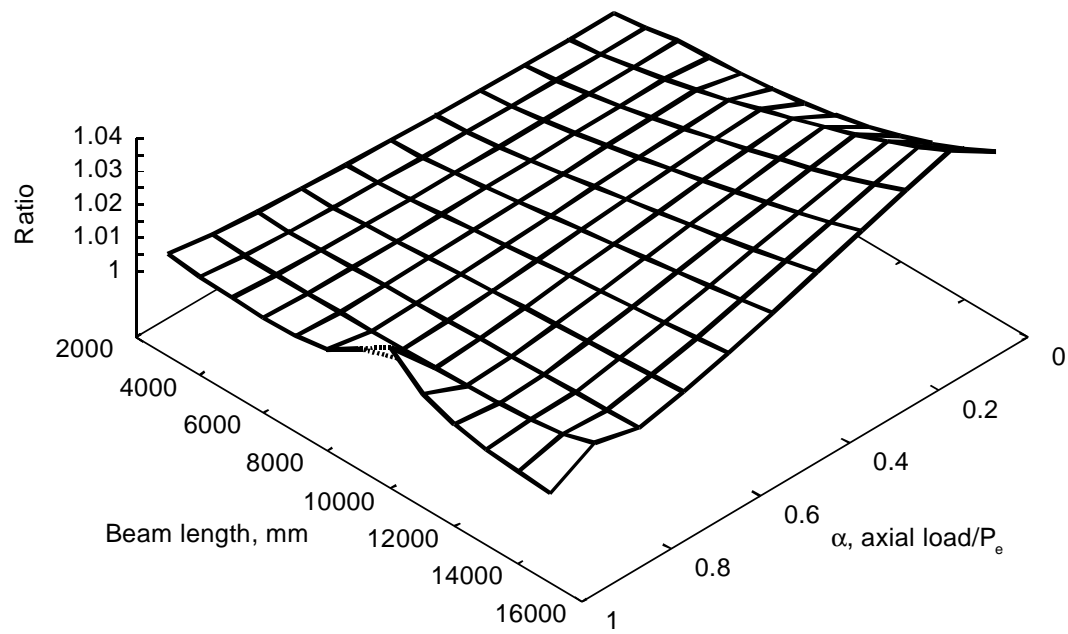


a)

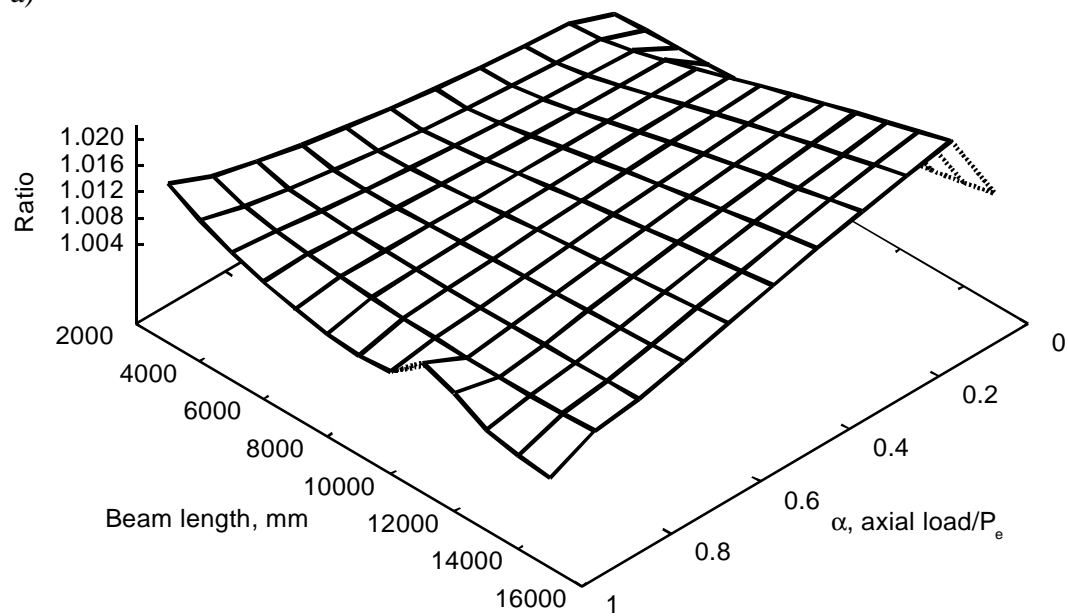


b)

**Figure 4-24** Ratio of strengths for direct warping to reversed warping, a) 3 m and b) 4 m columns, W200x27 frame, fixed column bases, unbraced.

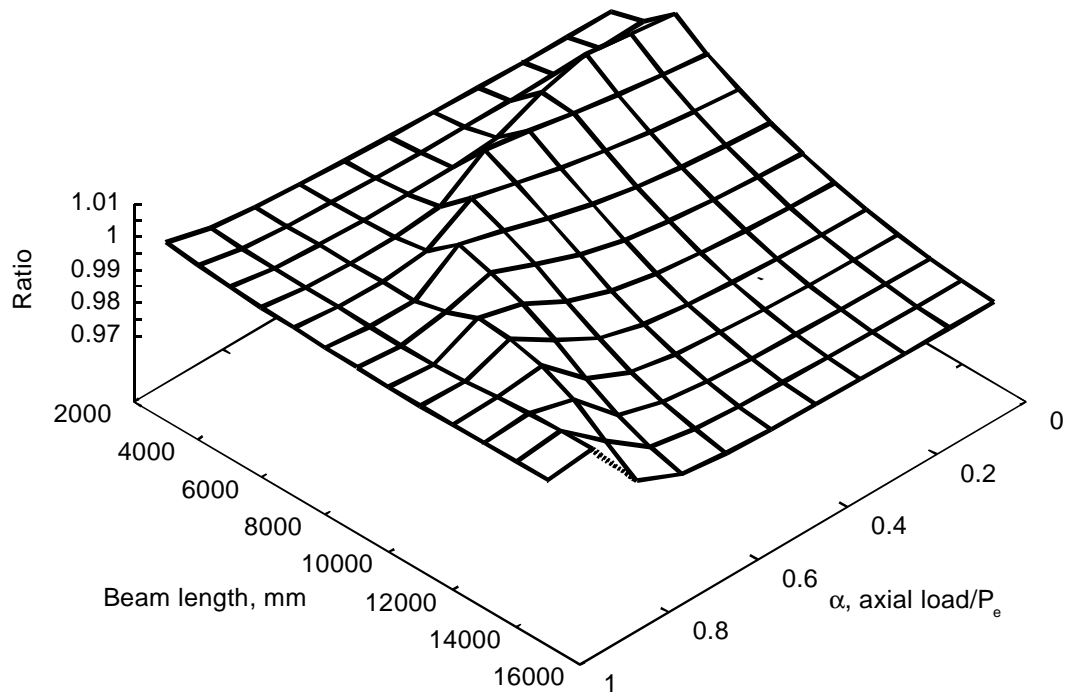


a)

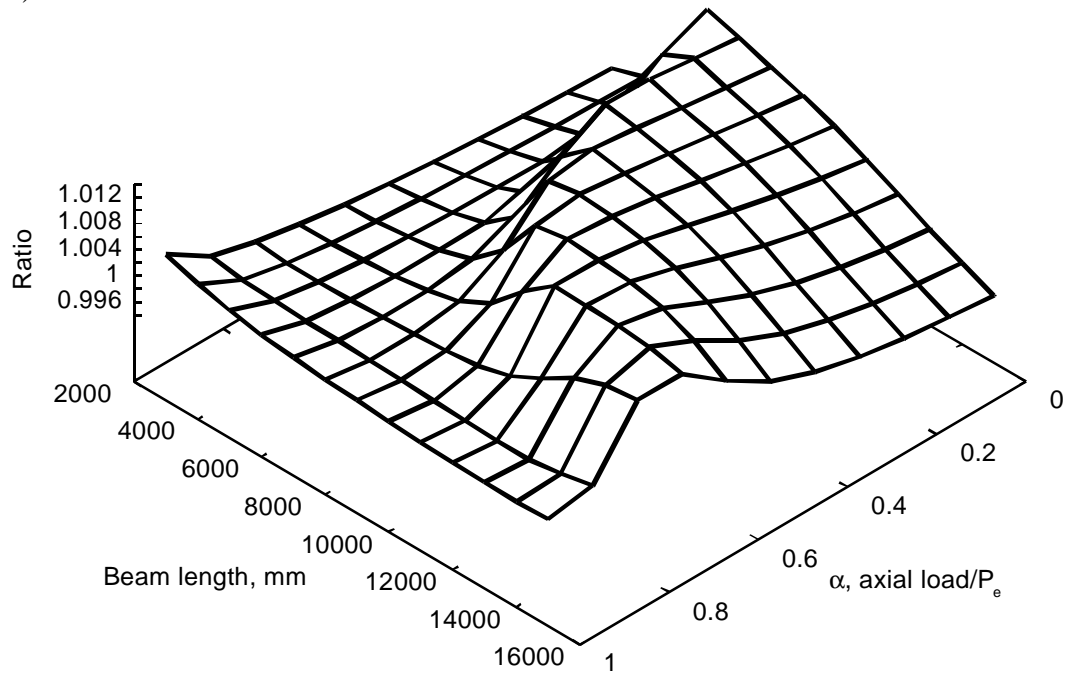


b)

**Figure 4-25** Ratio of strengths for direct warping to reversed warping, a) 3 m and b) 4 m columns, W200x27 frame, simply supported column bases, unbraced.

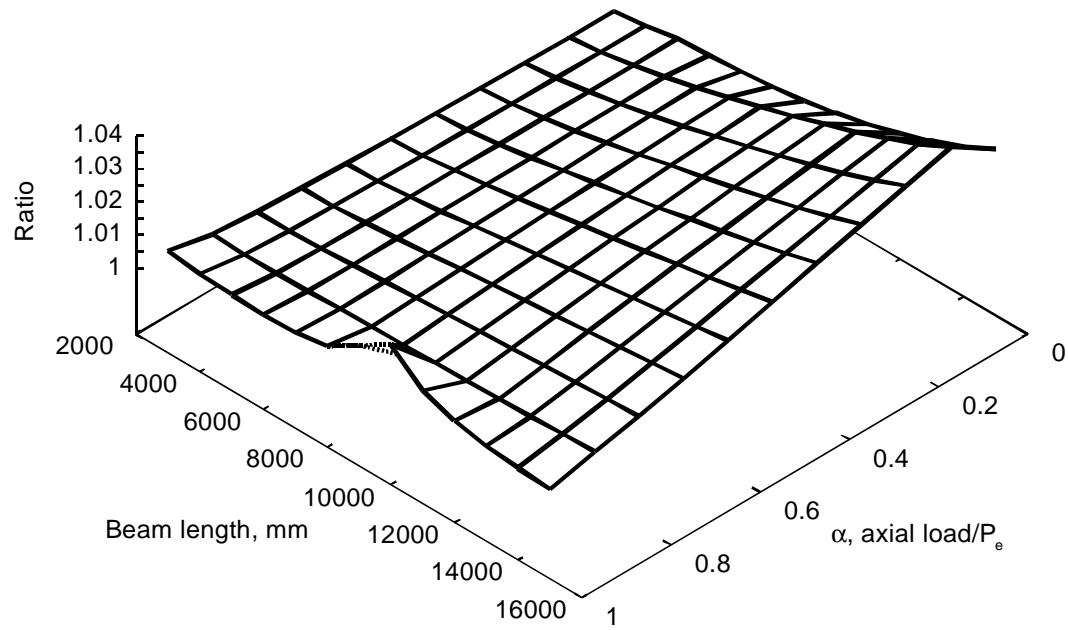


a)

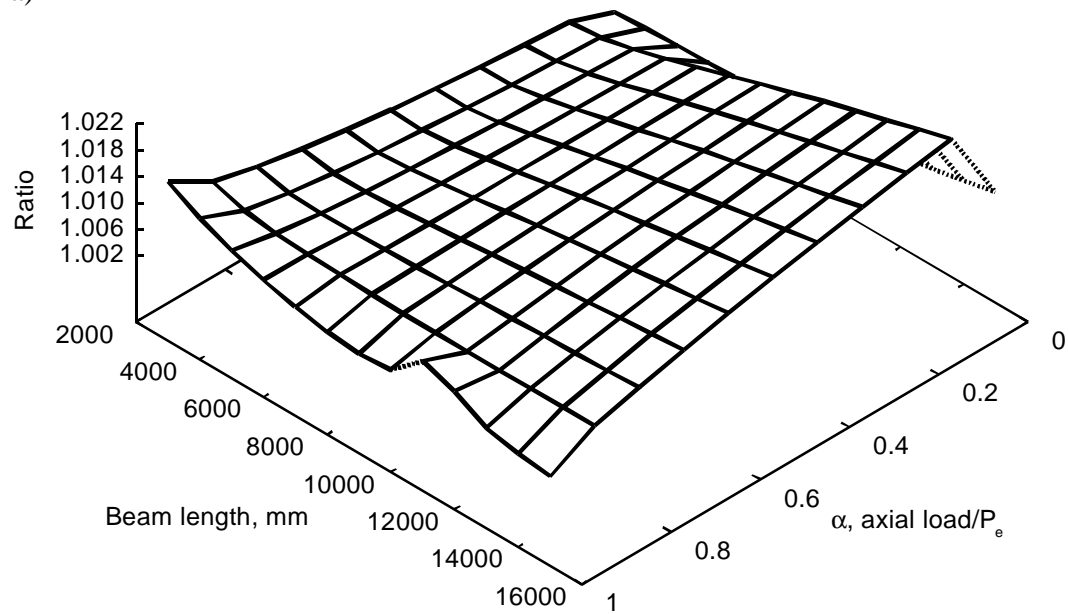


b)

**Figure 4-26** Ratio of strengths for direct warping to reversed warping, a) 3 m and b) 4 m columns, W200x27 frame, fixed column bases, braced.

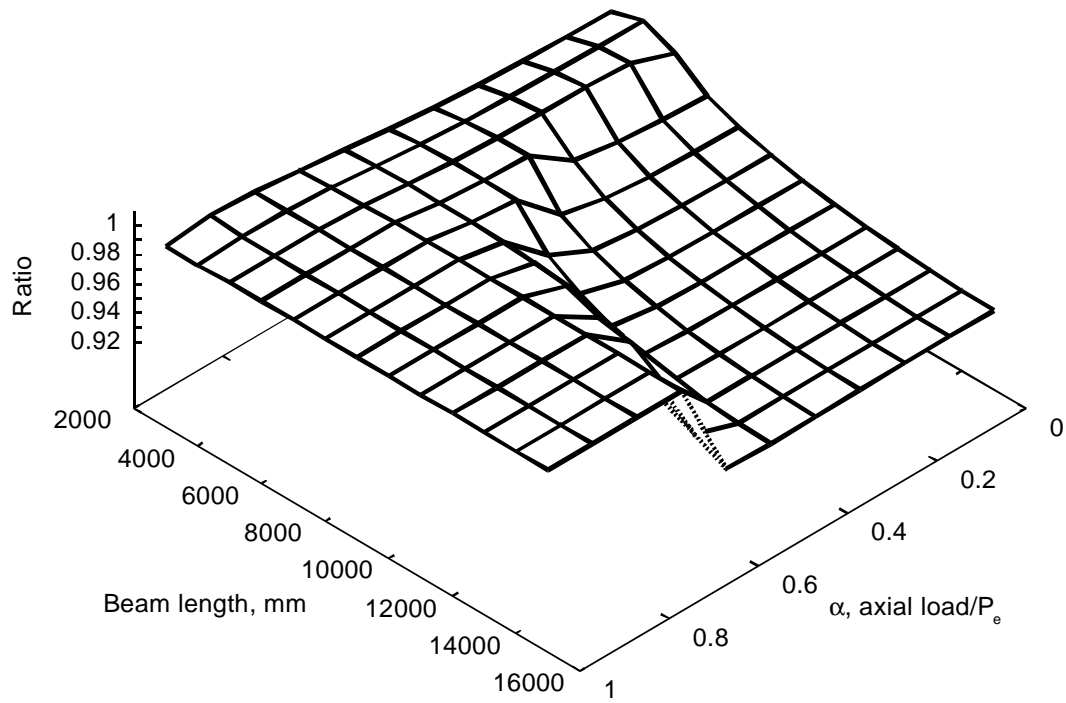


a)

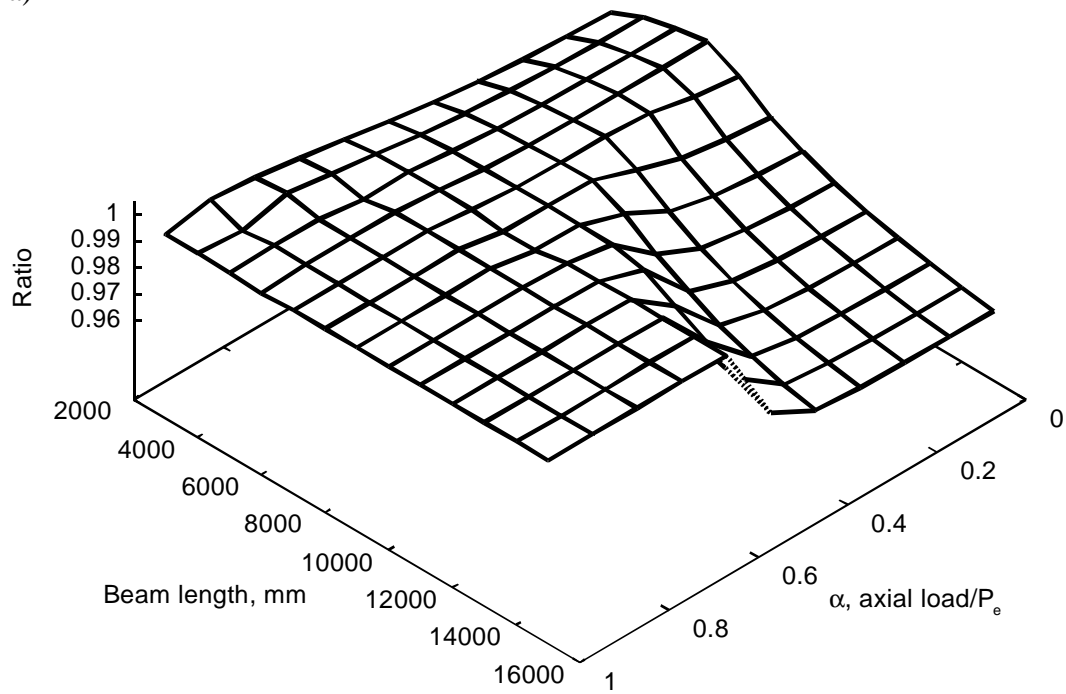


b)

**Figure 4-27** Ratio of strengths for direct warping to reversed warping, a) 3 m and b) 4 m columns, W200x27 frame, simply supported column bases, braced.



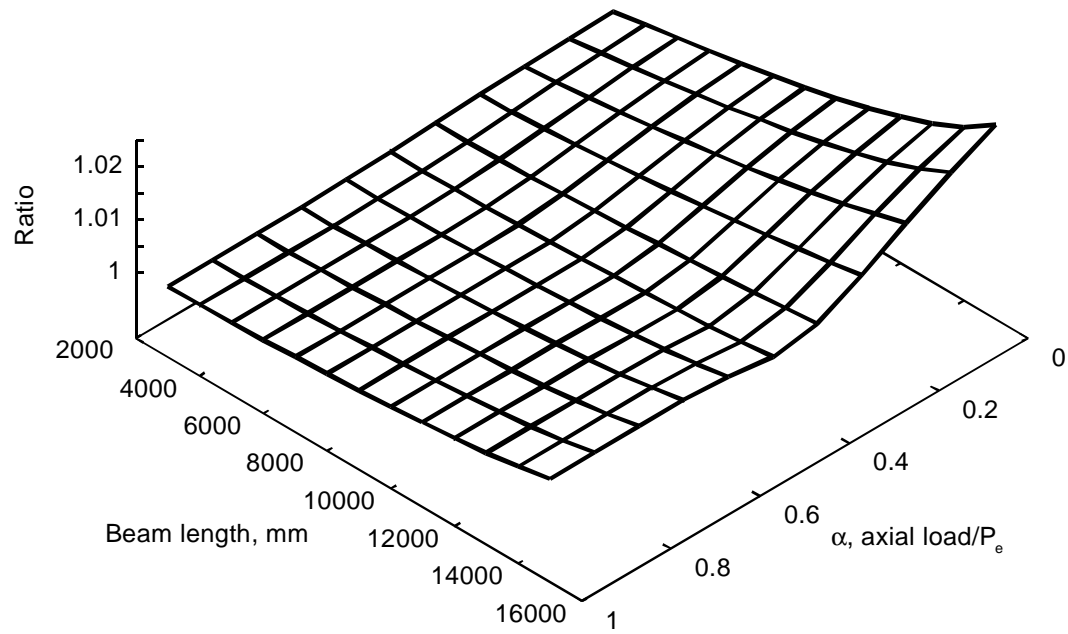
a)



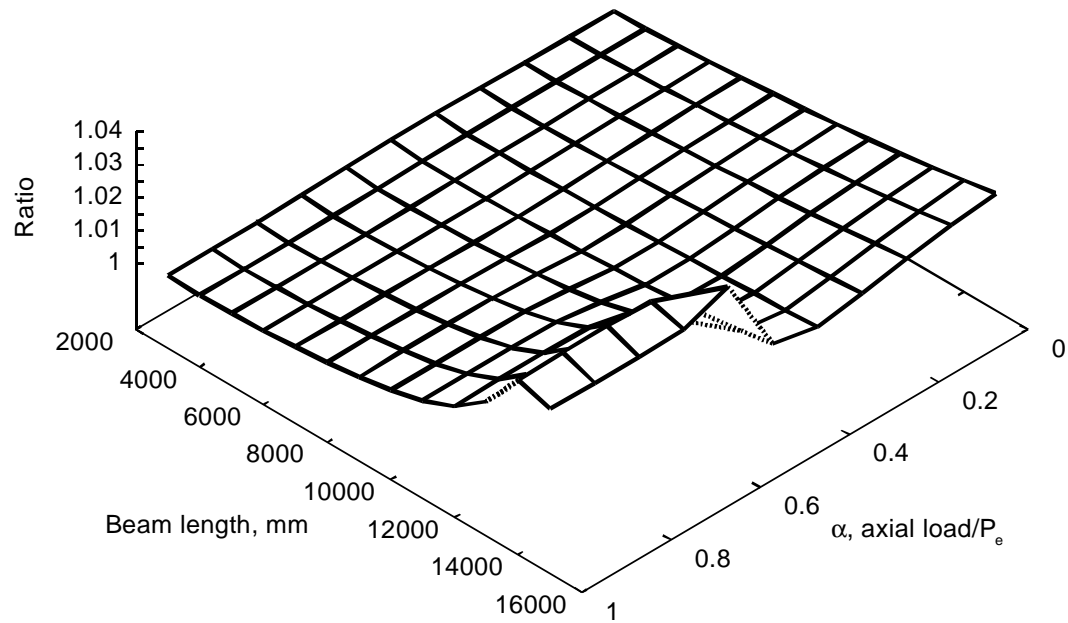
b)

**Figure 4-28** Ratio of strengths for direct warping to reversed warping, a) 3 m and b) 4 m columns, W360x134 frame, fixed column bases, unbraced



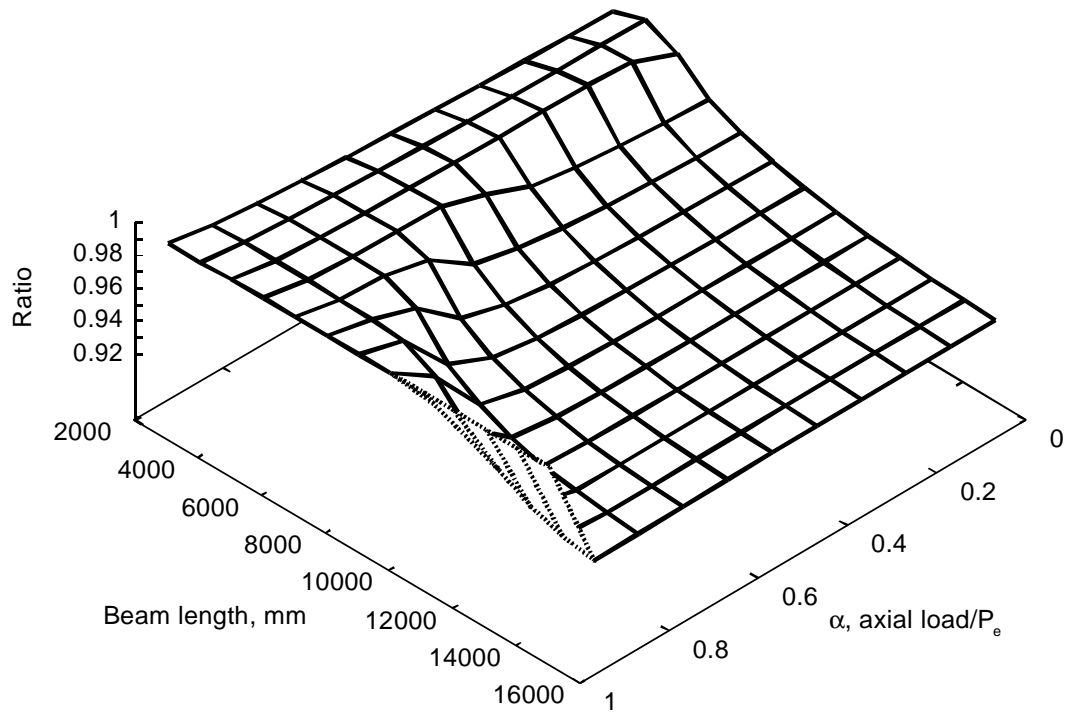


a)

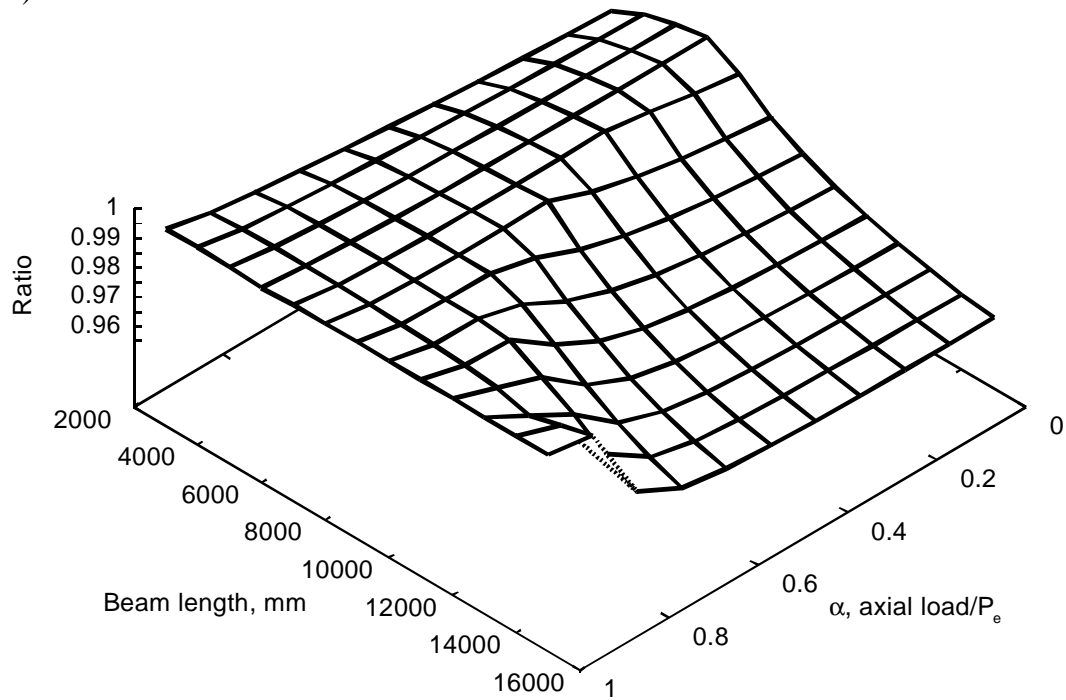


b)

**Figure 4-29** Ratio of strengths for direct warping to reversed warping, a) 3 m and b) 4 m columns, W360x134 frame, simply supported column bases, unbraced

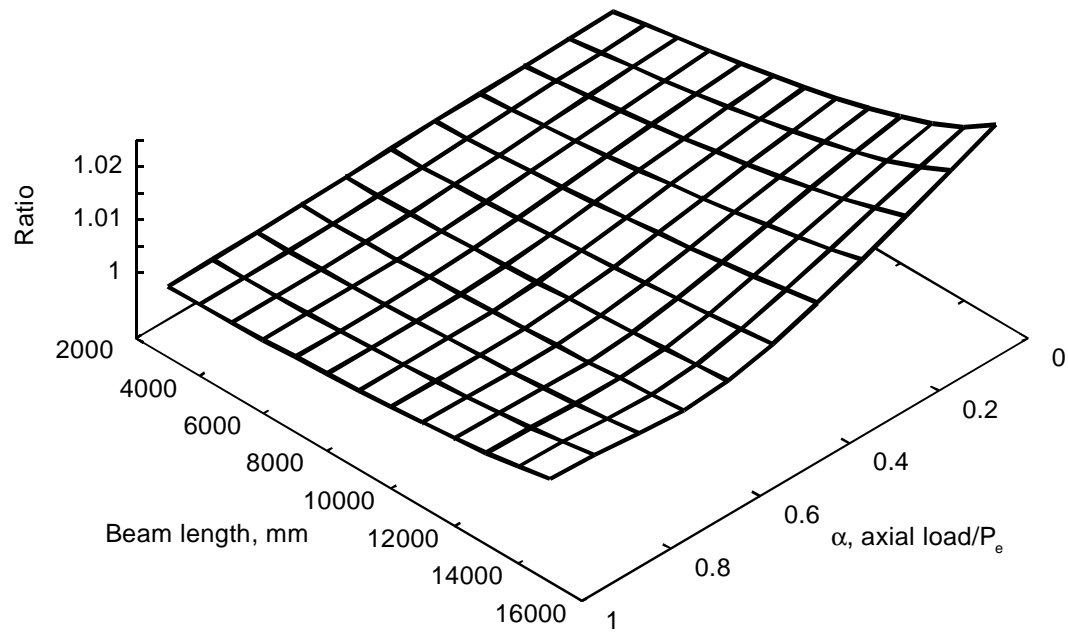


a)

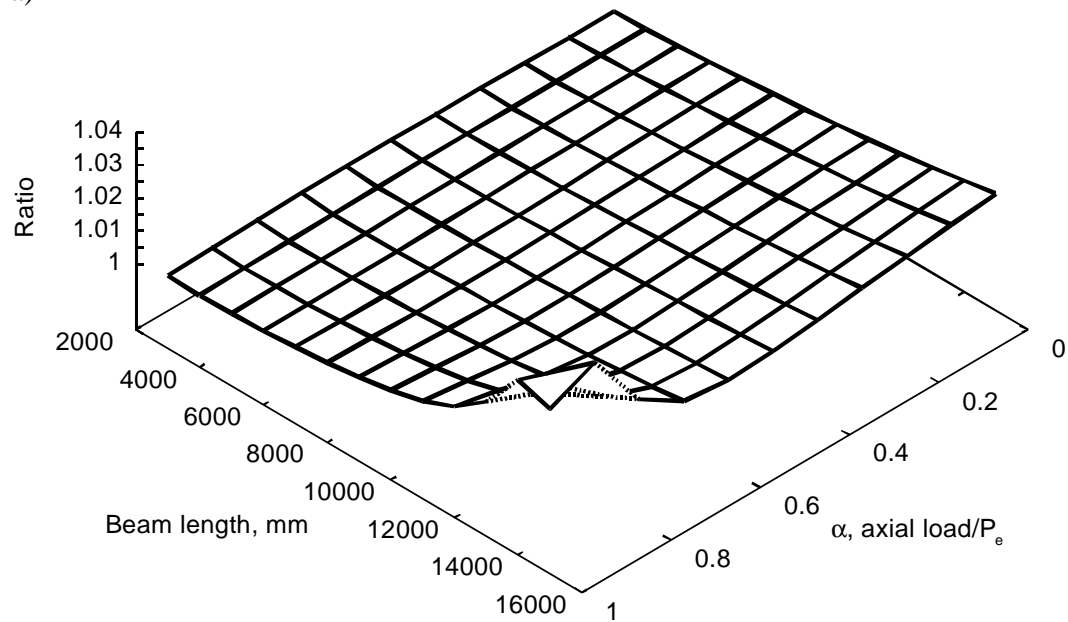


b)

**Figure 4-30** Ratio of strengths for direct warping to reversed warping, a) 3 m and b) 4 m columns, W360x134 frame, fixed column bases, braced



a)



b)

**Figure 4-31** Ratio of strengths for direct warping to reversed warping, a) 3 m and b) 4 m columns, W360x134 frame, pinned column bases, braced.

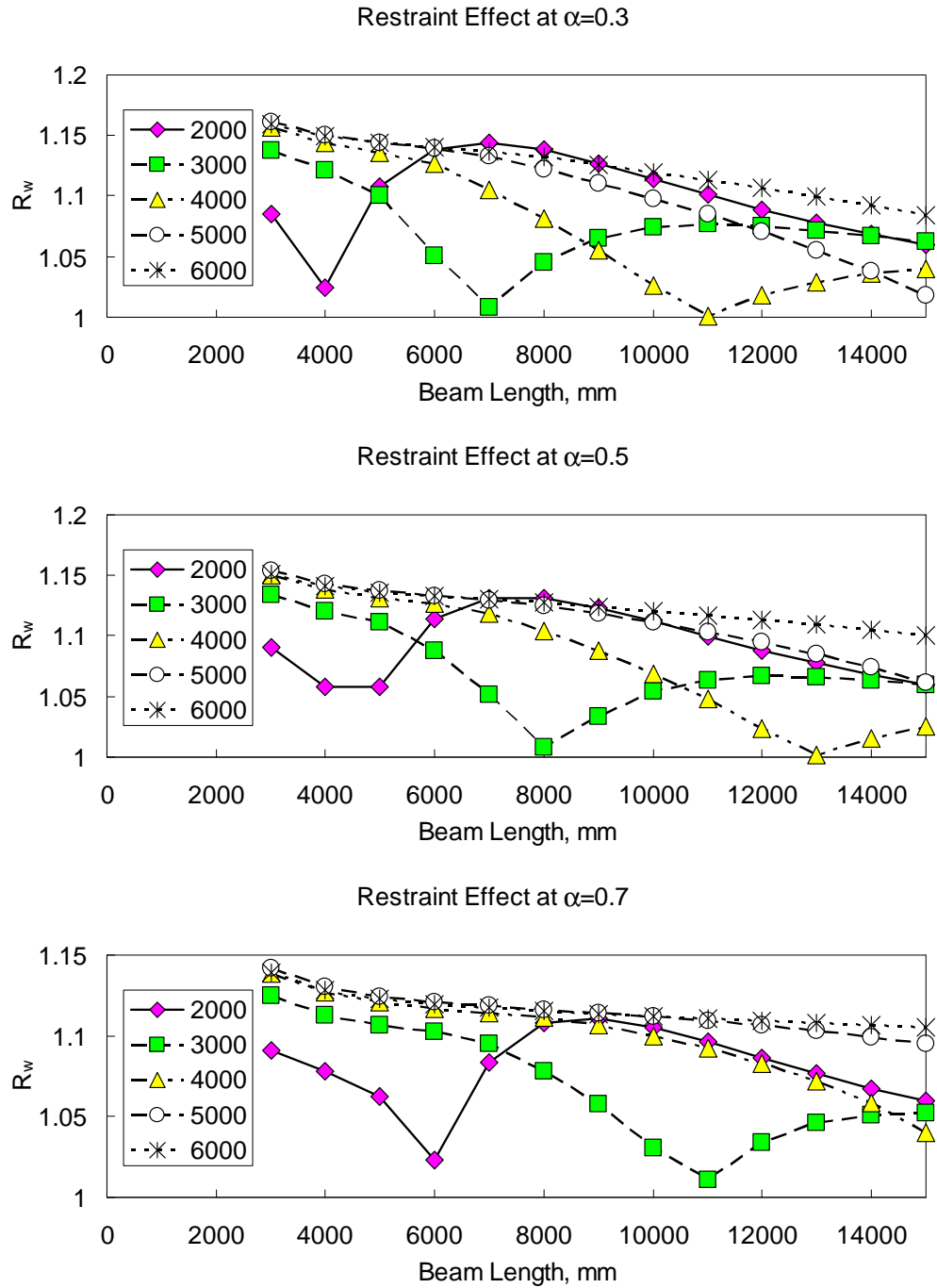


**Figure 4-32** Length effects, W200x27 members, fixed base, unbraced frame. Column lengths are shown in the figure legends.

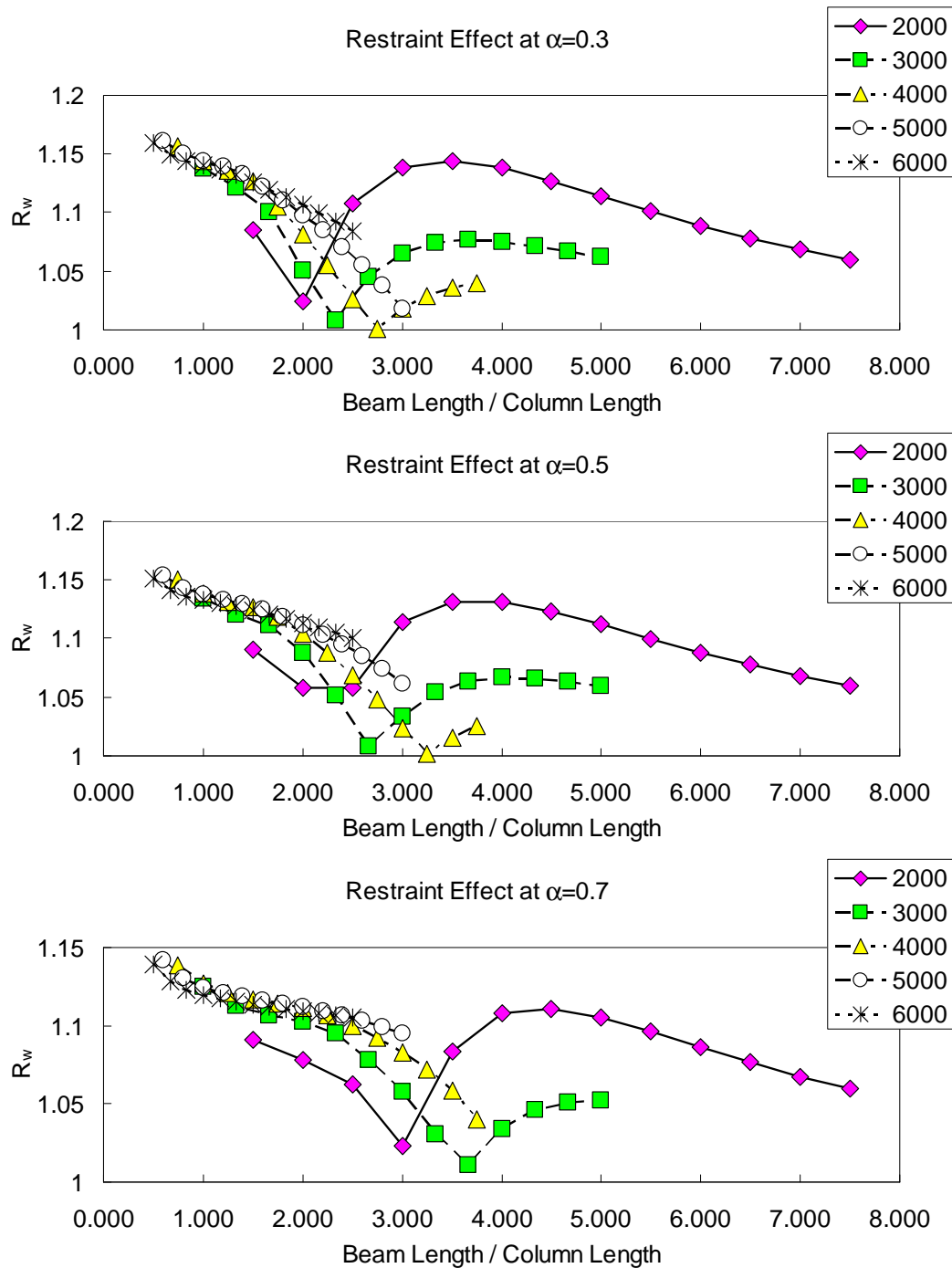


**Figure 4-33** Length effects, W200x27 members, fixed base, unbraced frame, normalised

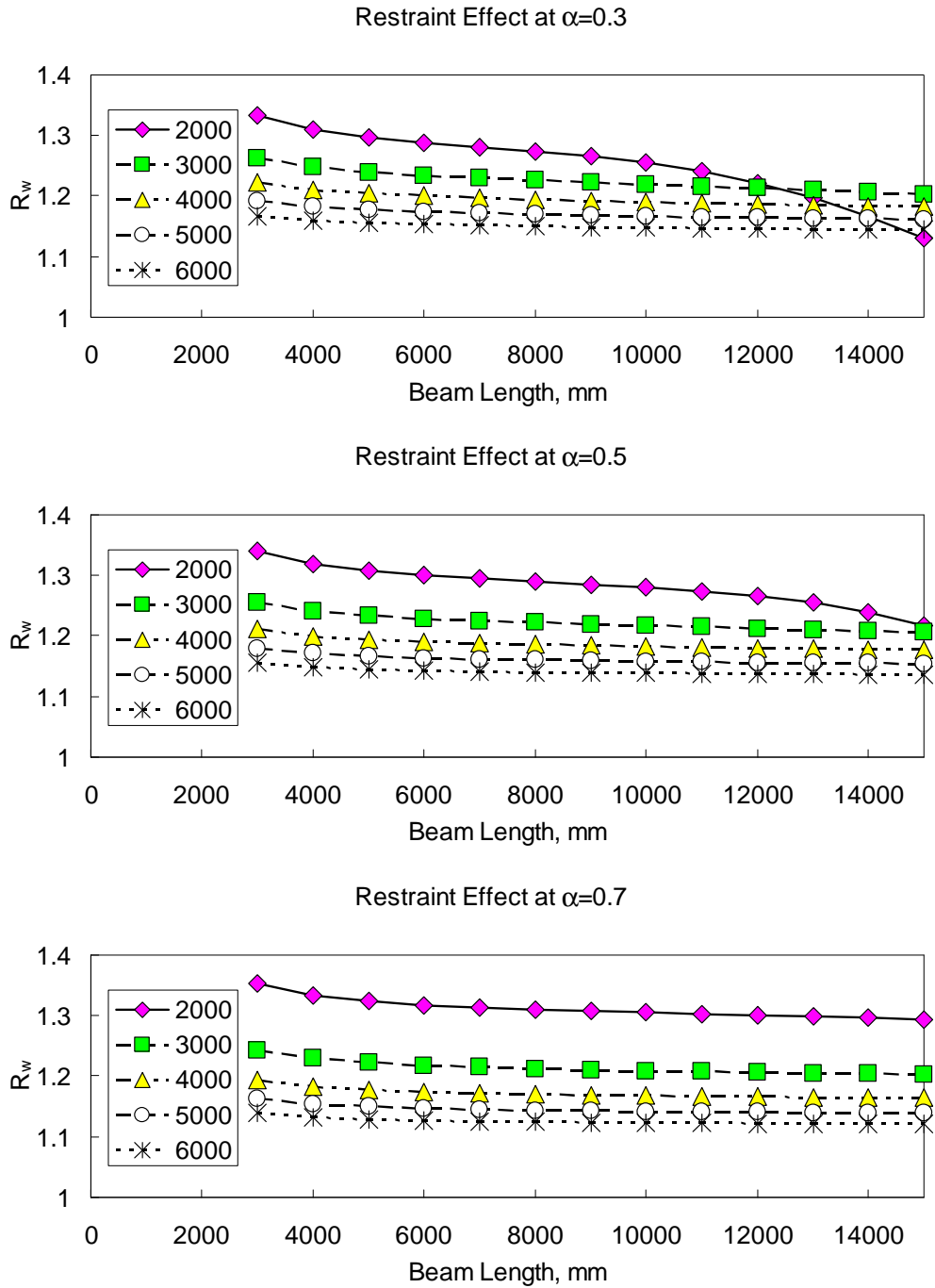


**Figure 4-34** Length effects, W200x27 members, pinned base, unbraced frame

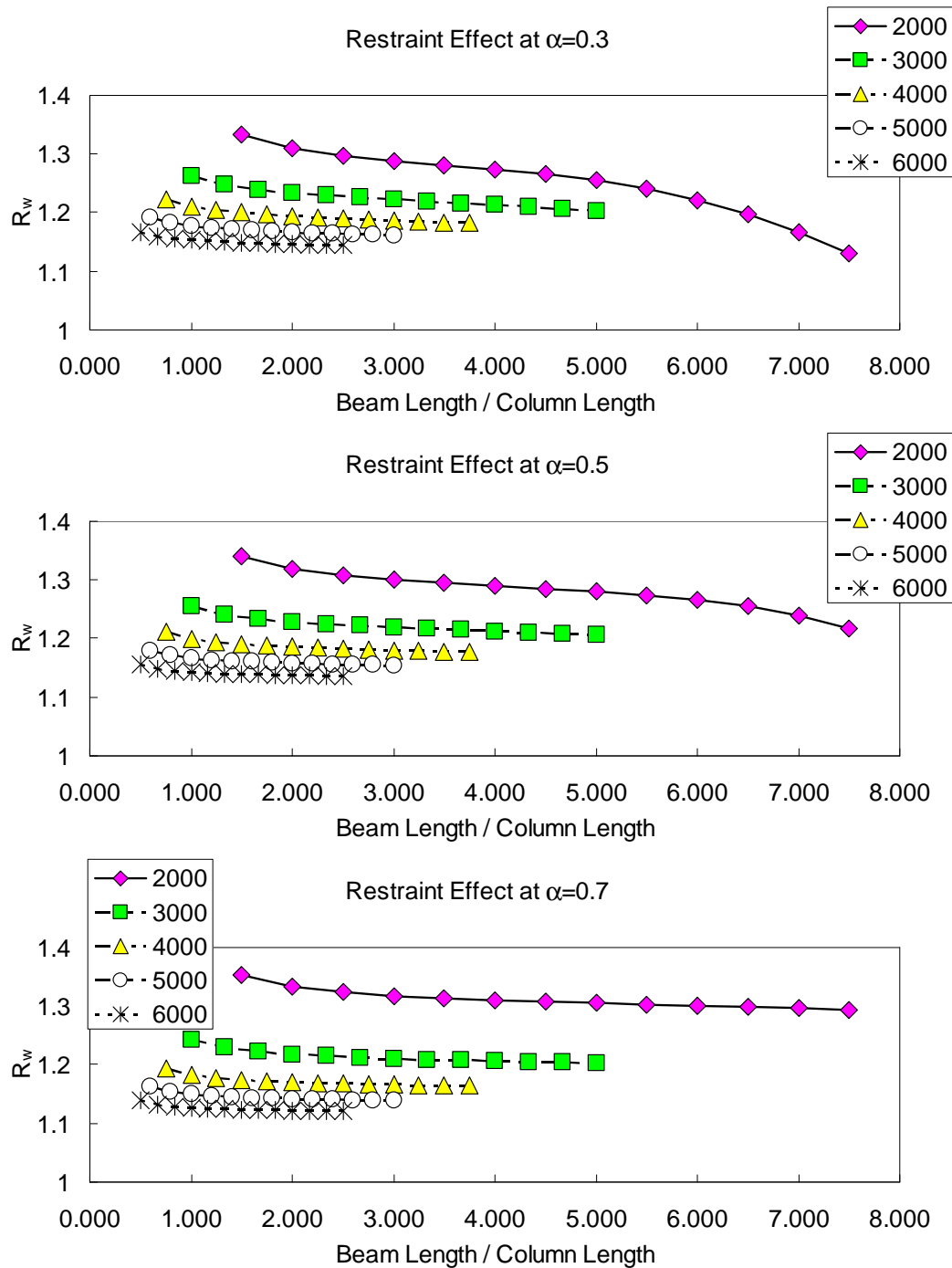


**Figure 4-35** Length effects, W200x27 members, pinned base, unbraced frame, normalised

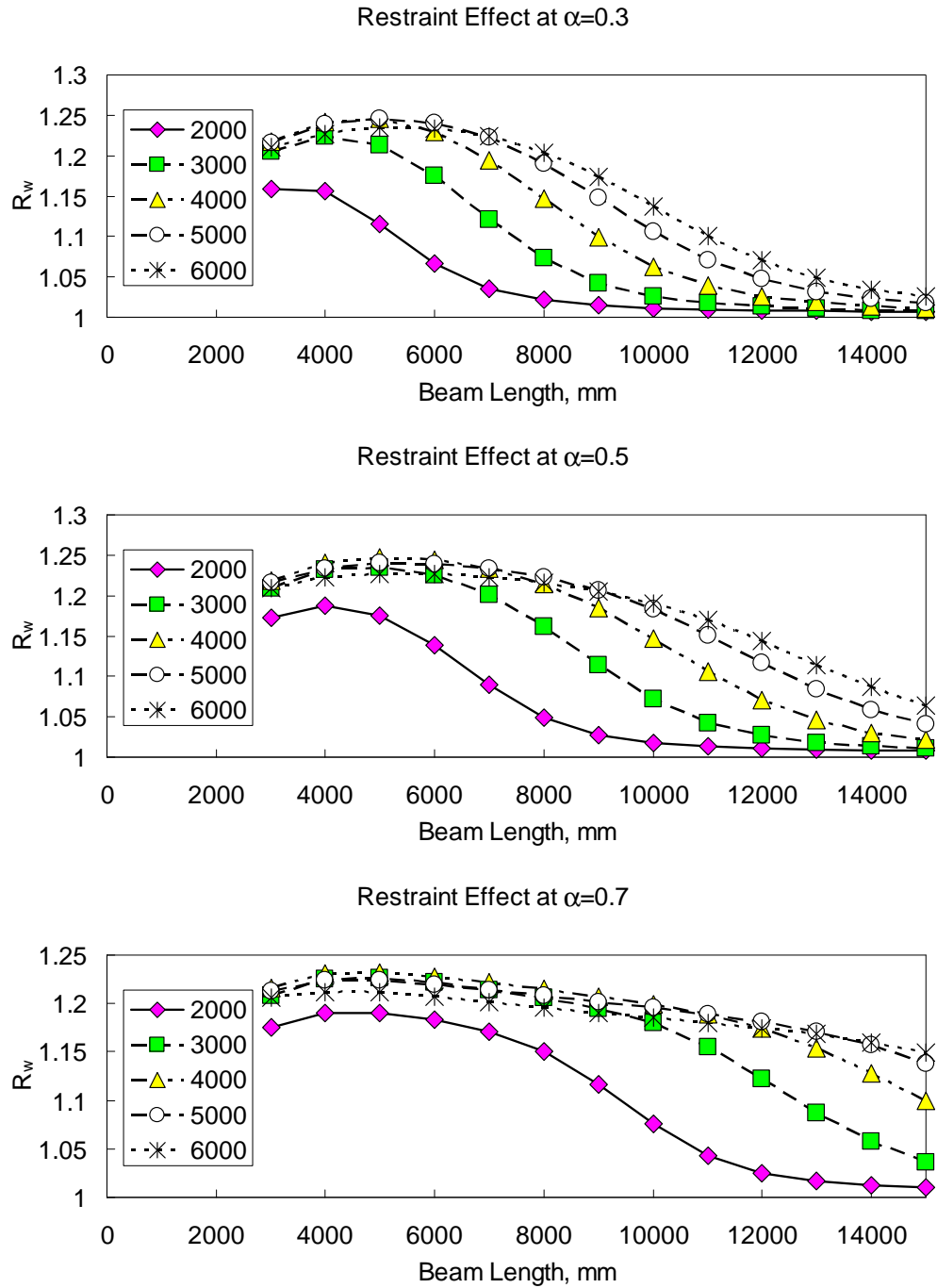


**Figure 4-36** Length effects, W200x27+W690x125 members, fixed base, unbraced frame



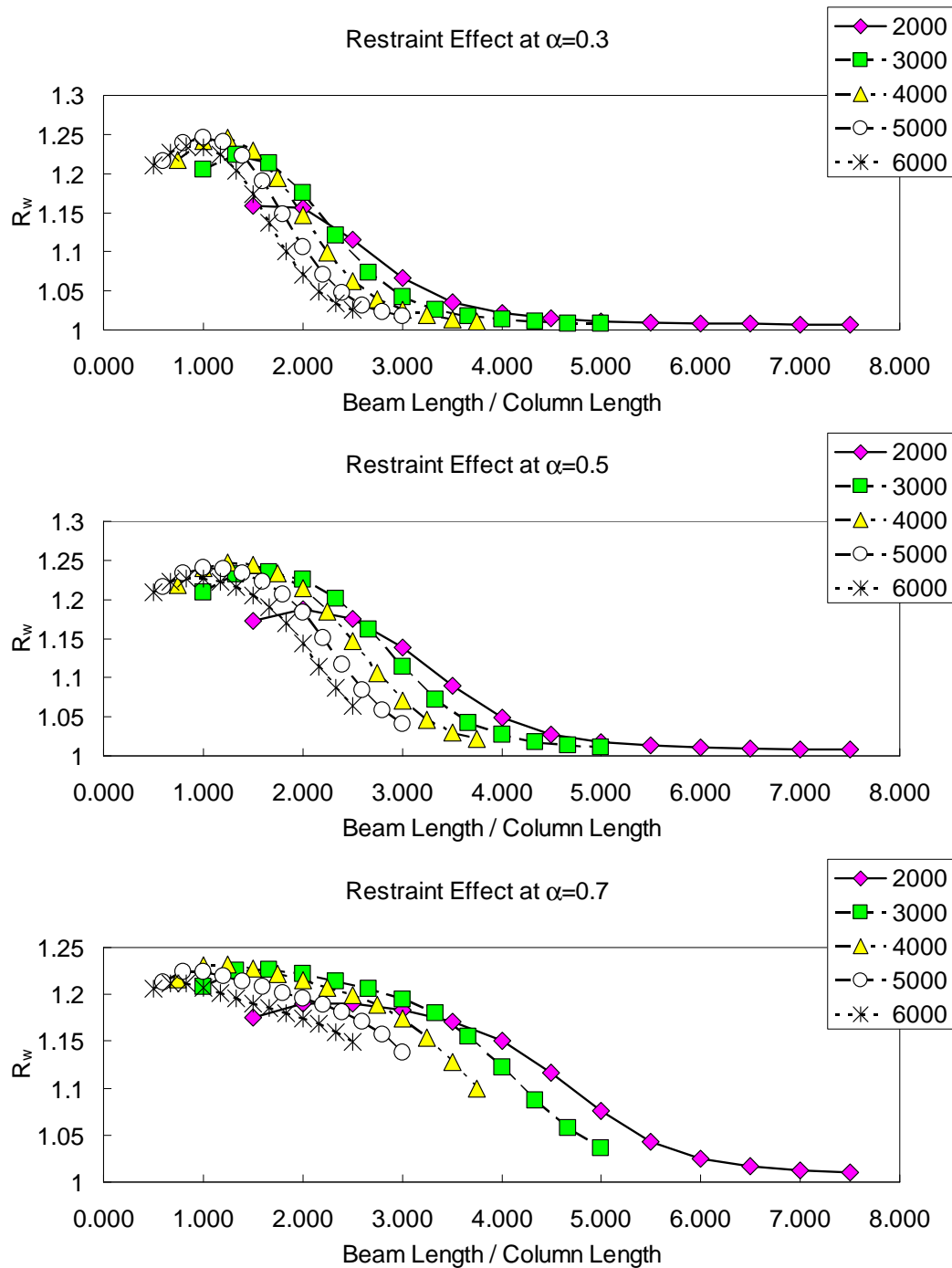


**Figure 4-37** Length effects, W200x27+W690x125 members, fixed base, unbraced frame, normalised

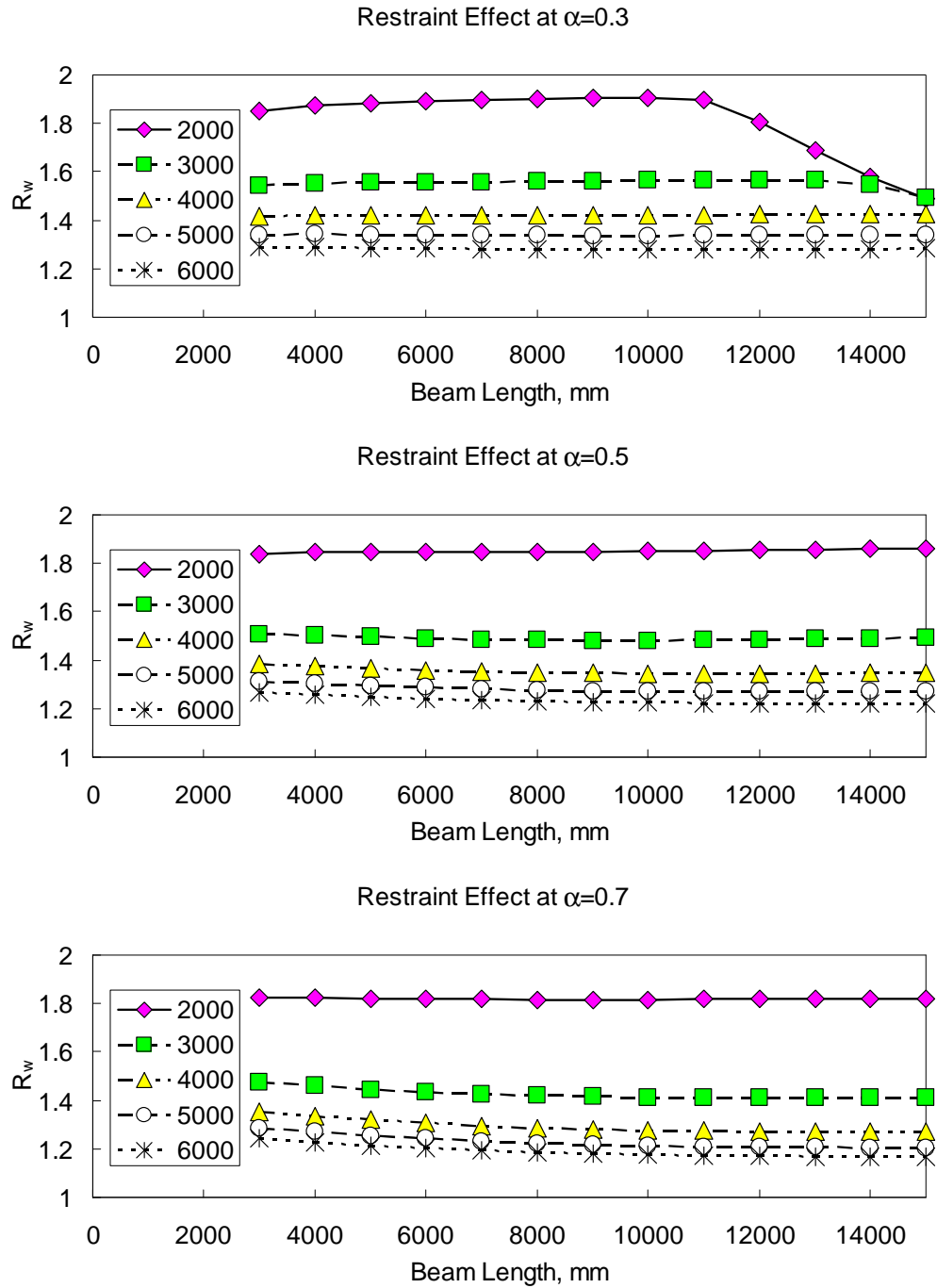


**Figure 4-38** Length effects, W200x27+W690x125 members, pinned base, unbraced frame

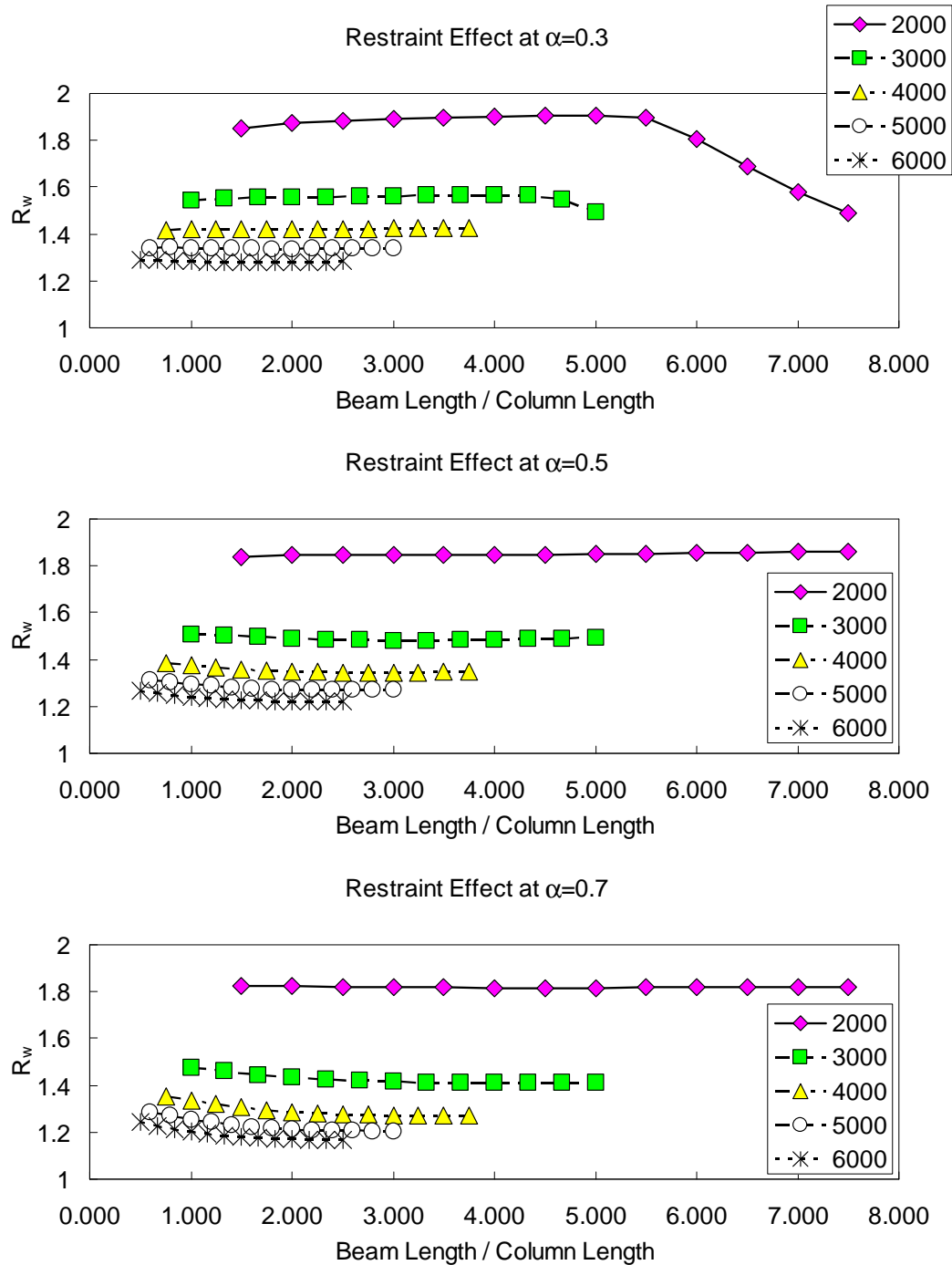


**Figure 4-39** Length effects, W200x27+W690x125 members, pinned base, unbraced frame, normalised

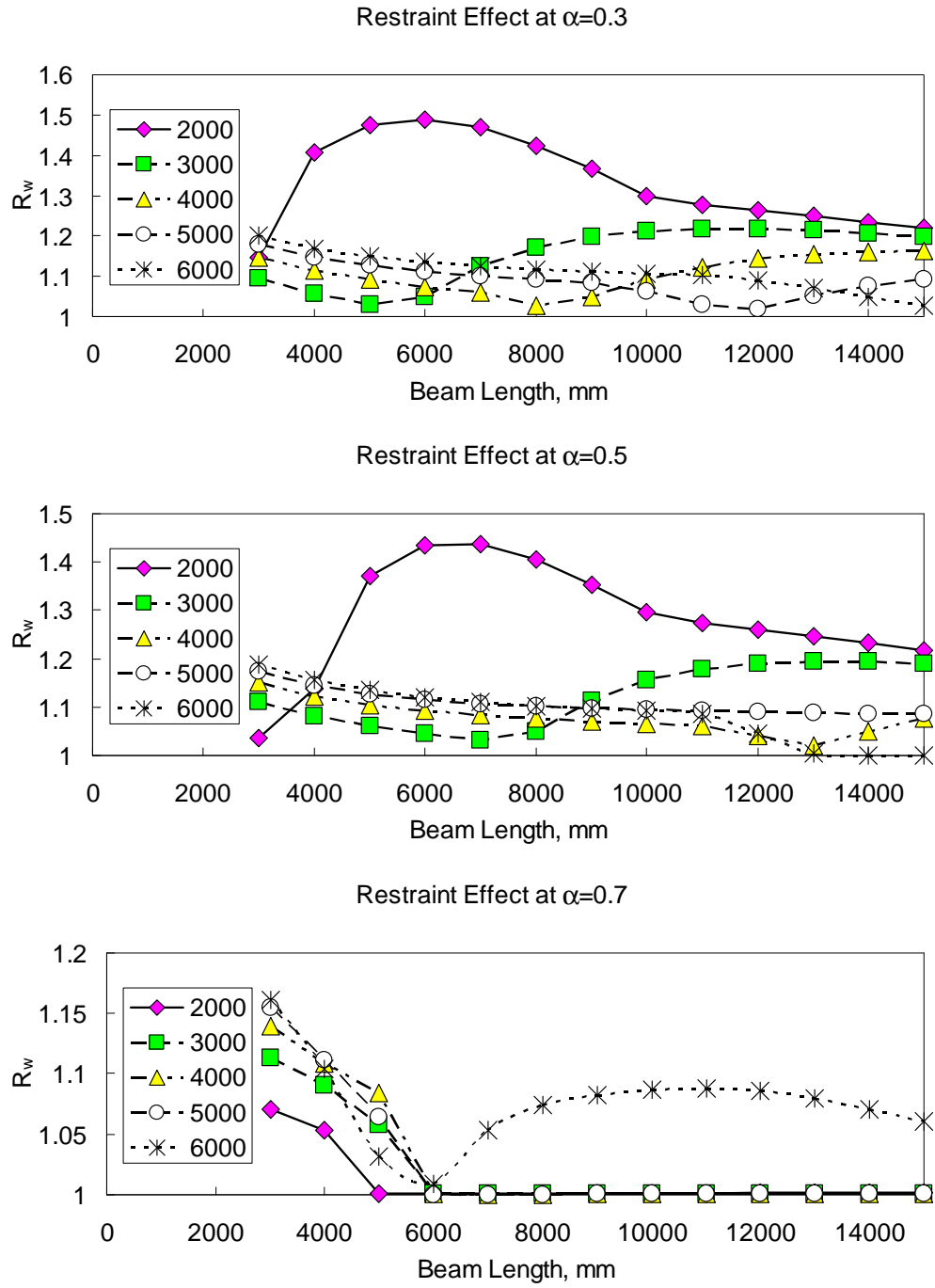


**Figure 4-40** Length effects, W360x134 members, fixed base, unbraced frame

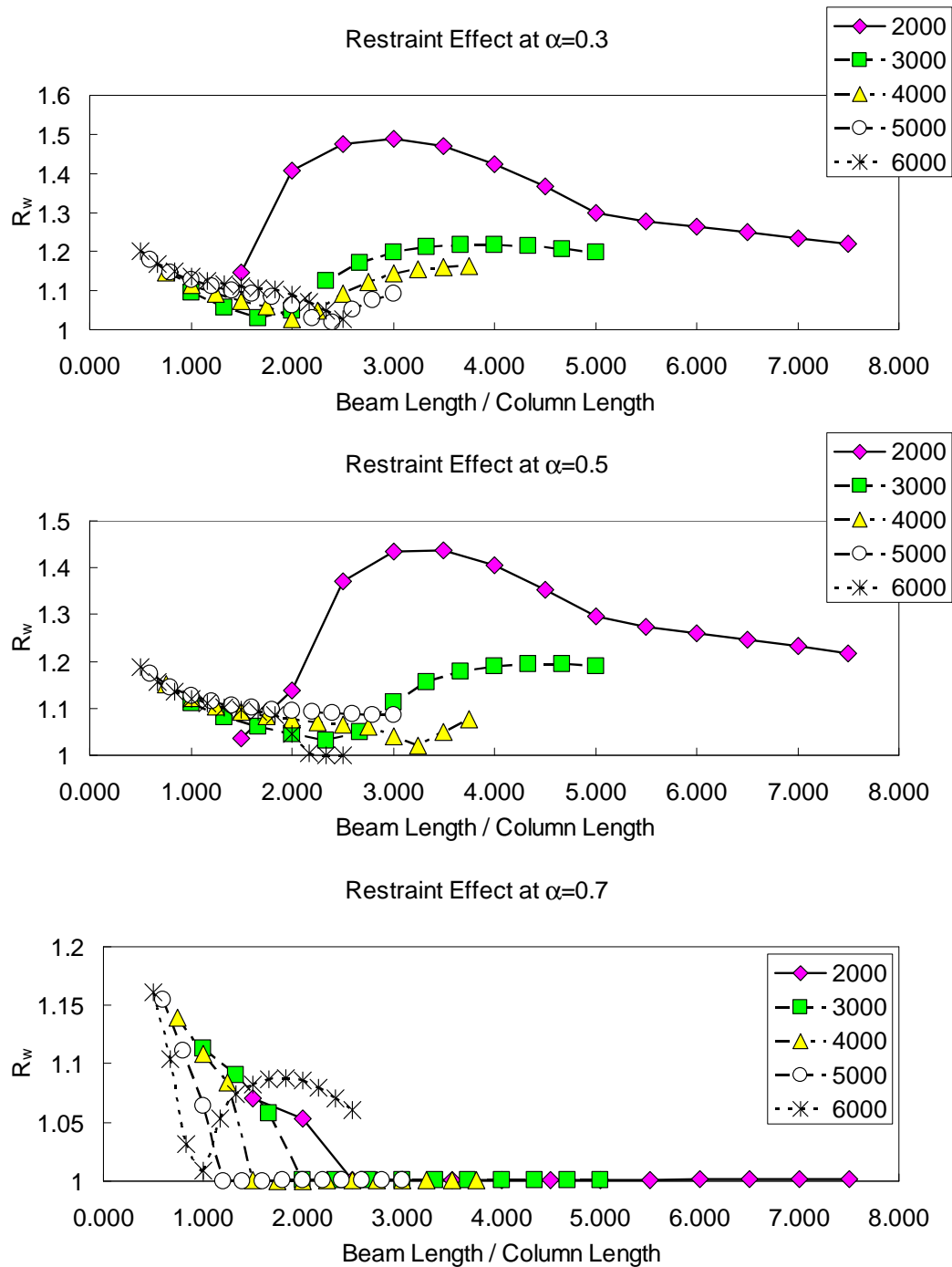


**Figure 4-41** Length effects, W360x134 members, fixed base, unbraced frame, normalised

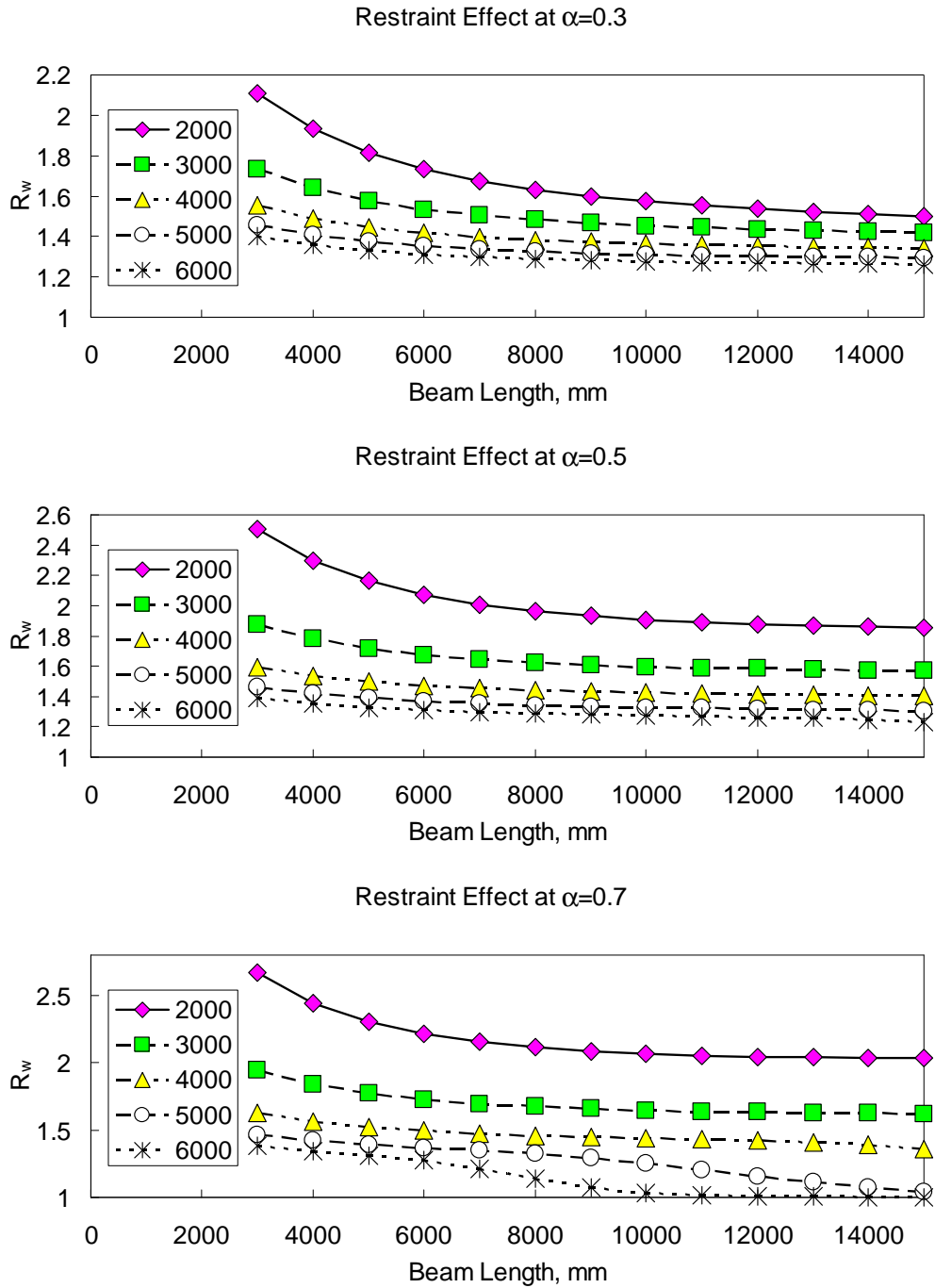


**Figure 4-42** Length effects, W360x134 members, pinned base, unbraced frame

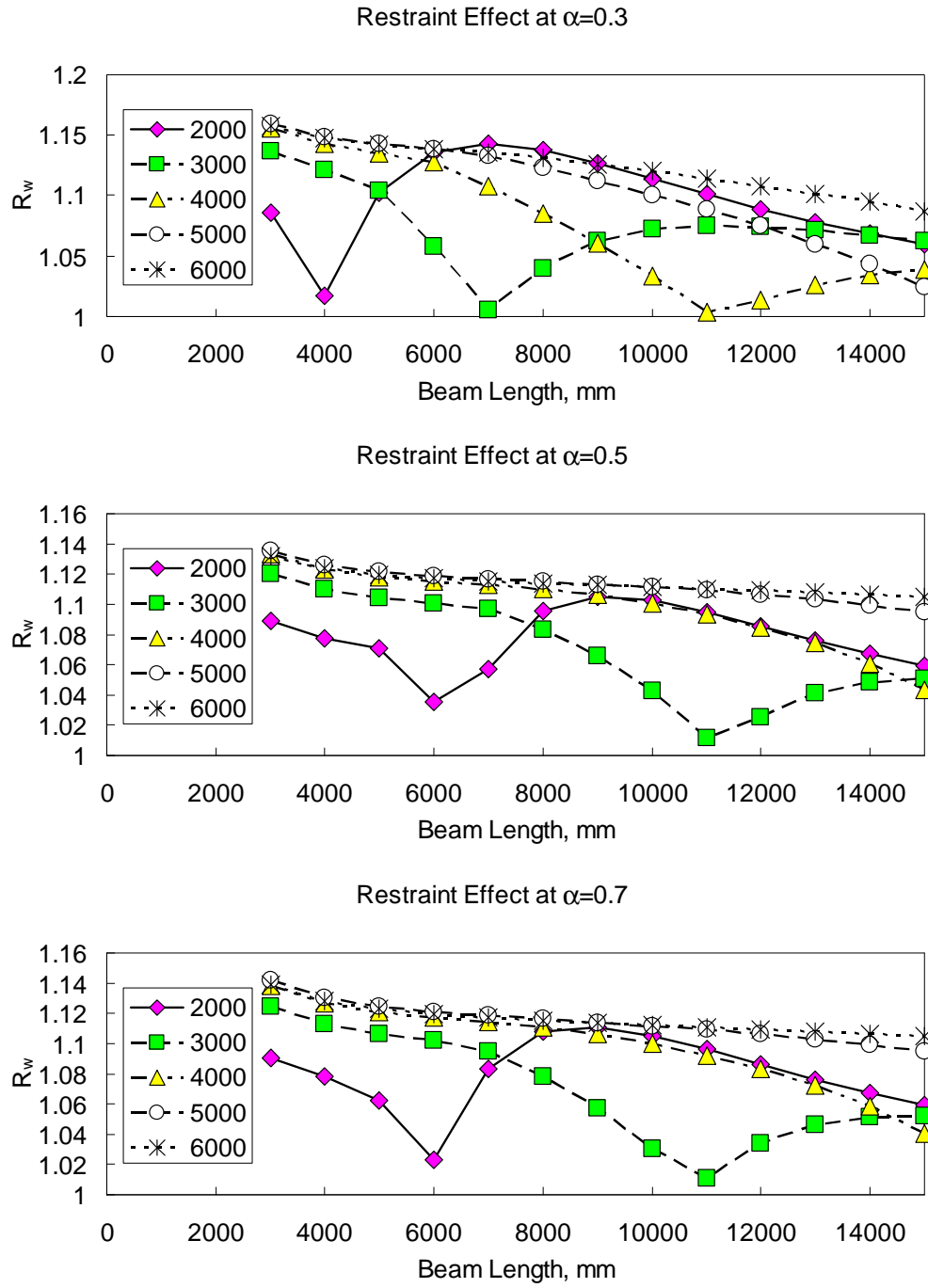


**Figure 4-43** Length effects, W200x27 members, fixed base, braced frame

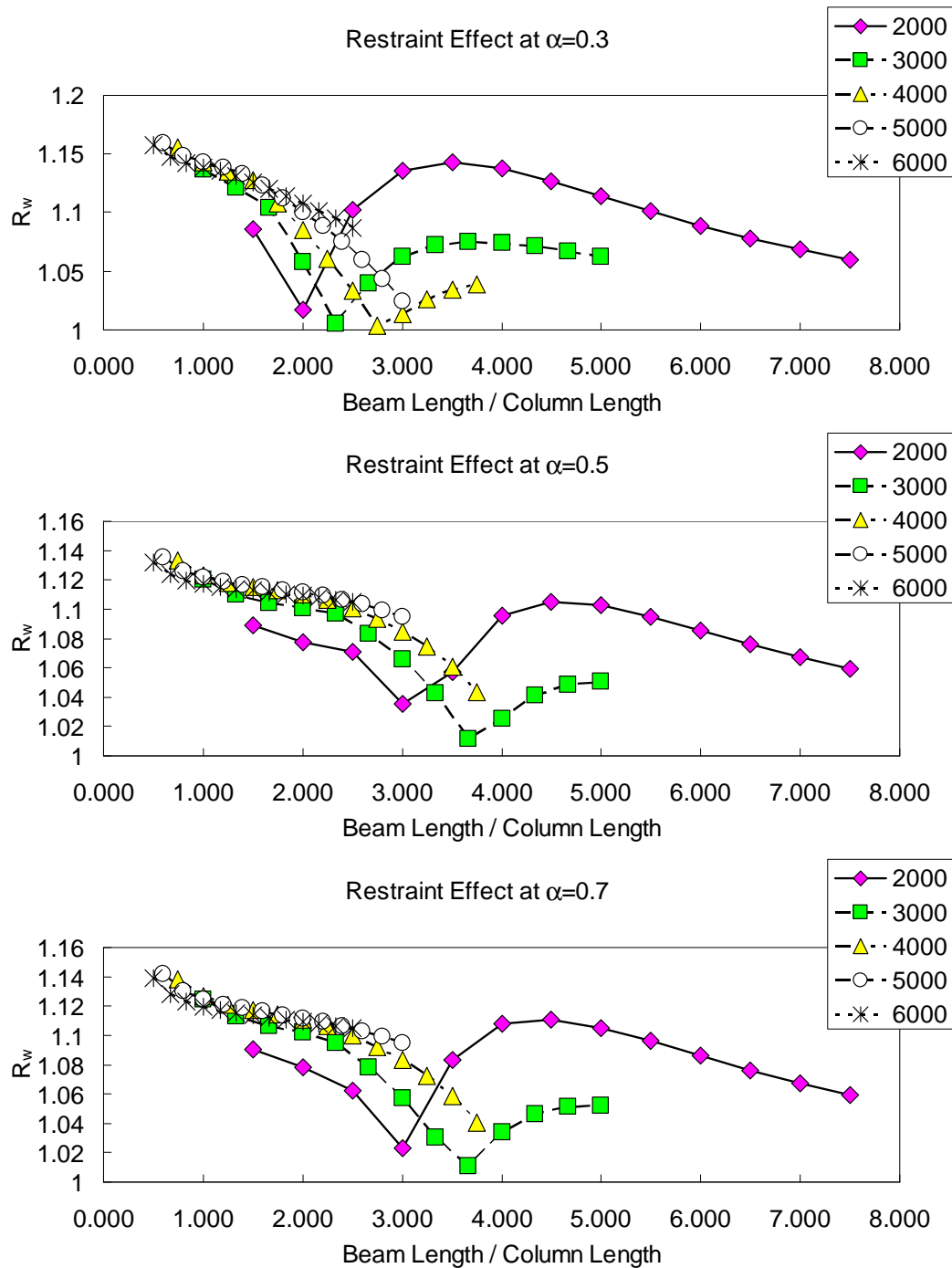


**Figure 4-44** Length effects, W200x27 members, fixed base, braced frame, normalised



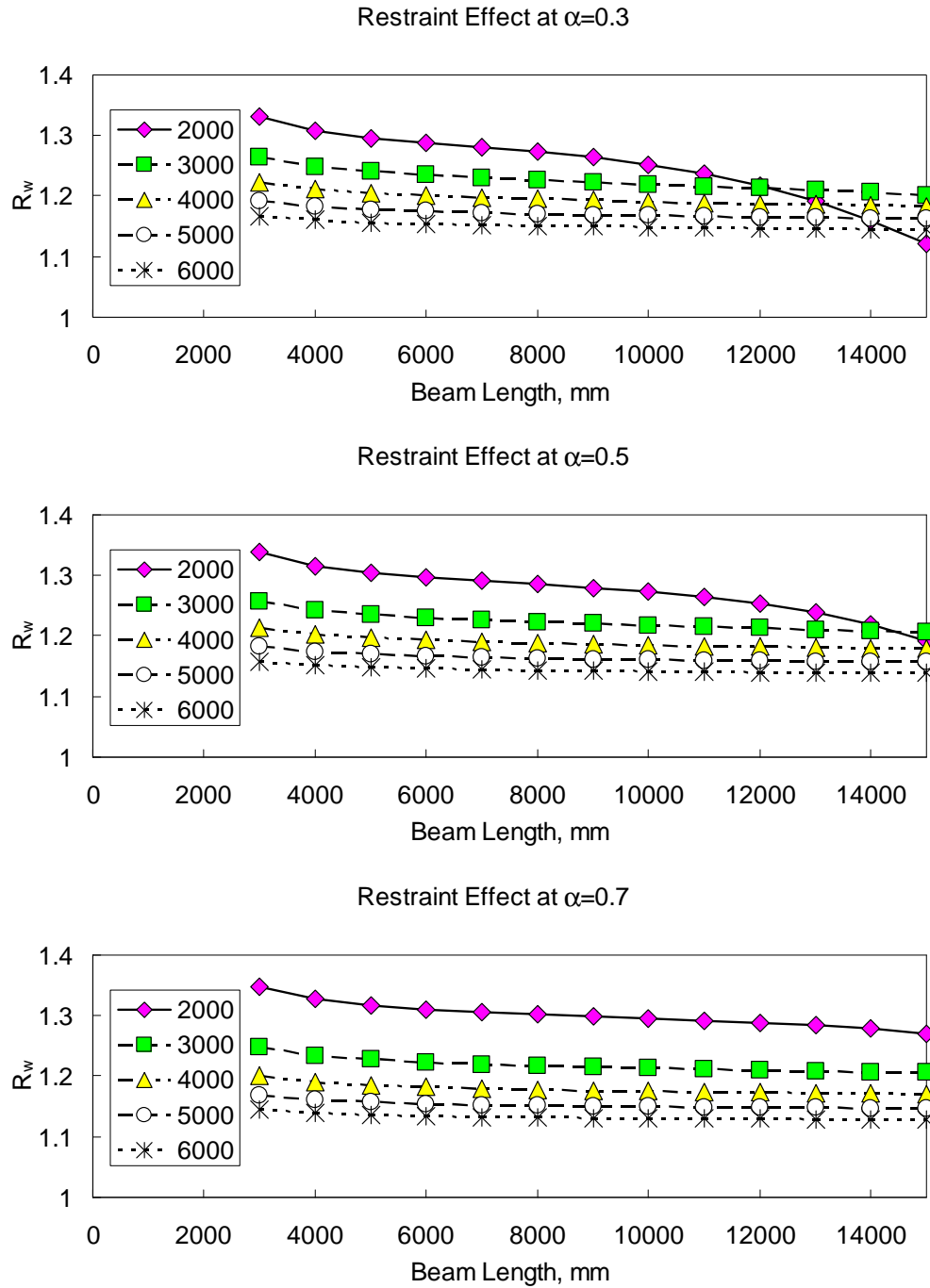


**Figure 4-45** Length effects, W200x27 members, pinned base, braced frame

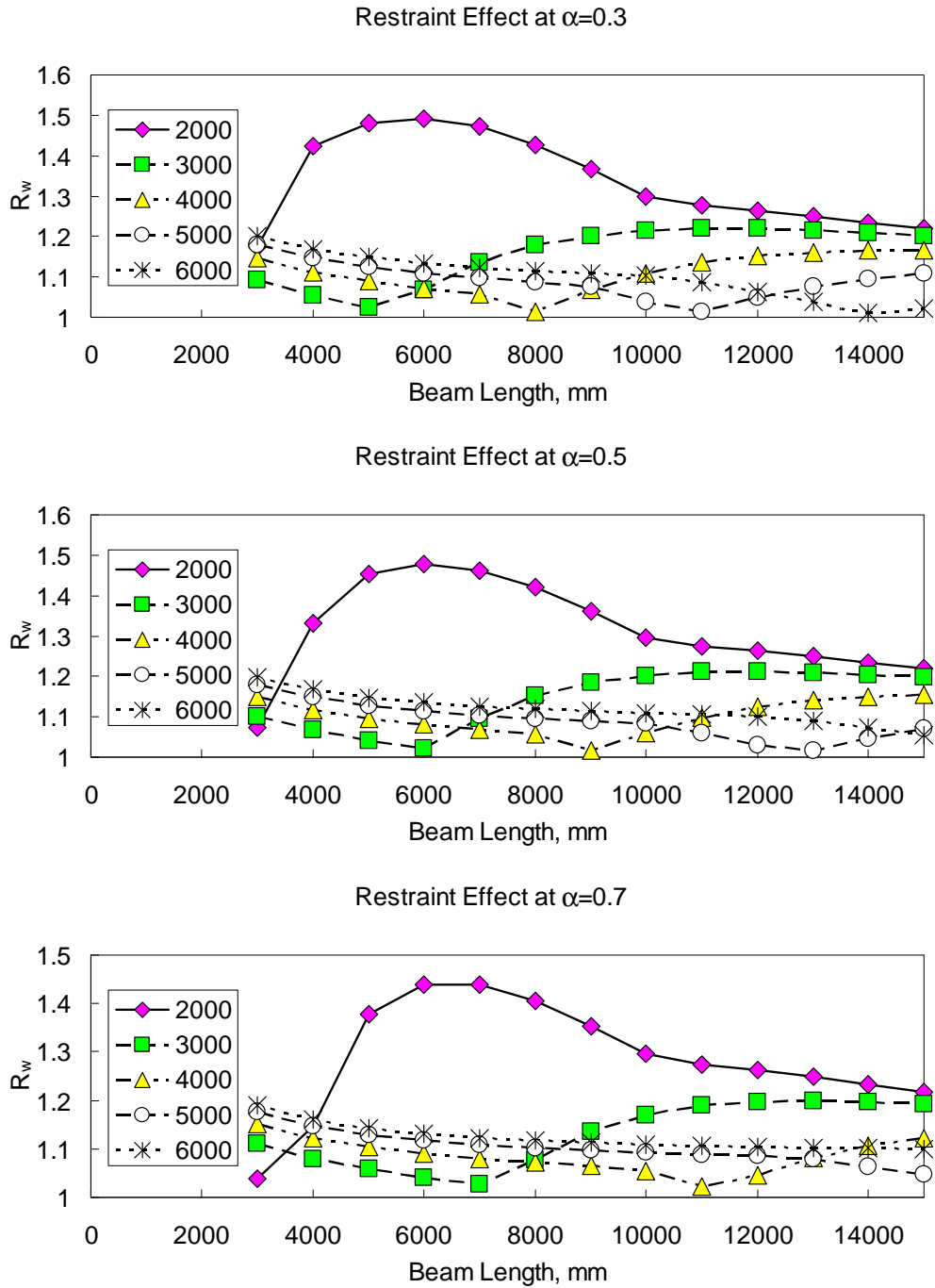


**Figure 4-46** Length effects, W360x134 members, fixed base, braced frame

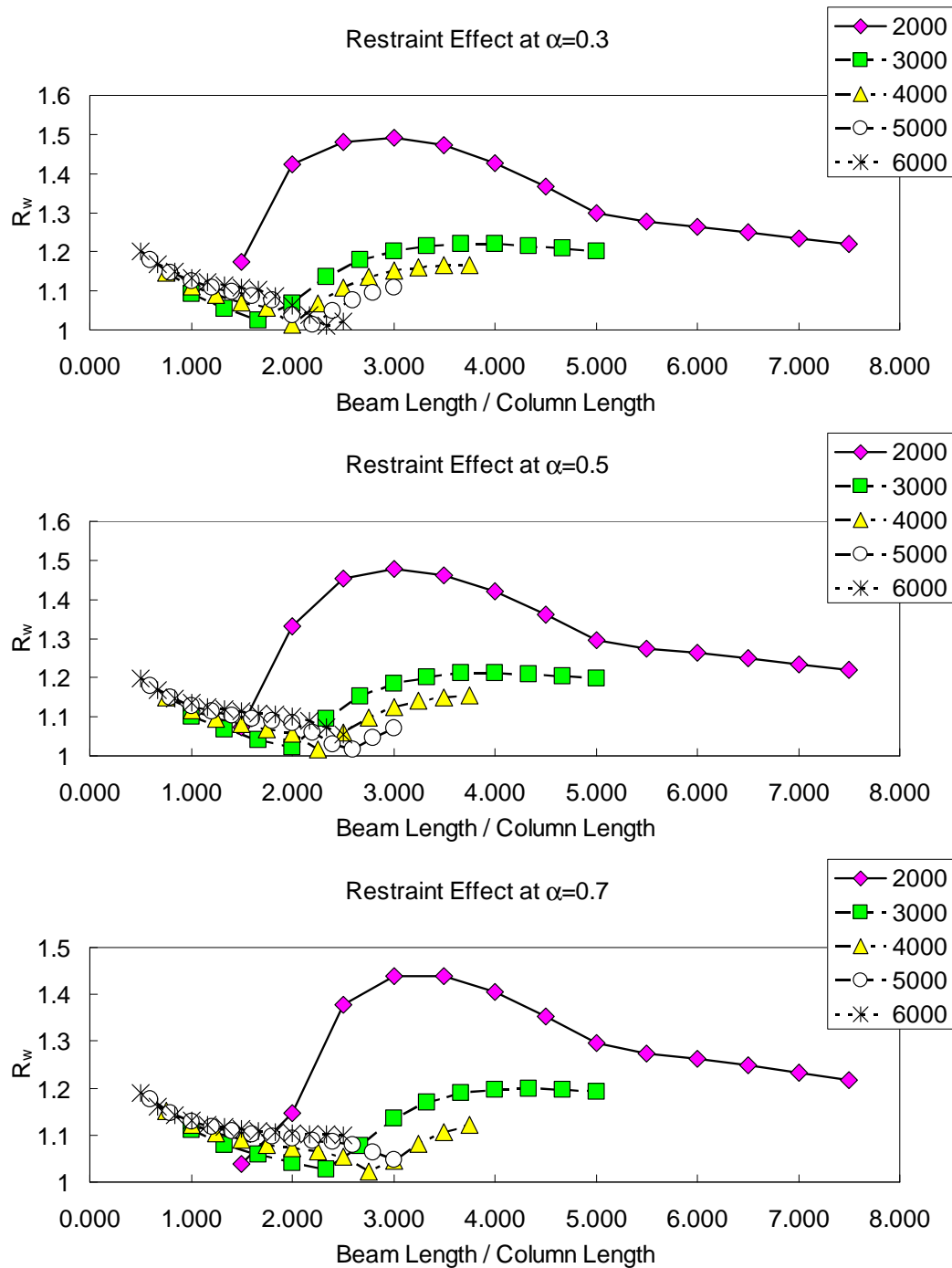


**Figure 4-47** Length effects, W360x134 members, fixed base, braced frame, normalised

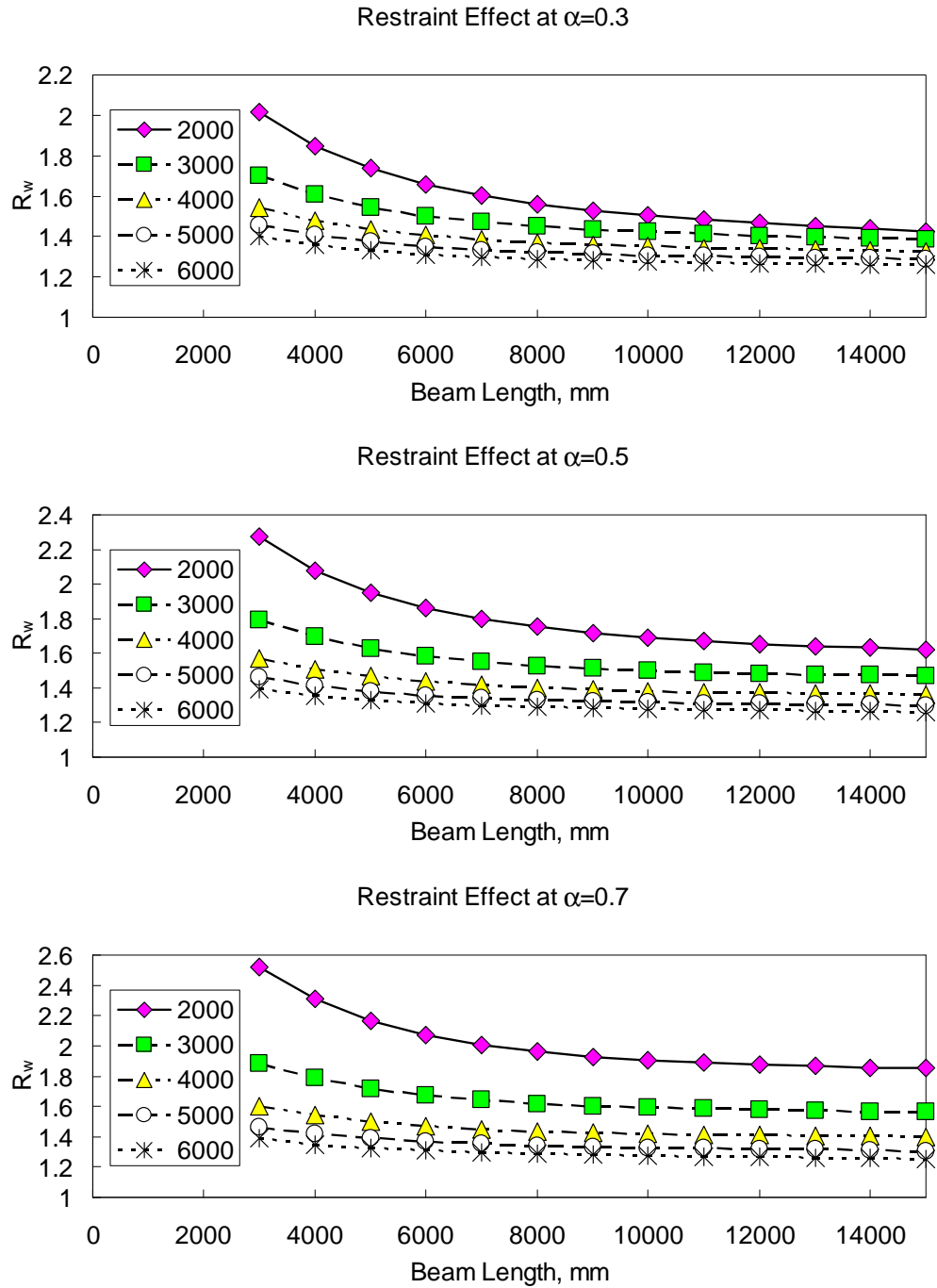


**Figure 4-48** Length effects, W360x134 members, pinned base, braced frame

## 5. Joint Element with Warping Capability

The proper continuity of warping displacements across member discontinuities (structural connections) is not ensured with the use of finite element beam elements, particularly for stiffened connections. This is due to the constraints on the beam element, which include the lack of a mechanism to model the restraint provided by the stiffeners in the joint. To circumvent this problem, a joint element was developed to join beam elements and maintain warping displacements through the connection.

The new element accepts the warping degrees of freedom from the connected beam elements and redistributes the warping to all connected members. This also permits small torsional displacements within the joint itself. However, there is no flexural nor translational stiffness provided by the element.

The basis for the element is Abaqus' shell element, S4. This element has several features that were deemed essential. Primarily, the element supports the “drilling” degree of freedom. This is the capability to support a moment whose action is within the plane of the element itself. Alternatively, this can be described as a moment vector perpendicular to the element.

As this element provides a flexible interface between the connected members, it will reduce the warping resistance experienced by the members at the joint. It acts as a partially restrained connection, allowing the connected members to warp with a “spring” type interface between them, rather than the rigid connection described in Chapter 4.

The new element forms the basis of a new set of elastic buckling analyses to investigate the effect of considering warping continuity on the elastic stability of frames.

## 5.1 Other joint elements

Special elements to model joints and connections in structures have been available for some time, though the frequency of their use seems to be increasing. These elements permit the analyst to model the characteristics of the connections between members, without the need for modifying the member elements themselves. However, there are arguments made for considering special cases in member elements, such as plastic hinges, as special joint elements (Krishnan, 2004).

Krishnan (2004) describes a special element that models the panel zone of a connection – the area of “web” that the connecting members share – in steel moment frames. This permits analysis of the shear deformations in the joint and how this affects the connected members and the frame behaviour.

A similar joint for reinforced concrete structures is described by Lowes, *et al.* (2004) for earthquake analyses. As reinforced concrete members and structures are usually more massive than their counterparts in structural steel, the connections take up considerable distances in most directions, affecting the geometry of the frame model. With this joint element, the reinforced concrete beams and columns can be modelled using their clear spans between joints and the joints can be modelled individually to account for local effects within the joint.

## 5.2 The shell element

The joint element discussed here is composed of S4 shell elements within Abaqus. This element is chosen in preference to other element types, such as the hexahedral “brick” element, as the shell element permits the direct inclusion of moments as well as forces. This allows the direct mapping of the flexural and axial degrees of freedom of the beam element to the corresponding degrees of freedom in the shell element. In order to accommodate all of the degrees of freedom required, a shell element supporting all six degrees of freedom in the

translational and rotational directions is selected. As the plate thicknesses are small compared to the other dimensions in the joint, thick element theory, where higher order effects on the stresses through the element's thickness are considered, are not applicable and thin shell theory will be used.

The shell element stiffness matrix can be thought of as being divided into two sub-elements, one for the out-of-plane (bending and shear) actions and one for the in-plane (membrane) actions. These are shown in Figure 5-1. One of the in-plane actions is the drilling degree of freedom that permits a torque to be applied perpendicularly to the element, causing rotation of the element in its own plane. This is very important in the analyses performed herein, as the drilling degree of freedom will map to one of the flexural degrees of freedom of the connecting beam element or the beam's torsional degree of freedom.

As the sensitivity of the entire joint element relies on that of the base element type, an analysis of the suitability of the elements was conducted. The available shell elements from Abaqus, S4 and S4R, are compared to one used in the program Aladdin (Austin, *et al.* 2000) as developed by Jin (1994), in Table 5-1. This table compares the displacements for a cantilever beam example used in Jin (1994). The structure being modelled is a plate acting as a cantilever beam 12 inches deep, 48 inches long and 1 inch thick. The material used has a modulus of elasticity of 30000 psi, and a Poisson's ratio of 0.25. A point load of 40 pounds is applied to the tip. The theoretical solution is 0.3553 inches of deflection. The first four models use a mesh of square elements. The two columns denoted by an asterisk (\*) employ a mesh of irregularly spaced nodes, as shown in Figure 5-3.

There are some problems noted with S4R, the element with a reduced number of integration points. This element uses one integration point in its formulation, compared to four in the case of S4. This reduced number of integration points can soften the element's apparent stiffness, as shown by the very large displacements for small numbers of elements. While the error does disappear with more elements in the joint model, the S4R does not perform as well as the full

integration element, S4. Therefore, the S4 element was selected as the basis for the assemblage.

However, there is less error if the structure is modelling using more elements. A comparison of models of an open shape with several elements shows less difference for models using S4 and S4R elements. The structure in question is a cantilever beam composed of an I-shaped cross section, with flange widths of 10 inches, a web depth of 10 inches, plate thicknesses of 0.25 inches and a length of 40 inches. The material has a modulus of elasticity of 10000 ksi and a Poisson's ratio of 0.3. The loading is composed of two opposing point loads applied in the plane of the flanges of 1600 pounds each, producing a torque on the beam. The mesh size in Table 5-2 is twice the number of elements across the height of the web or the number across the width of the flange. The number of elements along the beam is the same as the number across the flange. The results as reported by Jin (1994) and results from Abaqus are summarised in Table 5-2.

### **5.3 The assemblage, or joint element**

The beam elements that are used to model the beam-columns in the frame support, among other degrees of freedom, the warping degree of freedom. The other degrees of freedom, bending and lineal displacements, will be transmitted directly between members at the nodes of the model. The warping degrees of freedom for connected members connect via the joint element. In order for the warping displacements to be transmitted from one member to another at a joint in a frame, the joint element must accept the warping displacements from both members.

The joint itself is to be modelled as an assemblage of shell elements, each using the S4 element described above. However, the natural degrees of freedom of the shell elements and those it is meant to capture from the beam element are not compatible, in that there is no direct method of connecting the beam element's warping degree of freedom to the shell element. Also, the number of elements in



the joints would outnumber those in the rest of the frame. This would mean that a fairly simple structure's model could become overly complex with the inclusion of the joint element, and the results of interest – those of the beam-columns – would be lost in the detail results of the joint element. To alleviate these problems, some additional computation is required to reduce the complexity of the joint element and to align its degrees of freedom to those applied from the beam elements.

The joint configuration chosen for this element is one where the flanges of the column are continued vertically through the connection, and “continuity plates”, or horizontal stiffeners, are welded to both sides of the web and to the column flanges. There are, of course, many configurations that can be used in these connections, as shown in Figure 3-7, but the “box” configuration was chosen as it: represents a fairly common configuration; is compatible with multilevel frames; and provides physical continuity between all nodes. The last condition would not be satisfied for a mitre joint, for example. This geometry is shown in Figure 5-2.

Each of the four faces of the element formed by one of the “flange plates” will need to provide support for a degree of freedom that connects with an attached beam-column element's warping degree of freedom. While not modelled in this element, it is possible that the out-of-plane faces may need to provide this degree of freedom if there were the need to model torsional warping continuity for beam framing into the “open” sides of the joint. This configuration is unlikely, as the beams framing in that direction would typically use only a shear connection. It is not practical to establish a moment connection for beams framing into the weak axis of a column.

Figure 5-4 shows the degrees of freedom for one “face” of the joint assemblage that provide the warping displacement to support the warping degree of freedom of the beam element that frames into that face. A unit warping displacement from the beam will cause unit deformations at each corner of the plate forming this face, in the directions shown. This will provide a twisting displacement in the

assemblage that will produce the deformed shape shown in Figure 5-5 (in the same orientation as Figure 5-4) and in Figure 5-6 (looking into the open face of the joint). Note that both Figures 5-5 and 5-6 have the warping deformation acting in the opposite direction to the degrees of freedom shown in Figure 5-4.

The joint in the frame is to be considered as a rigid joint with respect to bending, so that the connected members are considered to rotate together. Therefore, the joint element will not be rotationally flexible. Also, the panel zone is not considered to be flexible with respect to the axial or shearing loads in the connected member. Therefore, the translational and rotational degrees of freedom are all expressed at the centre of the assemblage, represented by the three lines at the centre of the assemblage shown in Figure 5-7. The diagonal lines indicate the face to which warping is applied and the arrows at the corner nodes show the direction of the degree of freedom expressed in the joint element for the warping behaviour of the beam column.

### **5.3.1 Sensitivity test**

There are a number of considerations for determining the appropriate density for the mesh of the joint element. While the final condensed matrix is the same size, that being determined by the number of degrees of freedom that are expressed, it still reflects the complexity of the parent mesh used. More complex meshes will take more time to generate initially, but should not affect the general solution time, once condensed. However, the complexity of the original joint model should be kept reasonably low.

The joint element was modelled using S4 elements and various configurations to find how large the aggregate element should be, in terms of the number of shell elements. The base configuration is as shown in Figure 5-2 with four elements across the face of the joint element. The base number of elements of the joint element was varied to produce the results in Figures 5-8, 5-9 and 5-10. For the first two figures, the base model employed 32 elements across the face of the

joint, and only reflected S4R elements. Figure 5-9 presents the results of the analysis excluding the outlier point in Figure 5-8, that being the point for 2 elements across the face of the section. This better illustrates the trend of the other points. A more complex model using 64 elements as the basis was also modelled using a later version of Abaqus, version 6.7, and the results of that analysis are presented in Figure 5-10. Two element types were used for the models – the fully integrated S4 shell element and the reduced integration S4R shell element. The S4 element shows a larger error for coarse meshes than does the S4R element. However, the S4 element shows a smoother, more predictable curve. The differences in error between the S4 and S4R elements are very small after reaching 28 elements. A comparison of these two studies indicates that the mesh may be not yet be optimal, in that the error is still not zero even with the 64 element mesh density. However, the time required to condense one of these larger matrices is several times the solution time for the entire frame model.

A total of eight S4 elements across the face of the joint was chosen as a compromise between solution time and error in the joint model. The error is approximately 3% but the number of degrees of freedom is reasonable at about 3300. While the S4R elements appear to perform better at this density, their tendency to produce a more erratic error curve was considered to be a factor against using them.

## 5.4 Substructuring

Substructuring is the process used by Abaqus to generate the joint element. “Substructure” is the term used in the Abaqus documentation for a technique that other finite element analysis products call “super-elements.” A substructure is an assembly of several individual finite elements for which only certain degrees of freedom are “exposed” and available for use in the global stiffness matrix (Abaqus, 2002<sup>1</sup>). The other degrees of freedom of the individual elements are hidden internally by a process called “static condensation” (Bathe and Wilson,

---

<sup>1</sup> Section 7.2, “Substructuring” Abaqus Analysis User’s Manual

1976<sup>2</sup>). This can be thought of as the solution of the stiffness matrix formed by the individual elements for unit displacements applied in succession to the desired degrees of freedom, while the other expressed degrees of freedom have a zero displacement. As the degrees of freedom from the substructure are more closely connected than would be the degrees of freedom of a regular element matrix, the condensed stiffness matrix will typically be more fully populated than standard element stiffness matrices. That is, there will be relatively fewer zeroes in the condensed matrix than a typical element stiffness matrix.

The substructuring capabilities of the finite element analysis program were used, rather than assembling the super element “manually” and then eliminating the undesired degrees of freedom. The manual method would require incorporating a subroutine that pre-calculates the reduced stiffness matrix in a closed form solution that incorporates the local geometry, such as plate thicknesses and widths, and material properties, such as the modulus of elasticity, as parameters. This approach is known in Abaqus as a “user element.” This method would be a more complex process for the analyst, requiring generation and compilation of the routine outside Abaqus. The substructure method is implemented entirely within Abaqus.

To map the warping degree of freedom from the beam element to the displacements in the substructure element, the corner displacements in the direction of the beam’s axis are constrained to be equal to each other through the use of the \*EQUATION<sup>3</sup> command. The \*EQUATION constraint sets up linear equations where the displacement of one degree of freedom is tied to other degrees of freedom. In this case, each alternate corner node of the joint element is set to have equal and opposite displacements in the direction of the attached beam. This requires three constraint equations per face, and removes the relevant degrees of freedom for the first node in each equation.

---

<sup>2</sup> Section 10.3.1, pages 388-395

<sup>3</sup> Section 20.2.1, “Linear constraint equations” Abaqus Analysis User’s Manual

$$DOF = 6(2(N_x + 1)(N_y) + 2(N_x + 1)(N_z) + (N_z - 1)(N_y - 1)) \quad [5-1]$$

The total number of degrees of freedom in the full joint element can be found from Equation [5-1] where  $N_x$  is the number of elements across the face of the joint,  $N_y$  is the number of elements “down” one vertical face and  $N_z$  is the number along a horizontal face. The total number of degrees of freedom would increase at about the same rate as  $N_x^2$ . An aspect ratio of 3:2 for both  $N_y: N_x$  and  $N_z: N_x$  produces a total of 870 degrees of freedom for 4 elements across the joint face, 3318 for 8, 12966 for 16 and 203910 for 64. The solution of a stiffness matrix of this size would be relatively slow, especially when compared to the stiffness matrix for a small frame.

While it may be noted that the final element still only expresses 10 degrees of freedom, no matter how detailed the underlying geometry, this more complex geometry still needs to be calculated. The large original matrix must be condensed to the smaller desired matrix and this requires processing time, even if it is done once per typical joint.

As the forcing degree of freedom for the substructure is still a force, while that on the warping degree of freedom is a bi-moment, the stiffness from the substructure must be converted from a force to a bi-moment by multiplying by the flange width,  $b$ , and depth between flange centroids,  $h$ , as per Equation [5-2] from Chen and Atsuta (1977)<sup>4</sup>. This simplification can be done as the flange moments,  $M_{ft}$  in the top flange and  $M_{fb}$  in the bottom flange, will be opposite and equal to each other and equal to  $b P$ , where  $P$  is the flange tip force.

$$M_\omega = \frac{h}{2} [M_{ft} - M_{fb}] = hM_{ft} = hbP \quad [5-2]$$

---

<sup>4</sup> Equation 6-9, page 273.

## 5.4.1 Deficiencies of the joint element as a substructure

The connection element is not as accurate as detailed models of the connection using shell or solid elements to model all the members and the connections. The major reason for this is imposed by the limitation that the beam elements framing into the connection consider warping only by a single degree of freedom. While this is consistent with other simplifications of the beam element, it does not allow for the discontinuous warping of the cross section, experienced when the connection has differing support conditions for opposite flanges. An example of this is the connection at the top “corner” of a frame, with the lower flange of the horizontal member connected rigidly to the vertical member, and the upper flange free. In this instance, the upper flange has a larger distortion than the lower flange. At a joint where the vertical member is continuous, the warping of the beam flanges are closer to being equal. (See Table 3-1 for numerical values of this phenomenon.)

The joint element also does not fully capture the torsion within the joint. This could be incorporated fairly readily by expressing the torsional, or drilling, degree of freedom of each flange plate in the substructure. However, this almost doubles the nodes and, thus, the complexity of the joint. However, because the joint covers a very short length, the warping behaviour would be the primary torsional component for the joint, and the additional effects from twisting within the joint would be small.

The substructure cannot be used with Eigenvalue buckling analyses in Abaqus as the program does not generate the geometric stiffness matrix for the element, and will not allow the element to act as a complex “spring” restraint otherwise.

While the constraint equations use the local coordinate system for the element in defining the warping degree of freedom as local displacement degrees of freedom, these are translated into global coordinates in Abaqus in general analyses. When

the local coordinates do not align with the global coordinate system, as is the case with non-linear geometric analyses involving the co-rotational aspects of the elements, there is a cross-link between the degrees of freedom at a node that are related to the substructure's faces, and should be handled separately. The two supposedly independent degrees of freedom become related to each other through the global degrees of freedom. This cross-linking leads to a situation whereby the local degrees of freedom become related to each other, and ultimately to themselves, causing a dilemma that Abaqus cannot resolve. This is an over constrained problem, however the cross-linking of the degrees of freedom is only required for the static condensation, and if the resulting reduced stiffness matrix was used in place of the substructure, this over-constraint would be avoided.

As noted previously, the stiffness from the substructure must be converted from a force degree of freedom to a bi-moment degree of freedom.

To avoid the above mentioned problems, the joint element is converted from the substructure to a user element that allows eigenvalue analysis. This also negates the problem of cross linking of constraints, as the exposed degrees of freedom can be manipulated outside the constraints of the super element.

The element does not fully incorporate the interaction that the joint experiences with other forces, particularly the bending moments that are applied to the faces of the joint. To partially account for these, the plates forming the box element were restrained from bending about their weak axis at the edge of the joint. This would result from the restraint provided to the plates by the moment causing strong axis bending in the joint, already considered in the rigid connection formed by the beam-column members framing directly into each other at the joint. This modification did not greatly affect the stiffness of the joint element.

## **5.4.2 Using the substructure in Abaqus**

While other finite element analysis programs employ this method of substructures, albeit under other names, each has its own terminology and

syntaxes for using the process in its program. A short description of the specifics of the Abaqus implementation is included here to explain the process.

The substructure is generated the same way that any model is created in Abaqus. The nodes are laid out to follow the geometry of the model. The elements are meshed between these nodes and are given the material and geometric section properties they require. A “load step” is then run to perform the static decomposition of the substructure to produce the reduced stiffness matrix with the expressed degrees of freedom. The substructure is stored as a database file in the same directory as the analysis will be executed.

Once the substructure has been formulated, it is treated as another element. The substructure nodes that support expressed degrees of freedom are matched with nodes in the full model. That is, the analyst must place nodes in the full model that are at the same locations as those in the substructure. These nodes are used to define the orientation of the substructure as an element in the full model. The degrees of freedom at these nodes will be connected to the degrees of freedom from the connecting elements. This sharing of degrees of freedom would typically be done through constraint equations. Simply using the same nodes as the beam would not connect the flexural and axial degrees of freedom. Also, if the substructure element is defined at one location, the element must be “translated” to the appropriate location with a “\*SUBSTRUCTURE PROPERTY” command. As the translation is represented by the distances moved in three dimensions from the original definition to the new location, it is convenient to define the substructure centered at the origin, and use the nodal coordinates at which the members meet for the translation distances.

A PERL script to generate the required substructure in Abaqus commands is included in Appendix “A”. PERL is a programming language that is available for most computer platforms (Wall *et al.*, 2000).



The stiffness matrix from a substructure is generated by the use of the Abaqus command “\*SUBSTRUCTURE MATRIX OUTPUT” during the run that creates the substructure.

## **5.5 Frame analysis with the joint element**

To illustrate the effect that the stiffened connection has on frame stability, the frames composed of W200x27 members and columns with fixed base plates, discussed in the previous chapter, were re-analysed incorporating the substructure element in the model.

In the first step of the analysis, the joint element was formed as a substructure and its stiffness matrix was generated. In this particular case, the stiffness matrix was collected for the joint element having only two expressed degrees of freedom: the warping degree of freedom for the vertical face; and the warping degree of freedom for the horizontal face. These two degrees of freedom provide three stiffness components: one for each warping degree of freedom, plus an interaction between the two warping degrees of freedom. As the warping deformation produces no net force on the element, the warping stiffness can be thought of as a single degree of freedom stiffness, affecting only the displacements of the joint element. The stiffness matrix from the substructure was multiplied by the depth and width of the connection as described in Equation [5-2] to maintain consistency between the expected “force” degrees of freedom.

These three stiffness components were applied as three springs on the frame. It is also possible to use the stiffness matrix directly as a “user element”, but since both approaches result in the same stiffness being applied to the model, the same buckling capacities result from either procedure. If any stiffness component is negative, the user element would have to be used, but all stiffness values are positive for this substructure.

Unfortunately, the Abaqus spring element will not directly operate on the warping degree of freedom, so an indirect method of connecting the springs was required.

New “dummy” nodes were created to match each of the end nodes of the beam elements meeting at the joint. The warping degrees of freedom at the end nodes of the beam elements meeting at the joint were each tied to a supported (i.e. lineal) degree of freedom of one of these dummy nodes. The direct warping stiffness from the corner joint matrix was attached as a SPRING1 element to the dummy node. The SPRING1 element is an element that connects to one degree of freedom and acts as a spring to produce a force on that degree of freedom when it is displaced. This is considered to be a spring that links the degree of freedom with the “ground”. This physically represents the restraint of the joint node on the warping degree of freedom of the beam or column. The interaction between the warping of the elements meeting at the joint is expressed as a SPRING2 element between the two supported degrees of freedom of the dummy nodes. As a comparison to the SPRING1 element, the SPRING2 element links two degrees of freedom and generates a force between them as the two degrees of freedom experience displacement. This model is illustrated as schematic in Figure 5-11. The rectangular beam elements are connected to the dummy nodes via constraint equations, linking the beam elements’ warping degrees of freedom to the dummy nodes’ lineal degrees of freedom. The SPRING1 elements connect the dummy nodes to ground and the SPRING2 element connects the two warping degrees of freedom.

The results of these analyses are displayed in Figures 5-12 to 5-16. These figures show the relative change (always an increase) in buckling capacity between frames that are modelled without a connection between members on their warping degrees of freedom, and members that have their warping degrees of freedom connected through a joint element. The frames are the same general format as those presented in Chapter 4 – a beam supported by two identical columns. Each graph shows the results for one column height, but with several beam lengths. The horizontal axes of the graphs are the beam length and ratio of the applied axial load to the column buckling load,  $P_e$ , considering the effective length of the columns (an effective length factor of  $k_y = 0.7$  is used). The immediate observation is that the strength increase is significantly lower than that found in

the rigidly connected frames presented in Chapter 4. Apparently, the rigid connection over-estimates the warping restraint when compared to the joint element.

However, it is difficult to completely restrain, or in this case transmit, warping displacements in structures. Work by Ojalvo and Chambers (1977) included testing of I-shaped beams with channel sections welded to the beam ends. These channel sections were intended to prevent warping of the flanges as the webs of the channels were welded to the beam flange tips, and the channel flanges were welded to the web of the beam. This is a greatly stiffer connection than any modelled herein. The test results are summarised in Table 5-3. The first two columns in the table designate the particular test by beam section and length. The third column is a ratio of the test load to the unrestrained buckling capacity. The fourth column is the ratio of the theoretical buckling moment for a beam with warping completely restrained to the buckling moment for a simply supported beam. The last column presents the ratio of these two values – the test result over the fully restrained moment capacity. This shows that the very stiff restraints were able to provide only about 90% of the theoretical value.

The rigid connections between the members' warping degrees of freedom used in Chapter 4 illustrate the maximum effects of mutual warping interaction. The weaker interaction demonstrated by the joint element indicates that this maximum may be significantly more than the amount of warping that can be transmitted by the connection.

As the increase in stiffness is small, there is not a great deal of detail visible in Figures 5-12 to 5-16. However, the buckling multiplier is largest for shorter beams at low axial load ratios, as in Figure 5-12 for the shortest column, and dropping to one or near one at the maximum axial load ratio. As the columns increase in length, the increase in strength affects longer beams, as can be seen in the progression from 3 m columns in Figure 5-13, where only the shorter beam lengths are affected, through the 4 m columns presented in Figure 5-14, showing a

rather steep drop-off in strength increase for longer beams. The trend is almost complete in Figure 5-15, for 5 m columns where only the longest beams at the lowest axial load show the decrease in strength and finishes in Figure 5-16, where the entire graph shows a uniform plateau for buckling capacity increase.

As a check on the influence of the stiffness of the joint element, the stiffness of the springs was increased by a factor of 1000 and another set of analysis models generated. These are presented in Figures 5-17 to 5-21 and show a significant increase in buckling strength. With the larger increase in capacity, the progression of a change in strength following the length of the column from 2 m in Figure 5-17, to 3 m in 5-18, 4 m in 5-19, 5 m in 5-20 and 6 m in 5-21 is illustrated better than with the unmodified element. This parallels some of the findings in the rigidly connected frames discussed previously, where the ratio of the length of the beam to the length of the column was shown to be a predictor of this buckling behaviour.

## 5.6 Summary

This chapter outlined the creation of an assemblage of elements to represent the warping at a stiffened moment connection in a steel frame. It also presented how this could be adapted to form a mechanism to directly model the warping stiffness at the joint in a frame situation.

The joint element acts as a spring, and is much more flexible than the direct connections provided by rigidly connecting the beam-column elements together. This reduces the strengthening contributions of the mutual warping interaction. Because of the reduced stiffness introduced by the joint element when compared to the rigidly connected warping degrees of freedom in the analyses presented in Chapter 4, it is likely that the results from simple buckling analyses connecting the members together may be optimistic. However, the frame does not experience any weakening due to this interaction, strengthening the conclusion that the warping interaction in frames is not deleterious to the frame behaviour, and that

ignoring that contribution in the design of frames is not unconservative. Also, the strengthening effect considering the flexibility of the joints appears to be negligible, at least in some cases.

**Table 5-1** Comparison between Aladdin and Abaqus elements, tip deflection of a fixed cantilever with rectangular cross section (inches)

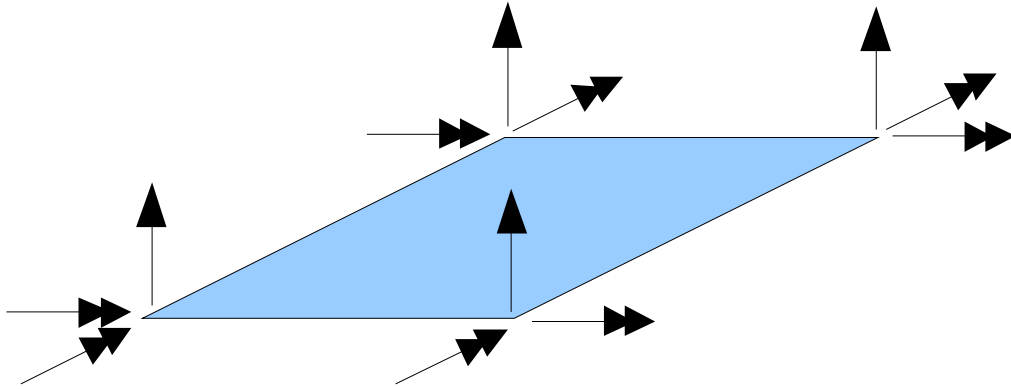
<b>Meshes</b>	<b>4 x 1</b>	<b>8 x 2</b>	<b>16 x 4</b>	<b>4 x 1*</b>	<b>8 x 2*</b>
Jin (1994)	0.34	0.35	0.35	0.31	0.35
% error	3.04%	1.38%	0.282%	13.71%	2.76%
Abaqus S4 Element	0.35	0.35	0.36	0.55	0.38
% error	1.83%	0.619%	0.873%	54.5%	7.94%
Abaqus S4R Element	55.01	0.47	0.39	33.30	0.47
% error	15400%	33.4%	8.98%	9270%	33.4%

**Table 5-2** Lateral displacement of flange tip for I-shaped cantilever experiencing torque, (inches)

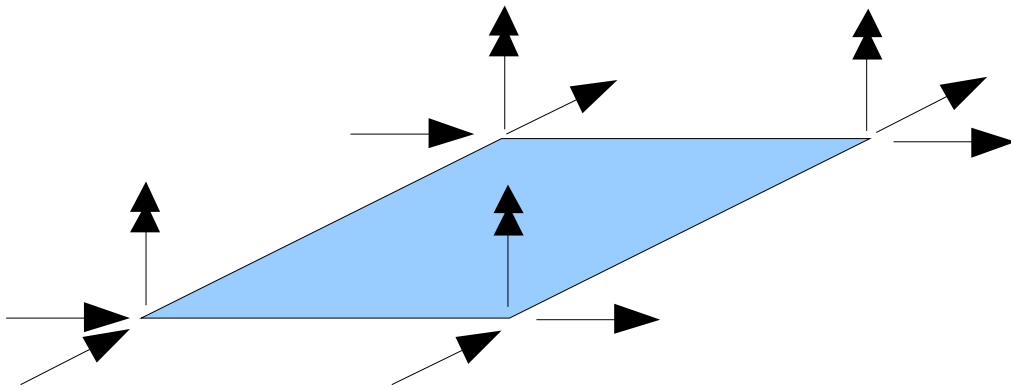
<b>Meshes</b>	<b>2</b>	<b>4</b>	<b>8</b>	<b>16</b>
Jin (1994)	0.139	0.147	0.149	0.150
ANSYS 5.0 (From Jin, 1994)	0.063	0.111	0.137	0.146
SAP 90 (From Jin, 1994)	0.104	0.131	0.144	0.148
Abaqus S4 Element	0.140	0.149	0.152	0.153
Abaqus S4R Element	0.181	0.158	0.154	0.154

**Table 5-3** Results from tests from Ojalvo and Chambers (1977) compared to theoretical warping fixed beam.

Shape	Normalised Length (L/a)	Normalised Test Strength	Theory	Ratio Test / Theory
W21x49	2.73	3.28	3.62	0.91
	4.10	2.89	3.15	0.92
	5.47	2.63	2.82	0.93
	6.83	2.46	2.61	0.94
	8.20	2.34	2.46	0.95
W30x99	2.18	3.45	3.85	0.90
	3.27	3.09	3.42	0.90
	4.36	2.81	3.08	0.91
	5.45	2.61	2.83	0.92
	6.54	2.47	2.65	0.93
W18x50	2.26	3.42	3.81	0.90
	3.39	3.05	3.37	0.90
	4.52	2.78	3.03	0.92
	5.65	2.58	2.79	0.93
	6.78	2.45	2.61	0.94
W24x100	1.89	3.55	3.97	0.89
	2.84	3.22	3.58	0.90
	3.79	2.94	3.24	0.91
	4.74	2.73	2.98	0.92
	5.68	2.58	2.78	0.93
W21x112	1.91	3.55	3.96	0.90
	2.86	3.22	3.57	0.90
	3.81	2.94	3.24	0.91
	4.77	2.73	2.97	0.92
	5.72	2.58	2.78	0.93
W12x53	1.67	3.63	4.06	0.89
	2.51	3.33	3.71	0.90
	3.34	3.06	3.39	0.90
	4.18	2.85	3.13	0.91
	5.02	2.68	2.92	0.92
Average				0.9142
CoV				0.0170



a)



b)

**Figure 5-1** Shell element with degrees of freedom separated into a) flexural (out of plane) and b) membrane (in-plane) degrees of freedom



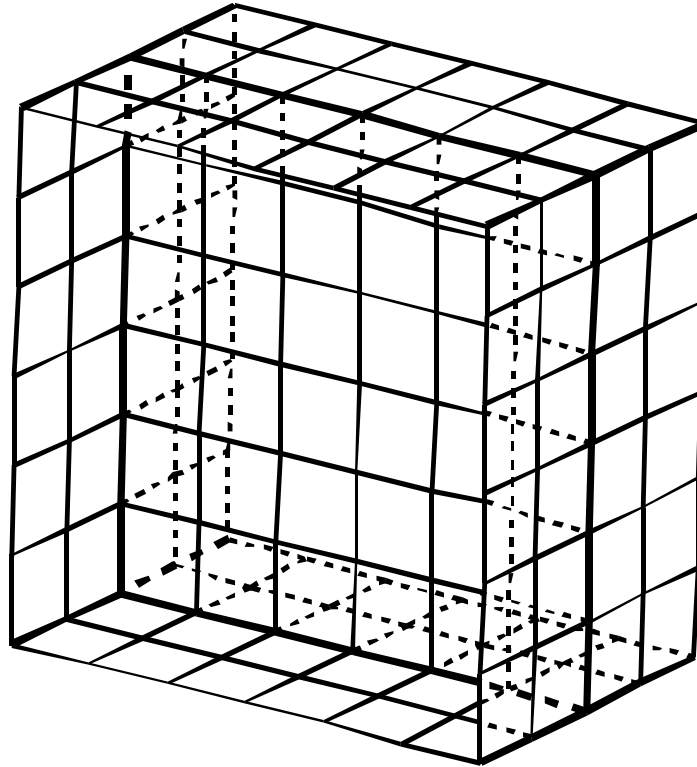


**Figure 5-2** Joint element mesh, 4 elements across the face

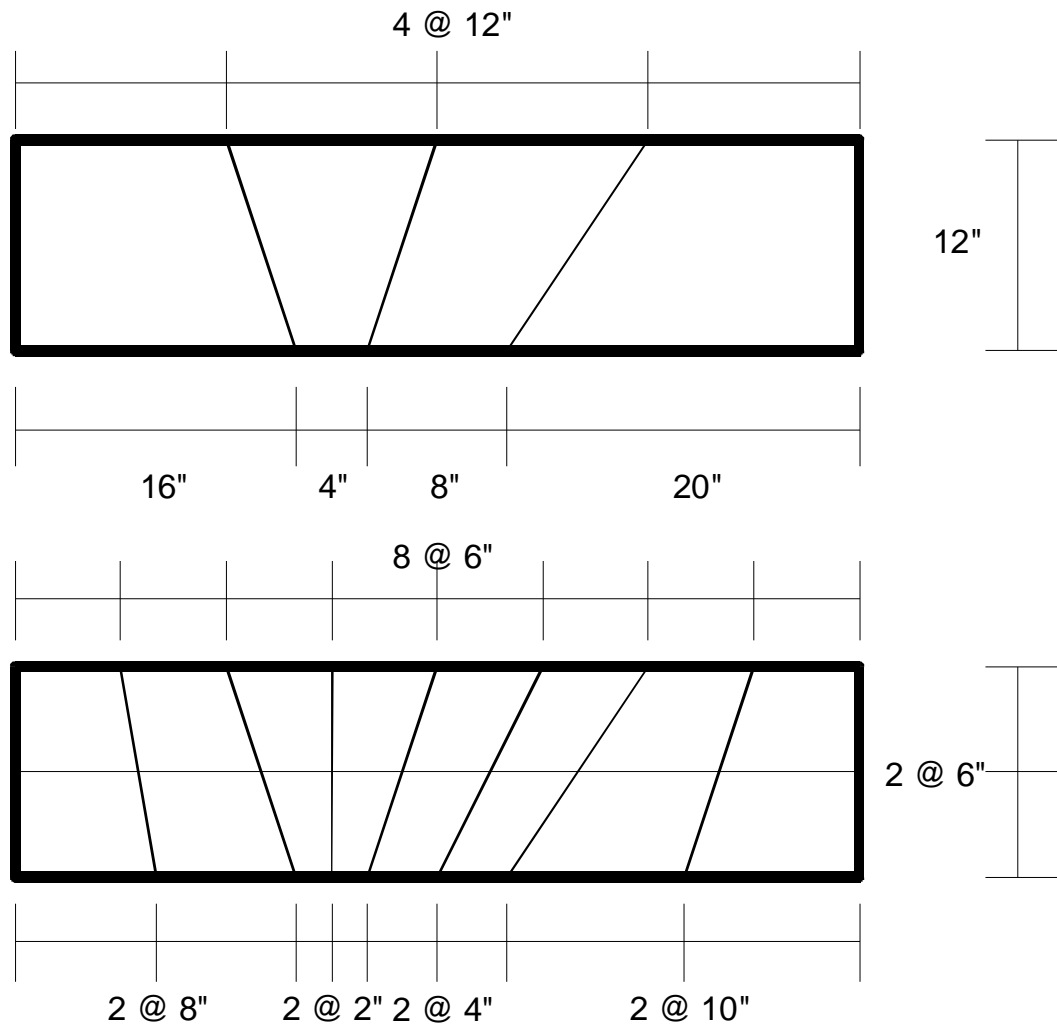


**Figure 5-3** Irregular mesh for cantilever (Jin, 1994)

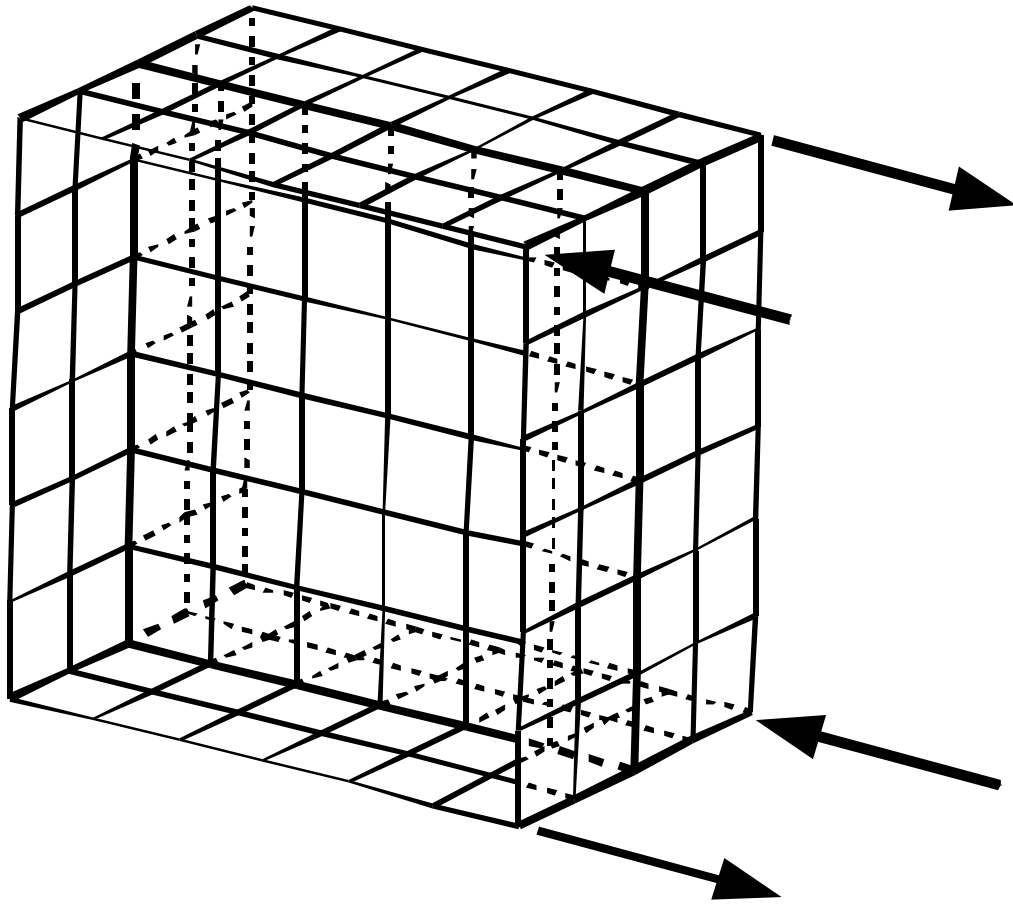


**Figure 5-4** Displacement degrees of freedom in the joint element that form a single warping degree of freedom.

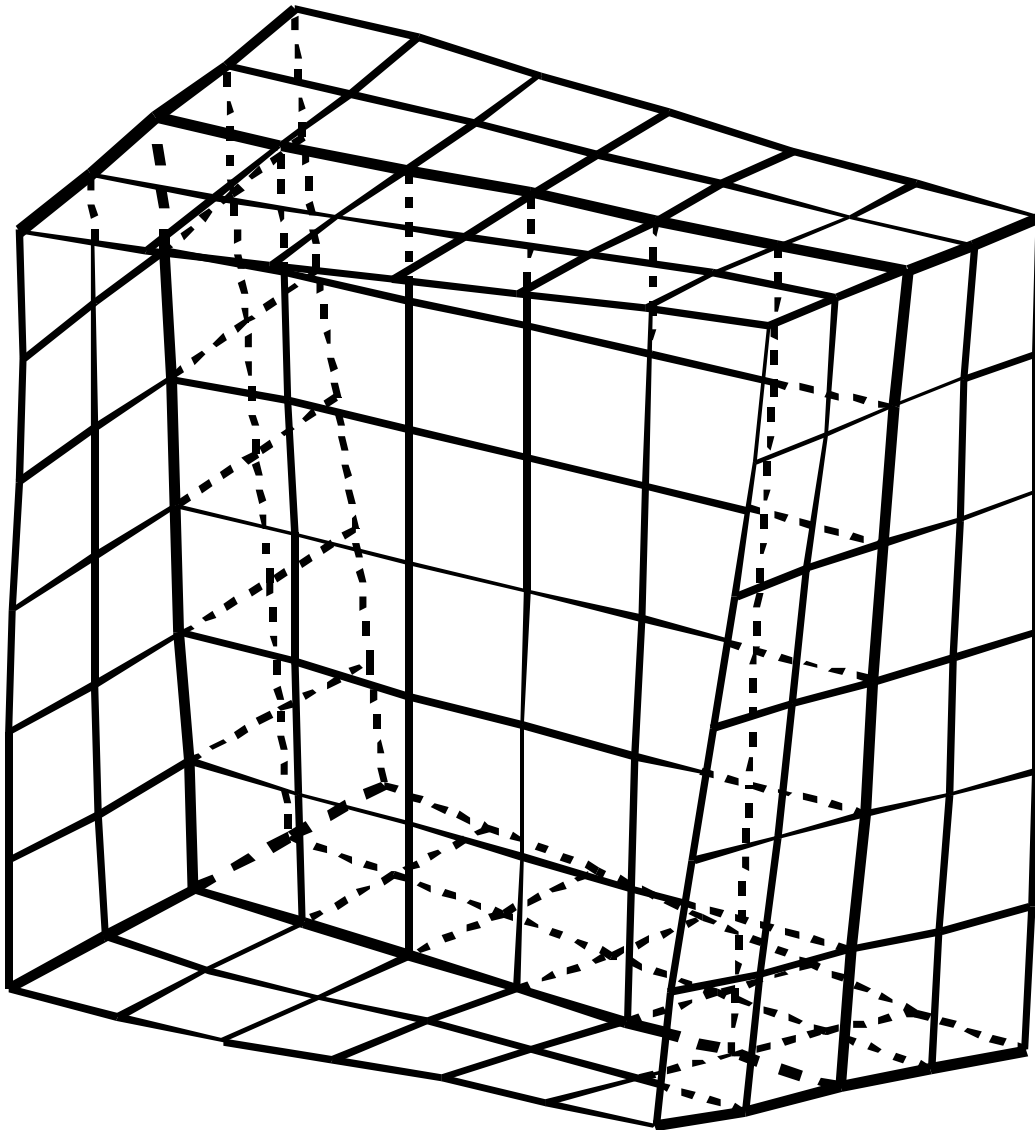


**Figure 5-5** Joint element with warping displacement applied to one face, through the unified degree of freedom.

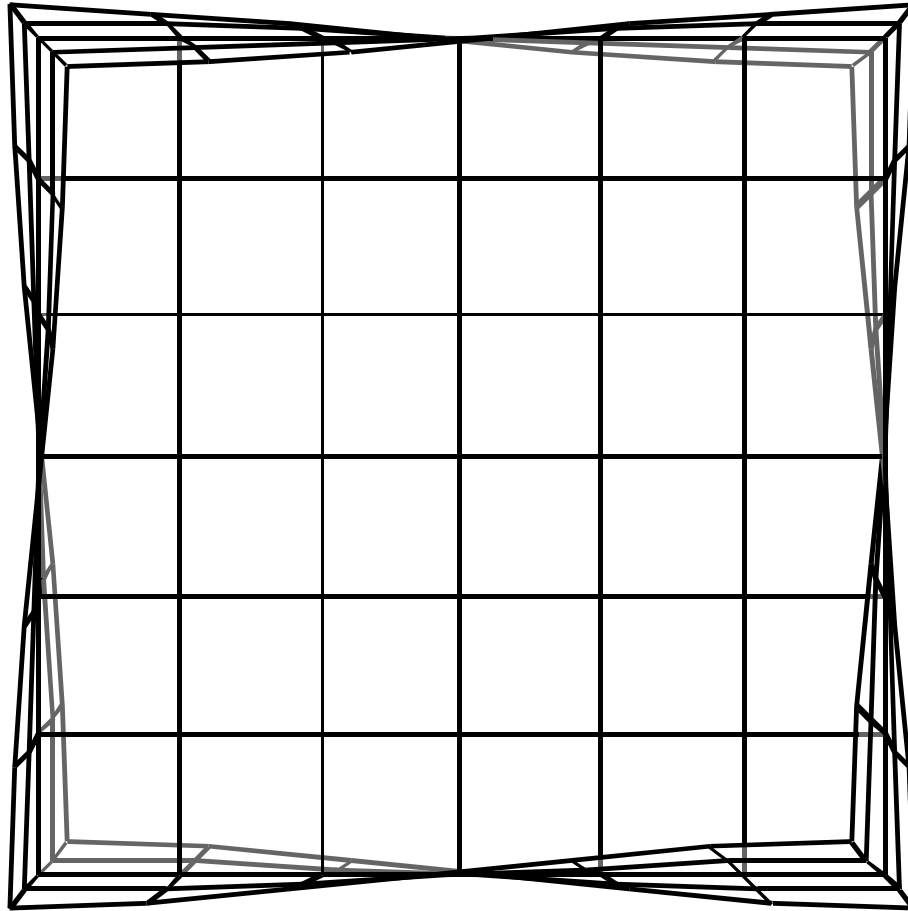


**Figure 5-6** Side view of element with displacement on the warping degree of freedom.

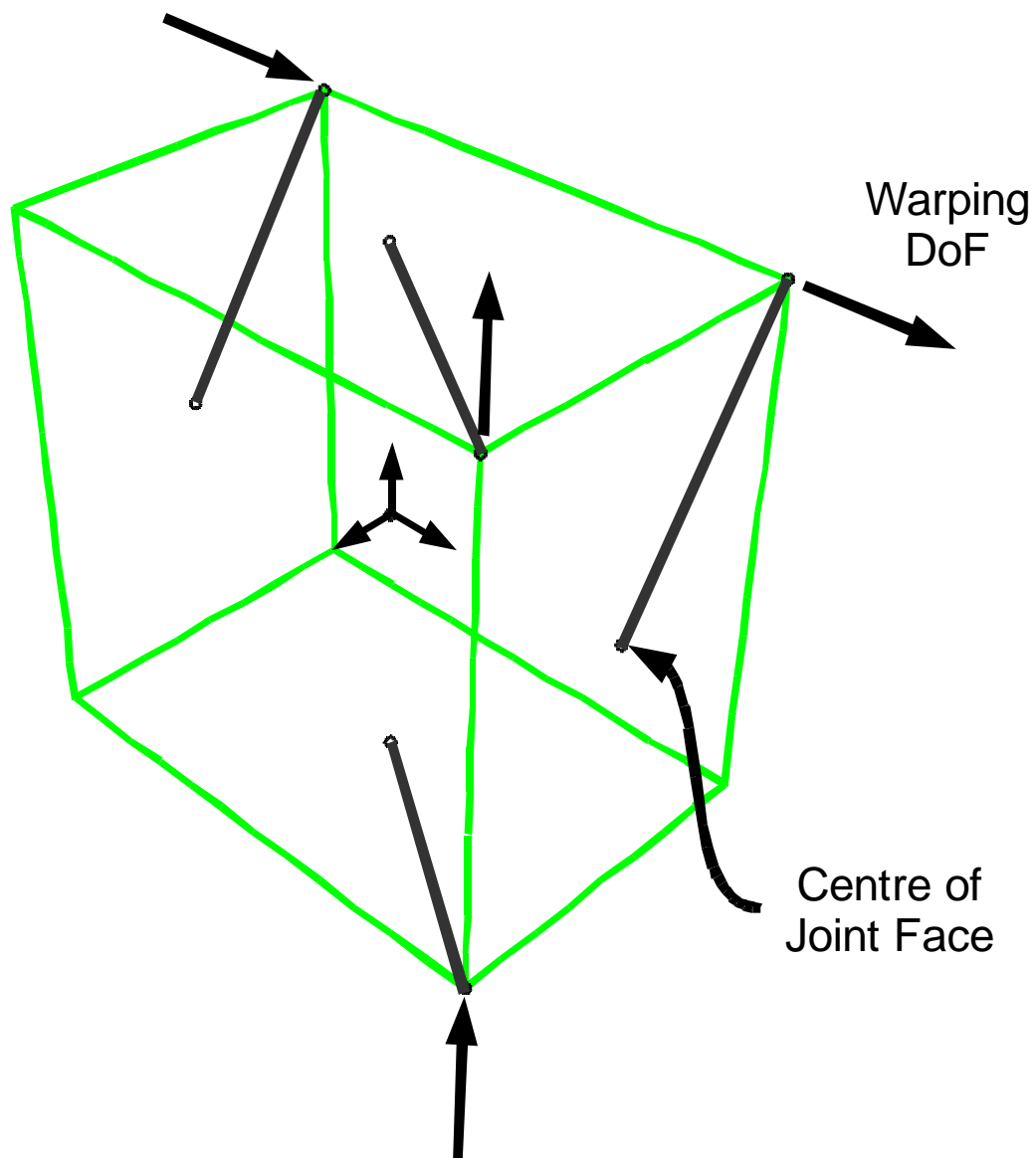


**Figure 5-7** Schematic of joint element showing the linear degrees of freedom expressed for the warping displacement.

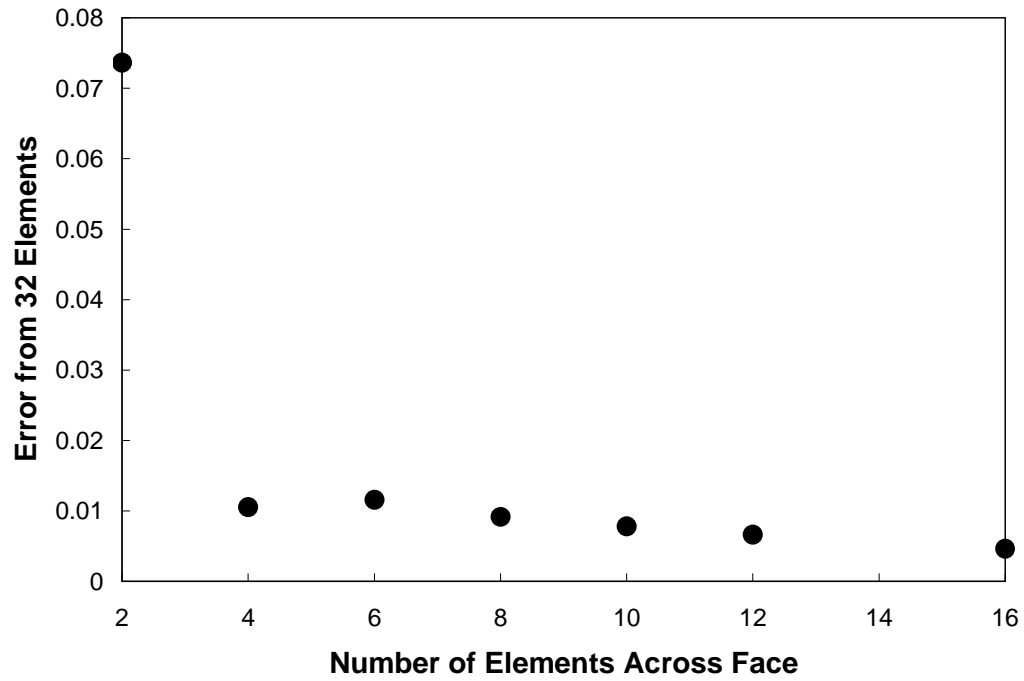


**Figure 5-8** Error in the S4R shell element model, relative to results from 32 element wide model.

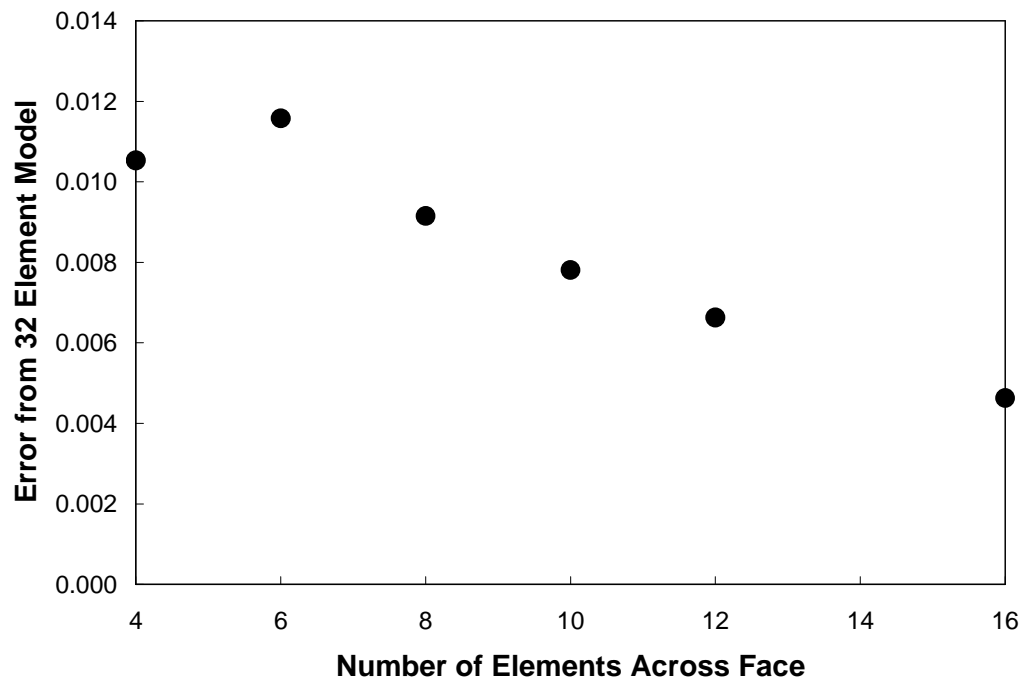


**Figure 5-9** Relative error in the S4R shell element model, based on 32 divisions on the edge

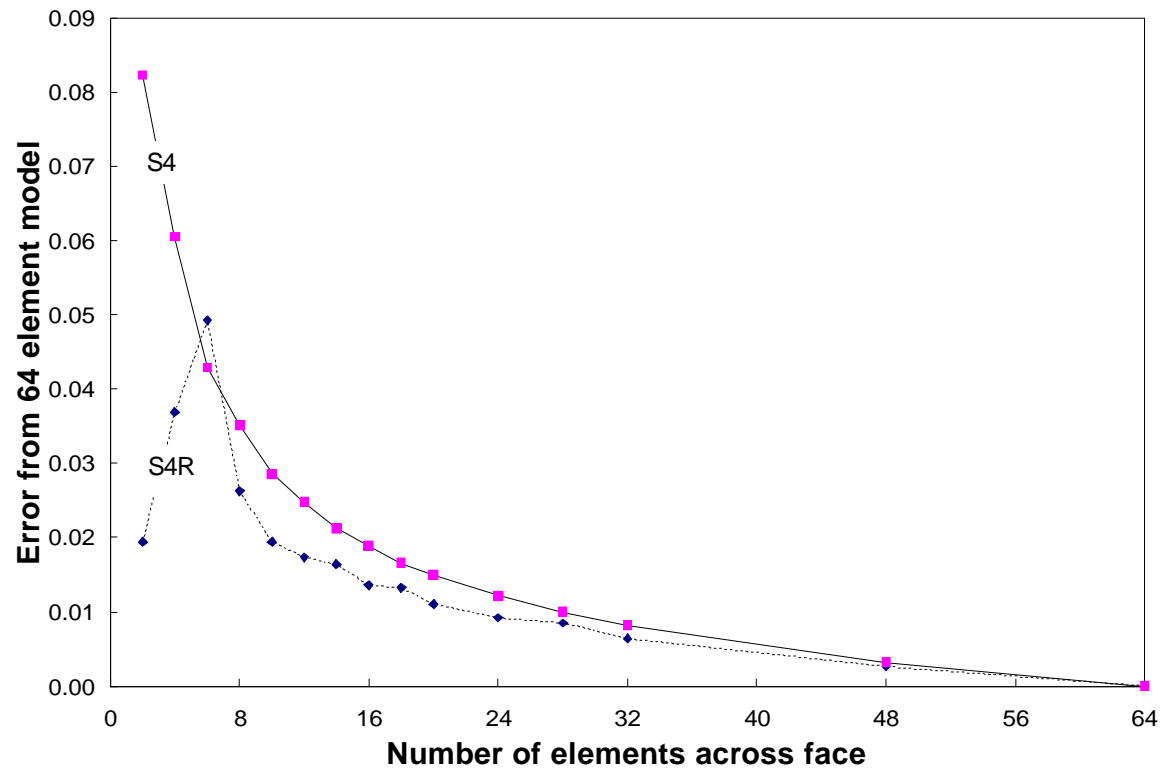


**Figure 5-10** Error in corner displacement relative to 64 elements across the face of the joint element.



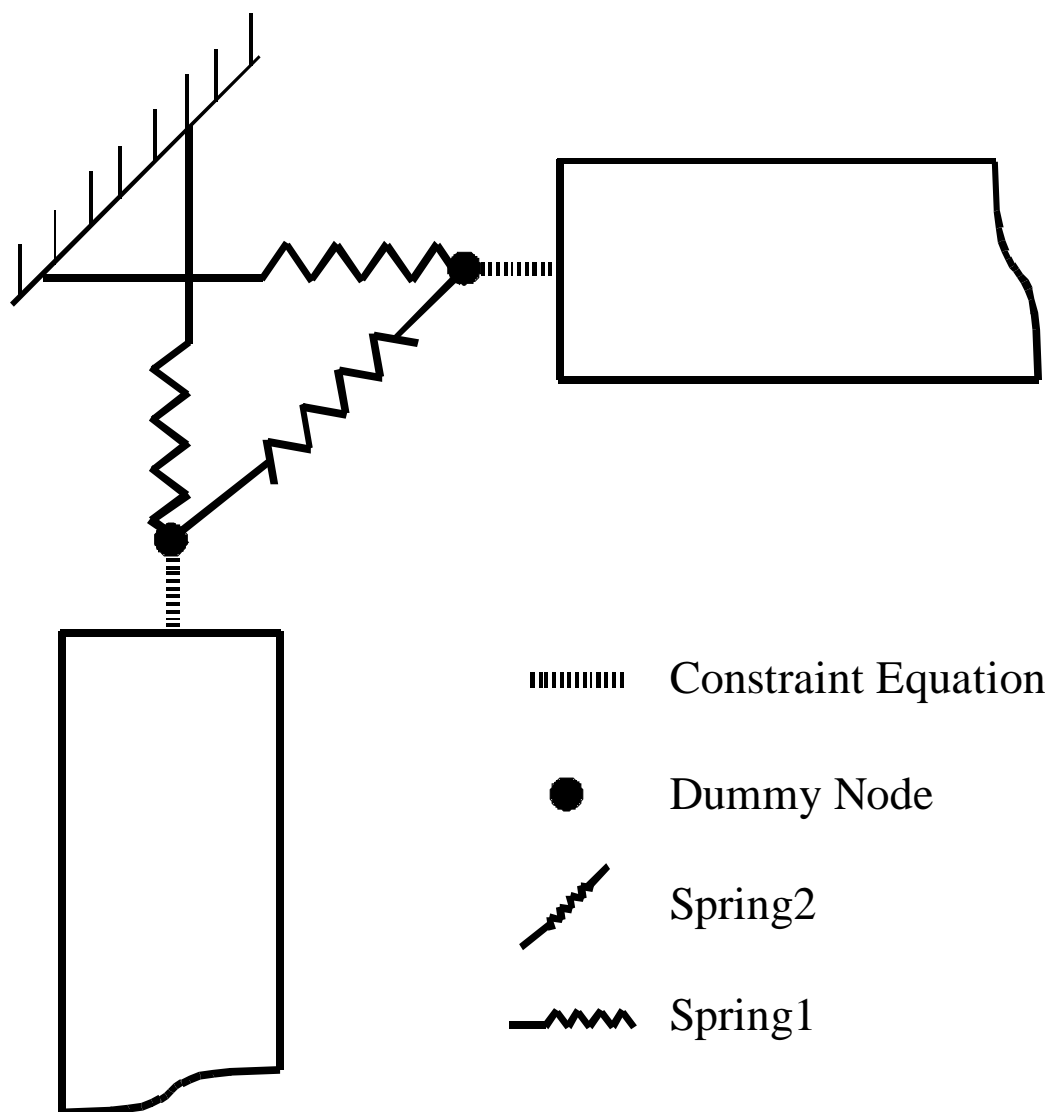


**Figure 5-11** Schematic of spring model.

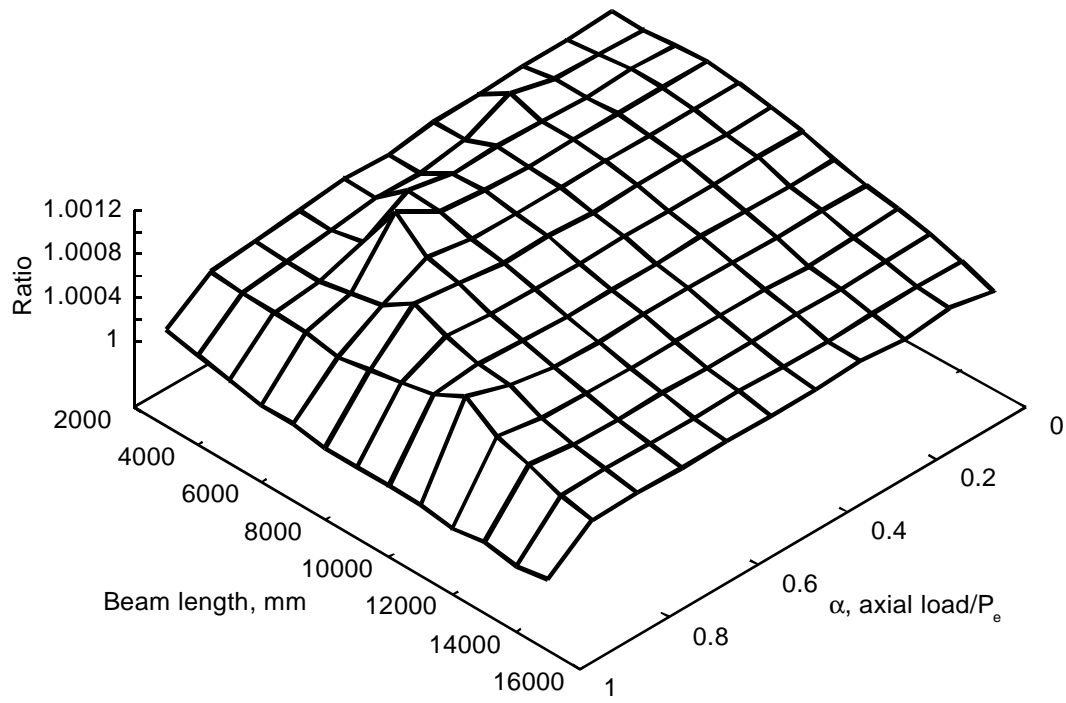


**Figure 5-12** W200x27 frame – fixed base 2000 mm columns, joint element.

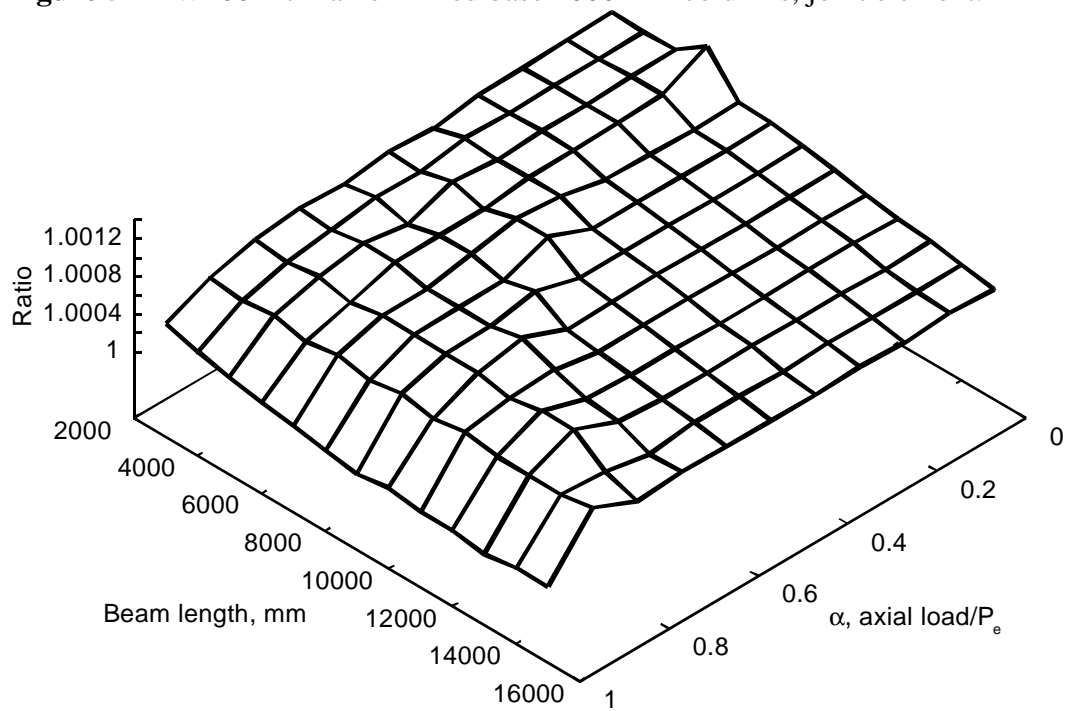


**Figure 5-13** W200x27 frame – fixed base 3000 mm columns, joint element.

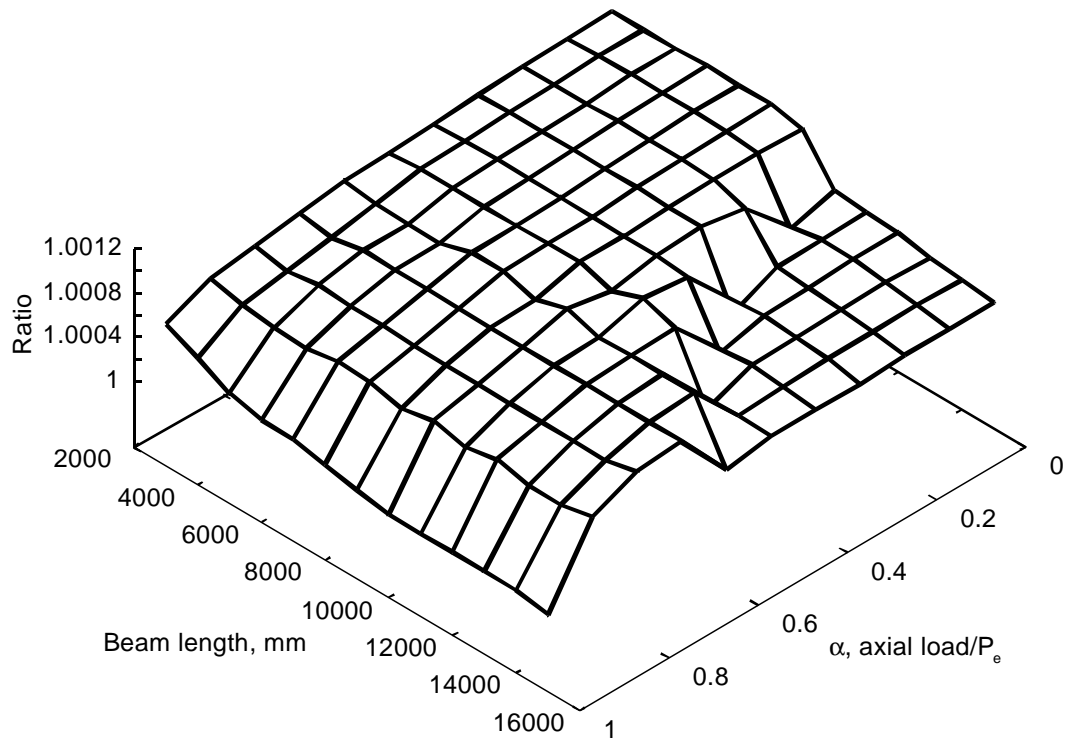


**Figure 5-14** W200x27 frame – fixed base 4000 mm columns, joint element.

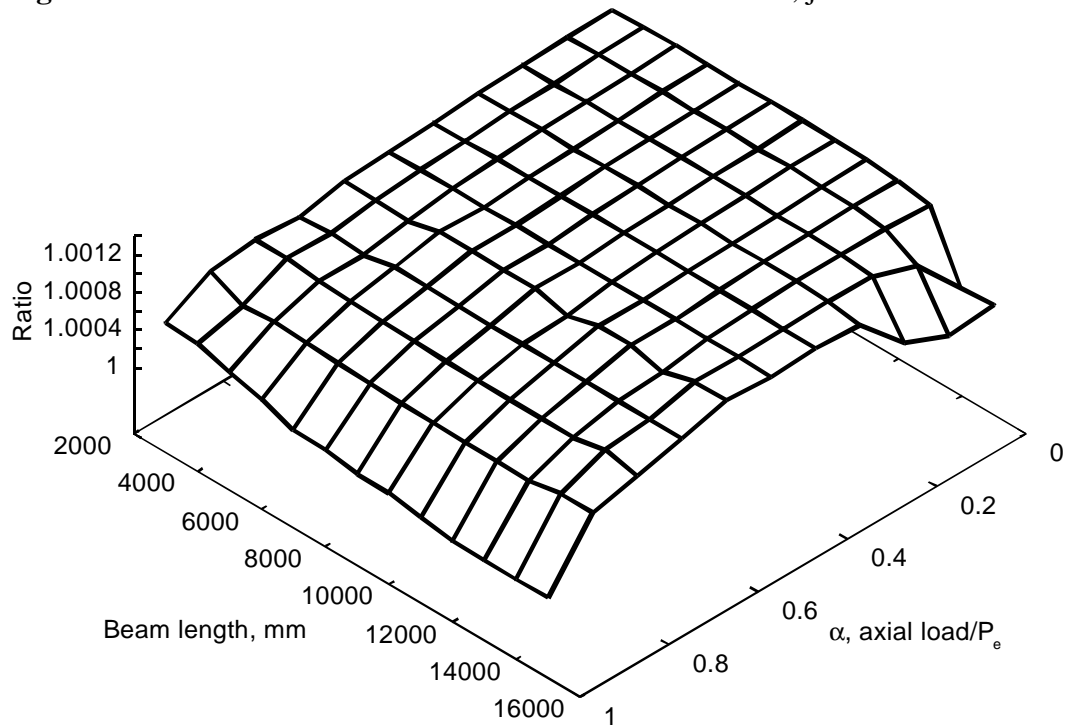


**Figure 5-15** W200x27 frame – fixed base 5000 mm columns, joint element.

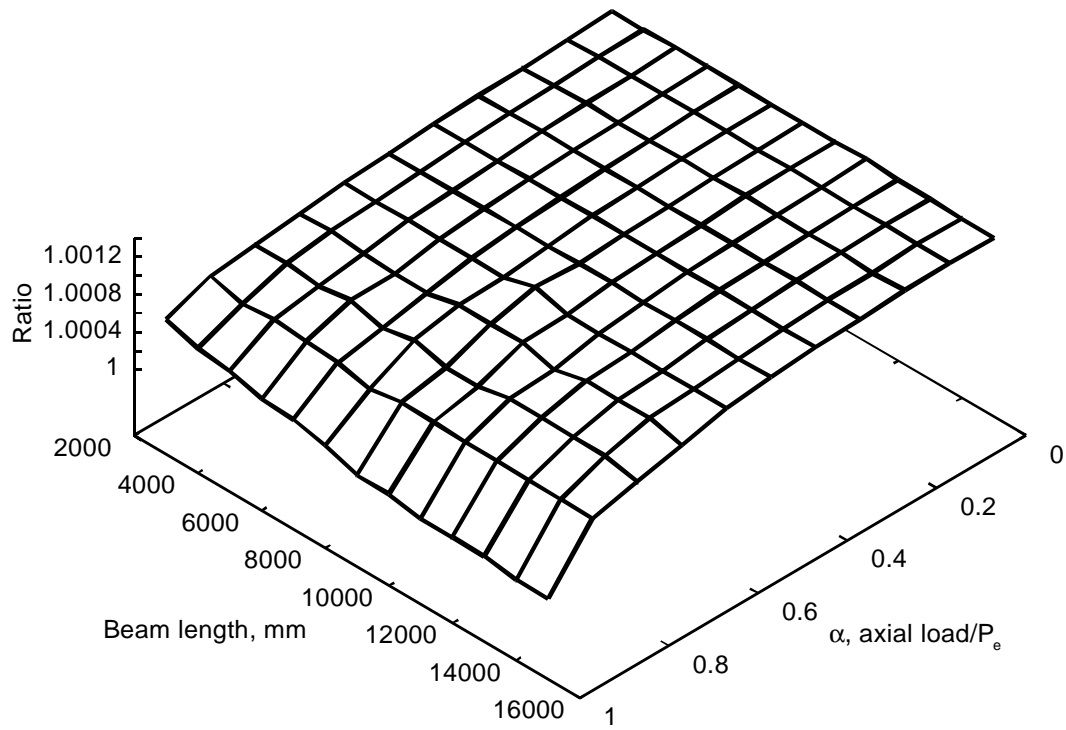


**Figure 5-16** W200x27 frame – fixed base 6000 mm columns, joint element.

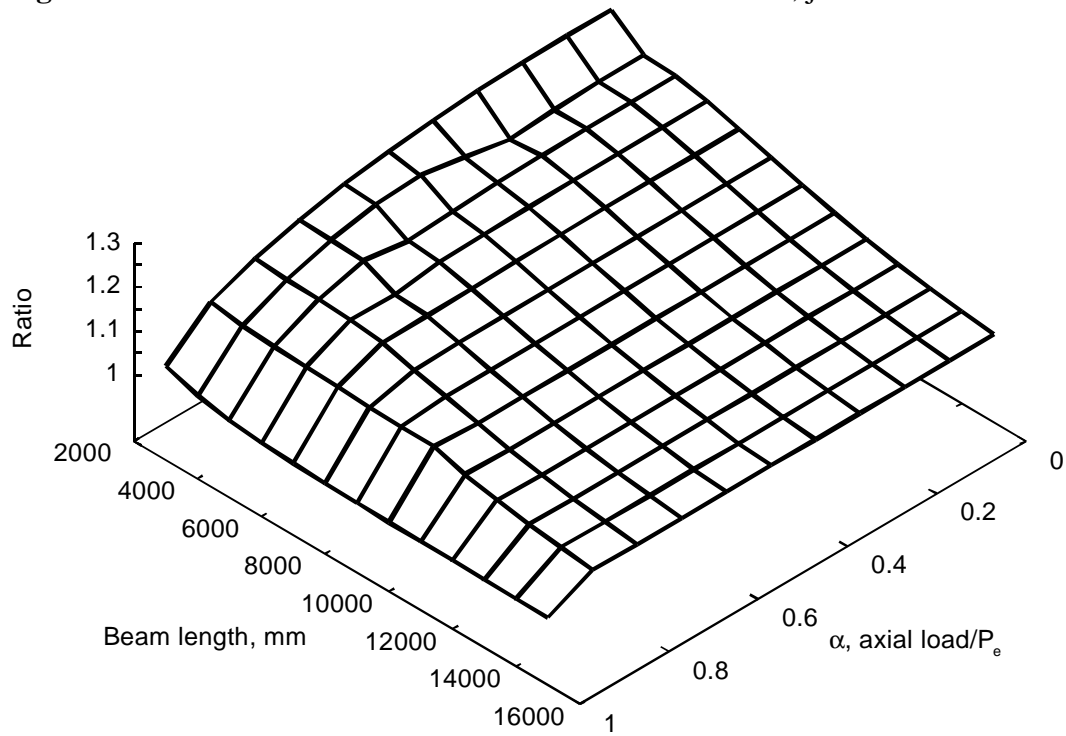


**Figure 5-17** W200x27 frame – fixed base 2000 mm columns, stiffer joint element.

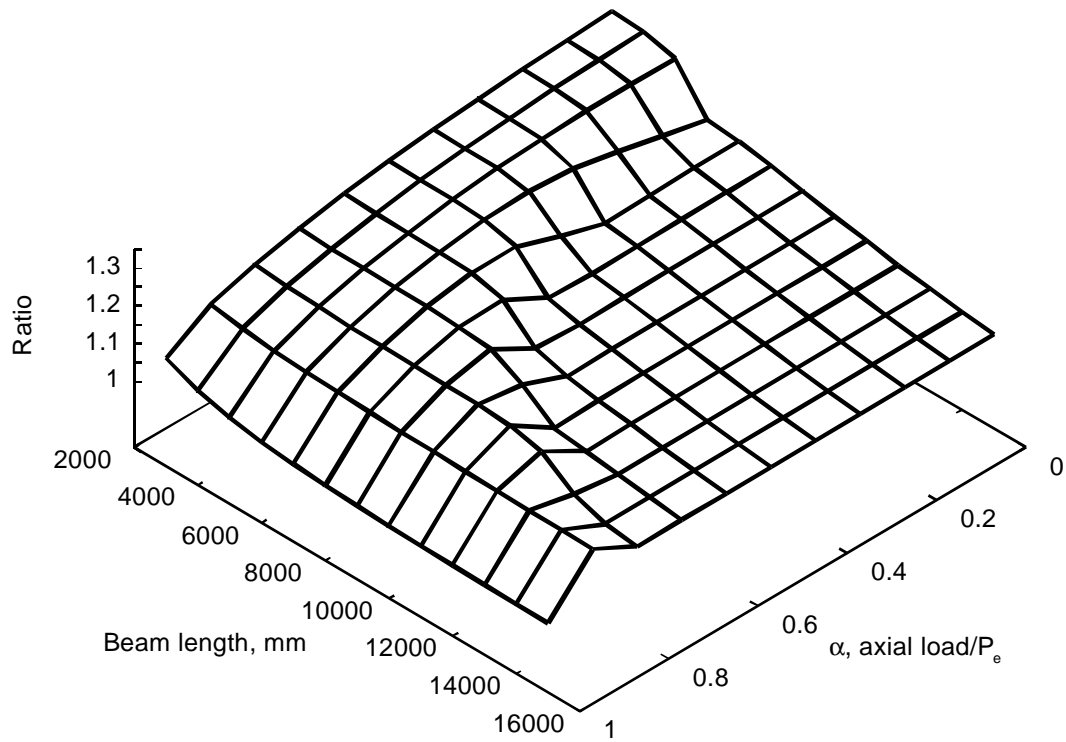


**Figure 5-18** W200x27 frame – fixed base 3000 mm columns, stiffer joint element.

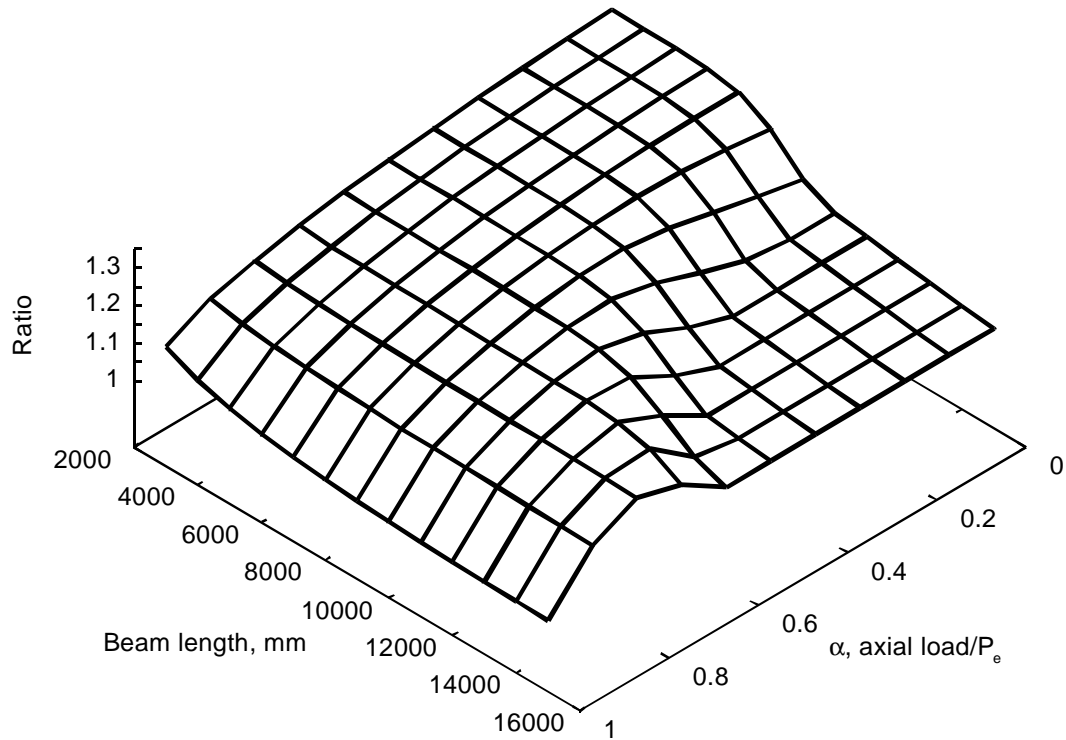


**Figure 5-19** W200x27 frame – fixed base 4000 mm columns, stiffer joint element.

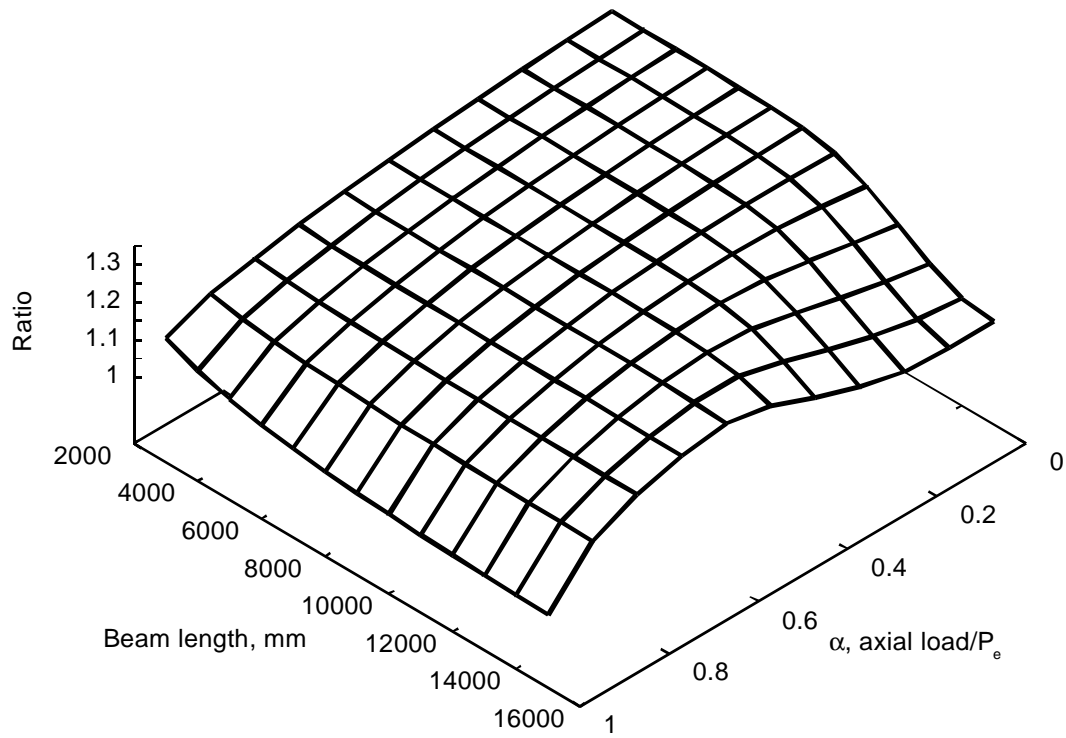


**Figure 5-20** W200x27 frame – fixed base 5000 mm columns, stiffer joint element.

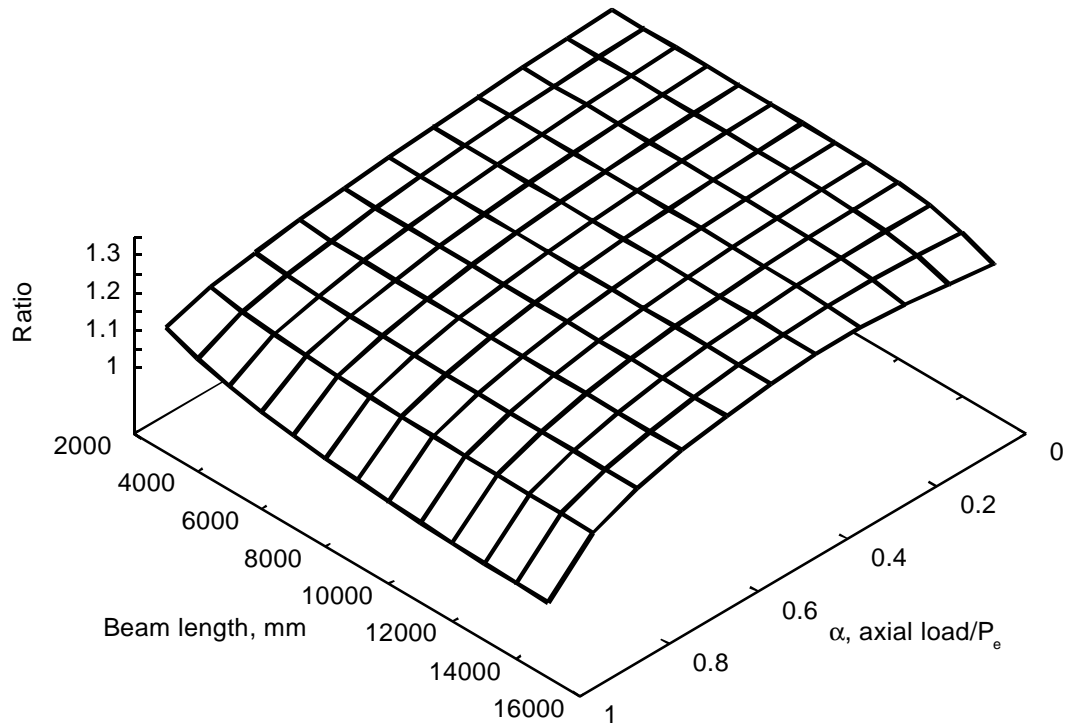


**Figure 5-21** W200x27 frame – fixed base 6000 mm columns, stiffer joint element.

## **6. Inelastic frame behaviour**

The frame analyses performed in this work also included consideration of inelastic behaviour. This is an important aspect of the behaviour of steel structures, and is an important limit state for structural stability, for all forms of buckling. Part of the reason for the importance of inelastic behaviour is that an attractive aspect of steel in structural design is the ductility that steel provides beyond its first yield. However, inelastic behaviour is not accounted for in the linear buckling analyses, nor fully in the joint element analyses presented in Chapter 5. This work was done as the second phase of this project (MacPhedran and Grondin, 2006).

Inelastic lateral torsional instability has been investigated for over 60 years (Galambos, 1998). The results of investigations on several restraint conditions have been presented in numerous texts such as Chen and Lui (1991) and Trahair (1993). The results presented here show the same effect as shown elsewhere – the inelastic behaviour places limits on the maximum strength of the frame. The analyses also show interesting behaviour in the frame as the dominant modes change from those determined by stiffness to those determined by yield strength. This helps illustrate post-buckling behaviour of the frame.

### **6.1 Inelastic buckling considerations**

While elastic buckling and fully plastic behaviour are generally well understood and defined limit states for structures, their inelastic buckling is not as straightforward. Several approaches have been proposed to approximate inelastic buckling behaviour in design. Examples for lateral-torsional buckling behaviour in steel beams include ECCS (1976), which gives a smooth curve over the full range of behaviour, and CSA-S16 (CSA, 2005) and the AISC Specification (AISC, 2005) which both provide a three part design curve with specific sections considering fully plastic behaviour, inelastic buckling and elastic buckling joined at limiting values for the slenderness ratio. Both the ECCS and S16 approaches

use a slenderness ratio based on the fully plastic capacity of the beam divided by the elastic buckling capacity. The AISC approach is based on the length of the beam and specified lengths below one of which the beam is considered to develop its full plastic moment capacity and beyond the other where elastic buckling is assumed to be unaffected by residual stresses.

Part of the work presented herein was to investigate the effect of end conditions that provide varying amounts of warping restraint on the inelastic lateral torsional buckling of beams. These end restraint conditions of members in steel frames were generated using several common frame joint geometries as shown in Table 6-1. These were modelled in the context of a simple single bay, single storey frame (Figure 6-1). Various beam lengths were used in the frame, incorporating the effect of elastic and inelastic lateral torsional buckling as well as attainment of the plastic moment capacity as the ultimate limit state.

The elastic buckling moment for a beam, not considering higher order effects, can be represented as

$$M_{crw} = \sqrt{\frac{\pi^2 E I_y G J}{k_y^2 L^2}} \cdot \sqrt{1 + \frac{\pi^2 a^2}{k_w^2 L^2}} \quad [6-1]$$

where the value  $a$ , the torsional bending constant, relates both material and cross-section properties, including  $C_w$ , the warping constant, and is expressed as  $a = \sqrt{(E C_w)/(G J)}$ . The effective length factors,  $k_y$  and  $k_w$ , associated with the lateral buckling and warping lengths, are both 1.0 for a simply supported beam. The flexural component can be removed from the flexural torsional buckling capacity for a restrained beam by dividing by the capacity for a similar simply supported beam, leaving only the effective length factors related to the end restraint conditions, and a value relating  $L$  to the torsional constant ( $L/a$ ). This ratio was expressed previously as  $R_w$  in Equation [3-4].



However, when yielding is considered, the effects of axial, flexural and warping strains and stresses become much more tightly coupled. This is because the strains developed from all loading conditions can interact to cause differing yielding patterns, and the effects of warping and flexure can not be treated separately as they can in the elastic case. This interaction of yielding patterns leads to complex yield surfaces as illustrated by Daddazio *et al.* (1983) who studied warping in Z sections. The work of Yang *et al.* (1989), although less broad in its scope than that of Daddazio *et al.*, shows the complex interaction of yielding in various modes for I shaped sections. Both of these works illustrate that the interactions between yielding stresses due to the applied loadings are too complex to uncouple easily. For this reason, the results of the elastic eigenvalue analyses of the frames should not be directly compared to the inelastic instability analyses. However, these can be contrasted to show the general effects of inelastic behaviour and how it would affect the predictions based on the elastic behaviour.

Current research on the topic of inelastic buckling, such as Trahair and Hancock (2004) and Ziemian *et al.* (2008) use reduced stiffness to predict buckling, but include the use of elastic end restraints.

It is usual to include residual stresses in studies of inelastic buckling, as these tend to reduce the overall buckling capacity of the members. However, the softening effect was considered to reduce the influence of the warping displacements from the perspective of stability. In order to maximize the effects of the warping interactions, residual stresses are not included in the models here. It is recognised that this will over-predict the capacity for the structure compared to the real structure, the effects under investigation will be increased by neglecting the residual stresses.

## 6.2 Modelling

The finite element analysis reported in this chapter was conducted using the finite element program Abaqus, version 6.4, running on Sun W1100z computers. The

frame models were discretised using the shell element type S4R. A discussion of S4R and S4 elements was presented in Chapter 5. However, there are two points not included there. First, the reduced integration allows the shell element to avoid shear locking to which the fully integrated element may be prone. However, there can be some zero-mode instability problems with the reduced integration element (also known as hour-glassing). This mode is caused by a lack of apparent in-plane shear stiffness with the integration scheme. Abaqus provides a mechanism to resist this by providing extra in-plane stiffness. This has been shown to avoid hourglassing with minimal side effects. The element has a large displacement formulation, with finite strains. The S4R element has been used successfully to model the complex behaviour of structural members with geometric and material non-linear behaviour in stiffened steel plates (Sheikh *et al.*, 2003), in beam – column – infill plate assemblies (Schumacher *et al.*, 1999) and multi-storey steel plate shear walls under cyclic loading (Behbahani, *et al.* 2003). While it has been noted in the previous section on the elastic corner element that the S4R element has some disadvantages when compared to the S4 element, these were not considered to be relevant for this part of the work.

The beam and columns of the portal frame model were meshed using 4 shell elements across the flange width and 6 elements through the web. Element dimensions along the length of the beam were determined to produce an element aspect ratio of 1.00 in the flanges. The aspect ratio for the elements in the web was 1.05. The web elements were slightly larger in the through-beam direction than they were along the beam length. The mesh for the box joint with diagonal stiffener is presented in Figure 3-6.

Five joint conditions, illustrated in Table 6-1, were explored in the study. While the mitred end condition is not a usual connection detail in hot rolled steel construction, it has been extensively studied in previous works, for example Krenk and Damkilde (1991). The column through and beam through conditions represent moment connections with no stiffeners. The others are moment connections with varying amounts of stiffeners added.

Figure 6-1 shows a typical portal frame used for this investigation. The columns were 2000 mm long and the beam length varied from 1000 mm to 8000 mm. This range was used to include a wide range of beam behaviour, from full plastic moment to elastic lateral torsional buckling.

The beam and columns cross-section chosen for this study was a W200x27 wide flange hot rolled section. This section was chosen for its large torsional bending constant, noted as “ $a$ ” in this work. The value of “ $a$ ” is 1088 mm for this section. It is also one of the sections that will experience lateral torsional buckling when used as columns in side sway permitted frame. This is a class 2 (compact) section in flexure for yield strengths up to 460 MPa. The critical unbraced length ( $L_u$ ) at a yield strength of 300 MPa is 2.04 m, based on CAN/CSA-S16-01 (CSA, 2005). This is the length at which the member is assumed to be too short to buckle either elastically or inelastically, and at which it will carry its full plastic capacity.

The frames were loaded with a uniformly distributed load acting vertically down through the shear center of the beam. The analyses determine the critical load in terms of a multiplier for this load.

Each frame was analysed using the elastic eigenvalue solver of Abaqus, which provided an indication of the elastic buckling (or bifurcation) load for later comparison to the inelastic analysis results. The eigenvalue analysis also produced a set of eigenvectors used for creating initial imperfections in the model. For the models represented here, only the first beam buckling mode was incorporated in the initial imperfection. These initial imperfections were scaled to limit the maximum initial imperfection to 1/200 of the member length (0.005L). Higher modes were included in preliminary models in this part of the study, but these did not appreciably affect the buckling loads, nor the deflected shape. The higher mode imperfections had been scaled to half of the first mode value. A nonlinear analysis was then performed, using these initial imperfections, an elastic / perfectly plastic material model using two yield strengths of 300 MPa and

400 MPa, and updated Lagrangian formulation technique using the modified Riks procedure (Riks, 1984) available in Abaqus.

Two sets of end restraints were modelled on the beams: full restraint and flange restraint. In the flange restraint set, the out-of-plane displacement of the bottom flange of the beam was restrained all along the beam-to-column connection. This boundary condition was implemented to prevent out-of-plane buckling of the columns while allowing twisting via the distortion of the beam's web at the supports. For the full restraint set, all nodes of the cross-section of the beam at the beam-to-column joints were constrained to move only within the plane of loading, thus preventing twisting of the beam's cross-section without preventing warping. These two end restraint conditions are presented in Figure 3-6, in Chapter 3.

## **6.2.1 Analysis results**

The elastic buckling analyses are relatively easy to interpret. The result is a single load multiplier for each buckling mode extracted. The inelastic buckling results are more difficult to interpret in that there is no easily identifiable point of instability for some cases. The load versus lateral displacement loads must be examined to determine the “buckling load”.

The plots for applied load and lateral displacement are presented in Figures 6-2 through 6-11 for the cases analysed. In each set the upper diagram is for a frame constructed of 300 MPa steel and the lower is for 400 MPa steel. Figures 6-2 through 6-6 are for the fully restrained beam end, and Figures 6-7 through 6-11 are for the analyses where only the bottom flange was restrained. The lateral displacement plotted on the horizontal axis was obtained at the centre node of the beam. The vertical axis on the graphs represents the load proportionality factor – the load multiplier for the initial loading.

Figures 6-2 and 6-7, which represent the shortest beam lengths (2 m), show the expected buckling phenomenon. The load rises to a peak, and then falls off. Later in the load path, the beam centre moves back to its original position with no

change in load. This is due to a decrease in the lateral stiffness of the member, which can result from either reaching the buckling capacity of the member or the plastic moment capacity. At that point, the beam does not have the stiffness to hold the beam away from the plane of the frame, and will return back to a zero lateral deflection. This can be a fairly abrupt transition, also known as a snap-through buckling mode.

The stiffer joint details retain this behaviour in the next beam length of 4 m, shown in Figures 6-3 and 6-8, but the more flexible details show an increased load accompanying the return of the beam centre towards its original position, particularly in Figure 6-8. This trend continues in the 6 m beam frames, shown in Figures 6-4 and 6-9, to the point where the load resistance developed on the return path is higher than the load experienced in the rise to the peak load.

In all of the preceding figures, the frames reach a peak load, and the load drops before the beam starts its return to the original position. This peak load is considered the failure load and all of the other behaviour – the load decrease, the reversal in lateral deflection and any subsequent strength gains – are all post-failure mechanisms.

This trend does not appear to be continued in the longer beams. Figures 6-5, 6-6, 6-10, and 6-11 show the behaviour of frames where the load is increasing up to the point of reversal of lateral deformation, and then continues to increase after the point on the curve where the reversal occurs. Because the reversal in lateral displacement indicates a change in the stiffness of the structure, the load at which the reversal occurs was considered to be the failure load. The failure load may have been before this, even though the load carried by the structure was still increasing, but the load – displacement relationship does not give a good indication of where the failure should be considered to have happened. The results of the analyses considering these criteria for determining the failure load will be used in the following section.

The process is shown by the progression of an analysis with a typical frame. In the series of pictures starting with Figure 6-12, a frame formed with a 6 m beam and using a yield strength of 300 MPa is followed through the load-displacement path. In the first figure, lateral movement has just begun. The analysis results for this frame were presented in Figure 6-9(a) as the beam through end condition. In Figure 6-13, the lateral displacement of the beam continues, even with large rotations the frame capacity is increasing. After the peak loads are achieved, the situation shown in Figure 6-14 is approached, where the beam's lateral movement is back towards its original location. In the final stages, illustrated in Figure 6-15, the beam and frame have failed completely. The beam's axes have changed orientation at midspan and the columns have buckled. The beam's centre is almost back to the original plane of the frame.

The results of the analysis for the stiffer end conditions of the entire beam end being restrained are presented in Figure 6-16 for a 300 MPa yield strength and in Figure 6-17 for 400 MPa yield strength. These charts represent the strength determined from all of the frame analyses previously presented in Figures 6-2 through 6-11. The horizontal axis is the length normalised by the torsional bending constant,  $a$ . As the value of  $a$  is just over one meter for the members considered in these graphs, so these are close to the length in meters. The values are converted from the uniformly distributed load,  $w$ , in the solution to an end moment of  $wL^2/12$ , the theoretical maximum elastic end moment. For both yield strengths, there is a noticeable difference between the beam capacity based on the end restraints. This is considered an indication that the moments at the ends of the beam could not reach the full capacity for those end details and the connections acted as partially restrained details, offering a reduced end capacity. The rapid drop in capacity for the shortest beam in all cases is due to the location of failure moving to the column from the beam. The higher strength steel has a higher capacity than the 300 MPa steel, as expected.

The inelastic analyses are compared to the elastic eigenvalue analyses in Figures 6-18, for 300 MPa, and 6-19, for 400 MPa. There is a trend in all of the frames

analysed for the ratio of results of the inelastic analysis to those of the elastic analysis to decrease linearly with the length of the beam. While this is somewhat expected, the inelastic strength shows a higher capacity than the elastic capacity for longer beams. This is due to the post-buckling strength in the beam permitting the beam to carry more load than predicted by the buckling analysis.

The same data is presented for the weaker end restraint condition where only the bottom flange at the beam-to-column connection is restrained from displacing out of the plane of the frame. The moment capacities, as described above, are presented in Figure 6-20, for 300 MPa yield strength, and Figure 6-21, for 400 MPa. These figures show a larger difference between the “weaker” joint details of column through, beam through and mitre joints. However, Figures 6-22 and 6-23 show that the same general trend is present as in the results from the full beam end restraint presented in Figures 6-18 and 6-19.

The yield strength of the material does influence the buckling strength of the beam. Given two yield strengths of 300 MPa and 400 MPa, the ratio of the critical loads for similar conditions were in proportion to the square root of the ratio of the yield strengths, as predicted by Kirby and Nethercot (1979). Table 6-2 presents the critical moments for five beam lengths and five joint types and the ratio between the moments for the two yield strengths presented. The ratio of the critical strengths for the 300 MPa steel versus the 400 MPa steel has a mean value of 0.832 with a standard deviation of 0.036. The approach from Kirby and Nethercot indicates a value of 0.866. This indicates that the phenomenon investigated for most frames is actually inelastic buckling, and not plastic hinge formation. For shorter (and stiffer) beams, the ratio decreases. For extremely short beams, inelastic buckling would be replaced by full section yield, and the strength ratios would become that of the yield strength ratio of 0.75.

An extensive numerical investigation of elastic lateral torsional buckling of beams was presented by Nethercot and Rockey (1971). This was one of the first studies of elastic lateral-torsional buckling to use computer methods, and was completed

before the release of the first beam-column elements that supported warping (Barsoum, 1972). The technique used approximate methods for determining the effects of loading and restraint and determined effective moment factors for various lengths of beams. One of the results from that investigation was an equivalent moment factor ( $C_b$ ) for uniformly distributed loads and various end support conditions. For beams loaded with a uniformly distributed load at their shear centres, these factors are expressed as Equation [6-2] for beams fixed at their ends with respect to warping, and Equation [6-3] for beams fixed at their ends with respect to bending about their weak axis. The class II and III designations are those of Nethercot and Rockey.

$$C_b = 1.2 + \frac{4.106}{(L/a)^2} + \frac{1.263}{(L/a)} \quad (\text{Warping fixed: Class II}) \quad [6-2]$$

$$C_b = 1.9 - \frac{1.184}{(L/a)^2} + \frac{0.02}{(L/a)} \quad (\text{Laterally fixed: Class III}) \quad [6-3]$$

Figures 6-24 and 6-25 present a comparison of  $C_b$ , as proposed by Nethercot and Rockey with the results from the elastic eigenvalue analysis conducted in this study. The curves from Nethercot and Rockey appear as solid lines for laterally and warping fixed conditions. The data presented here appear as broken lines. The three weaker end conditions are found to be considerably weaker than the laterally fixed condition presented by Nethercot and Rockey. The stiffened connections appear to be at least as strong as the laterally fixed condition, but no end condition appears to provide full warping restraint. However, all those conditions follow the same trends as the curves presented by Nethercot and Rockey for a laterally fixed condition. The stronger end joint conditions from this study lies between Nethercot and Rockey's curves for the laterally fixed and warping fixed conditions.

While it was expected that the short beams would experience more benefit from the connections that have higher warping rigidity, the results appear to show that



the longer members also experience proportionally greater benefits from the stiffer connections. This is due to the greater stiffness in connecting the beam to the columns, and the resulting increase in mobilising the post buckling strength of the full structure for the beam.

As a comparison, the current Canadian structural steel design standard, CAN/CSA S16-01 (CSA, 2005) recommends a value of 1.0 for  $C_b$  (or in the nomenclature of S16,  $\omega_2$ ) in that the end moments are equal. There is no explicit guidance for load cases such as the uniformly distributed load applied here. This will be remedied in a future edition to account for the moment distribution in similar cases. In any event, the value of  $\omega_2$  cannot exceed 2.5, while Nethercot and Rockey's values can exceed 2.5. In all, the design standard is conservative in its recommendations.

## 6.3 Summary

This chapter presents the results of a series of inelastic analyses for a set of steel frames to determine the effect of plasticity on the behaviour of the frames. The results of the inelastic analyses were compared with bifurcation or eigenvalue buckling analyses of similar frames.

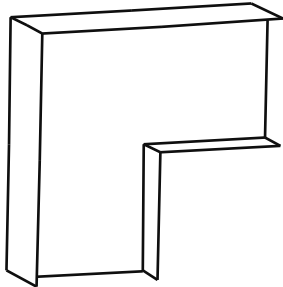
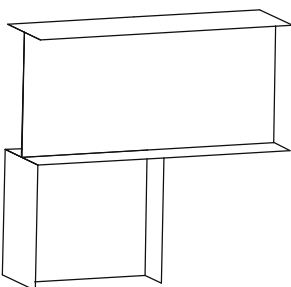
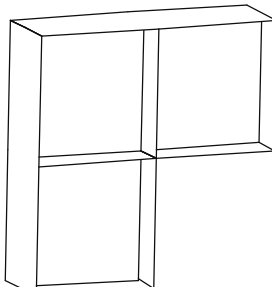
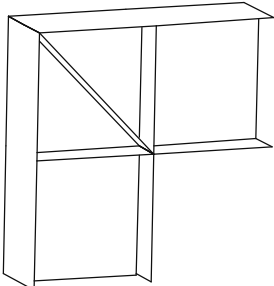
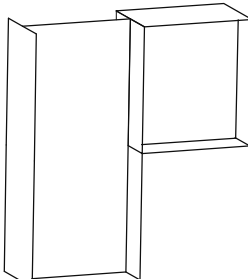
The inelastic analyses do not have a definitive point of instability in the same fashion that bifurcation buckling does, and the point for instability was chosen considering the shape of the graph of load and lateral displacement. This could give some optimistic values when compared to elastic buckling analyses for long members, as there can be some significant post-buckling strength reserve in beams experiencing lateral-torsional buckling (Trahair, 1996). As well, as has been noted earlier in this work, there can be an increase in buckling capacity for shallower sections due to the pre-buckling deflection of the member. (The first approximation for the W200x27 sections investigated here would be on the order of a 7% increase.)

As could be expected, the inelastic effects dominate the behaviour of shorter members, and significantly reduce the capacity from the predicted elastic buckling capacity. Longer members experience some benefit in the inelastic analysis over the elastic buckling analysis, due to effects ignored in the buckling analysis. These would include the effect of the relative stiffnesses about the major and minor axes of the member and the post-buckling increase in strength for beams, as discussed in Chapter 3.

The weaker end conditions, the “column through”, “beam through” and mitre joints do not provide sufficient restraint to develop the strength predicted by current design equations.

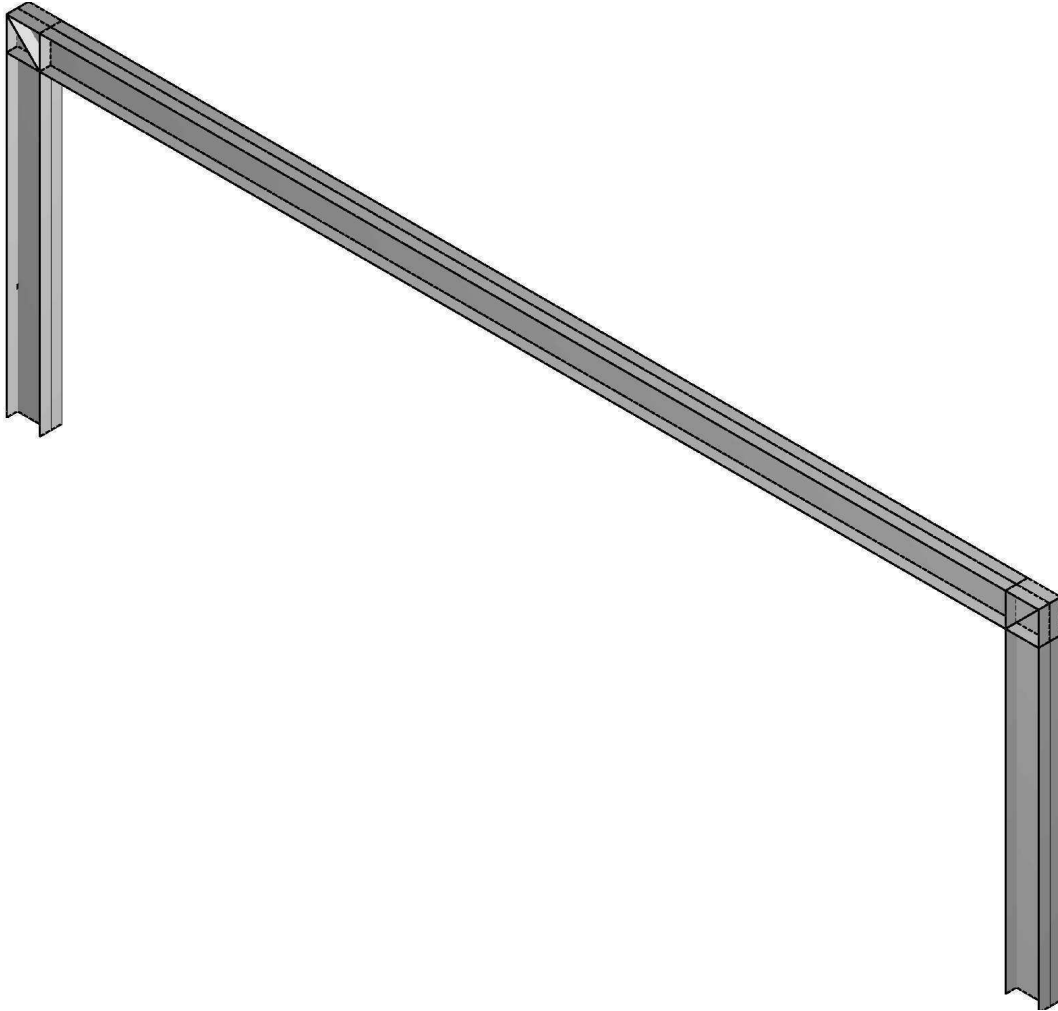
However, the major effect of inelastic buckling is the obvious one. As shown in Figures 6-18, 6-19, 6-22, and 6-23 the effects of plasticity significantly reduce the capacity of the structure for shorter members from that predicted by elastic buckling. As the warping effects predominate for shorter members, plasticity does negate at least some of the effects of warping restraint in increasing the buckling strength of steel members. However, there may still be benefits for the frame's stability to have greater warping restraint, even over the range of intermediate beam lengths.

Table 6-1 Frame joint configurations

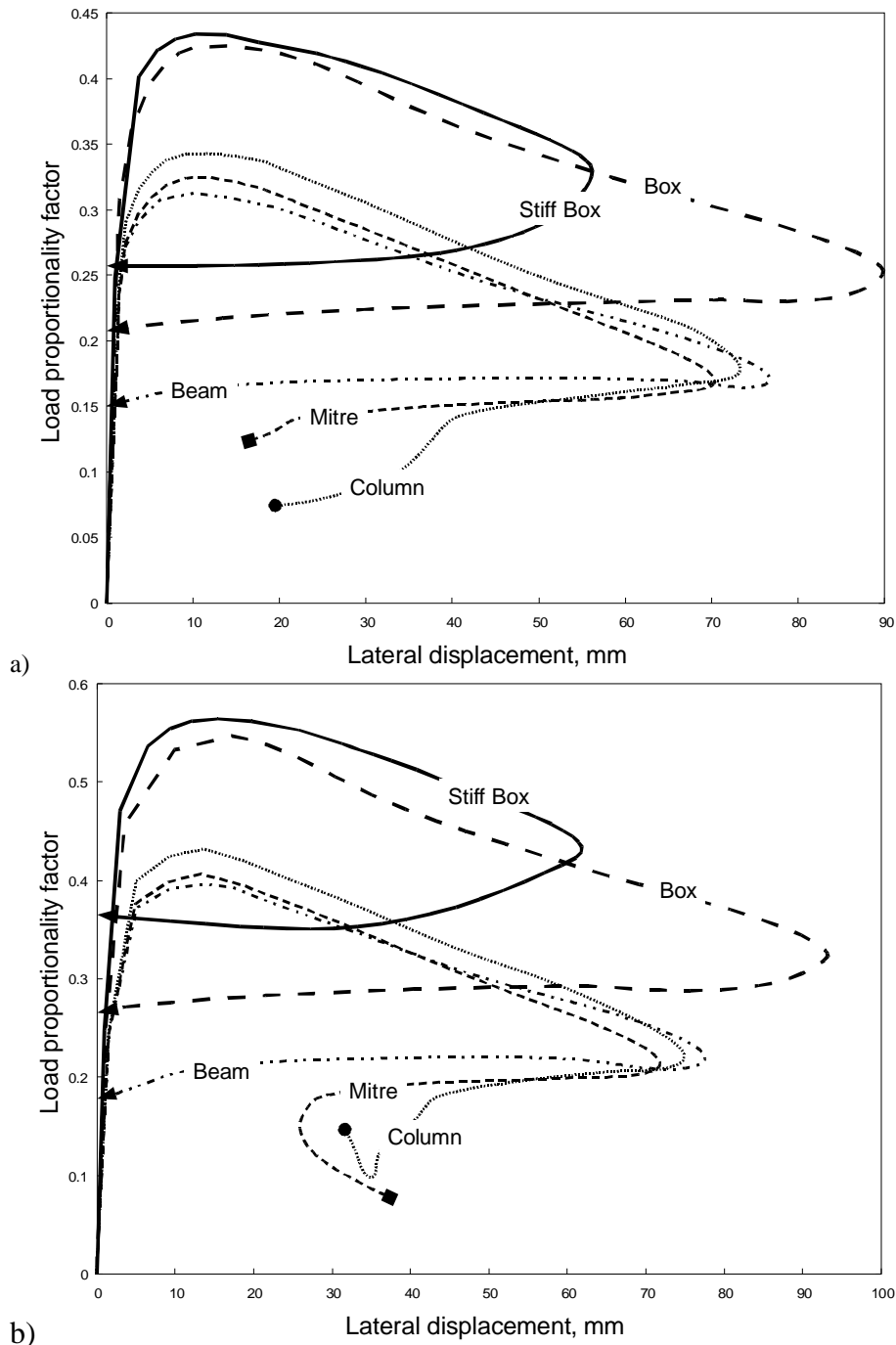
		
Mitre Joint	Beam Through	Box
		
Stiff Box	Column Through	

**Table 6-2** Summary of inelastic critical moments (kN m) and ratios for modelled yield strengths

Joint Type	Yield Strength (MPa)	Beam Length (mm)				
		2000	3000	4000	6000	8000
Beam Through	300	30.0	32.5	32.5	30.6	28.7
	400	34.3	37.1	37.1	35.5	33.5
	Ratio	0.875	0.877	0.877	0.862	0.855
Mitre	300	46.5	41.0	37.1	33.0	30.0
	400	55.2	47.8	42.8	37.3	33.4
	Ratio	0.842	0.858	0.867	0.885	0.898
Column Through	300	63.8	56.2	49.2	41.3	37.2
	400	80.1	67.9	59.4	50.1	45.1
	Ratio	0.797	0.827	0.829	0.823	0.826
Box	300	74.4	69.3	62.1	52.3	47.2
	400	93.9	85.9	76.1	64.5	60.6
	Ratio	0.793	0.807	0.816	0.812	0.779
Stiffen Box	300	81.4	81.8	75.4	67.0	63.4
	400	104.6	101.9	92.0	84.6	80.2
	Ratio	0.779	0.803	0.819	0.792	0.791



**Figure 6-1** Typical frame model, fully stiffened joints (box and diagonal stiffeners).



b)

**Figure 6-2** Results for 2000 mm beam second order analyses, full restraint. a)  $F_y = 300$  MPa, b)  $F_y = 400$  MPa.

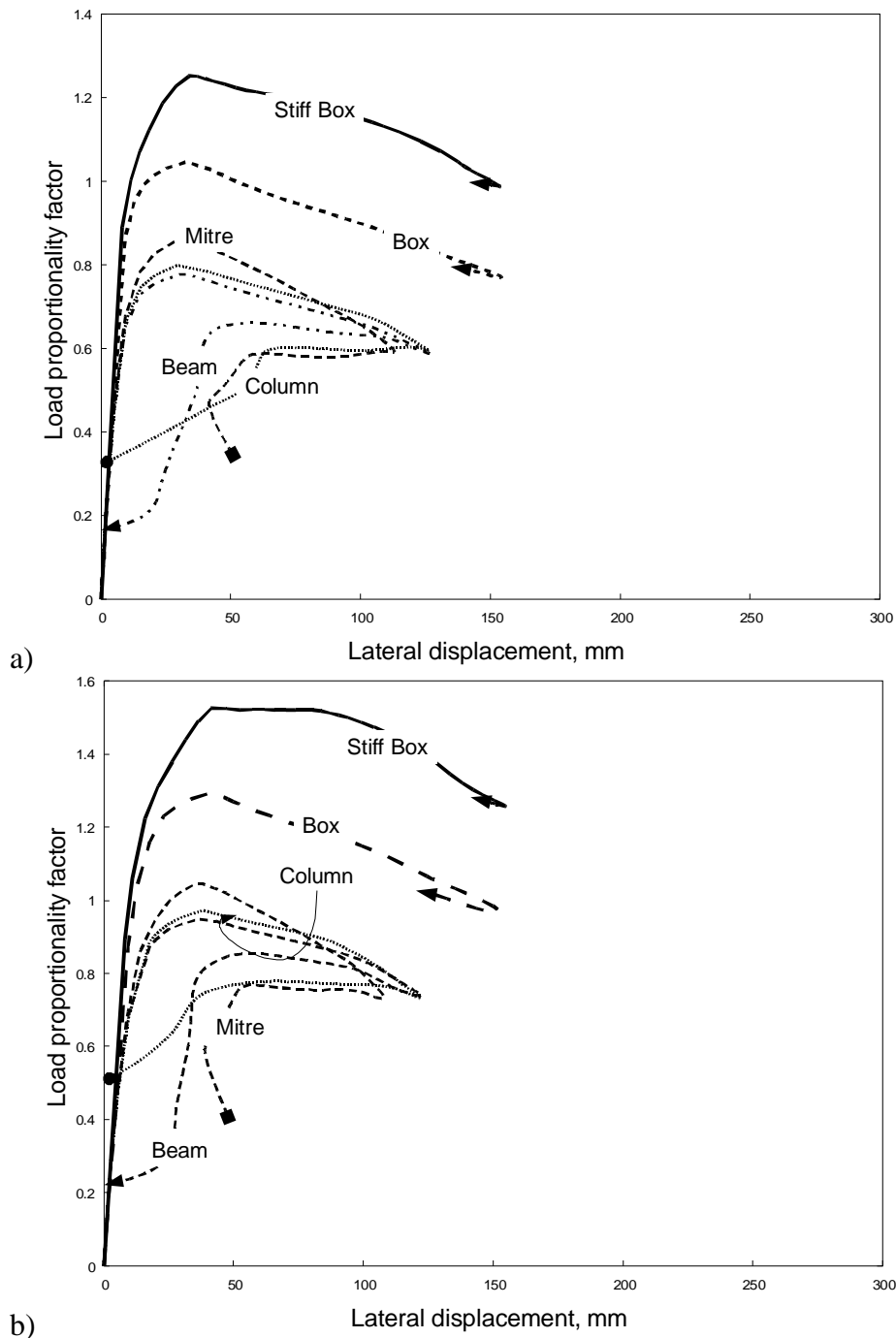
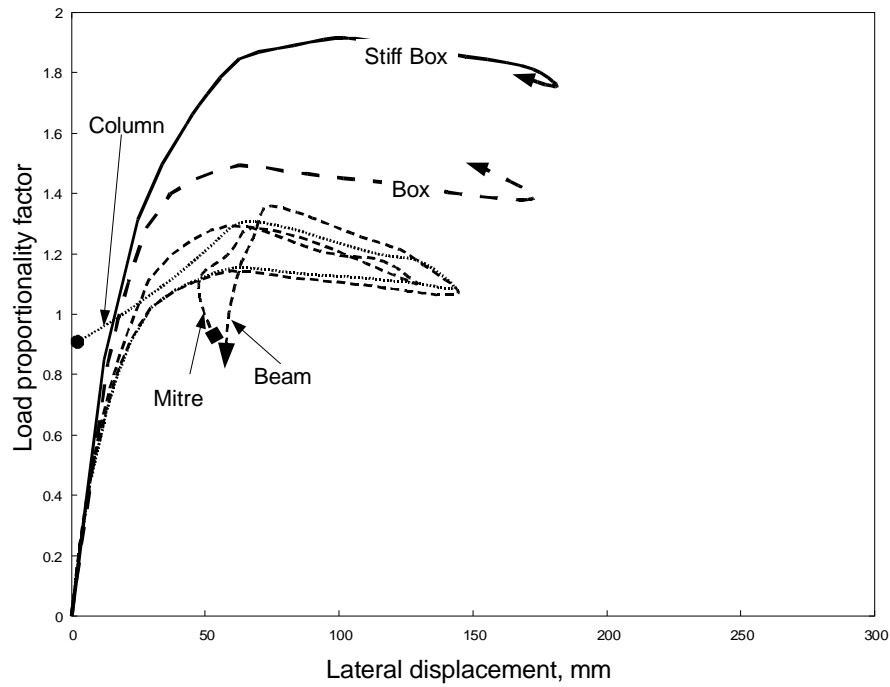
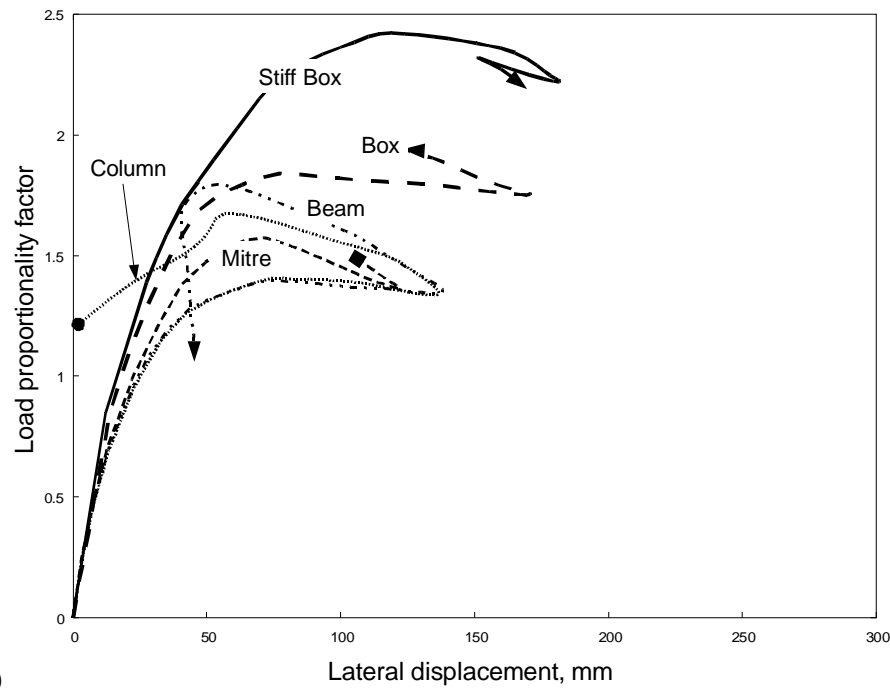


**Figure 6-3** Results for 4000 mm beam second order analyses, full restraint. a)  $F_y = 300$  MPa, b)  $F_y = 400$  MPa.



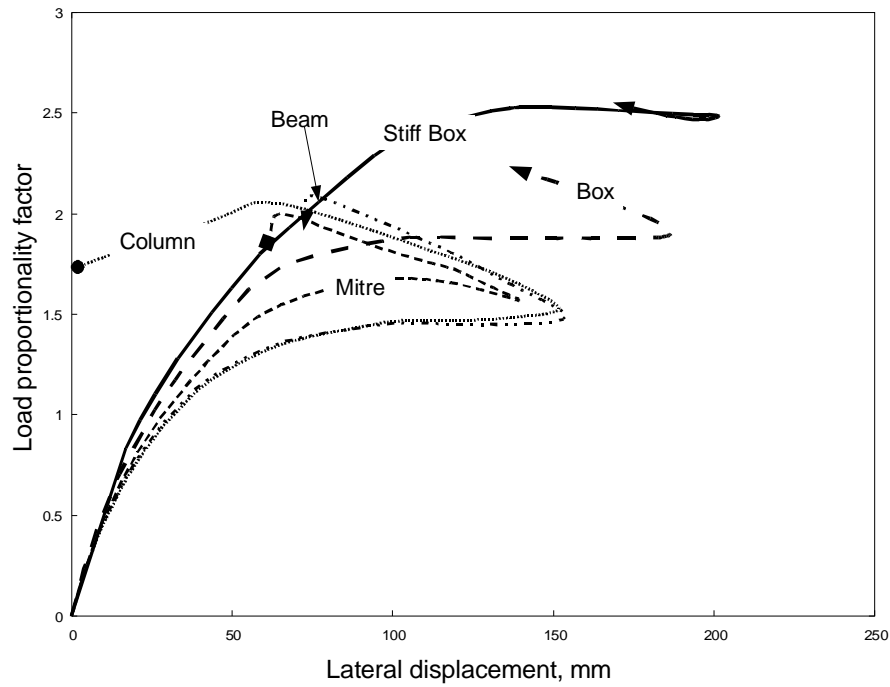
a)



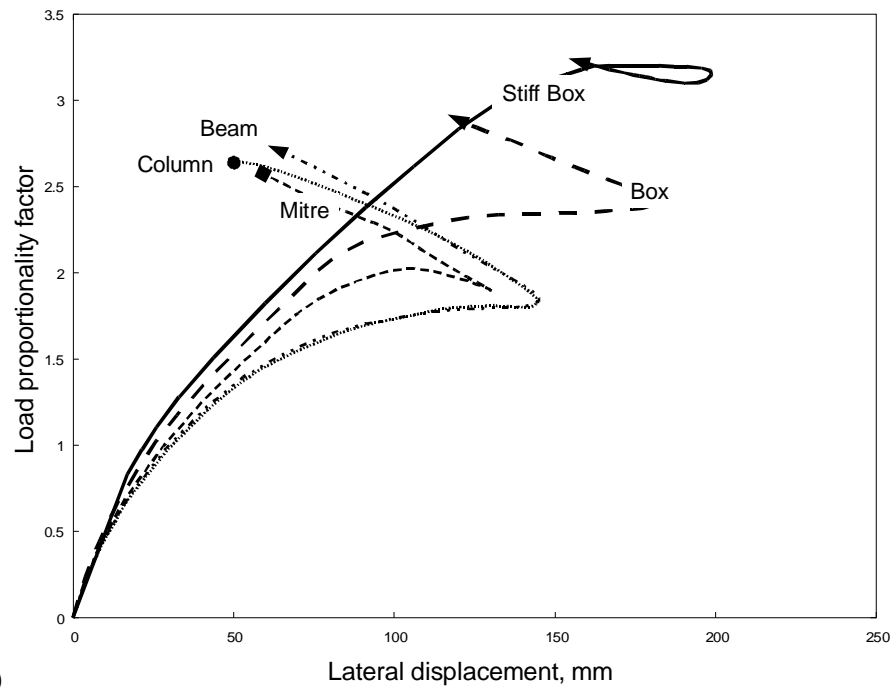
b)

**Figure 6-4** Results for 6000 mm beam second order analyses, full restraint. a)  $F_y = 300$  MPa, b)  $F_y = 400$  MPa.



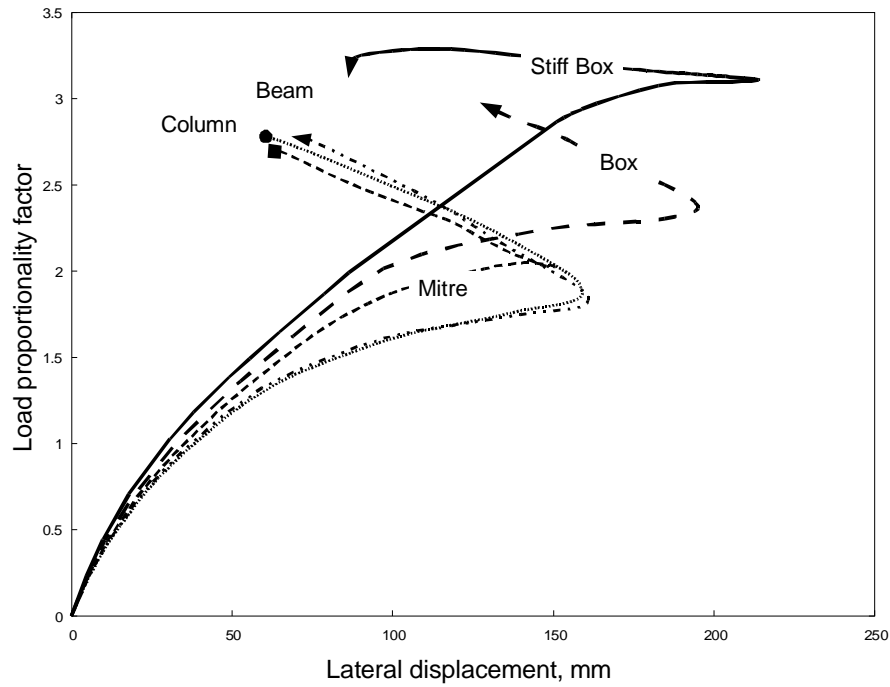


a)

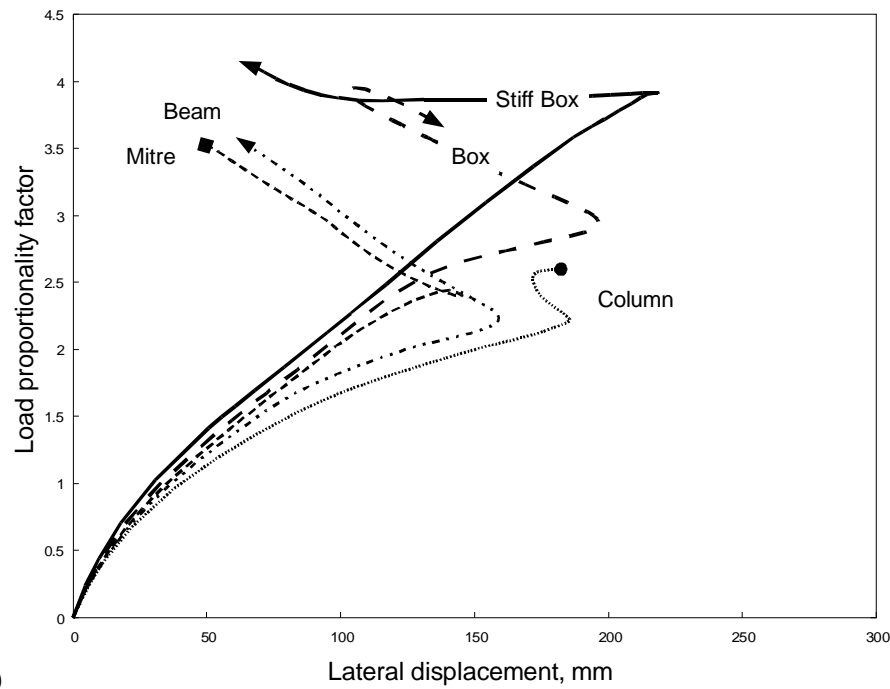


b)

**Figure 6-5** Results for 8000 mm beam second order analyses, full restraint. a)  $F_y = 300$  MPa, b)  $F_y = 400$  MPa.



a)



b)

**Figure 6-6** Results for 10000 mm beam second order analyses, full restraint. a)  $F_y = 300$  MPa, b)  $F_y = 400$  MPa.

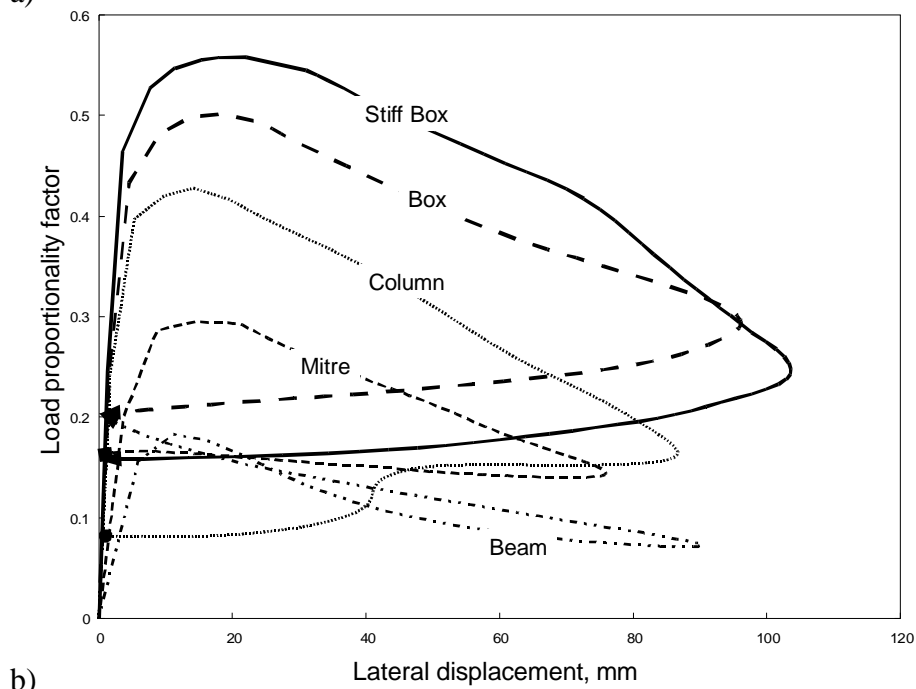
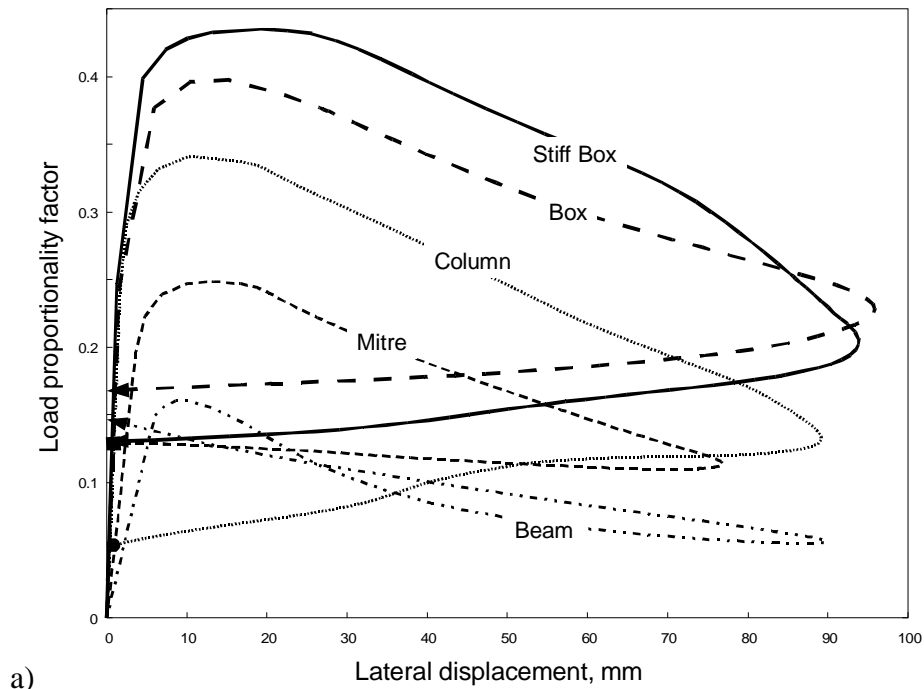


**Figure 6-7** Results for 2000 mm beam second order analyses, bottom flange restraint. a)  $F_y = 300$  MPa, b)  $F_y = 400$  MPa.

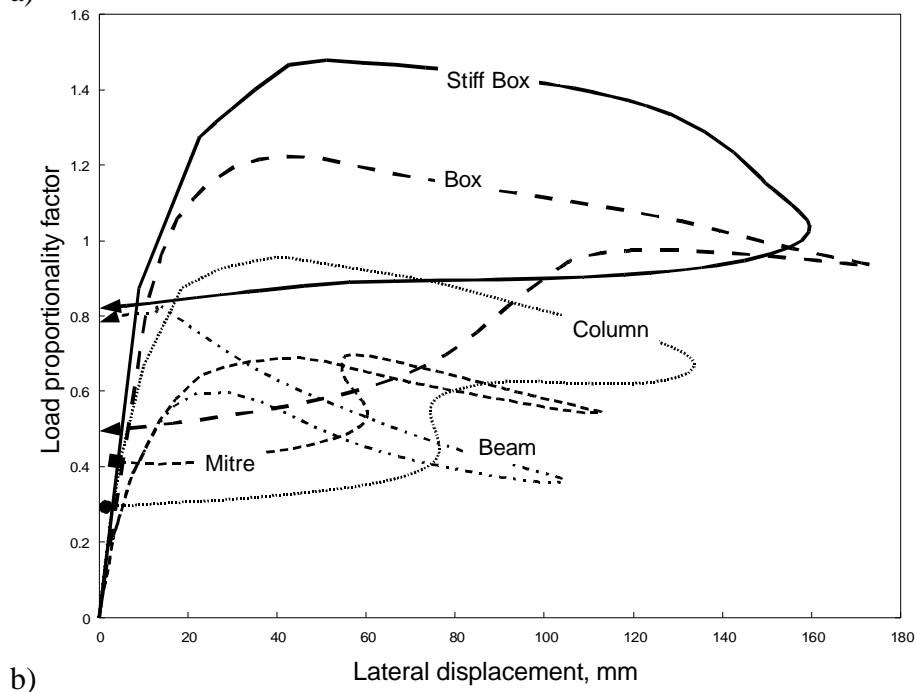
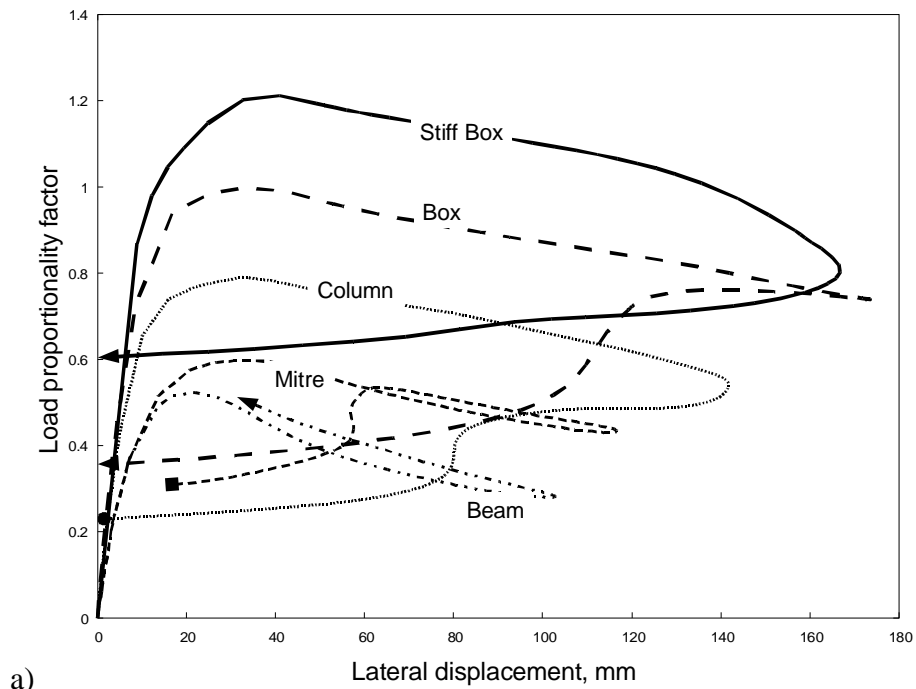
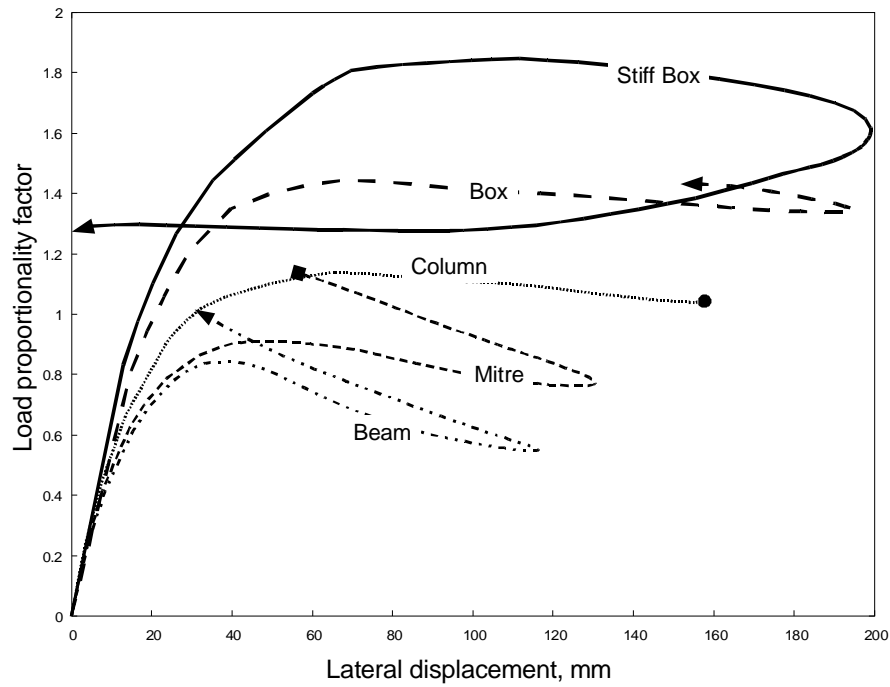
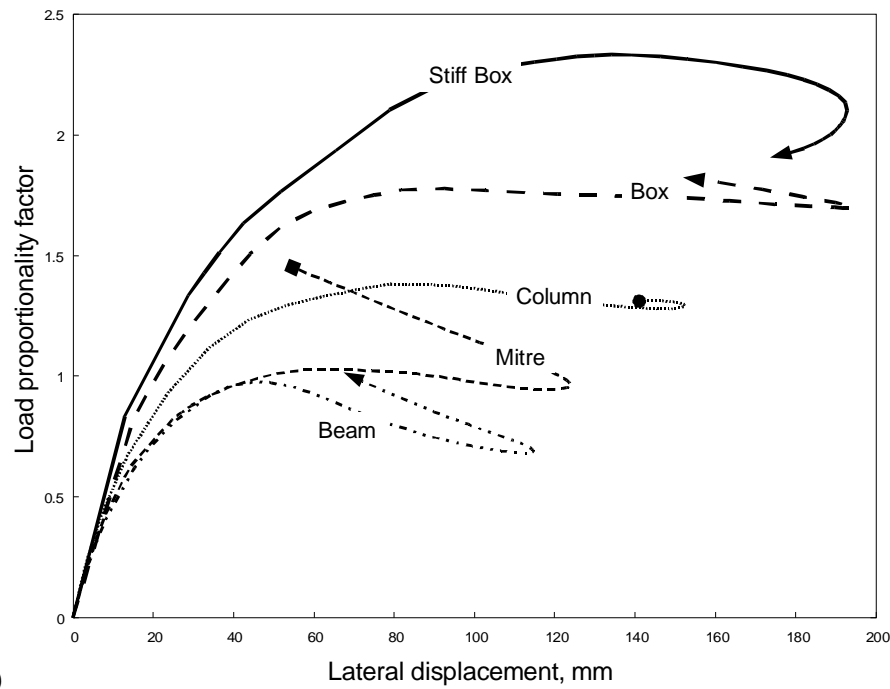


**Figure 6-8** Results for 4000 mm beam second order analyses, bottom flange restraint. a)  $F_y = 300$  MPa, b)  $F_y = 400$  MPa.

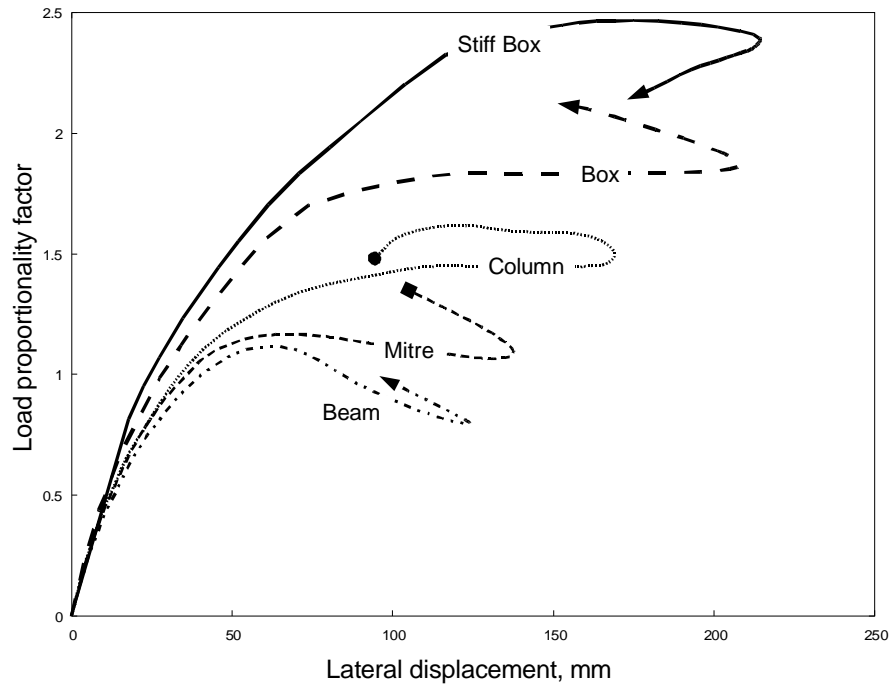


a)

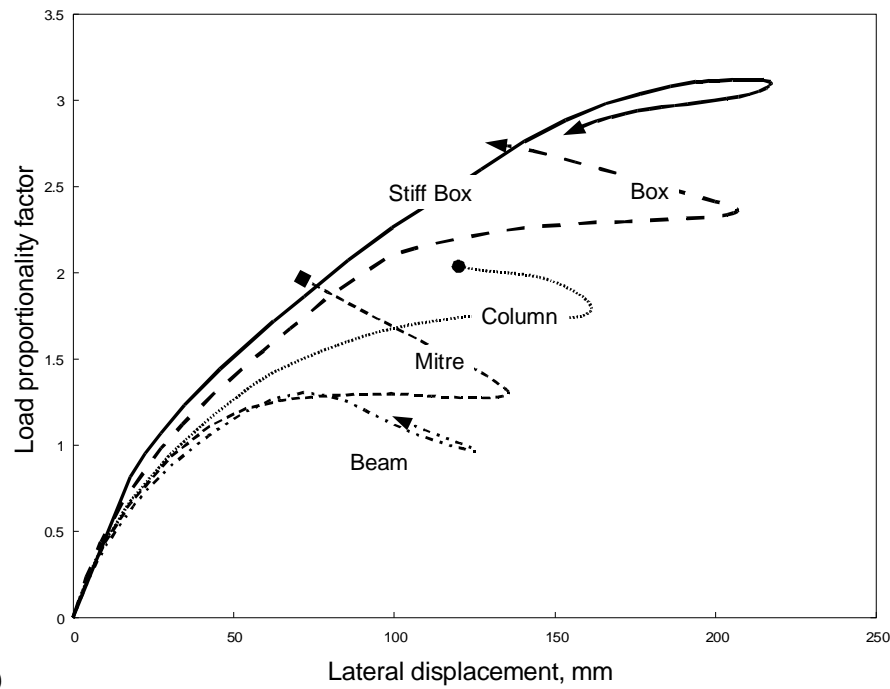


b)

**Figure 6-9** Results for 6000 mm beam second order analyses, bottom flange restraint. a)  $F_y = 300$  MPa, b)  $F_y = 400$  MPa.

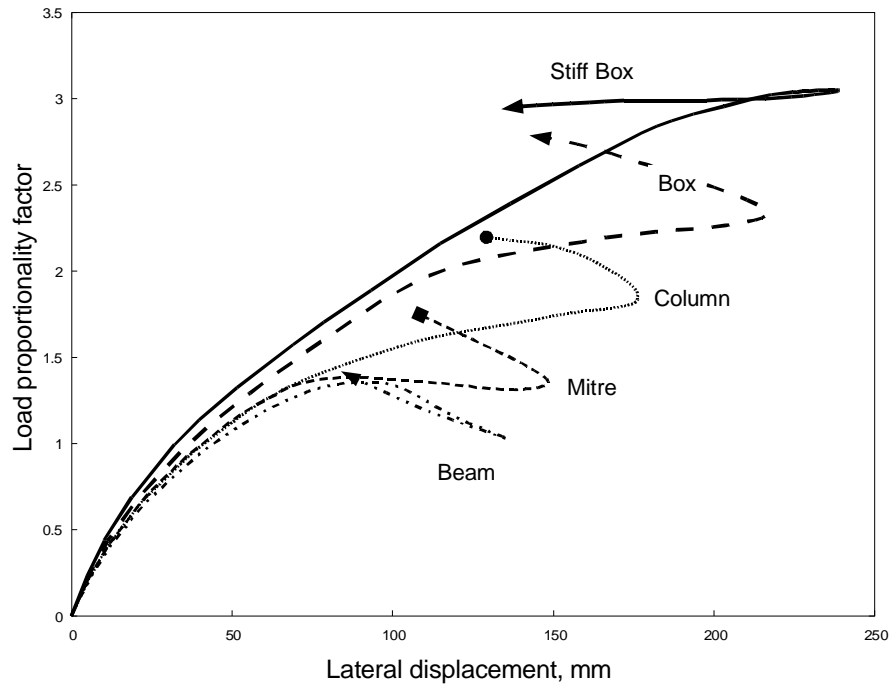


a)

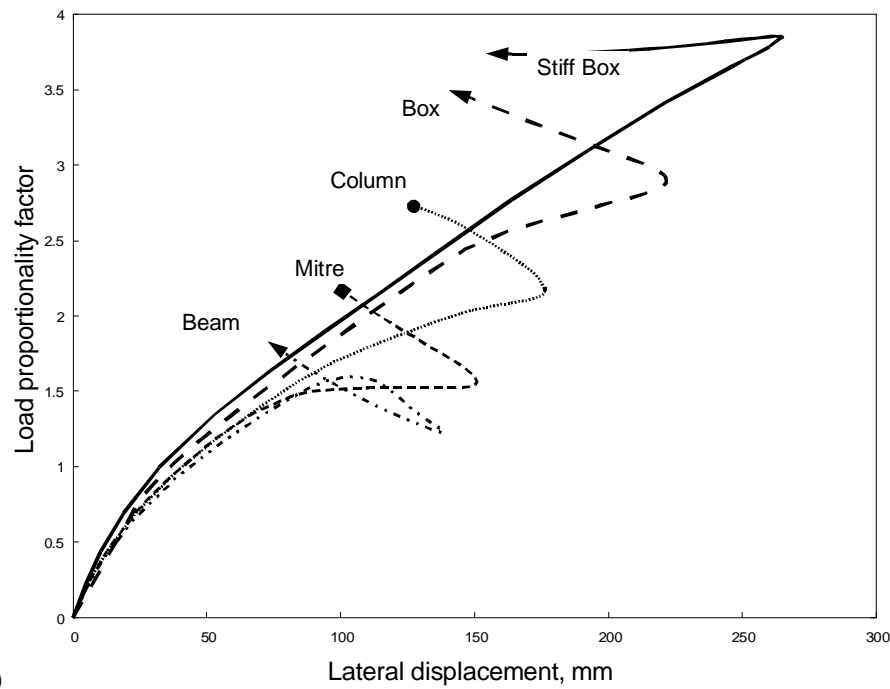


b)

**Figure 6-10** Results for 8000 mm beam second order analyses, bottom flange restraint. a)  $F_y = 300$  MPa, b)  $F_y = 400$  MPa.



a)



b)

**Figure 6-11** Results for 10000 mm beam second order analyses, bottom flange restraint. a)  $F_y = 300$  MPa, b)  $F_y = 400$  MPa.

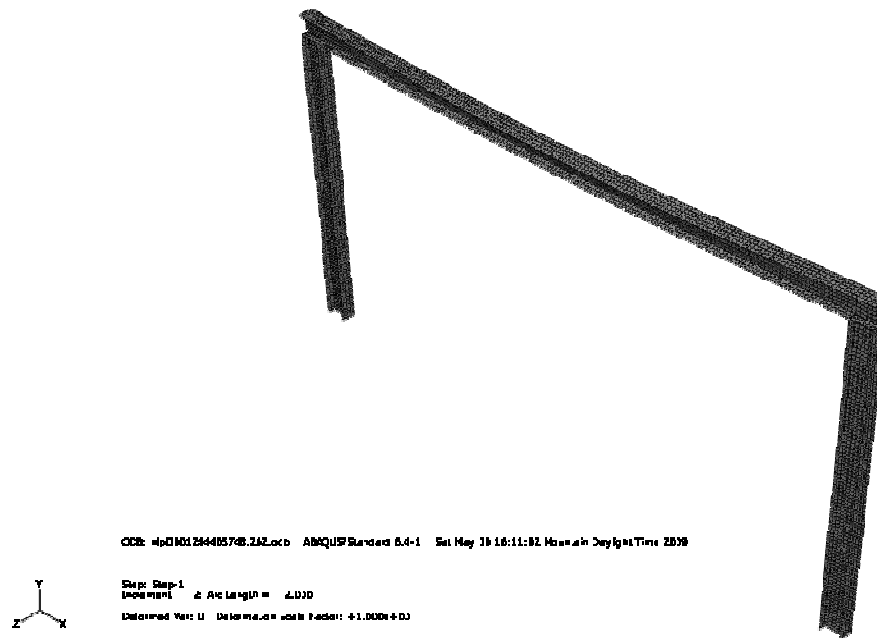


**Figure 6-12** Initial lateral displacement, in frame with 6 m beam and 2 m columns, out of plane restraint on all nodes at beam to column interface. All members W200x27, Grade 300W.

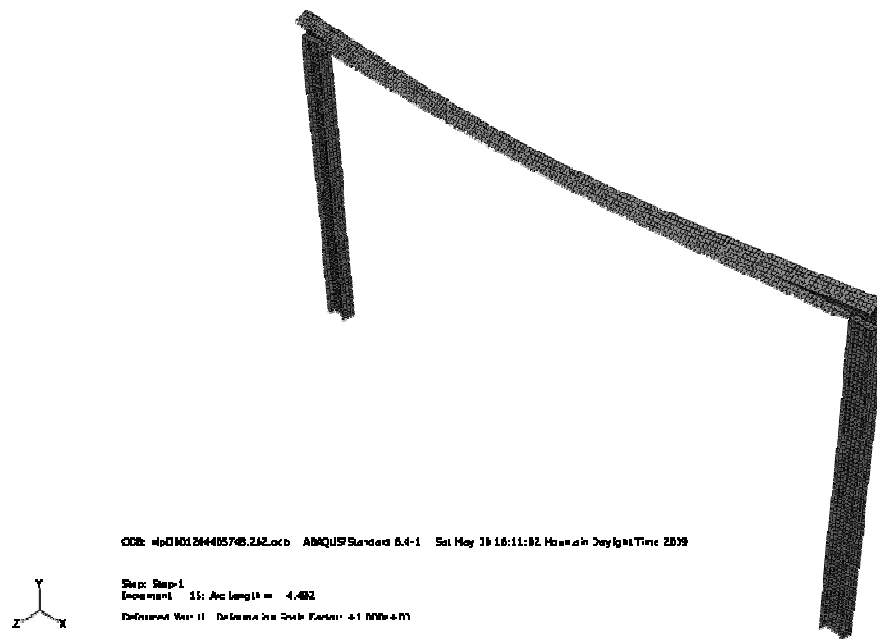


**Figure 6-13** Further lateral displacement, same frame as in Figure 6-12.



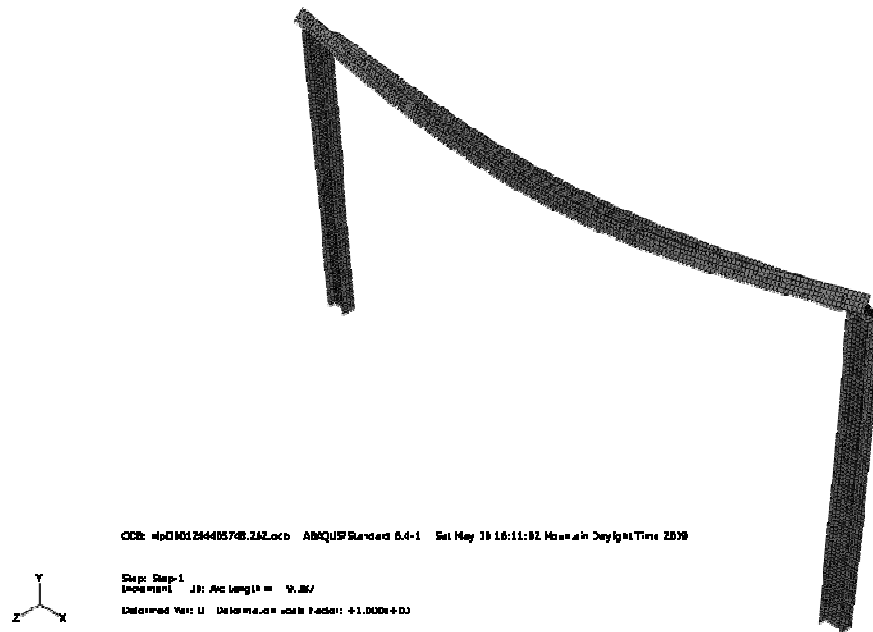


**Figure 6-14** Beam returning towards plane of frame, same frame as in Figure 6-12.

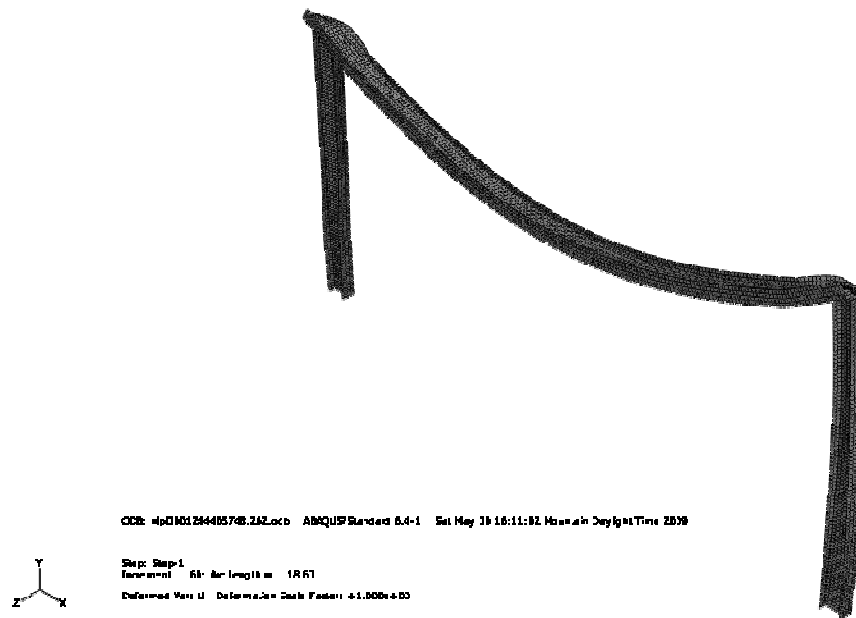


**Figure 6-15** Beam acting as catenary / weak axis bending, same frame as in Figure 6-12.

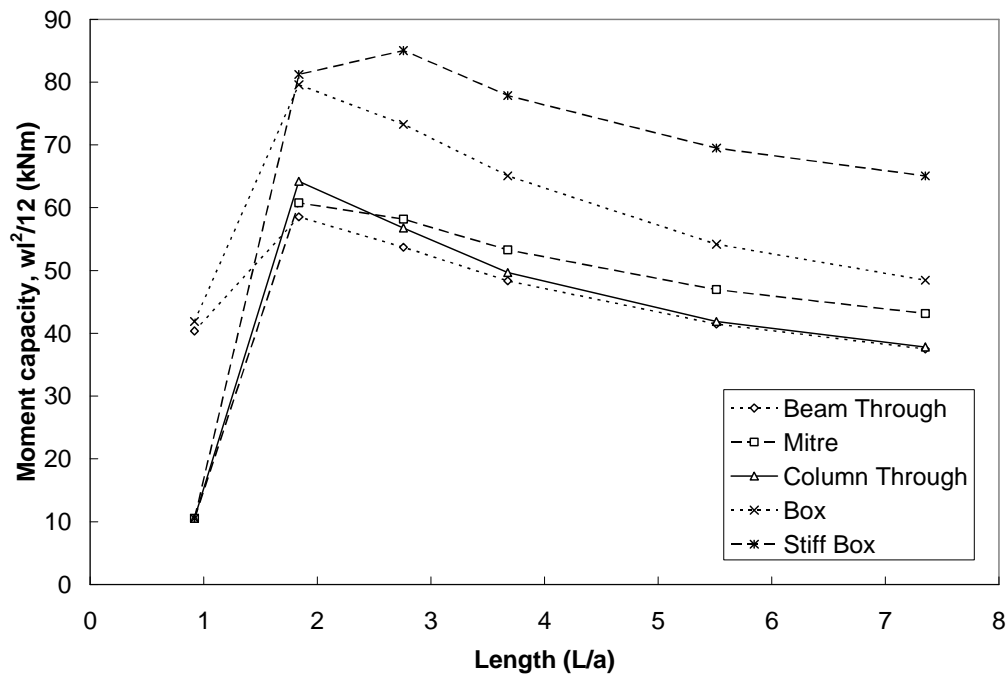


**Figure 6-16** Moment capacity based on  $wl^2/12$  for a frame with full beam restraint,  $F_y=300$  MPa. ( $l$  is the beam length, in mm)

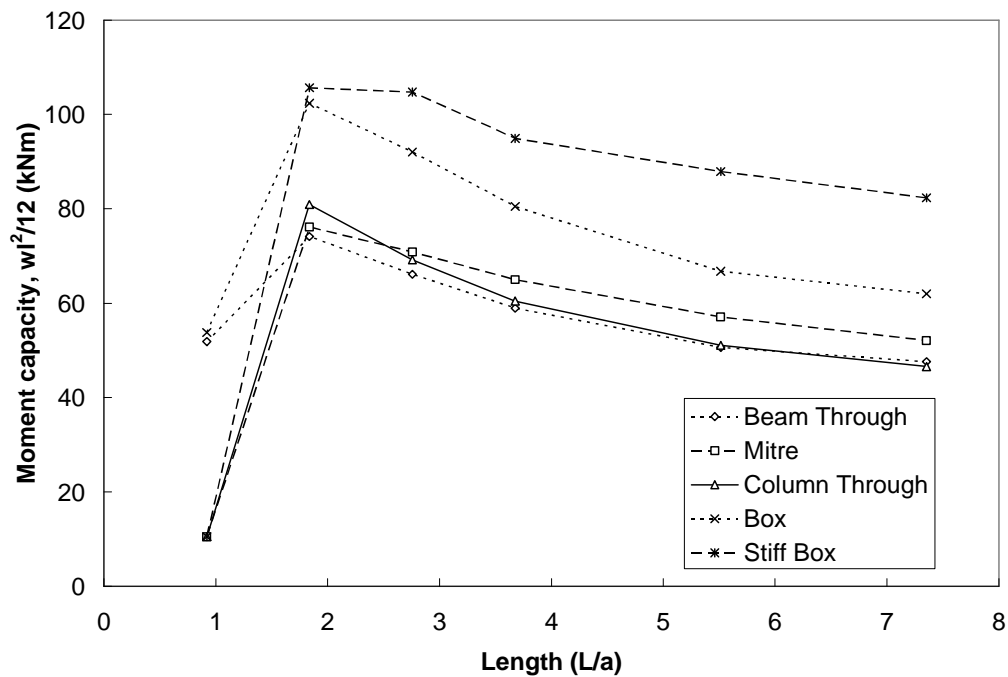


**Figure 6-17** Moment capacity based on  $wl^2/12$  for a frame with full beam restraint,  $F_y=400$  MPa. ( $l$  is the beam length, in mm)

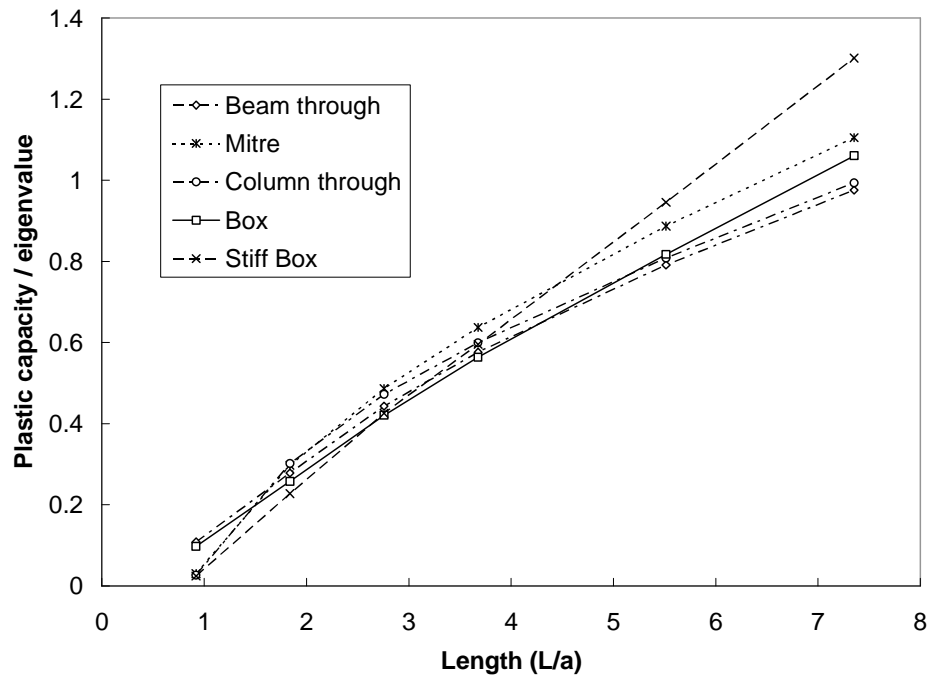


**Figure 6-18** Second order inelastic analysis compared to elastic buckling capacity for a frame with full beam restraint,  $F_y=300$  MPa.

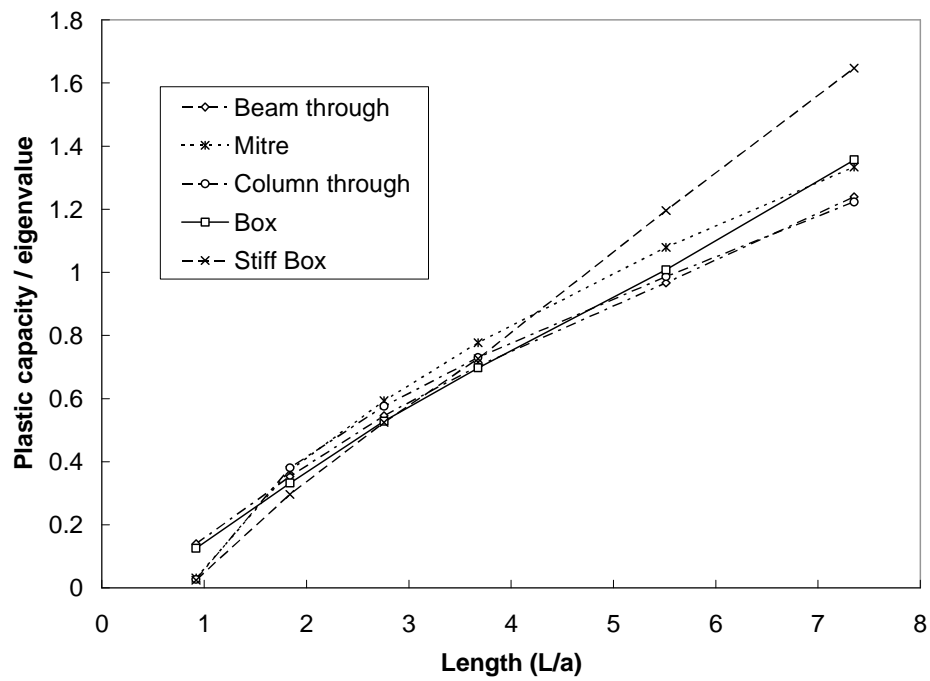


**Figure 6-19** Second order inelastic analysis compared to elastic buckling capacity for a frame with full beam restraint,  $F_y=400$  MPa.

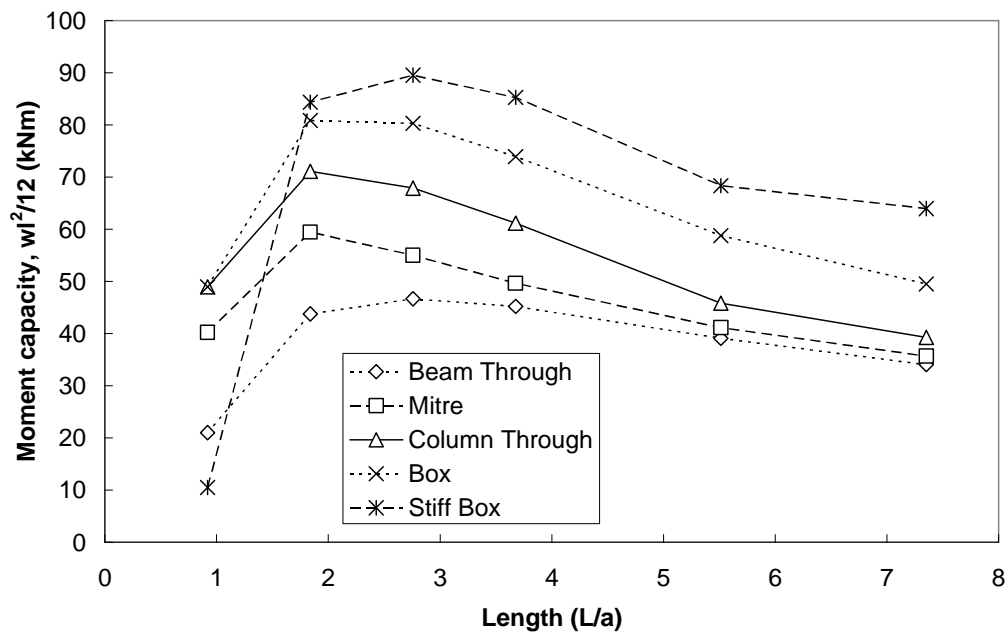


**Figure 6-20** Moment capacity based on  $wl^2/12$  for a frame with bottom flange restraint,  $F_y=300$  MPa. ( $l$  is the beam length, in mm)

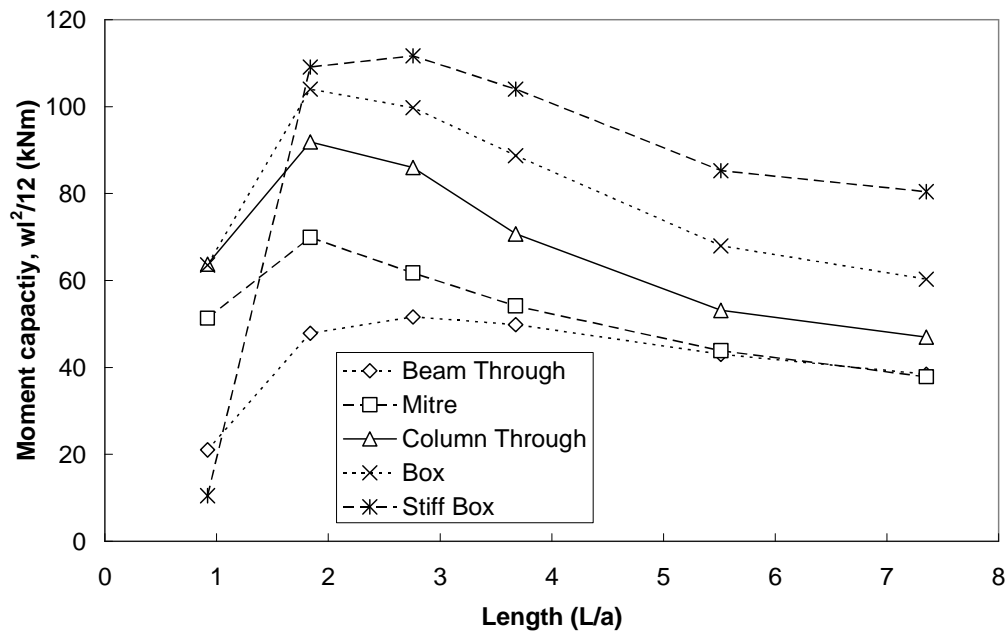


**Figure 6-21** Moment capacity based on  $wl^2/12$  for a frame with bottom flange restraint,  $F_y=300$  MPa. ( $l$  is the beam length, in mm)

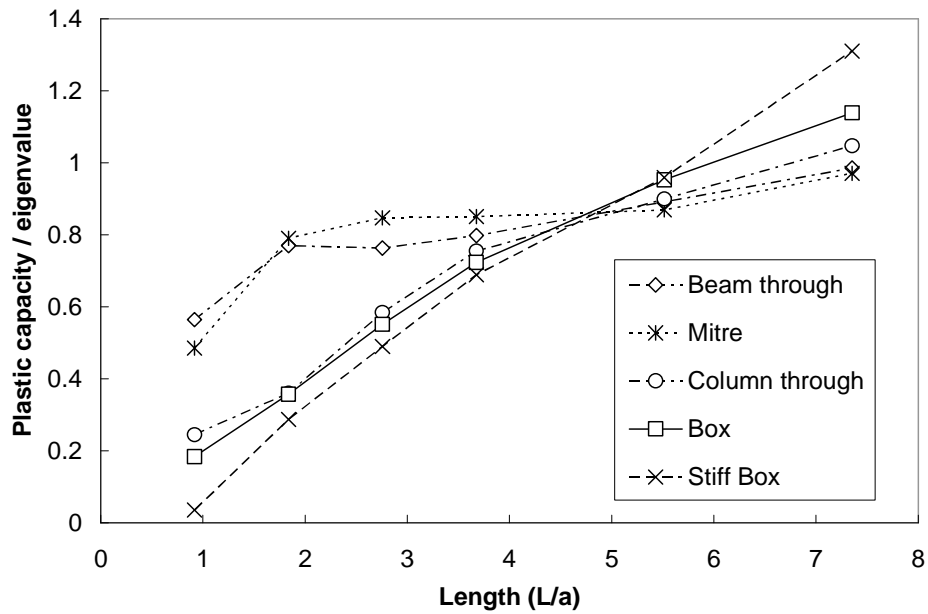


**Figure 6-22** Second order inelastic analysis compared to elastic buckling capacity for a frame incorporating bottom flange restraint,  $F_y=300$  MPa,

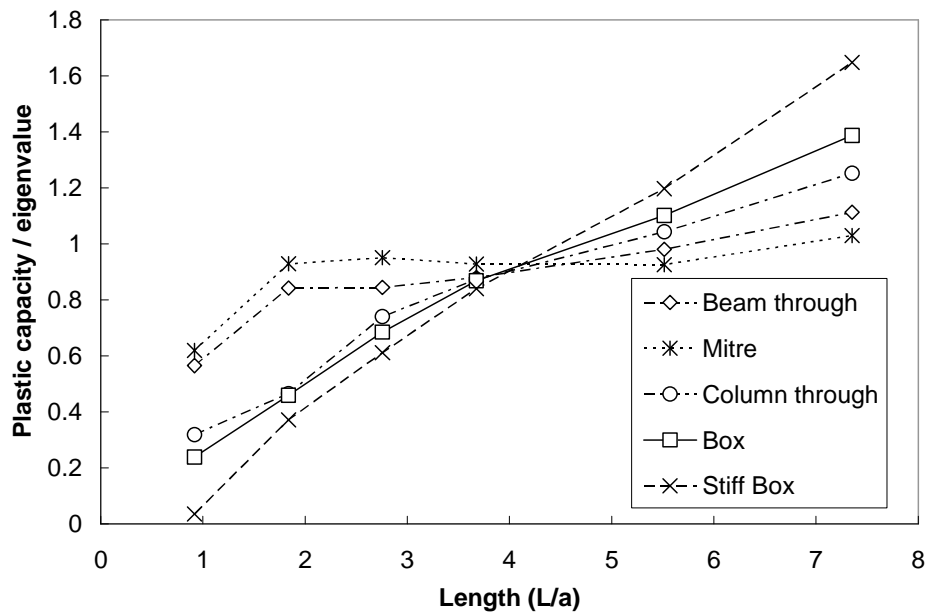


**Figure 6-23** Second order inelastic analysis compared to elastic buckling capacity for a frame incorporating bottom flange restraint,  $F_y=400$  MPa,

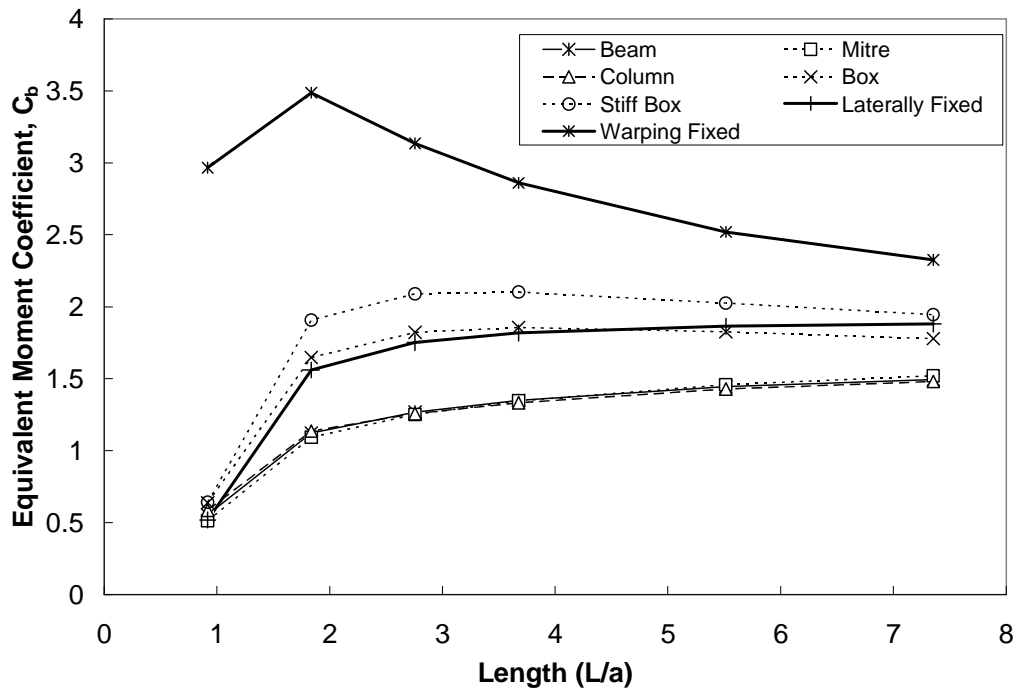


**Figure 6-24** Equivalent moment coefficient from elastic analysis, full beam restraint.

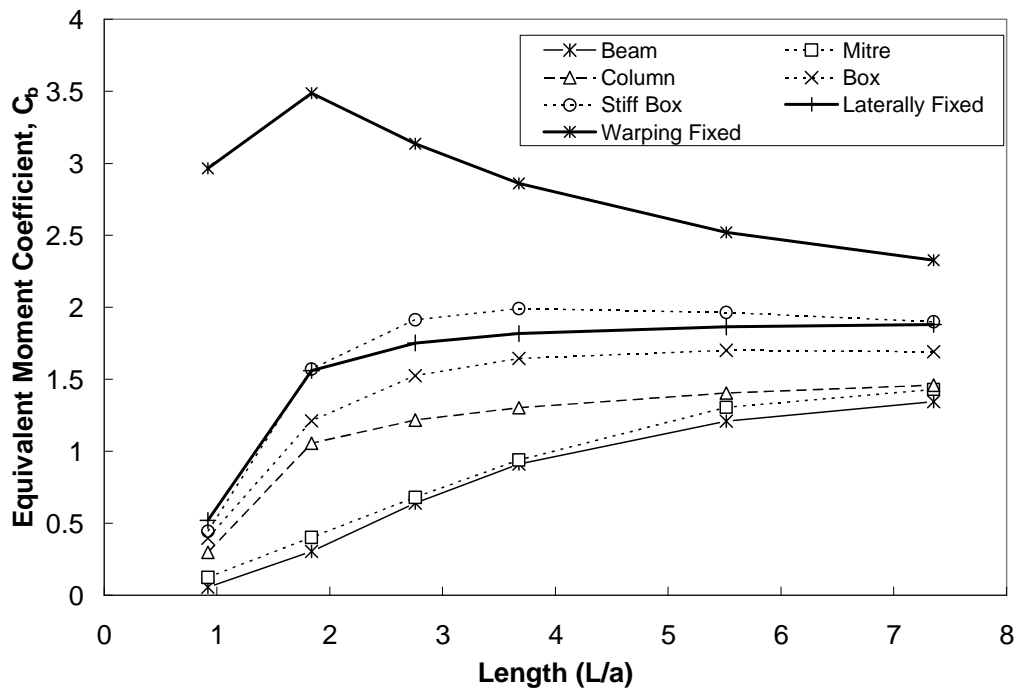


**Figure 6-25** Equivalent moment coefficient from elastic analysis, compression flange restrained

## 7. Design Implications

To this point, discussion has focussed almost exclusively on analysis. However, a guiding interest in structural engineering research is into applications for incorporating the results of structural analysis into the design of safer and more economical structures.

Thus, the question that must now be answered is “what are the implications of this work on the design of structures?” The initial hypothesis of this study was that the interaction of warping between members of a structure would reduce the structure’s capacity. If this were the case, there would be a need to require a correction for member loads used in design.

On the face of this presentation, the conclusion is that the effects of warping in the joints of steel frames can be safely ignored in their design. The analyses that include them are more complex than would normally be required for such structures and ignoring these effects is a conservative assumption, much like the current practice of ignoring any stiffening effects of major axis curvature. The warping effects also dominate the torsional behaviour for shorter members. This is the same range of lengths that are governed by local buckling. In the case of the members considered in this work, this means that at least part of the cross section will have yielded before the design capacity is achieved.

### 7.1 Increase in Strength

Current design methods already neglect a component of extra strength. If the extra stiffness of beams with respect to major axis curvature<sup>1</sup> (as per Trahair and Woolcock, 1973) were included in design consideration, there could be significant increase of the member capacity. For example, using the moments of inertia for a W360x216 section would require a simple calculation to determine the ratio of the

---

<sup>1</sup> Also noted in Chapter 3 of this work.

buckling moment,  $M_{u+}$  (calculated using the procedure proposed by Trahair and Woolcock), to the nominal lateral-torsional buckling moment,  $M_{u0}$ .

$$\frac{M_{u+}}{M_{u0}} = \frac{1}{\sqrt{1 - \left( \frac{I_y}{I_x} \right)}} = \frac{1}{\sqrt{1 - \frac{(283 \times 10^6 \text{ mm}^4)}{(712 \times 10^6 \text{ mm}^4)}}} = 1.288 \quad [7-1]$$

This would increase the elastic buckling moment by over 25%, and thus increase the design capacity for any but the shortest members, for which the inelastic behaviour would govern. However, this is not included in standard practice (MacPhedran and Grondin, 2008).

The calculation to determine the strength increase due to the inclusion of the warping contribution is much more involved than the relatively simple Equation [3-6], and would provide a much smaller increase in strength. The results from the previous chapter show increases only of the order of a few percent, and those are for shorter members, where plasticity consideration are more important than the elastic buckling strength.

## 7.2 Post Failure Considerations

While not part of the scope of this project, a discussion of the tests from Chi and Uang (2002) and Zhang and Ricles (2006) was raised earlier. These tests looked at the effect of plastic hinging and large rotation of reduced beam sections (typically used as “fuses” in seismic resisting frames) on the behaviour of a frame. There was significant plastic deformation of the members involved, mostly resulting from the localised warping of the connection, following plastic hinging in the adjacent reduced beam sections. These tests were conducted past the point that normal design methods would consider the ultimate strength of the frame members. The warping displacements experienced in those tests would be considered to occur after structural failure. There may be a need for these displacements to be considered for the structural “robustness” or structural



integrity design of the structure to ensure that extreme loading events do not cause disproportionate failure.

## 7.3 Design Interaction Equations

S16-01 (CSA, 2005) standard has a separate equation that considers lateral torsional buckling in beam-columns that will not experience local buckling before the development of full plastification of the cross-section (noted as Class 1 or Class 2 sections). This equation was introduced in S16.1-M89 (Kennedy, Picard, and Beaulieu, 1990) to address previous problems with lateral torsional buckling in S16 (Trahair, 1986; Kennedy and Qureshi, 1988). The current equation uses “shape” specific factors to reduce the moment contribution to the beam-column equation of 0.85 for strong axis bending and  $(0.60 + 0.40\lambda_y)$ , but not greater than 0.85, for weak axis bending. These mirror the factors used for the strength interaction equation, which in turn reflect approximate linear expressions for the idealized plastic behaviour. The strength relationships are based on earlier plastic design expressions, Equations 7-2 and 7-3, (ASCE, 1971)<sup>2</sup>. Previous editions of S16, from 1984 (CSA, 1984) and dating back to 1974, used factors of 1.0 for stability checks (MacPhedran and Grondin, 2007). The current S16 also uses factors of 1.0 for sections that will experience local buckling between the conditions of first yielding of the cross section and full plastic behaviour of the cross section (Class 3 sections).

$$\frac{M_{pcx}}{M_{px}} = 1.18 \left( 1 - \frac{P}{P_y} \right) \quad [7-2]$$

$$\frac{M_{pcy}}{M_{px}} = 1.19 \left( 1 - \left( \frac{P}{P_y} \right)^2 \right) \quad [7-3]$$

A case can certainly be made for the moment ratio reduction factors if the members are reasonably short, that is, if they are governed by inelastic or fully

---

<sup>2</sup> Page 137

plastic behaviour. Longer, or more slender, members will act in a fashion closer to the fully elastic behaviour, so that the inelastic effects, and thus the reduction factor, are reduced. The increase in the moment ratio factor for weak axis bending indicates that this has been considered in the equations.

However, the S16 cross section strength curve (Equation [2-9 (a)]) approximations appear to be unconservative for low ratios of  $P/P_y$  (Galambos and Surovek, 2008)<sup>3</sup>. This may appear to conflict with data from Dawe and Lee (1993), which show that the test data fall mostly above the design curve<sup>4</sup>. This discrepancy can be explained by noting the ultimate flexural strength of a number of short beam tests exceeding the calculated plastic moment. This can be found in collections of such data, as in White and Kim (2004), but is also shown in two of the tests by Dawe and Lee.

The American steel design specification (AISC, 2005) approximates the interaction curve with the two part equation in Equation [7-4]. For the portion of the curve with higher axial loads (Equation [7-4 (a)]) a reduction factor of 8/9 is applied to the factored moments. This equation is slightly more conservative than the S16 equivalent, as the AISC expression uses moment reduction factors of (approximately) 0.89 compared to the maximum S16 factor of 0.85. As well, for the portion of the curve where the moments are dominant, (Equation [7-4 (b)]) the moments are not reduced.

$$\begin{aligned} \frac{P}{P_r} + \frac{8}{9} \left( \frac{M_x}{M_{rx}} + \frac{M_y}{M_{ry}} \right) &\leq 1.0, \quad P > 0.2P_r & (a) \\ \frac{P}{2P_r} + \left( \frac{M_x}{M_{rx}} + \frac{M_y}{M_{ry}} \right) &\leq 1.0, \quad P \leq 0.2P_r & (b) \end{aligned} \quad [7-4]$$

Equation [7-4 (b)] addresses the portion of the S16 interaction equation that was noted above as being unconservative. Low values for the applied axial load

<sup>3</sup> An example that shows this unconservative prediction is Figure 4.36

<sup>4</sup> Table 4, ultimate  $M/M_p$ , this is not plotted in Dawe and Lee, 1993, but is plotted as Figure 9 in Essa and Kennedy, 2000.

(compared to the full yield strength of the cross section) do not greatly reduce the moment capacity. This lessened reduction is handled by the change in emphasis from the axial load in [7-4 (a)] to the moment load in [7-4 (b)].

Ziemian, *et al.* (2008) indicate that Equation [7-4] may be unconservative in some cases. One particular case is a beam-column of a W360x79 cross section, a 15 foot length (4572 mm), with an applied axial force of 382 kN and an applied moment of 349 kN·m. These loads are calculated to be right on the envelope defined by interaction Equation [7-4 (b)] using a resistance factor of 1.0. Finite element analysis shows this predicted capacity over-estimates the failure load by 20%. The interaction equation from S16 (CSA, 2005), Equation [2-9 (c)], is less conservative, predicting a nominal resistance that is 125% of the FEA result. (This is primarily due to the previously mentioned higher aggressiveness of the lower moment reduction factors in the S16 equation.) The interaction equation that does not use moment reduction factors gives a better prediction, though it predicts the beam-column capacity to be 11% higher than the FEA result. The failure loads predicted by the finite element analysis are too low to produce plastic hinging in the member. The member is too stocky to experience elastic lateral-torsional buckling, so the behaviour would be governed by inelastic buckling. It seems that even the unreduced moments may be optimistic in predicting member strength.

The plastic design manual (ASCE, 1971) does not use a similar reduction for lateral torsional buckling.<sup>5</sup> Also, a theoretical development of the interaction between the axial and lateral torsional instabilities<sup>6</sup> shows that there should be no reduction for cross-section shape, considering purely elastic behaviour.

---

<sup>5</sup> Page 162, ASCE 1971.

<sup>6</sup> As presented in Chapter 2 of this thesis.

## 7.4 Comparison With Standards

Figure 7-1 illustrates the results from one of the previous analyses as the raw magnifiers from the eigenvalue buckling analysis. Three points from these curves were selected to demonstrate how the predictions fit with the design equations. These points were selected to give a sample frame for each of the following cases: moment governed; column axial load governed; and an intermediate point, on the “ridge” of the surface. For each frame chosen, a nonlinear, elasto-plastic analysis was performed to obtain the ultimate strength of the frame for that loading, given the ratio between axial load and moment. The results from both the elastic eigenvalue buckling analysis and second-order elasto-plastic analysis are presented in Table 7-1. The strengths of frames analysed considering the warping displacements to be continuous through the joint connections are higher than the analyses that considered the warping to be free (unrestrained) at the joints. This held true for both eigenvalue and second-order analyses. In these frames, all members are W200x27 sections. The column height and the beam length are presented in Table 7-1.

The results from the second-order elasto-plastic analysis were used as the loadings for an elastic frame analysis for a typical frame analysis program (S-Frame v6.21) to generate the member forces using a P- $\Delta$  elastic analysis. These results were used with the AISC (Equation [7-4]) and CSA S16 design equations to produce the values presented in Table 7-2.

For the Canadian design procedure, a notional load of 0.5 % of the gravity loads was used in-plane, and for AISC, notional loads of 0.2 % of the gravity loads were applied in the in-plane direction, as the frame is braced in the out-of-plane direction. For the AISC design procedure, a reduced stiffness factor is applied to account for the inelastic effects for analysing the frame. The AISC Specification sets the reduced stiffness ( $EI^*$ ) as  $EI^* = 0.8\tau_b EI$ , where  $\tau_b$ , a factor that accounts for the softening due to yielding, is  $\tau_b = 4(P_f/P_y)(1 - P_f/P_y) \leq 1.0$ . The reduction factor used in this case was  $0.9\tau_b$ , as Surovek-Maleck and White (2004) note that

the  $0.8\tau_b$  value used in the AISC Specification has been factored with a resistance factor of 0.9.

The design equations appear to be conservative for the frames analysed. The capacity of the column in frame 3 would be estimated at about 52% of its capacity determined by analysis using the S16-01 approach and at about 62% using the procedure in the AISC Specification. Part of the reason for the apparently large difference between the design equations and the inelastic analysis is a lack of recognition by the elastic analysis of the redistribution of moments in the structure as yielding progresses in an indeterminate frame. This redistribution is also affected by the reduction of flexural member stiffness due to lateral torsional instability. This latter effect is also not usually recognised in the elastic analysis.

## **7.5 Costs**

The hidden face of the work is that of economy in construction. While ignoring the warping displacements at the joints of the frame may be safe, would including them in the design considerations improve the economy of the structure? In all, while there would be extra demands placed on joint design, and engineering time, taking advantage of the strength developed by the warping restraint would result in a reduction in the weight of steel.

One aspect that would be required to ensure the proper development of the warping resistances would increase effort in joint design and detailing. The extra demands placed on the joint from the bimoment would change the predicted local joint loading, including the potential for tensile demands on welds that may be assumed to carry only compression. This could necessitate more complex design of the joint connections. However, the effects of the warping interaction appear to be small enough that the current analyses, which neglect these effects, do not produce any significant under-estimation of the connection loads. In any event, the increased reliability index for connections would lead to member failure before connection failure.

Current construction trends are such that the cost of materials is a decreasing proportion of the total cost of a structure over time (Carter, *et al.*, 2000, Ruby and Matuska, 2009). Ruby and Matsuka show how, over the past 25 years, the proportion of the cost of the steel in a structure to the total cost of the completed steel erection has declined from about 40% in 1983 to 27% in 2008. This is not a uniform decline, but the trend is evident. It may be more economical to use heavier sections than are strictly required by the design standards. It is also advantageous to use less complex connection detailing, as shop costs (basically labour) have remained steady at about one-third of the total cost.

## **7.6 Summary**

In summary, ignoring the effect of warping of the joints appears to be safe. Analyses that include the interaction between the members of a frame result in a higher capacity than that predicted by the current analysis procedure. Including the effect of the interaction in design is complex, and would give minimal decreases in steel material costs. As fabrication costs are higher than material cost, the savings realised by incorporating the increase in strength due to mutual warping restraint may be more than offset by the increased design and fabrication costs. The implication for design is that maintaining the status quo would be the preferable course of action.

**Table 7-1** Analysis results for selected frame configurations for eigenvalue and second-order elastic-plastic analysis

	Frame 1	Frame 2	Frame 3
Column Height (mm)	4000	4000	4000
Beam Length (mm)	11000	12000	13000
Nominal $P_{app}/P_{ev}$	0.00	0.60	1.00
$P_{eigen}$ (warp free) kN	0.00	527	819
$P_{eigen}$ (warp cont.) kN	0.00	573	821
$P_{2nd}$ (warp free) kN	0.00	382	673
$P_{2nd}$ (warp cont.) kN	0.00	409	675
$M_{eigen}$ (warp free) kN·m	201	114	15
$M_{eigen}$ (warp cont.) kN·m	207	124	15
$M_{2nd}$ (warp free) kN·m	130	78	12
$M_{2nd}$ (warp cont.) kN·m	142	84	12

**Table 7-2** Design results from North American design guidelines

Frame	CSA-S16-01 Design Equations		AISC Design Equations	
	Column	Beam	Column	Beam
1	1.13	0.42	1.14	0.40
2	1.27	0.29	1.33	0.47
3	1.92	0.27	1.61	0.71

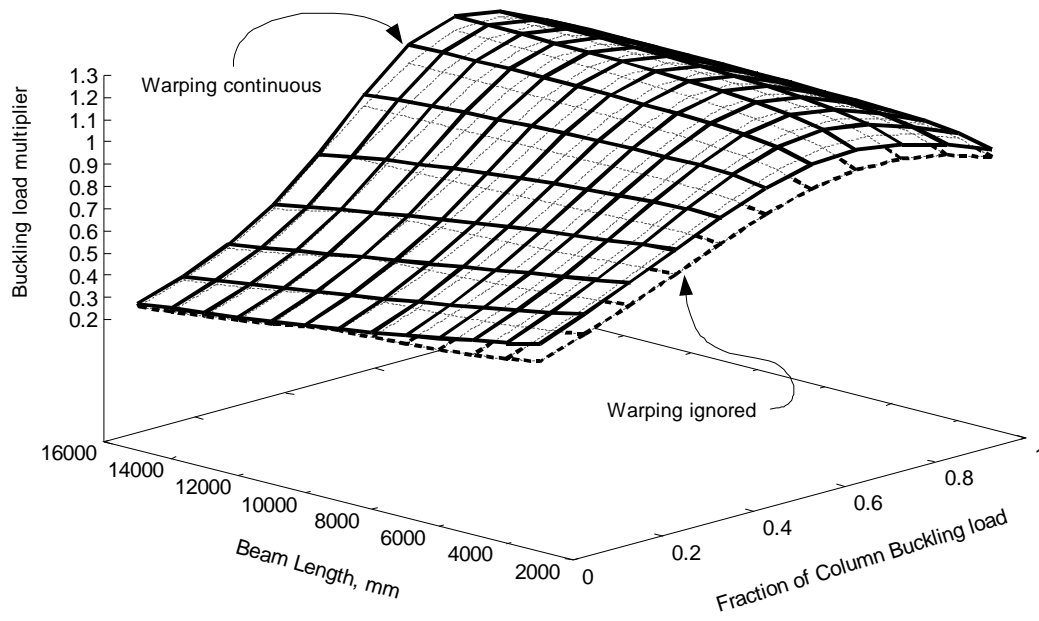


**Figure 7-1** Buckling load magnifier for 4 m W200x27 columns with W200x27 beam.



## 8 Summary and Conclusions

The current design approach of isolating members from rigid frames before considering the effect of warping does not account for the possible interaction between beams and columns. The purpose of this work was to investigate the possibility that the warping deformations experienced by members in a steel frame may cause failures at lower loads than would be expected in current design procedures. There was concern in this regard due to the possibility that the local warping deformation of the members at the joint would create additional forcing torque to decrease the lateral-torsional buckling capacity of the members. This project was considered to be a good candidate for investigation through finite element analysis because of the capability of beam elements to support the warping degree of freedom in current high-level analysis programs. The project does not lend itself to experimental examination, in that while we can, and do, separate the warping and flexural behaviours in the analysis and design of steel structures, the behaviours are inextricably linked. The warping of I-shaped sections is analogous to bending of the flanges in opposite directions about the member's weak axis. Thus it is inexorably linked to the weak axis flexure that is already included in moment connections.

As the work was analytical, an examination of available FEA elements was conducted to determine how well they perform for this type of analysis. The beam elements used were ones supporting warping degrees of freedom, but having quadratic formations, requiring several elements per member to better capture buckling effects. The elements behaved well when compared to Vlasov's (1961) theory when fully restrained end conditions were applied. Theoretical predictions for combined bending and axial loading were also well satisfied by the beam elements.

There are two cases where the elements deviate from expected behaviour. One case results in lowered capacity for very short elements or those that would be

very stiff torsionally. These members appear to have an inexplicable decrease in buckling strength compared to theory. The range of members affected by this phenomenon is small and not within the practical range of member sizes or shapes. The other case is for an effect where the in-plane curvature will affect the buckling strength. This effect prevents lateral-torsional buckling in a straight beam bent about its weak axis. This effect is ignored in the Abaqus buckling analysis and the analysis will give a buckling moment for a beam bent about its weak axis. This is presumably due to the increased capacity being a pre-buckling effect and not capable of being included in this type of analysis.

Despite these drawbacks, the elements were considered to be adequate for the required analyses.

The major part of the project involved using the beam elements to form a simple frame and these frames were analysed with and without warping continuity through the joints. The project analysed several frame configurations and found that the effects of mutual warping deformations did not negatively affect the frame capacity.

A “corner element” was developed using the substructuring capabilities of the Abaqus finite element analysis software to model the effects of a typical joint configuration. The stiffness provided by this linking element was considerably less than that of the continuous connection formed by directly connecting the warping displacements in the frame as described above. The more flexible connection means that the direct connection analyses described above will give unconservatively high values for buckling loadings on frames.

The elastic buckling analyses also neglect the limits placed on the structure by plastic behaviour. This will prevent the structure from achieving the upper bound given by buckling analyses for many structures with short members. The strengthening effect of considering warping continuity is higher for shorter members, so the net result is that the greatest elastic buckling capacity increases will not be reached in practical structures, as these will be limited by plastic

behaviour. Some shorter members may have capacity limits given by local or distortional buckling effects on the cross section or its component plates.

## 8.1 Conclusions

The current practice of neglecting the influence of mutual warping restraint between members in the analysis and design of steel frames appears to be a conservative practice. Certainly from the perspective of elastic buckling, this is a safe practice. The extra work involved to include these displacements in analysis is considerable. Developing the increased capacity derived from this relationship in the design of steel frames is likely not of benefit in the design process, particularly for frames constructed from rolled sections.

Any beneficial effect of this warping restraint is not applicable to members where the governing limit state is not lateral-torsional buckling, or a torsional buckling mode. This means that members that will fail in elastic buckling about their strong axis, which includes most columns in unbraced frames (Wongkaew, 2000), do not experience any increase in capacity due to this effect. Also, there is no benefit for those members in which formation of plastic hinges occurs before buckling or any significant second order effect develops. This would be the case for braced frames (Essa and Kennedy, 2000). The development of the first plastic hinge is often the governing limit state. Because of this criterion, there is less benefit to the frame's capacity from the mutual warping restraint than there is for fully elastic frames, as the hinge capacity represents the maximum loads that can be resisted by the frame.

Even in those members where there is a benefit, the advantage varies with respect to a number of variables, including the ratio of axial to flexural loadings, base conditions and relative stiffnesses of the joined members. This would mean that any attempts to take advantage of the benefits require significant analysis to judge their benefit for any given load case. There are numerous load cases that may be critical in the design of frames, due to the already complex nature of beam-column design and frame analysis. Even effects that are simpler to calculate, such

as the increase in theoretical buckling moment for stockier sections is not generally considered. (Eurocode 3 (CEN, 2005) includes these effects in a general sense, by including two separate design strength curves for stocky and slender beams.)

The joint element indicates that the warping stiffness developed in the connection is not as large as the rigid connection assumed by direct beam-element connections would indicate. While it is apparent that the joint element would be more flexible than a rigid connection, this element appears to be extremely flexible.

## **8.2 Further work**

It must be noted that the members and frames studied do not cover the multitude of all possible combinations. The structures and sections examined were thought to be the most sensitive to the effects of warping deformations on their torsional stability. However, there may be unexamined structures that provide further insight into the problem. In particular, sections with very wide flanges would provide more warping, but also have a larger weak axis moment of inertia that would increase the lateral torsional buckling capacity. Channel sections may also be affected more by reason of their torsional properties.

While the loads applied are also selected to maximise the effects of the warping, these are not typical of the loadings experienced by real structures. Actual loadings will give rise to different conditions that may trigger unexpected modes, and investigations of those conditions might also give an insight not provided by the ones used herein.

The joint element is very flexible relative to the rigid connections assumed in the direct beam to beam modelling. Its formulation could be revisited to determine if there should be incorporation of the other behaviours, such as weak axis flexure or twist. The interactions between all deformations are complex and may need to be assessed to gain a better understanding of the joint behaviour.

The entire problem of lateral-torsional buckling in beam columns is still open for greater exploration. There may be unconservative implications in the formulae used in design of very long Class 1 and Class 2 sections in the Canadian design standard, as compared to the design of Class 3 sections. That interaction equation is a different problem from the one addressed in this work.

There are instances beyond the scope of this work that indicate problems with warping in post-failure scenarios (Chi and Uang 2002, Zhang and Ricles 2006) when reduced section (“dog-bone”) beams are used in moment frames. Investigation of the effects of mutual warping restraint in conditions of extreme loadings may benefit structural integrity investigations in preventing progressive, or disproportionate, collapses.

The effects of warping deformation in the connections of moment frames are currently neglected in the analysis and design of the frames. A study of these effects and their impact on connection design and detailing may prove of value in the future. This is particularly of concern with the work above by Chi and Uang (2002), and Zhang and Ricles (2006).

## References

Abaqus, Inc (2002) ABAQUS/Standard Theory Manual, Version 6.3-1, Dassault Systemes, Providence, RI, USA.

AISC (2005) *Specification for Structural Steel Buildings*, ANSI/AISC 360-05, American Institute for Steel Construction, Chicago, IL, USA. March.

Albert, C., Essa, H. S., and Kennedy, D. J. L. (1992) "Distortional buckling of steel beams in cantilever-suspended span construction." *Canadian Journal of Civil Engineering*, Ottawa, Canada, Vol. 19, No. 5, pp. 767-780.

Alemdar, B.N. and White, D.W. (2008) "A new 3D co-rotational beam-column element." *Proc. Structural Stability Research Council Annual Conference*, April, Nashville, TN, USA. pp. 175-194.

ANSYS, Inc (2002) ANSYS 6.1, Finite Element Program. Canonsburg, PA, USA.

ASCE (1971) *Plastic design in steel: A guide and commentary*, ASCE Manuals and Reports on Engineering Practice No. 41, ASCE, New York, NY, USA.

ASCE Task Committee on Effective Length (ASCE) (1997) *Effective length and notional load approaches for assessing frame stability: implications for American steel design*, American Society of Civil Engineers.

Attard, M.M. and Lawther, R. (1989) "Effect of secondary warping on lateral buckling." *Engineering Structures*, Vol. 11, No. 2, April, pp. 112-118.

Austin, M., Lin W.-J., Chen, X. (2000) Aladdin FEA Program V2.1, URL "<http://www.isr.umd.edu/~austin/aladdin.html>", March.

Austin, W.J. (1961) "Strength and design of metal beam-columns." ASCE, *Journal of the Structural Division*, Vol. 87 (ST4) pp. 1-32.

Ayrton, W. E. & Perry, J. (1886) "On struts." *The Engineer*, Vol. 61, pp. 464-465 (Dec. 10) and pp. 513-514 (Dec. 24).

Baker, J.F. (1936) "The Rational Design of Steel Building Frames." *Journal of the I.C.E.*, Vol. 3, No. 7, pp. 127-210.

Barsoum, R.S. and Gallagher, R.H. (1970) "Finite element analysis of torsional and torsional-flexural stability problems." *International Journal for Numerical Methods in Engineering*, Vol. 2, pp. 335-352.

Basaglia, C., Camotim, D. and Silvestre, N. (2007) "GBT-Based Analysis of the Local-Plate, Distortional and Global Buckling of Thin-Walled Steel Frames" *Proceedings of the 2007 SSRC Annual Stability Conference*, April 18-21, pp. 391-412.

Basaglia, C., Camotim, D. and Silvestre, N. (2009) "Latest Developments on the GBT-Based Buckling Analysis of Thin-Walled Steel Frames" *Proceedings of the 2009 SSRC Annual Stability Conference*, April 1-4, pp. 325-344.

Bathe, K-J (1996) *Finite Element Procedures*. Prentice-Hall, Inc. Englewood Cliffs, NJ, USA.

Bathe, K-J, and Wilson, E.L. (1976) *Numerical Methods in Finite Element Analysis*. Prentice-Hall, Inc. Englewood Cliffs, NJ, USA.

Beaulieu, D. and Adams, P.F. (1980) "Significance of structural out-of-plumb forces and recommendations for design." *Canadian Journal of Civil Engineering*, Ottawa, Canada, Vol. 7, No. 1, pp. 115-113.

Behbahani, M.R., Grondin, G.Y. and Elwi, A.E. (2003) *Experimental and Numerical Investigation of Steel Plate Shear Walls*, Structural Engineering Report 254, Department of Civil and Environmental Engineering, University of Alberta, Edmonton, AB.

Bjørhovde, R. (1972) *Deterministic and probabilistic approaches to the strength of steel columns*, Doctoral dissertation, Lehigh University, Bethlehem, PA.

Bremault, D., Driver, R.G. and Grondin G.Y. (2008) *Limit States Design Approach for Rolled Wide Flange Beams Subject to Combined Torsion and Flexure*, Structural Engineering Report No. 279, Department of Civil and Environmental Engineering, University of Alberta, Edmonton, AB, Jan.

Carter, C.J., Murray, T.M., and Thornton, W.A. (2000) "Economy in Steel." *Modern Steel Construction*, American Institute of Steel Construction, April, 2000, (available on-line at [http://www.modernsteel.com/issue.php?date=April\\_2000](http://www.modernsteel.com/issue.php?date=April_2000)).

Chan, S.L. (2001) "Non-linear behavior and design of steel structures." *Journal of Constructional Steel Research*, Vol. 57, pp. 1217-1231.

Chang, J.-T. (2004) "Derivation of the higher-order stiffness matrix of a space frame element." *Finite Elements in Analysis and Design*, Vol. 41, Issue 1, Oct., pp. 15-30.

Chen, W.-F. and Atsuta, T. (1977) *Theory of Beam-Columns: Volume 2 Space behaviour and design*, McGraw-Hill, New York, NY.

Chi, B. and Uang, C.-M. (2002) “Cyclic response and design recommendations of reduced beam section moment connections with deep columns.” ASCE, *Journal of Structural Engineering*, Vol. 128, No. 4, April 1. pp. 464-473.

CISC (2002) *Torsional section properties of steel shapes*, Canadian Institute of Steel Construction, “<http://www.cisc-icca.ca/resources/tech/updates/torsionprop/>” August. Markham, ON.

CISC (2006) *Handbook of steel construction*, 9<sup>th</sup> ed., Canadian Institute of Steel Construction, Markham, ON.

Clarke, MJ, and Bridge RQ (1995) “The notional load approach for the design of frames.” The University of Sydney, School of Civil and Mining Engineering Research Report No. R718, Dec. (Also included as Chapter 4 and Appendices in: ASCE Task Committee on Effective Length (1997) *Effective length and notional load approaches for assessing frame stability: implications for American steel design*, American Society of Civil Engineers.)

Column Research Council (CRC) (1960) *Guide to design criteria for metal compression members*, Johnson, B. (ed.) First Edition, Column Research Council.

CSA (1984) *CAN/CSA S16.1-M84 Limit States Design of Steel Structures*, Canadian Standards Association, Mississauga, ON.

CSA (1989) *CAN/CSA S16.1-M89 Limit States Design of Steel Structures*, Canadian Standards Association, Mississauga, ON.

CSA (1994) *CAN/CSA S16.1-94, Limit States Design of Steel Structures*, Canadian Standards Association, Mississauga, ON.

CSA (2005) *CAN/CSA S16-01 Limit States Design of Steel Structures, including S16S1-05*, Canadian Standards Association, Mississauga, ON.

CSA (2007) *CSA S136-07 North American Specification for the Design of Cold-Formed Steel Structural Members*, Canadian Standards Association, Mississauga, ON.

Cuk, P. E. and Trahair, N., S. (1981) “Elastic buckling of beam-columns with unequal end moments.” Institution of Engineers, Australia, *Civil Engineering Transactions*, Vol. CE23, No. 3, pp. 166-171.

Daddazio, R.P., Bieniek, M.P. And DiMaggio, F.L. (1983) “Yield Surface for Thin Bars with Warping Restraint” ASCE, *Journal of Engineering Mechanics*, Vol. 109, No. 2, April 1983, pp. 450-465.



Davidson, J.F. (1952) "The elastic stability of bent I-section beams." *Proceedings of the Royal Society of London, Series A*, Vol. 212, No. 1108 1952, April 8, pp. 80-95.

Dawe, J.L. and Kulak, G.L. (1986) "Local buckling behavior of beam-columns." ASCE, *Journal of Structural Engineering*, Vol. 112, No.11, Nov. pp. 2447-2461. (Discussion by Frakes, J. and closure in ASCE, *Journal of Structural Engineering*, Vol. 114, No. 4, April, pp. 968-972.)

Dawe, J.L. and Lee, T.S. (1993) "Local buckling of Class 2 beam-column flanges." *Canadian Journal of Civil Engineering*, Vol. 20, No. 6, pp. 931-939.

Dinno, K.S. and Gill, S.S. (1964) "The plastic torsion of I-sections with warping restraint." *International Journal of Mechanical Sciences*, Vol. 6, pp. 27-43.

Essa, H.S. and Kennedy, D.J.L. (2000) "Proposed provisions for the design of steel beam-columns in S16-2001." *Canadian Journal of Civil Engineering*, Vol. 27, No. 4, pp. 610-619.

Ettouney, M.M. and Kirby J.B. (1981) "Warping restraint in three-dimensional frames." ASCE, *Journal of Structural Engineering*, Vol. 107, No. ST8, April 1. pp. 1643-1656.

European Committee for Standardization (CEN) (2005) Eurocode 3: *Design of steel structures – Part 1-1: General rules and rules for buildings*. European Committee for Standardization, Brussels, BE, May.

European Convention for Constructional Steelwork (ECCS) (1976) *Manual on the Stability of Steel Structures*. European Convention for Constructional Steelwork, Brussels, BE, June.

Felippa, C.A. and Haugen, B. (2005) "A unified formulation of small-strain corotational finite elements: I. Theory." *Computational Methods in Applied Mechanical Engineering*. Elsevier. Vol. 194, pp. 2285–2335.

Flint, A.R. (1951) "The influence of restraints on the stability of beams." The Institution of Structural Engineers' *The Structural Engineer*, Vol. 29, No. 9, September, pp. 235-246.

Galambos, T.V. (1968) *Structural Members and Frames*. Prentice Hall, Englewood Cliffs, NJ.

Galambos, T.V. (1998) *Guide to stability design criteria for metal structures* (5<sup>th</sup> ed.) Structural Stability Research Council, John Wiley & Sons, Inc. New York, NY.

Galambos, T.V. (2004) "Reliability of the member stability criteria in the 2005 AISC Specification." *International Journal of Steel Structures* of the Korean Society of Steel Construction, Vol. 4, No. 4, December, pp. 223–230. (Reprinted in *AISC Engineering Journal*, Fourth Quarter, 2006, pp. 257-265.)

Galambos, T.V. and Surovek, A.E. (2008) *Structural Stability of Steel: Concepts and Applications for Structural Engineers*, John Wiley & Sons, Inc., Hoboken, NJ.

Grondin, G.Y., Chen, Q., Elwi, A.E and Cheng, J.J.R. (1998) "Buckling of Stiffened Steel Plates – Validation of a Numerical Model," *Journal of Constructional Steel Research*, Vol. 45, No. 2, pp. 125-148.

Ioannidis, G., Mahrenholtz, O. and Kounadis, A.N. (1993) "Lateral post-buckling analysis of beams." Springer-Verlag, *Archive of Applied Mechanics*, Vol. 63, pp. 151-158.

Jin, L. (1994) *Analysis and Evaluation of a Shell Finite Element with Drilling Degree of Freedom*, MSc Thesis, Department of Civil Engineering and Institute for System Research, University of Maryland at College Park, MD, USA.

Kennedy, D.J.L., Picard, A., and Beaulieu, D. (1990) "New Canadian provisions for the design of steel beam – columns", *Canadian Journal of Civil Engineering*, Vol. 17, No. 6, pp. 837-893.

Kennedy, D.J.L., Picard, A., and Beaulieu, D. (1993) "Limit States Design of Beam-Columns: the Canadian Approach and Some Comparisons." *Journal of Constructional Steel Research*, Vol. 25, pp. 141-164.

Kennedy, D.J.L. and Qureshi, S. (1988) "Design strengths of steel beam-columns: Discussion." *Canadian Journal of Civil Engineering*, Vol. 15, No. 1, pp. 136-140.

Kim, S-E., Lee, J. and Park, J-S. (2002) "3-D second-order plastic-hinge analysis accounting for lateral torsional buckling." *International Journal of Solids and Structures*, Vol. 39, pp. 2109–2128.

Kim, Y.D., and White, D.W. (2008) "Lateral torsional buckling strength of prismatic and web-tapered beams." *Proc. SSRC 2008 Annual Stability Conference*, Nashville, TN, USA. April 2-5, pp. 155-174.

Kirby P.A. and Nethercot, D.A. (1979) *Design for Structural Stability*, Granada Publishing, London.

Krenk, S. and Damkilde L. (1991) "Warping of joints in I-beam assemblages." ASCE, *Journal of Engineering Mechanics Division*, Vol. 117, No. 11, pp. 2457-2474.

- Krishnan, S. (2004) "Three Dimensional Nonlinear Analysis of Tall Irregular Steel Buildings Subject to Strong Ground Motion." PhD Thesis, California Institute of Technology, Pasadena, CA, USA.
- Kulak, G.L. and Grondin, G.Y. (2006) *Limit States Design in Structural Steel*, 8<sup>th</sup> ed. Canadian Institute of Steel Construction, Markham, ON.
- Lowes, L. N., Mitra, N., and Altoontash, A. (2004) "A beam-column joint model for simulating the earthquake response of reinforced concrete frames." PEER Report 2003/10, Pacific Earthquake Engineering Research Center, College of Engineering, University of California, Berkeley, CA, US. February.
- MacPhedran, I., and Grondin, G.Y. (2005) "Warping restraint and steel frame instability." *Proc. SSRC 2005 Annual Stability Conference*, Montréal, QC. April 6-9.
- MacPhedran, I., and Grondin, G.Y. (2006) "Effects of plasticity on steel beam stability considering partial warping restraint." *Proc. SSRC 2006 Annual Stability Conference*, San Antonio, TX. February 8-11.
- MacPhedran, I., and Grondin, G.Y. (2007a) "Out-of-plane instability considering frame-member interaction." *Proc. SSRC 2007 Annual Stability Conference*, New Orleans, LA. April 18-21.
- MacPhedran, I.J., and Grondin, G.Y. (2007b) "A brief history of beam-column design." *Proc. Canadian Society for Civil Engineering 2007 Annual Conference*, June 6–9, Yellowknife, NT.
- MacPhedran, I.J., and Grondin, G.Y. (2008) "A simpler steel beam design strength curve." *Proc. Canadian Society for Civil Engineering 2008 Annual Conference*, June 10–13, Québec, QC.
- Maleck, A.E. (2001) *Second-Order Inelastic and Modified Elastic Analysis and Design Evaluation of Planar Steel Frames*, PhD thesis, Georgia Institute of Technology, Atlanta, GA, US.
- Masarira, A. (2002) "The effect of joints on the stability behaviour of steel frame beams", *Journal of Constructional Steel Research*, Elsevier. Vol. 58, pp. 1375-1390.
- Massonnet, C. (1959) "Stability considerations in the design of steel columns." ACSE, *Journal of the Structural Division*, Vol. 85, No. ST7, Sep., pp. 75-111.
- Massonnet, C. (1976) "Forty years of research on beam columns in steel," *Solid Mechanics Archives*, Vol. 1, No. 1, pp. 27-157.

Michell, A.G.M. (1899) "Elastic Stability of Long Beams under Transverse Forces." *The London, Edinburgh, and Dublin Philosophical Magazine and Journal of Science*, Vol. 48, No. 292, Sept., pp. 298-309.

Mohareb, M. and Nowzartash, F. (2003) "Exact finite element for nonuniform torsion of open sections." ASCE, *Journal of Structural Engineering*, Vol. 129, No. 2, pp. 215-223. (Discussion by Saadé, K., Espion, B. and Warzée, G. (2004) and Closure ASCE, *Journal of Structural Engineering*, Vol. 130, No. 9, pp. 1420-1421.)

Morrell, P.J.B. (1980) "The influence of joint detail on the behaviour of thin walled structures having an axial discontinuity." *Thin-walled Structures*, Rhodes, J. and Walker, A.C. editors, Granada, London, UK pp. 539-552.

Morrell, P.J.B., Riddington, J.R., Ali, F.A. and Hamid, H.A. (1996) "Influence of joint detail on the flexural/torsional interaction of thin-walled structures." *Thin-Walled Structures*, Elsevier, Vol. 24, pp. 97-111.

NRC (2005) *National Building Code of Canada*. Institute for Research in Construction, National Research, Council of Canada, Ottawa, ON.

Nethercot, D.A. and Rockey, K.C. (1971) "A unified approach to the elastic buckling of beams", *The Structural Engineer*, Vol. 49, No. 7, pp 321-330.

Nethercot D.A. and Trahair, N.S. (1976a) "Inelastic lateral buckling of determinate beams." ASCE, *Journal of the Structural Division*, Vol. 102, No.ST4, (April) pp. 701-717.

Nethercot D.A. and Trahair, N.S. (1976b) "Lateral buckling approximations for elastic beams." *The Structural Engineer*, Vol. 54, No. 6, (June) pp. 197-204.

Ofner, R. (1997) "Traglasten von Stäben aus Stahl bei Druck und Biegung." (Load Carrying Capacity of Steel Members Subjected to Compression and Bending.) Dissertation at the Technische Universität Graz, Graz, AT.

Ojalvo, M. (1975) Discussion on Vacharajittiphan, P. and Trahair N.S. (1974) "Warping and distortion at I-section joints." ASCE, *Journal of the Structural Division*, Vol. 101, No. ST1, pp. 343-345.

Ojalvo, M. and Chambers, R.S. (1977) "Effect of warping restraints on I-beam buckling", ASCE, *Journal of the Structural Division*, Vol. 103, No. ST12, pp. 2351-2360.

Rajasekaran, S. (1977) "Finite Element Method for Plastic Beam-Columns." in *Theory of Beam-Columns, Volume 2: Space behaviour and design*, W-F Chen and T Atsuta, McGraw-Hill, New York, NY, pp. 539-608.

Riks, E. (1979) "An incremental approach to the solution of snapping and buckling problems." *International Journal of Solids and Structures*, Elsevier. Vol. 15, No. 7, pp. 529-551.

Riks, E. (1984) "Some computational aspects of the stability analysis of nonlinear structures." *Computer Methods in Applied Mechanics and Engineering*, Elsevier. Vol. 47, No. 3, pp. 219-259.

Ruby, J. and Matuska, J. (2009) "Structural Steel Economy: Revisiting the Assumptions." AISC, *Modern Steel Construction*, January, 2009, (available on-line at [http://www.modernsteel.com/issue.php?date=January\\_2009](http://www.modernsteel.com/issue.php?date=January_2009)).

Schmitke, C.D. and Kennedy, D.J.L. (1984) *Effective lengths of laterally unsupported steel beams*, Structural Engineering Report No. 118, Department of Civil and Environmental Engineering, University of Alberta, Edmonton, AB, Oct. (available on-line at <http://www.engineering.ualberta.ca/structures/nav02.cfm?nav02=46539&nav01=36095>)

Schmitke, C.D. and Kennedy, D.J.L. (1985) "Effective lengths of laterally continuous, laterally unsupported steel beams." *Canadian Journal of Civil Engineering*, Vol. 12, No. 3, Sept., pp. 603-616.

Schumacher, A.S., Grondin, G.Y., and Kulak, G.L. (1999) "Connection of Infill Panels in Steel Plate Shear Walls," *Canadian Journal of Civil Engineering*, Vol. 26, No. 5, pp 549-563.

Seaburg, P.A. and Carter, C.J. (1996) *Torsional analysis of structural steel members*, AISC Steel Design Series No. 9, American Institute of Steel Construction, 2<sup>nd</sup> printing, October.

Southwell, R.V. (1932) "On the analysis of experimental observations in problems of elastic stability," *Proceedings of the Royal Society of London. Series A, Containing Papers of a Mathematical and Physical Character*, Vol. 135, No. 828., April, pp. 601-616.

Surovek-Maleck, A.E. and White, D.W. (2004) "Alternative approaches for elastic analysis and design of steel frames. I: overview", *Journal of Structural Engineering*, ASCE, Vol. 103, No. 8, pp. 1186-1196.

Surovek, A., Camotim, D., Hajjar, J., Teh, L., White, D. and Ziemian, R. (2006) "Direct Second-Order Analysis for the Design of Steel Structures." *Proceedings*

of the American Society for Civil Engineering's 2006 Structural Congress, St. Louis, MO, USA. May.

Surovek, A.E., White, D.W. and Leon, R.T. (2005) "Direct Analysis for Design Evaluation of Partially Restrained Steel Framing Systems." ASCE, *Journal of the Structural Division*, Vol. 131, No. 9, pp. 1376-1389.

Tong, G.S., Yan, X.X. and Zhang, L. (2005) "Warping and bimoment transmission through diagonally stiffened beam-to-column joints." *Journal of Constructional Steel Research*, Vol. 61, No. 6, pp. 749-763.

Trahair, N.S. (1968a) Discussion of "Elastic lateral buckling of continuous beams" by A.J. Hartmann, ASCE, *Journal of the Structural Division*, Vol. 94, No. ST3, pp. 845-848.

Trahair, N.S. (1968b) "Elastic stability of propped cantilevers." Institution of Engineers, Australia, *Civil Engineering Transactions*, Vol. 10, April, pp. 94 - 100.

Trahair, N.S. (1968c) "Interaction buckling of narrow rectangular continuous beams." Institution of Engineers, Australia, *Civil Engineering Transactions*, Vol. 10, Oct., pp. 167- 172.

Trahair, N.S. (1986) "Design strengths of steel beam-columns." *Canadian Journal for Civil Engineering*, Vol. 13, No. 6, pp. 639-645.

Trahair, N.S. (1993) *Flexural-Torsional Buckling of Structures*, CRC Press Inc., Boca Raton, FL, USA.

Trahair, N.S. (1996) "Laterally unsupported beams", *Engineering Structures*, Vol. 18, No. 10, pp. 759-768.

Trahair, N.S. (2003) *Non-Linear Elastic Non-Uniform Torsion*, Centre for Advanced Structural Engineering Research Report No R828, Department of Civil Engineering, Sydney, NSW, AU. (Also available as: "Nonlinear Elastic Nonuniform Torsion", ASCE, *Journal of Structural Engineering*, Vol. 131, No. 7, July 1, pp. 1135-1142.)

Trahair, N.S. and Chan, S.L. (2003) "Out-of-Plane Advanced Analysis of Steel Structures." *Engineering Structures*, Elsevier, Vol. 25, No. 13, pp. 1627-1637. (Also available as Centre for Advanced Structural Engineering Research Report No R823, Department of Civil Engineering, Sydney, NSW, AU. September 2002.)

Trahair, N.S., and Woolcock, S.T. (1973) "Effect of major axis curvature on I-beam stability." ASCE, *Journal of Engineering Mechanics Division*, Vol. 99, No. EM1, Feb., pp. 85-98.

Vacharajittiphan, P. and Trahair N.S. (1974) “Warping and distortion at I-section joints.” ASCE, *Journal of the Structural Division*, Vol. 100, No. ST3, pp. 547-564.<sup>1</sup>

Vlasov, V.Z. (1961) *Thin-Walled Elastic Beams*, 2nd edition, Israel Program for Scientific Translation, Jerusalem.

Wagner, H. (1936) “*Verdrehung und knickung von offenen profilen* (Torsion and buckling of open sections)”, NACA Technical Memorandum, No. 807.

Wall, L., Christianson, T., and Orwant, J. (2000) *Programming Perl, Third Edition*, O'Reilly Media.

White, D.W. and Kim, Y.D. (2004) “*Unified Flexural Resistance Equations for Stability Design of Steel I-Section Members – Moment Gradient Tests.*” Structural Engineering, Mechanics and Materials Report No. 04-28. School of Civil and Environmental Engineering, Georgia Institute of Technology, Atlanta, GA.

Wongkaew, K. (2000) “*Practical advanced analysis for design of laterally unrestrained steel planar frames under in-plane loads,*” PhD thesis, Purdue University, UMI number 3018291.

Wongkaew, K. and Chen, W.-F. (2002) “Consideration of out-of-plane buckling in advanced analysis for planar steel frame design.” *Journal of Constructional Steel Research*, Elsevier. Vol. 58, pp. 943-965.

Wood, B.R., Beaulieu, D. and Adams P.F. (1976a) “Column design by P-Delta method.” ASCE, *Journal of the Structural Division*, Vol. 102, No. ST2, pp. 411-486.

Wood, B.R., Beaulieu, D. and Adams P.F. (1976b) “Further aspects of design by P-Delta method.” ASCE, *Journal of the Structural Division*, Vol. 102, No. ST2, pp. 487-500.

Woolcock, S.T. and Trahair, N.S. (1974) “Post-buckling behaviour of determinate beams.” ASCE, *Journal of Engineering Mechanics Division*, Vol. 100, No. EM2, pp. 151-171.

Yang Y-B, Chern, S-M, and Fan, H-T (1989). “Yield Surfaces for I-Sections with Bimoments” ASCE. *Journal of Structural Engineering*, Vol. 115, No. 12, pp. 3044-3058.

---

<sup>1</sup> Note discussions by Renton and Ojalvo, *Journal of the Structural Division*, Vol. 101, No ST1, pp. 341-345

Yang, Y-B and McGuire, W. (1984) "A procedure for analysing space frames with partial warping restraint." *International Journal for Numerical Methods in Engineering*, Vol. 20, pp. 1377-1398.

Yang, Y-B and McGuire, W. (1986) "Joint rotation and geometric nonlinear analysis." ASCE, *Journal of Structural Engineering*, Vol. 112, No. 4, April, pp. 879-905.

Yura, J.A. (2006) "Five useful stability concepts." SSRC 2006 Beedle Award Paper, presented at the SSRC Annual Conference Feb. 8, San Antonio, TX.

Yura, J.A., and Widiyanto (2005) "Lateral buckling and bracing of beams – a re-evaluation after the Marcy Bridge collapse." *Proc. Structural Stability Research Council Annual Technical Session*, April, Montréal, QC, pp. 277-294.

Zhang, X. and Ricles, J.M. (2006) "Experimental evaluation of reduced beam section connections to deep columns." ASCE, *Journal of Structural Engineering*, Vol. 132, No. 3, March 1, pp. 346-357.

Ziemian, R.D., Seo, D-W. and McGuire, W. (2008) "On the inelastic strength of beam-columns under biaxial load." *Proc. Structural Stability Research Council Annual Technical Session*, April, Nashville, TN, USA. pp. 453-471.

Zinoviev, I and Mohareb, M (2004) "Analysis and design of laterally unsupported portal frames for out-of-plane stability." *Canadian Journal of Civil Engineering*, Vol. 31, No. 3, pp. 440-452.



## **Curriculum Vitae for Ian MacPhedran, P.Eng.**

### **Education**

M.Sc. 1989 Structural Engineering, University of Saskatchewan  
B.E. 1983 (Great Distinction) Civil Engineering, University of Saskatchewan

### **Submitted for publication**

July 2008 I .J. MacPhedran and G. Y. Grondin, “A simple steel beam design curve” submitted to the Canadian Journal of Civil Engineering, currently under review.

### **Conference Proceedings**

April 2009 I .J. MacPhedran\* and G. Y. Grondin, “A Proposed Simplified Canadian Beam Design Approach” presented at the 2009 Annual Stability Conference of the Structural Stability Research Council, Phoenix AZ (Awarded 2009 Vinnakota Award for best student paper)

June 2008 I .J. MacPhedran\* and G. Y. Grondin, “A Simpler Steel Beam Design Strength Curve” presented at the Canadian Society for Civil Engineering's Second International Structural Specialty Conference, Québec, QC

June, 2007 I .J. MacPhedran\* and G. Y. Grondin, “A brief history of beam-column design” presented at the Canadian Society for Civil Engineering's 2007 Annual General Meeting and Conference in Yellowknife, NT

April, 2007 I .J. MacPhedran\* and G. Y. Grondin, “Out-of-plane instability considering frame-member interaction” presented at the 2007 Annual Stability Conference of the Structural Stability Research Council, New Orleans, LA

August 2006 I .J. MacPhedran\* and G. Y. Grondin, “Fatigue of high strength bolted connections in tension” presented at the 7th International Conference on Short and Medium Span Bridges in Montréal, QC

August 2006 G. Y. Grondin\* and I .J. MacPhedran, “Prying action in bolted tension joints loaded at service load,” Tenth East Asia-Pacific Conference on Structural Engineering and Construction (EASEC-10) in Bangkok, Thailand.

Feb. 2006 I .J. MacPhedran\* and G. Y. Grondin, “Effects of plasticity on steel beam stability considering partial warping restraint” presented at the Structural Stability Research Council Conference in San Antonio, TX

April 2005 I .J. MacPhedran\* and G. Y. Grondin, “Warping Restraint and Steel Frame Instability” presented at the Structural Stability Research Council's 2005 Stability Conference in Montréal, QC

---

\* Presenter

May 1984     I.J. MacPhedran\* and M. U. Hosain\*, “Use of computers in teaching a basic course in steel design,” presented at the American Society of Civil Engineering 1984 Spring Convention, Atlanta, GA.

### **Other Presentations**

May 2000     I.J. MacPhedran, “Tracing Email Messages” invited presentation at the Campus Security Administrators’ Workshop, Saskatoon, SK

### **Other Publications**

Dec. 1988     Thesis: Development of an Educational Three Dimensional Structural Analysis and Design Package

1994 – 2008   Young, Roger and MacPhedran, Ian. Internet Finite Element Resources. Available online at:  
<[http://homepage.usask.ca/~ijm451/finite/fe\\_resources/fe\\_resources.html](http://homepage.usask.ca/~ijm451/finite/fe_resources/fe_resources.html)>

2008     Contributions to *Guide to Stability Design Criteria for Metal Structures*, 6th Edition, R. D. Ziemian, editor, to the chapters on Frame Stability, Stability of Angle Members, and Centrally Loaded Columns.

### **Awards**

2009            SSRC annual conference Vinnakota Award, best student paper  
2005-2009     Alberta Ingenuity Fund (AIF) Studentship  
1983-1985     NSERC Postgraduate Scholarship  
1980-1982     University of Saskatchewan Undergraduate Scholarship  
1980            GEM Centennial Bursary  
1979            Canadian Association of Physicists’ Provincial Prize

### **Professional Affiliations**

Professional Engineer registered with APEGGA (Alberta) and APEGS (Saskatchewan)

Member of the Canadian Society for Civil Engineering

Member of the Structural Stability Research Council

## **Appendix A: Substructure generation**

The substructure described in Chapter 6 can be difficult to form by hand. However it can be easily generated with an automated program. The following script is presented as one method of generating the box connection substructure element.

There are several variables that can be initialised by the analyst to enable customisation of the substructure for various configurations. The first is the number by which the substructure will be referenced. The others are the geometric parameters for the depth between the flange (or continuity) plates in the joint, and their thickness. The script uses the same thickness for both plates. While differing thicknesses could be used, the beam element attached to the substructure is defined assuming uniform warping resistance and would not accept the non-uniform warping restrained provided by unsymmetric conditions. The same data is entered for the vertical plates, and the thickness of the web.

The last parameter is the width of the substructure, in terms of shell elements. This gives the analyst the option of using a different mesh density.

```

#!/usr/local/bin/perl -W
#
# Define substructure element for box joint
#
# Element number for library
$ElemNum = 200;
# Required inputs for "box" type joint
# Centre to centre depth of beam, thickness of horizontal plates
$depthb = 210 - 10.2;
$thik1 = 10.2;
# Centre to centre width of column, thickness of vertical plates
$depthc = 210 - 10.2;
$thik2 = 10.2;
# web thickness
$webt = 5.8;
# full width of joint
$width = 133;
#
# Width by number of elements
$nelem = 16;
#
# This part writes the substructure element(s)
#
print "*HEADING\n This is a superstructure for a box type
joint\n";
#
# define geometry for joint
#
# The centre of the element is nominally at 0,0,0
#
$nelemup = int($depthb/$width * $nelem);
if (($nelemup % 2) == 1) {$nelemup++;}
$nelemfr = int($depthc/$width * $nelem);
if (($nelemfr % 2) == 1) {$nelemfr++;}
$nodenum = 1;
# Generate all nodes for joint
$dx = $depthc/$nelemfr;
$dy = $depthb/$nelemup;
$dz = $width/$nelem;
print "*NODE\n";

for ($h=0; $h<=$nelemfr; $h++) {
  $x = ($h - $nelemfr/2)*$dx;
  for ($i=0; $i<=$nelemup; $i++) {
    $y = $dy*($i - $nelemup/2);
    for ($j=0; $j<=$nelem; $j++) {
      $z = $dz*($nelem/2 - $j);
      print $nodenum,",", $x,",", $y,",", $z,"\n";
    }
  }
  # Flag corner nodes
  if ($h == 0) {
    if ((($j==0) || ($j == $nelem)) && (($i==0) || ($i ==
$nelemup))) {
      if (($j==0) && ($i==0)) {
        $nodea = $nodenum;
      } elsif (($j==0) && ($i==$nelemup)) {
        $nodec = $nodenum;
      } elsif (($j==$nelem) && ($i==0)) {

```

```

        $nodeb = $nodenum;
    } else {
        $noded = $nodenum;
    }
}
} elseif ($h == $nelemfr) {
    if (((($j==0) || ($j == $nelem)) && (($i==0) || ($i ==
$nelemup)))) {
        if (($j==0) && ($i==0)) {
            $nodee = $nodenum;
        } elseif (($j==0) && ($i==$nelemup)) {
            $nodeg = $nodenum;
        } elseif (($j==$nelem) && ($i==0)) {
            $nodef = $nodenum;
        } else {
            $nodeh = $nodenum;
        }
    }
} elseif (($x == 0) && ($y == 0) && ($z == 0)) {
    $cntrnode = $nodenum;
}
$nodenum++;
}
}
}
# Nodes for "back" plate
print "*NSET, NSET=NODEA\n ".$nodea."\n";
print "*NSET, NSET=NODEB\n ".$nodeb."\n";
print "*NSET, NSET=NODEC\n ".$nodec."\n";
print "*NSET, NSET=NODED\n ".$noded."\n";
print "*NSET, NSET=FACEBA\n
" . (($nelemup/2)*($nelem+1)+$nelem/2+1) . "\n";
# Nodes for "front" plate
print "*NSET, NSET=NODEE\n ".$nodee."\n";
print "*NSET, NSET=NODEF\n ".$nodef."\n";
print "*NSET, NSET=NODEG\n ".$nodeg."\n";
print "*NSET, NSET=NODEH\n ".$nodeh."\n";
print "*NSET, NSET=FACEFR\n
" . (($nelemup/2)*($nelem+1)+$nelem/2+1+($nelem+1)*($nelemup+1)*$ne
lemfr) . "\n";
print "*NSET, NSET=FACETP\n
" . ($cntrnode+($nelemup/2)*($nelem+1)) . "\n";
print "*NSET, NSET=FACEBO\n " . ($cntrnode-
($nelemup/2)*($nelem+1)) . "\n";
# Node for "centre"
print "*NSET, NSET=CENTRE\n ".$cntrnode."\n";
#
# set up elements
#
print "*ELEMENT, TYPE=S4R, ELSET=BACK\n";
$elem=1;
for ($n=0; $n<$nelemup; $n++) {
    for ($m=1; $m<=$nelem; $m++) {
        print
$elem.", " . ($n*($nelem+1)+$m) . ", " . ($n*($nelem+1)+$m+1) . ", " .
(($n+1)*($nelem+1)+$m+1) . ", " . (($n+1)*($nelem+1)+$m) . "\n";

```

```

        $selem++;
    }
}
#
print "*ELEMENT, TYPE=S4R, ELSET=FRONT\n";
$noffset = ($nelem+1)*($nelemup+1)*$nelemfr;
for ($n=0; $n<$nelemup; $n++) {
    for ($m=1; $m<=$nelem; $m++) {
        print
$selem.",",".($n*($nelem+1)+$m+$noffset).",",".($n*($nelem+1)+$m+1+$no
ffset).",",".

        (($n+1)*($nelem+1)+$m+1+$noffset).",",".(($n+1)*($nelem+1)+$m
+$noffset)."\n";
        $selem++;
    }
}
#
print "*ELEMENT, TYPE=S4R, ELSET=TOP\n";
$noffset = ($nelem+1)*($nelemup);
for ($n=0; $n<$nelemfr; $n++) {
    for ($m=1; $m<=$nelem; $m++) {
        print $selem.",",".
            ($noffset+$m+$n*($nelem+1)*($nelemup+1)).",",".
            ($noffset+$m+1+$n*($nelem+1)*($nelemup+1)).",",".
            ($noffset+$m+1+($n+1)*($nelem+1)*($nelemup+1)).",",".
            ($noffset+$m+($n+1)*($nelem+1)*($nelemup+1))."\n";
        $selem++;
    }
}
#
print "*ELEMENT, TYPE=S4R, ELSET=BOTTOM\n";
$noffset = 0;
for ($n=0; $n<$nelemfr; $n++) {
    for ($m=1; $m<=$nelem; $m++) {
        print $selem.",",".
            ($noffset+$m+$n*($nelem+1)*($nelemup+1)).",",".
            ($noffset+$m+1+$n*($nelem+1)*($nelemup+1)).",",".
            ($noffset+$m+1+($n+1)*($nelem+1)*($nelemup+1)).",",".
            ($noffset+$m+($n+1)*($nelem+1)*($nelemup+1))."\n";
        $selem++;
    }
}
#
print "*ELEMENT, TYPE=S4R, ELSET=WEB\n";
$noffset = int($nelem / 2)+1;
for ($n=0; $n<$nelemfr; $n++) {
    for ($m=0; $m<$nelemup; $m++) {
        print $selem.",",".
            ($noffset + $m*($nelem+1) +
$n*($nelem+1)*($nelemup+1)).",",".
            ($noffset + ($m+1)*($nelem+1) +
$n*($nelem+1)*($nelemup+1)).",",".
            ($noffset + ($m+1)*($nelem+1) +
($n+1)*($nelem+1)*($nelemup+1)).",",".
            ($noffset + ($m)*($nelem+1) +
($n+1)*($nelem+1)*($nelemup+1))."\n";
    }
}

```

```

        $elem++;
    }
}
#
print "*SHELL SECTION, ELSET=BACK, MATERIAL=STEEL1\n";
print $thik2, "\n";
print "*SHELL SECTION, ELSET=FRONT, MATERIAL=STEEL1\n";
print $thik2, "\n";
print "*SHELL SECTION, ELSET=TOP, MATERIAL=STEEL1\n";
print $thik1, "\n";
print "*SHELL SECTION, ELSET=BOTTOM, MATERIAL=STEEL1\n";
print $thik1, "\n";
print "*SHELL SECTION, ELSET=WEB, MATERIAL=STEEL1\n";
print $webt, "\n";
#
print "*MATERIAL, NAME=STEEL1\n";
print "*ELASTIC\n 200E3, 0.3\n";
print "*DENSITY\n 7.7E-9\n";
#
# Constraints
#
print "*EQUATION\n";
print "*** Back face\n";
print "2\n";
print "NODEC, 1, 1, NODEA, 1, 1\n";
print "2\n";
print "NODEA, 1, 1, NODEB, 1, 1\n";
print "2\n";
print "NODEB, 1, 1, NODED, 1, 1\n";
print "*** Front face\n";
print "2\n";
print "NODEG, 1, 1, NODEE, 1, 1\n";
print "2\n";
print "NODEE, 1, 1, NODEF, 1, 1\n";
print "2\n";
print "NODEF, 1, 1, NODEH, 1, 1\n";
print "*** Top face\n";
print "2\n";
print "NODEC, 2, 1, NODED, 2, 1\n";
print "2\n";
print "NODED, 2, 1, NODEH, 2, 1\n";
print "2\n";
print "NODEH, 2, 1, NODEG, 2, 1\n";
print "*** Bottom face\n";
print "2\n";
print "NODEA, 2, 1, NODEB, 2, 1\n";
print "2\n";
print "NODEB, 2, 1, NODEF, 2, 1\n";
print "2\n";
print "NODEF, 2, 1, NODEE, 2, 1\n";
#
# Generate element
#
print "*STEP\n";
# Note that type is of format Zn where 0<n<10000
printf "*SUBSTRUCTURE GENERATE, TYPE=Z%d, OVERWRITE, RECOVERY
MATRIX=YES\n", $ElemeNum;

```

```

print "*RETAINED NODAL DOFS, SORTED=NO\n";
# Lines to generate dof's - NodeNumber, dof_start, dof_end
print " ".$cntrnode.", ".1,6". "\n";
print " ".$noded.", ".1". "\n";
print " ".$nodeh.", ".1". "\n";
print " ".$nodeg.", ".2". "\n";
print " ".$nodee.", ".2". "\n";
# End of definition
print "*END STEP\n";

```